A kainic acid-induced status epilepticus model of epileptogenesis in the C57BL/6J mouse. Interventions targetting nitric oxide and NMDA receptor-mediated pathophysiology

Thesis submitted in accordance with the requirements of the University of Liverpool for the degree of Doctor of Philosophy by Edward Beamer

ACKNOWLEDGEMENTS

I would like to thank the following people both for their direct help and their tireless support: Swamy Thippeswamy, Richard Morris, Graeme Sills, Beatrice and Cyril Dodd, Barbara and Gary Beamer, Laura Macdonald, Maya Wardeh, Matthew Bradman, Chrysanthi Fergani, Maria Poveda Villalón, Catherine Quinn, Tracy and Laura Fleming

Abstract

In this thesis, the behavioral, electrographic and neurobiological effects of a period of kainic acid-induced status epilepticus (SE) on the C57BL/6J inbred mouse strain are characterised. The severity of epileptic behaviour was scored, used immunohistochemistry to investigate the anatomical distribution of c-Fos expression in the hippocampal formation following SE and recorded EEG during and after SE using an implantable, wireless telemetry device. Further to assessing the severity of SE, changes subsequent to seizures related to the emergence of chronic epilepsy were investigated, including reactive gliosis and synaptogenesis and epileptiform discharges in the EEG trace.

I investigated the potential of a range of pharmacological agents for modulating the severity of induced seizures and disease progression. These included drugs targetting the NR2B subunit of the NMDA receptor (RO 25-6981), neuronal nitric oxide synthase (L-NPA), The post synaptic density protein 95 (Tat-NR2B9a) and inducible nitric oxide synthase (1400W).

L-NPA, when administered prior to the induction of SE was found to profoundly suppress the emergence of epileptiform activity, including behavioural, electrographic and neurobiological indicators. Further, L-NPA's modulation of the precipitating event lead to a decrease in neurobiological changes associated with epileptogenesis, such as reactive gliosis in the CA3 region of the hippocampus and

elevated synaptogenesis in th molecular layer of the hippocampus. This correlated with a marked decrease in epileptiform discharges in the EEG trace.

A novel method of kainic acid administration was trialed, involving multiple small doses of the drug, titrated by the severity of behaviour. This method led to a decrease in mortality and an increase in the severity and inter-individual uniformity of SE, assessed by the analysis of behaviour, EEG and c-Fos expression in the hippocampus. Furthermore, this method induced neurobiological changes associated with epileptogenesis 3 days following SE and was associated with an increased frequency of epileptiform discharges for 7 days post SE.

Contents

Chapter 1. Introduction

1.1 Summary

Initially, the clinical characteristics of seizures and epilepsy will be described and the mental and social problems associated with the pathology (1.2). A brief anatomical description of the anatomy of brain regions implicated in seizure generation will then be given, alongside a discussion of their physiological function (1.3). An overview of basic research into the epilepsies will then be given, with an emphasis on temporal lobe epilepsy (TLE) (1.4). Some background to the history and development of the methods used in our studies will be given, including animal models of seizures and epilepsy (1.5). The development of pharmacological interventions will be discussed, both in terms of their development and clinical applications (1.6). Finally, a discussion of the physiological and pathophysiological role of nitric oxide in a range of disorders of the central nervous system will be presented, with a particular emphasis on epilepsy (1.7), before a brief introduction to the specific aims of the research described in subsequent chapters (1.8).

1.2 Seizures and epilepsy in the clinic

1.2.1 Overview

Epilepsy is a brain disorder characterized by an enduring predisposition to generate seizures, and by emotional and cognitive dysfunction (Duncan et al, 2006). Epilepsy effects approximately 50 million people worldwide and is strongly linked to depression, both through direct physiological causation and secondary effects mediated by restrictions on lifestyle, living with the fear of seizures, intellectual deterioration, exclusion from driving and low self-esteem (Gilliam et al, 2008). 30% of sufferers are refactory to currently available pharmacological interventions (Kwan & Brodie, 2000) and, in many cases, highly invasive surgery often involving severe side-effects (Wiebe et al, 2001) is the only option available.

1.2.2 Seizures

The word *seizure* derives from the Latin ‘sacīre’ meaning simply *to take hold of.* A seizure is a paroxysmal event that can be triggered by physiological (organic) or psychological disturbances. Not all seizures are epileptic. Seizures that are triggered by events outside the brain, or psychological disturbances, are described as non-epileptic seizures. These include, but are not limited to: febrile convulsions in infants, hypoglycaemic seizures and parasomnias, such as ‘night terrors’. Seizures can involve involuntary muscle activity or abnormal experiences, ranging from visual disturbances to phenomonological experiences that defy linguistic description.

1.2.3 Epileptic seizures

An epileptic seizure is, by definition, generated in the brain and involves the abnormal, rhythmic discharges of cortical neurons (Ricker, 2003). Epileptic seizures can be categorised according to either the anatomical distribution of epileptiform activity, or the emergent behaviour or phenomenological experiences. The challenge involved in creating a system of seizure classification of sufficient precision and breadth, however, is exemplified by the complications in the most simple dichotomy between partial (focal) and generalised seizures. Partial seizures are restricted to a specific focus in a single hemisphere, while generalised seizures effect both sides of the brain. The distinction, however, is blurred in cases of secondarily-generalised partial seizures and non-generalised, multi-focal seizures. Here follows a brief overview of different seizure types described by currently accepted nomenclature of the international league against epilepsy (ILAE) (Fisher et al, 2005) and a figure illustrating the hierarchical structure of seizure types (Figure 1).

A simple partial seizure (SPS) is restricted to a narrow focus, described by John Hughlings Jackson (1890) as a 'discharging lesion', can often produce an 'aura', which can be used to predict more serious and potentially damaging secondarily-generalised seizures. The site of the seizure focus largely dictates the way SPS is experienced, with a temporal lobe focus (most common) typically inducing epigastric rising sensations, feelings of familiarity (deja vu) or unfamiliarity (jamais vu), intense bursts of emotion and highly vivid flashbacks of memory. A parietal lobe focus often causes sensations of numbness, tingling or burning. In the occipital lobe, a distortion

of vision, flashing lights, coloured shapes and hallucinations can be experienced, while, in the frontal lobes, a ‘wave’-like sensation going through the head and body is commonly reported.

Complex partial seizures (CPS) effect larger areas of the brain, but are usually still restricted to a single hemisphere. A CPS can inhibit conciousness, responsiveness and memory of the seizure. A period of severe post-ictal confusion is often difficult to demarkate from the seizure itself. The temporal lobe is the most common site for CPS, where it often induces manual and oral automatisms.. CPS in the frontal lobe is often of shorter duration and and characterised by the adoption of strange limb postures, juddering movements and a swift post-ictal recovery. Generalised seizures affect both hemispheres and involve the full loss of conciousness and tonic-clonic convulsions. Partial seizures that spread are referred to as secondarily-generalised seizures.

Seizures are also often defined primarily from the behavioural and experiential perspective. Absence seizures (petit mal), underpinned by a disruption of corticothalamic and thalamocortical pathways (Snead III, 1995) involve the temporary loss of conciousness. Typical absence seizures often last for just a few seconds and may often go unnoticed. Tonic, atonic, myoclonic and clonic seizures involve disruptions in the motor cortex and respectively produce the involuntary contraction, relaxation, twitching and alternating contraction and relaxation muscles. Tonic-clonic (grand mal) seizures involve alternate phases of tonus and clonus and usually result in the loss of conciousness. A period of 30 minutes or more of either

continuous or repeating seizure activity is classified as status epilepticus (Treiman, 1993). Up to 25% of seizures fail to fulfill the criteria for any seizure 'type' and remain unclassified.

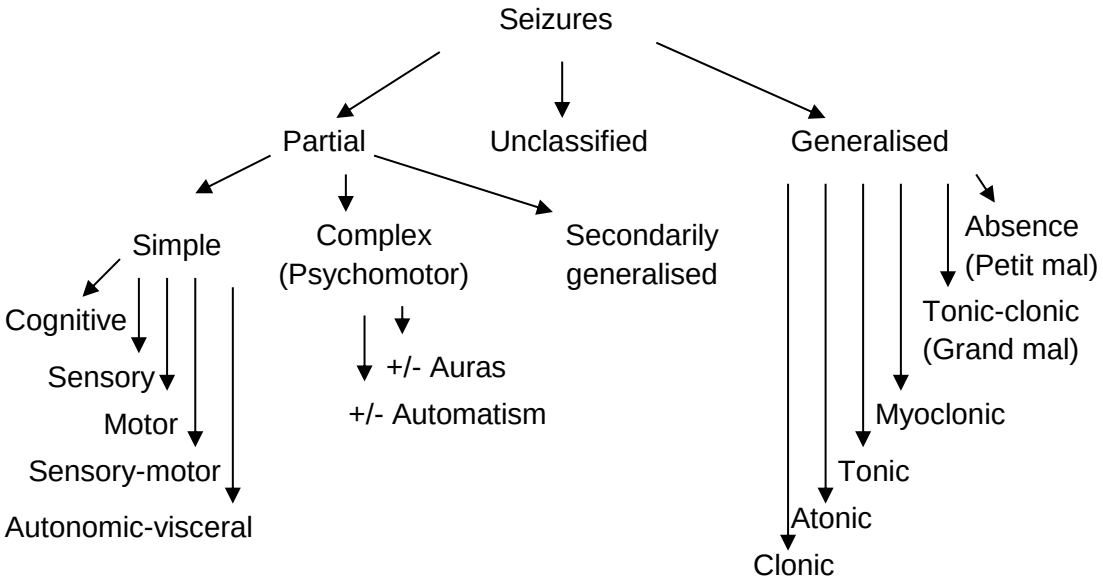

Figure 1.1. Categorisation of seizures according to the international league against epilepsy (Fisher, 2005).

1.2.4 Epilepsy

Epilepsy is the recurrence of unprovoked epileptic seizures, implying a permanent brain pathophysiology supporting abnormal hypersynchronous neuronal firing (Fisher, 2005). Rather than a single disorder, 'epilepsy' refers to a diverse group of syndromes with different symptoms and etiologies. Epilepsies are classified according to five criteria: etiology, se miology, anatomical site of seizure origin, syndrome and trigger (Fisher, 2005). Common epilepsy syndromes include

childhood absence epilepsy, caused by disruptions to thalamocortical and corticothalamic circuitry (Snead III, 1995) and benign familial neonatal convulsions, an inheritable ‘channelopathy’ effecting potassium channel kinetics (Baulac, 2010). Many epilepsy syndromes are idiopathic, like the relatively rare Landau-Kleffner syndrome (Landau & Kleffner, 1957), which involves acquired aphasia related to epileptiform activity during sleep. Of particular interest to us, and discussed in detail below is temporal lobe epilepsy (TLE).

1.2.5 Temporal lobe epilepsy

John Hughlings Jackson first described the semiology of what would later become known as TLE in the 1860 as *uncinate fits*; seizures arising from the uncal part of the temporal lobe. Gibbs, et al (1936) introduced the term *psychomotor epilepsy* to describe the same set of symptoms. In 1981, the international classification of epileptic seizures replaced this term with *complex partial seizures* and in 1985, the ILAE classified TLE as a condition characterised by spontaneous recurrent seizures (SRS) originating from the medial or lateral temporal lobe (Fisher, 1985).

TLE is the most common form of new-onset epilepsy in adults and is clinically characterised by complex focal seizures with oral or manual automatisms and secondarily generalised tonic-clonic seizures (Aronica & Gorter, 2007). It is a condition of diverse etiologies, however, it is often precipitated by abnormalities within the hippocampus (Ben-Ari & Cossart, 2000). TLE is also the most common

indication for epileptic surgery (Berg, 2008), which can involve the resection, disconnection or stimulation of the temporal lobe. Electrophysiological recordings from the human brain during surgery and histology on resected tissues has contributed to our understanding of the disease, however, because patients will invariably have tried numerous drug treatments prior to surgery, a basic understanding of the 'natural history' of TLE in humans is lacking (Berg, 2008).

An initial precipitating insult (IPI), such as traumatic brain injury, ischaemic brain injury or a seizure sets in motion a process known as epileptogenesis (De Lanerolle et al, 1989), involving a seizure-free 'latent' phase, followed by chronic susceptability to sponateous recurrent seizures (SRS). In humans, the latent phase will often last for years. Animal models, in vitro preparations and computational models have all contributed to our understanding of TLE. An overview of the contribution of basic research and an in depth discussion regarding the underlying biology of the condition is tackled later in this chapter.

1.3 Physiological function of brain regions implicated in seizures and epilepsy

1.3.1 Summary

Hughlings Jackson (1890) described seizures as a collection of neurons firing in a hypersynchronous manner. In order to understand this disrupted activity, it is necessary to first need to understand a little about how neurons and neuronal circuits behave under physiological conditions. Here, the basic anatomy of neurons and neuronal circuits is discussed, before switching emphasis to a description of the anatomy and physiology of brain regions implicated in TLE. A detailed discussion regarding the pathophysiology of epilepsy, however, is reserved for later in the chapter.

1.3.2 Neurons – the basic unit of network activity

1.3.2.1 Anatomy of the neuron

Neurons are cells specialised for the integration and transmission of information (Hebb, 1949). This information is transmitted between neurons chiefly through chemical transmission at synapses, and transmitted across long-distances in the CNS by the progression of action potentials (APs) axons. The prototypical neuron (Figure 1.2) consists of dendrites, a soma (cell body), and an axon. The axon

arborises and forms terminal boutons on many target neurons, as well as proximate boutons along its length.

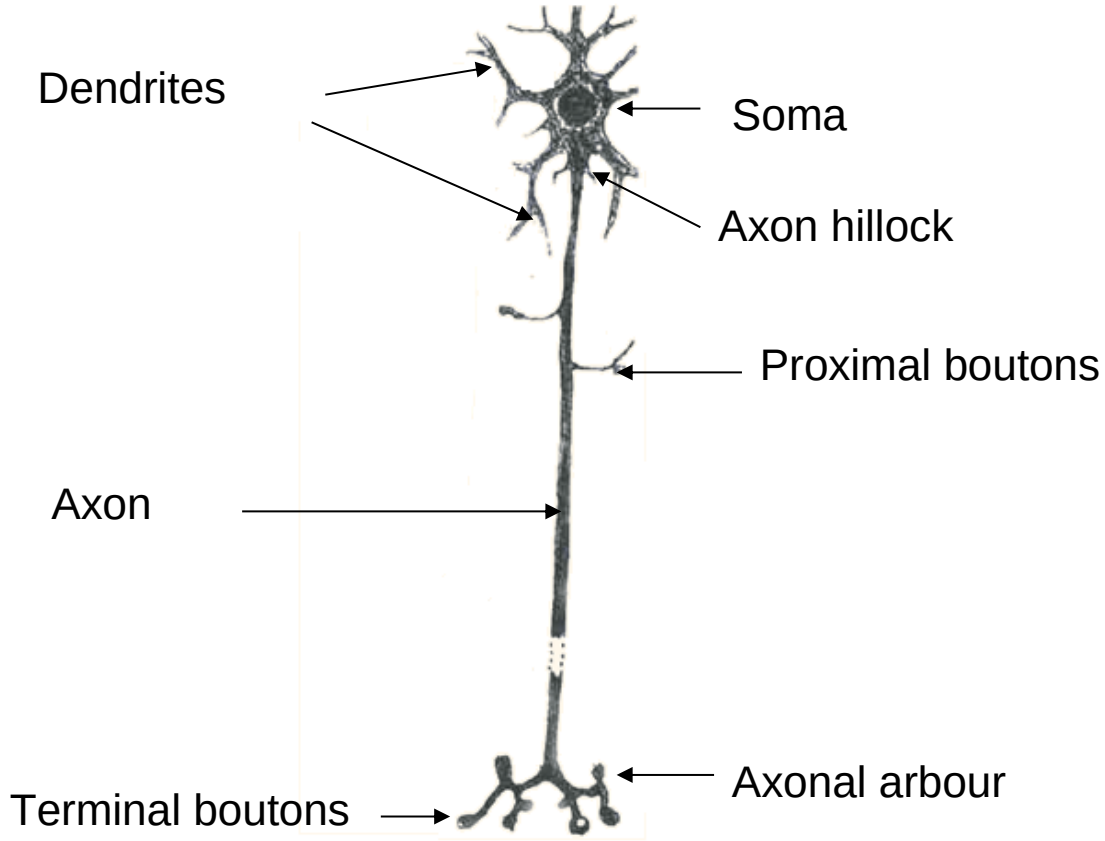

Figure 1.2. Prototypical neuron (Drawing from Ramon Y Cajal & Azoulay, 1894)

1.3.2.2 The resting membrane potential

The cytosol is seperated from the extracellular environment by an insulatory lipid bylayer facilitating the formation of an electrochemical gradient. This gradient is created and maintained by an ATP-driven Na^+/K^- pump. A resting potential (V_m) of around -65mV is maintained across the lipid bilayer by the action of voltage-gated ion channels in the lipid membrane. This resting potential provides the store of

energy required for the swift transmission of information down the axon via the action potential (AP) (Hodgkin & Huxley, 1952).

1.3.2.3 The action potential

The AP (Figure 1.3) was first described in the giant axon of the squid, by Hodgkin & Huxley (1952) in four landmark papers published simoultaneously in the same issue of the Journal of Physiology. In the dendrites and soma, the membrane potential is depolarised by excitatory post-synaptic potentials (EPSPs) from excitatory input (typically mediated by glutamate in the CNS (Meldrum, 2000)), and hyperpolarised by inhibitory post-synaptic potentials (IPSPs) from inhibitory input (typically mediated in the CNS by Gamma-amino butyric acid (GABA) (Sivilotti & Nistri, 1991)). The membrane potential in this region fluctuates in a graded manner, depending on inputs from other neurons. An AP is produced at the axon hillock when the net effect of EPSPs and IPSPs is a depolarisation beyond the threshold potential, which varies across neurons, but is typically in the range of -40 to -55mV.

Depolarisation beyond the threshold leads to the opening of local voltage-gated Na^+ channels, further depolarising the memberane and leading to a cascade of Na+ influx (rising phase), a reversal in the potential (overshoot) that typically peaks around +40mV. At this reversal potential, Na+ channels are shut, preventing further influx and K+ channels open, leading to outflux of K+ and a return towards (falling phase) and often beyond (undershoot), V_m. Voltage-gated ion channels, particularly Na+ channels, propagate action potentials down an axon, with a high level of fidelity,

towards the pre-synaptic terminal. The great value of the AP is that it is an all or nothing event, translating graded inputs into a binary signal, which can be conducted quickly over long distances without degradation. At pre-synaptic terminals, the AP is translated into the vesicular release of neurotransmitters (Sudhof, 1995).

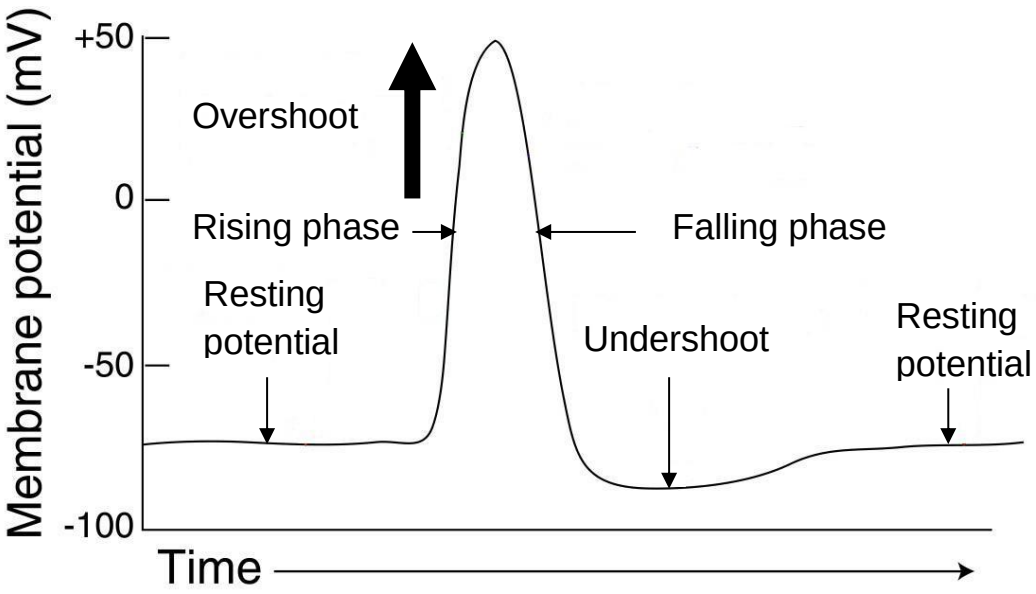

Figure 1.3. Phases of the action potential

1.3.2.4 Synaptic transmission

Chemical signalling at the synapse was first demonstrated at the neuromuscular junction by Otto Loewi (1921). Subsequently, it has become clear that the vast majority of synaptic signalling in the CNS is mediated via chemical rather than bioelectrical transmission. The details and variety of synaptic transmission is a topic of huge and ever-expanding complexity. The basic mechanisms understood to underpin the signalling of a prototypical chemical synapse will be briefly outlined and

give an account of how the synaptic machinery can be modulated to alter responses to excitatory and inhibitory inputs; a topic of great importance to an understanding of brain function and pathophysiology, including epilepsy.

At the pre-synaptic terminal, neurotransmitters are stored in pools of synaptic vesicles. In localised nanodomains or 'active zones', a proportion of these synaptic vesicles are docked in close proximity to a high density of voltage-gated Ca^{2+} channels (Zucker, 1996). When an AP arrives down the axon, a transient and local influx of Ca^{2+} interacts with proteins associated with the vesicles and promotes the formation of a 'fusion complex' (Neher & Sakaba, 2008) involving a host of protein-protein interactions; notably synatotagmin and synaptobrevin associated with vesicles and syntaxin and SNAP-25 associated with the plasma membrane. These fusion complexes allow for the exocytosis of neurotransmitters into the synaptic cleft (Sudhof, 2004). Ca^{2+} localised to nanodomains can mediate the fast signalling without triggering other pathways associated with Ca^{2+}. Llinas et al (1992) reports a delay of only 0.2ms between Ca^{2+} channel opening and vesicular release. Other sources of Ca^{2+} can interact with this basic mechanism to effect longer-term modulation of synaptic transmission, providing one mechanism for synaptic plasticity (Kandel, 2001).

Neurotransmitters released into the synaptic cleft bind to receptors on the post-synaptic terminal, initiating a number of events. Receptors can be grouped according to whether they are ligand-gated ion channels or metabotropic G-protein coupled receptors, with the majority of neurotransmitters having receptors of both types.

Generally, ion channels mediate fast, transient responses, while metabotropic receptors mediate slower, longer term responses, such as transcription (Conn & Pinn, 1997). Receptors are not restricted to the post-synaptic terminal, with many found on the pre-synaptic terminal and at extrasynaptic sites, where they generally play a regulatory role (Fellin et al, 2004). Neuronal signalling depends not only on the release of neurotransmitters, but also on their removal or degradation. Some neurotransmitters, such as acetylcholine (Ellman et al, 1961) are degraded in the cleft while others, such as serotonin (Amara & Kuhar, 1993) are taken back up by reuptake channels in the pre synaptic terminal.

In the adult CNS, excitatory and inhibitory transmission is generally mediated by glutamate and GABA respectively (Bradford, 1995). Edward George Gray (1959) defined two types of synapse, based on their differing appearance in electron micrographs. Type I synaspes were assymetrical, with a higher synaptic density on the post-synaptic terminal, while type II synapses had a symetrical appearance. The view that type I, assymetrical synapses largely mediate excitatory, glutamatergic neurotransmission, while type II, assymetrical synaspes largely mediate inhibition through GABA has subsequently crystalised, however there are significant exceptions (Klemann & Roubos, 2011). Besides the two dominant amino acids, a broad range of CNS neurotransmitters have been discovered, including monoamines, such as dopamine and serotonin (Twarog, 1954), peptides, such as the opiods (Malick & Bell, 1976) and others, such as acetylcholine (Loewi, 1921) and nitric oxide (Bredt & Snyer, 1992).

Glutamate receptors can be grouped into three main classes; N-Methyl-D-aspartic acid (NMDA) receptors, 2-amino-3-(5-methyl-3-oxo-1,2-oxazol-4yl)propanoic acid (AMPA) receptors and kainate receptors, named according to their affinity for pharmacological agents. The majority of EPSPs are mediated through AMPA receptors, while kainate receptors are largely found at extracellular sites and at the pre-synaptic terminal where it is thought to play a modulatory role (Ozawa, 1998). The NMDA receptor functions as a coincidence detector, opening a Ca^{2+} channel only when activated by glutamate and the membrane is sufficiently depolarised to remove a Mg^{2+} block in the channel (Nowak et al, 1984). The calcium permeability of the NMDA receptor and its ability to function as a coincidence detector allows it to function as a key mediator of synaptic plasticity (Tsien, 2000).

The primary means of modulating glutamatergic synaptic transmission is by changes in the activity and abundance of post-synaptic AMPA receptors (Manilow & Malenka, 2002). The primary mechanism for modulating this is via Ca^{2+} signalling through the NMDA receptor, which can induce long-term depression (LTD) or long-term potentiation (LTP) in response to different patterns of stimulation. Ca2+ influx through the post-synaptic NMDA receptor can also modulate activity in the pre-synaptic terminal through retrograde NO signalling (Hawkins et al, 1998). A wide variety of NMDA-independent mechanisms also exist for modulting synaptic transmission, including alterations in pre-synaptic Ca^{2+} influx and subsequent volume of vesicle release (Kandel, 2001), Ca^{2+} permeable AMPA receptor-mediated plasticity (Mahanty & Sah, 1998), kainate receptor-mediated plasticity, particularly at mossy fibre synapses in the hippocampus (Bortolotto et al, 2003).

The synaptic and intrinsic machinery briefly described here, allow neurons to function as units in an information-processing system. An ever greater diversity in synaptic and electrophysiological properties of neurons is being discovered (Llinas, 1992). The functional significance of this is that different neurons can respond differently to different inputs, depending on the frequency, ampliture and spatial characteristics of the input. Synaptic and intrinsic machinery allow neurons to act as 'resonators', responding preferentially to certain frequencies, or even intrinsic oscillators (Llinas, 1992). Later, neurons functioning as units in a network will be described.

1.3.3 The emerging importance of glia

Glial cells in the CNS include microglia, which are derived from immune cells, astrocytes, oligodendrocytes, ependymal cells, radial glia and NG2 cells (Verkhratsky & Butt, 2007). Previously the unglamorous cousins of neurons and relegated to the role of a 'glue' to offer structural support, the importance of the role that glial cells, also called 'neuroglia' or simply 'glia', play in information processing is becoming increasingly clear. As well as providing metabolic support (Tsacopoulos & Magistretti, 1996), regulating the ionic balance of the extracellular space (Sykova & Chvatal, 2000), regulating development (Song et al, 2002) and mediating neuronal survival (Vezzani et al, 2008) and apoptosis (Bal-Price & Brown, 2001), glia also play

a role in synaptogenesis (Ullian et al, 2004) and synaptic plasticity (Vernadakis, 1996).

Although Glia cannot conduct an AP, they express receptors for neurotransmitters and release 'gliotransmitters' in response to intracellular Ca^{2+} signalling. Astrocytes can also communicate with each other over long distance through Ca^{2+} 'waves' that propagate through gap junctions in wide-ranging astrocytic syncytia (Verkhratsky & Kettenmann, 1996). A better understanding of communication between glia, and between neurons and glia is likely to yield important information regarding the way the brain performs computations. Rather than neural networks, neuroglial networks may soon be considered of greater importance.

Glial cells provide an important link between neurons and the neurovascular system, where they can regulate the permeability of the blood-brain barrier Bannerjee & Bhat, 2007). Glial cells have a key involvement in every single physiological function that the brain performs. Likewise, they are involved in every pathophysiology. Glia are heavily involved in mediating the neuroinflammatory response to brain insults (Vezzani et al, 2008), which will be discussed in greater detail later In this chapter, with a particular emphasis on the glial contribution to temporal lobe epilepsy.

1.3.4 Neural circuits and oscillations

While it is important to understand the functional units, information processing in the CNS can only really be understood in the context of interactions between units. Seizures and epilepsy, also, generally arise as a consequence of dysfunctions at a network level. A network made up entirely of glutamatergic, excitatory neurotransmission, would be of limited use for information processing. In the absence of inhibition, any external input would generate a unidirectional avalance of excitation involving the whole population (Hopfield & Tank, 1986), with propagation of activity independent of time, wiring complexity, strength of excitation or any other factor (Buzsaki, 1997). GABAergic, inhibitory input does not function purely to dampen excitatory activity, but allows for the emergence of non-linearity. Feed-forward and feed-back mechanisms, highly-dependent on the specifics of wiring allow mixed networks of excitatory and inhibitory neurons to self-organise and generate complex properties (Buzsaki, 1997).

In the brain, The temporal coherence of large groups of neurons is coordinated by GABAergic signalling, which functions as a distributed clock, decreasing the probability of neuronal firing outside a window of disinhibition (Buzsaki, 1997). This distributed clock mechanism can modulate the activity of whole networks. Rather than being dormant in the absence of input, the CNS generates rhythmic activity endogenously. Signalling in the brain is carried out in the context of a system of nested oscillations, with oscillations often phase-locking (Palva et al, 2005). A strong inverse relationship between the spatial extent of rhythms and their frequency exists, with high frequency rhythms occuring for short durations in relatively limited areas of the brain.

Although previously understood as the epiphenomena of neuronal signalling, the role that network-wide oscillations play in computation is becoming increasingly clear. Network oscillations effect synaptic and intrinsic mechanisms underlying functions such as attention (Buzsaki et al, 1997). Many pathophysiological conditions can be understood as an 'oscillopathy', including schizophrenia, depression and epilepsy (Uhlhaas & Singer, 2006). The hippocampus has been a focus for studies into oscillatory mechanisms, with the CA3 region, in particular, an important pacemaker for generating network-wide activity (Ben-Ari & Cossart, 2000). It may be this feature that makes the region so susceptable to producing the pathological paroxysmal discharges associated with seizures.

1.3.5 Gamma frequency and seizures

As a general rule, during normal brain function, slower oscillations tend to be of higher amplitude, while higher frequency oscillations tend to be of lower amplitude. Approximately, the amplitude of oscillations in the brain are inversely proportional to their frequency. These 1/f dynamics are referred to as pink noise, because when similar distributions of wavelengths of light are observed, the effect of the spectrum of colours is a pink hue (Bak et al, 1987). Under physiological conditions, gamma activity (20 – 70Hz), thought to play an important role in the processing of episodic memory, is of short duration, not widely distributed and of low amplitude.

During seizure, the pink noise, 1/f dynamics of brain activity are disrupted and higher frequency oscillations occur at higher amplitudes than are present during normal

brain function. The high amplitude of these oscillations represents the pathological hypersynchrony of neuronal networks. Moreover, whereas oscillations in EEG during physiological function largely represent field oscillations reflecting EPSPs in the dendrites, during highly synchronous firing during seizures, the influence of action potentials on extracellular field potentials increases (Dudek, 2003) and is likely to contribute significantly to the EEG signal. Lehmuke et al (2009) demonstrated that the dynamic power in the gamma frequency range (20 – 70 Hz) was a good measure of seizure severity during KA-induced SE in rats.

1.3.6 The hippocampal formation

1.3.6.1 History of hippocampal research

The hippocampus has long been of great interest to anatomists, with members of the alexandrian school of medicine naming the structure *cornu ammonis*, horn of the ram, in reference to its curved shape. The name *hippocampus* was first coined by venetian anatomist Giulio Cesare Aranzi around 1564, in reference to its likeness for the seahorse. Modern biologists have also been fascinated by the structure. As well as its aesthetic merits, the hippocampal formation plays an important role in many brain functions and its highly organised stratified structure makes it particularly attractive for studying universal neuronal processes.

The nomenclature of terms describing the anatomy of the hippocampus and hippocampal formation is confused, with different authors ascribing the terms ‘hippocampus’ and ‘hippocampal formation’ to a varyingly broad array of structures. In this study, ‘hippocampus’ is reserved for the hippocampus proper, or ammon’s horn, while the ‘hippocampal formation’ refers to the hippocampus, dentate gyrus and the subiculum. The pre- and para- subiculum and the entorhinal cortex are also discussed, but are referred to as structures outside the hippocampal formation.

The circuitry of the hippocampal formation (Figure 1.4) has been traditionally viewed in terms of an excitatory ‘trisynaptic circuit’, propagated by glutamatergic synapses and modulated by a broad range of GABAergic local-circuit inhibitory interneurons (Sik, et al, 1997; McBain & Fisahn, 2001). The ‘trisynaptic circuit’ consists of input, via the perforant path, from layer II of the entorhinal cortex, with synapses formed on dentate granule cell dendrites in the molecular layer of the dentate gyrus. Mossy fibre projections from the dentate gyrus form synpases with CA3 pyramidal neurons in the stratum lucidum. CA3 axons or ‘Schaffer collaterals’ are found in the stratum radiatum and stratum lacunosum-moleculare, where they form synapses with CA1 pyramidal cell dendrites. CA1 sends projections to layer V of the entorhinal cortex completing the trisynaptic loop. While this is the primary pathway for transmission in the hippocampus, other pathways also exists, including, but not limited to, a projection from layer III of the entorhinal cortex, direct to CA1 dendrites in stratum lacunosum-moleculare and a ‘backprojection’ from the CA3 region to the dentate gyrus (Scharfman, 2007). The main input into the hippocampus, and therefore the starting point of the ‘tri-synaptic’ circuit is the dentate gyrus.

1.3.6.2 The dentate gyrus

A coronal section of the brain reveals the dentate gyrus as a V-shaped structure, with the two blades of the V sandwiching the proximal pyramidal cell layer (PCL) of the hippocampus (Figure 1.4). The two blades of the dentate gyrus are referred to as the supra- (above) and infra- (below) pyramidal blades, respectively. The Dentate gyrus is made up of three distinct layers. The granule cell layer (GCL) is a 4 – 8 somata thick layer of densely-packed excitatory granule neurons. Superficial to the GCL is the molecular layer, in which the entire dendritic tree of the granule cells is found, alongside the fibres of the perforant path and a small number of inhibitory interneuron cell bodies (Freund & Buzsaki, 1996). Subjacent to the GCL is the polymorphic zone (hilus) which encloses the proximal end of the CA3 PCL (Freund & Buzsaki, 1996). The hilus hosts a variety of neuronal cell bodies, including a range of inhibitory interneurons and excitatory mossy cells (Anderson et al, 2006)

Perforant path afferents from the lateral entorhinal cortex layer II terminate in the outer molecular layer (OML) of the dentate gyrus and those from the medial entorhinal cortex layer II terminate in the middle molecular layer (MML), where they form synapses with granule cell dendrites (Freund & Buzsaki, 1996). Granule cell axons (mossy fibres) originate at the opposite pole of the soma and enter the hilus, where they give rise to several local collaterals (Anderson et al, 2006). The main axon of the granule cells leaves the hilar region and courses adjacent to the

pyramidal cell layer in stratum lucidum of the CA3 subfield, where they form giant en passant boutons, on the proximal dendrites of pyramidal cells.

1.3.6.3 The hippocampus

A coronal section of the brain reveals the hippocampus as an elongated C-shaped structure, with one end of the structure sandwiched between the blades of the dentate gyrus (Figure 1.4). The hippocampus is subdivided into regions CA1, CA2 and CA3, with CA3 proximal to the dentate gyrus. The laminar organization of the hippocampus comprises the PCL, which is densely packed with excitatory pyramidal neurons bordered on its superficial and deep sides by the stratum radiatum and stratum oriens respectively. In CA3, a thin stratum, comprising the mossy fibre input from the dentate gyrus, stratum lucidum, separates the PCL from stratum radiatum.

The stratum radiatum contains Shaffer collateral fibres, projecting from CA3 to CA1 where they form the third synapse in the trisynaptic circuit. Both stratum radiatum and oriens contain high densities of associational fibres, linking pyramidal cells in the same subfield and commissural fibres, linking the two hippocampi across hemispheres. Superficial of the stratum radiatum, the thin stratum lacunosum-moleculare is found, where Schaffer collaterals and perforant path inputs from layer II of the entorhinal cortex terminate on CA1 pyramidal cell dendrites. Outside the PCL, a variety of non-pyramidal neurons are found, including a variety of subpopulations of inhibitory interneurons, subdivided according to their

morphological characteristics and neuropeptide and calcium-binding content (Freund & Buzsaki, 1996).

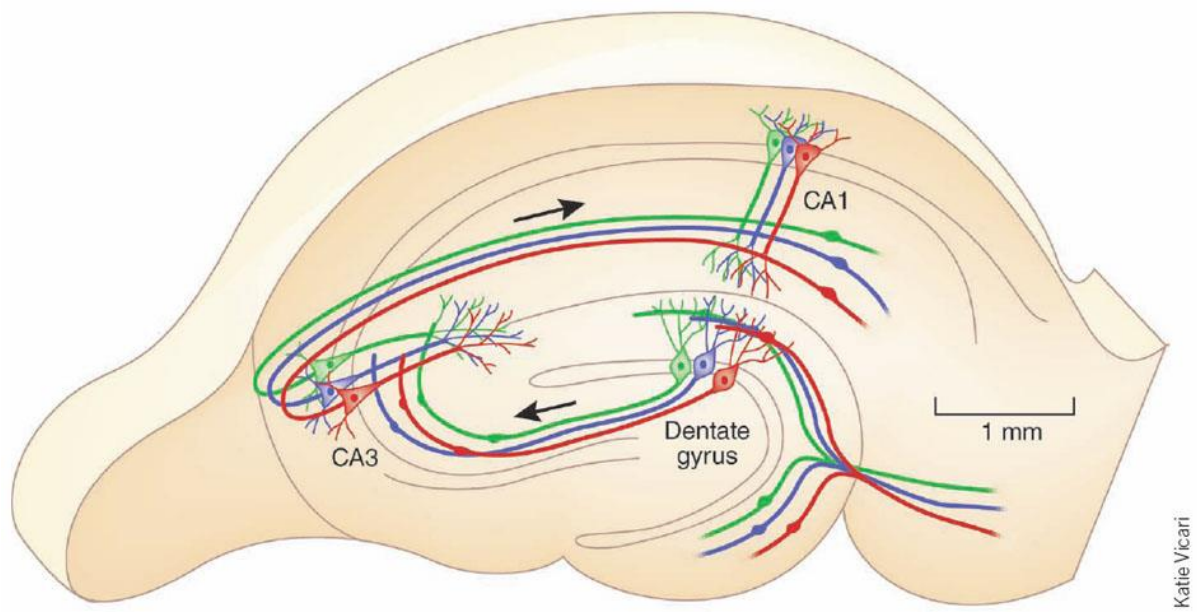

Figure 1.4. Hippocampal formation with main excitatory pathways. Taken from Moser (2011).

1.4 Seizures and epilepsy

1.4.1 Summary

I will give a brief historical perspective of the development of our understanding of seizures and epilepsy, and review some of the evidence for popular hypotheses regarding how dysfunctions in the physiological mechanisms described previously can contribute to ictogenesis and epilepstogenesis. The history of progress in the understanding of TLE will then be described and an in depth discussion of the mechanisms underpinning the development of chronic epilepsy will be offered. Research techniques specifically used in this project, pharmacological interventions and the contribution of nitric oxide will be touched upon, but will be covered in greater depth later in the chapter.

1.4.2 Research in the generation of seizures

The first known written accounts of the symptoms and causes of seizures and epilepsy were produced by the ancient Babylonians around 1000 BC. Hippocrates recommended a diet based method for controlling seizures that could be thought to anticipate the ketogenic diet, developed in the 1920s and still widely recommended for controlling epilepsy today (Kim & Rho, 2008). Epilepsy was referred to as ‘falling sickness’ during the middle ages and no significant developments in either treating

or understanding the disease were made through the renaissance or enlightenment. It was as late as the mid-19th century until significant progress was made, with the English physician John Hughlings Jackson building a platform for future research, accurately attributing seizures to the hypersynchronous firing of collections of neurons (Jackson, 1890).

Based on clinical and electroencephalographic (EEG) evidence, Penfield and Jasper (1954) contributed a conceptual model for brain mechanisms responsible for seizures. Partial and generalised seizures were considered the consequence of discrete cortical abnormalities in the cortex and subcortical structures (with diffuse projections to the forebrain responsible for the generalised nature of EEG abnormalities). In this conceptual model, secondarily generalised seizures were understood to be caused by the spread of paroxysmal activity from the cortex to deeper structures. Experimental models reproducing both motor convulsions and epileptiform EEG activity were developed to study the roles of different brain structures and anatomic pathways in the development and spread of epileptic activity (Dichter & Ayala, 1987).

In the late 50's and early 60's, pioneering methods for extracellular and intracellular and recording, first described by Brock et al (1951) began to be used routinely to elucidate mechanisms underlying both intrinsic neuronal excitability and synaptic function. This provided the platform for epilepsy research focussed at the cellular level. The most widely used in vivo models for seizure research in this era, such as the topical application of penicillin (Greenwood et al, 1983) modelled acute or

chronic focal epilepsies, offering the opportunity to investigate the contribution of individual neurons and synaptic function to ictogenesis and regional epileptiform activity (Dichter & Ayala, 1987).

The paroxysmal depolarisation shift (PDS) was first described by Greenwood et al (1983). A PDS consists of a giant EPSP, enhanced by the activation of voltage-regulated intrinsic currents (Johnstone & Brown, 1981; Timofeev et al, 2004). PDS occur in neurons in chronic epileptiform foci, with spontaneous long (100-200 μs) and high (10-15 mV) depolarisations, representing the cellular manifestation of epileptiform spikes recorded from the scalp EEG (Heinemann et al, 1999; Rogawski & Loscher, 2004). Contributors to enhanced EPSPs include both synaptically mediated (Disinhibition, frequency potentiation, changes in the density and morphology of dendritic spines, activation of NMDA receptors and potentiation by neuromodulators) and intrinsic mechanisms (high-threshold Ca^{2+} and slowly inactivating Na^{+} currents) (Dichter & Ayala, 1987).

A seizure (or ictus) requires not only the hyperexcitability of neurons, but also the hypersynchrony of neural circuits. Mechanisms responsible for synchronising neural circuits also include both synaptic and non-synaptic processes. The connectivity of networks can play a major role in synchronizing excitatory activity (McCormick & Contreras, 2001). In the healthy brain, different regions have different densities of recurrent connections, underlying different propensities to fire in synchrony. The dentate granule cells have relatively low numbers of interconnections, while the pyramidal cells of the CA3 region are highly interconnected, acting as a local

pacemaker and making the region particularly susceptible to becoming a focus of epileptiform activity under aberrant conditions (Colom & Saggau, 1994).

Other processes that encourage synchronous firing include ephaptic interactions between neurons due to large currents that flow through extracellular spaces and changes in extracellular ionic concentrations (Jeffreys, 1995) and the diffuse synaptic connections of inhibitory interneurons, which allow excitatory neurons to 'fire' synchronously mediated by the release of inhbibition (Von Krosigk et al, 1993; Pinault et al, 1998) Neuromodulators, such as ACh can also alter the spike thresholds for populations of neurons synchronously. A role for astrocyte-neuronal signalling in mediating both the excitability of neurons and the synchrony of neural circuits is also becoming increasingly clear. Astrocytes modulate the extracellular ionic balance, regulate extracellular glutamate concentrations and release gliotransmitters that bind to receptors at both synaptic and extrasynaptic sites, modulating the electrophysiological properties of neurons (Fellin & Haydon, 2005).

1.4.3 Interictal epileptiform discharges

The term 'interictal spike' is the widely-used name for what may be more appropriately described as a non-ictal epileptiform spike or sharp wave in the EEG trace. The term was initially used to describe the shape of EEG activity recorded from epilepsy patients and was therefore observed between ictal events; however, it is now recognized that it is an important predictive phenomena, prior to the first

seizure (Williams et al, 2006). The term ‘spike’ is inappropriate both because it causes confusion with the ‘spike’ referring to AP’s in individual neurons and because epileptiform events also include sharp-waves. Although lacking in accuracy, the wide use of the term ‘interictal’ means that improving the terminology is likely to cause more confusion than it clears up. In this work, the term ‘interictal epileptiform discharge’ (IED) is used to refer to both spikes and sharp waves.

IEDs are high-amplitude (50 mV), EEG transients, including both ‘spikes’ (< 50ms) and ‘sharp waves’ (50 – 200ms) habitually followed by a slow wave that lasts several hundreds of milliseconds. IEDs recur periodically and may cluster in brief paroxysms that can remain local or spread as a result of the involvement of subcortical structures. Underlying an IED is a focussed PDS contained spatially and temporally by a large after hyperpolarisation (AHP) (Ayala et al, 1973) caused by GABA-mediated opening of Cl^- and K^+ channels (Kaila, 1994), voltage-sensitive K^+ channels and Ca^{2+}-sensitive K^+ and Cl^- channels (Sah & Louise-Faber, 2002). The relative contribution of each of these mechanisms depends heavily on the specifics of the cell involved and dictates the dynamics on neuronal activity. Although the relationship between IED and ictal events is not entirely clear, the relative strength of the AHP may be an important difference between the two phenomena.

While it was previously assumed that a seizure developed from an IED (Ralston, 1958), more recent research has revealed that the two phenomena but are characterised by different EEG patterns are are, in part mediated by different neuronal mechanisms. The causal relationship between IEDs and seizures is far

from clear (Gotman, 1991; Janszky et al, 2001). Katz et al (1991) demonstrated a decrease in IED activity prior to seizures, while numerous studies have suggested that IED activity actually inhibits seizures (Engel & Ackermann, 1980; Barbarosie & Avoli, 1997). There is certainly a causal relationship in the reverse direction. IED activity is consistenly observed post seizure, with the focus diffusing away from the seizure focus with increasing time intervals (Kaibara & Blume, 1988; Gotman & Koffler, 1990).

1.4.4 Temporal lobe epilepsy – overview of disease progression

TLE is an acquired epilepsy, associated with a distinct pattern of neurological damage in the hippocampal formation. The association between the clinical features of TLE such progressive susceptability to complex-partial seizures and the underlying anatomical changes, such as neuronal cell loss and gliosis in the dentate hilus and the CA3 and CA1 regions of the hippocampus has been recognised for many years (Cazauvieilh, 1825). Following a seizure, or other IPI, a symptomless 'latent' phase precedes the emergence of spontaneous reccurent seizures (SRS) characterising chronic epilepsy; a process referred to as epileptogenesis. The disease often then continues to progress beyond the point of diagnosis (Pitkanen & Sutula, 2002). The dominant theory is that of a circular causality between seizures and anatomical changes, with seizure activity causing neuronal death in the hippocampus and this cell loss in turn, reducing the threshold for paroxysmal activity: 'seizures beget seizures' (Gowers, 1881). While there is a great deal of experimental

evidence to support the first part of this (Cavazos & Sutula, 1990; 1994), evidence that the loss of neurons exacerbates seizures is inconclusive (Sills, 2007).

Seizures, or other IPI initiate an inflammatory response mediated by glial cells and pro-inflammatory cytokines. This inflammatory response, if sufficiently severe and of sufficient duration initiates a series of anatomical and physiological changes, including neuroinflammation (Vezzani & Granata, 2005), fibrillary gliosis, aberrant axonal sprouting (Buckmaster & Dudek, 1997; Sloviter, 1999), reactive synaptogenesis (Mori et al, 1998), dispersion of the dentate granule cell layer (Houser, 1990), the altered expression of neurotransmitters and their receptors (Koyama & Ikegaya, 2005) and a highly selective pattern of neuronal cell death (Buckmaster & Dudek, 1997). These changes underly an alteration in neuronal excitibility and network dynamics, including intricate structural changes, reducing the seizure threshold and preceding the emergence of chronic epilepsy. (Pitkanen & Lukasiuk, 2011).

Because of the high level of interconnectivity between principal neurons, the hippocampus is particularly susceptable to becoming a focus for ictal activity. The CA3 region is extremely dense in associational and collaterall fibres, consequentially firing with a high level of synchrony and is believed to function as a ‘pacemaker’ for physiological activity in the hippocampus (Dragoi & Buszaki, 2006). The same anatomical features make the region susceptable to peturbations in neuronal excitibility, the balance between excitatory and inhibitory drive and to alterations in network dynamics, with relatively small changes sufficient to elicit pathophysiological

hypersynchronised, epileptiform neuronal firing (Colom & Saggau, 1994). Following an IPI, neurons in the hippocampal formation have varying degrees of susceptability to neurodegeneration. Principal cells in the CA3 and CA1 regions of the hippocampus and dentage granule cells of the dentate gyrus, as well as populations of inhibitory interneurons are susceptable to loss, whereas neurons in CA2 are highly resistant.

1.4.5 Gliosis and the inflammatory response

1.4.5.1 Overview

Inflammation is a homeostatic mechanism induced by innate immunity mechanisms in response to infection or injury in order to remove the pathogens and promote tissue repair (Vezzani et al, 2008). Under specific circumstances, such as allergies and auto-immune diseases, inflammation contributes to tissue damage, cellular dysfunction and apoptosis. While the CNS has traditionally been considered an ‘immuno-privileged’ site, shielded from systemic immune responses by the BBB (Vezzani et al 2012), it is becoming increasingly clear that inflammatory responses, mediated by glial cells, play an important role in the development of a broad range of CNS disorders, including epilepsy (Vezzani et al 2010). Evidence from clinical and experimental studies indicate that brain inflammation is an intrinsic feature of the

hyperexcitable pathologic brain tissue in a broad range of pharmacoresistant epilepsies, with a variety of causes (Vezzani et al, 2011).

The role of inflammatory processes in the CNS was first observed in patients with Rasmussen encephalitis (Rasmussen et al, 1958). Chronic brain inflammation involves the activation of astrocytes, microglia, endothelial cells of the BBB, peripheral immune cells, and the concomitant production of inflammatory mediators (McGeer & McGeer, 1995). In experimental models of TLE, the increased expression of pro-inflammatory cytokines initially occurs in neurons undergoing excitotoxic stress. Cytokine signalling induces the rapid hypertrophic and hyperplastic changes and migration to the site of insult of both astrocytes and microglia (Shapiro et al., 2008) where they form a 'glial scar'. Reactive glial cells amplify cytokine signalling (Mrak & Griffin, 2005), have a direct effect on abnormal neurotransmission and neurodegeneration preceding the emergence of paroxysmal discharges.

Gliosis, the extensive proliferation of glia that occurs near or at the site of lesion, constitutes a pathological hallmark of damaged CNS tissue. The glial scar is not only formed by reactive astrocytes and microglia, but also complemented by the involvement of endothelial cells, fibroblasts and exracellular matrix factors. Experimental studies have shown that seizure activity *per se* can induce brain inflammation and gliosis and that recurrent seizures perpetuate chronic inflammation (Vezzani et al, 2010). Inflammation and gliosis also contributes to an increase in BBB permeability (De Vries et al, 1997), degeneration of neurons (Glass et al, 2010) and the direct modulation of synaptic transmission.

The activation of glia and cytokine signalling are mutually reinforcing phenomena which can contribute to either neuronal cell death or neuroprotection and can either exacerbate or subdue the development of chronic epilepsy (Vezzani et al, 2008). The manner in which gliosis might influence the neuropathological condition is determined by the congruence of specific factors, such as severity, duration, time after insult, damage location, and the specifics of inter- and intra-cellular signalling (Foresti et al, 2011). These factors are determined by the severity of the primary tissue insult and genetic and epigenetic factors. Evidence has shown that subconvulsive doses of KA can protect against the damage of a subsequent convulsive dose of KA (Kelly & McIntyre, 1994), while other kindling regimens can have the opposite effect. This testifies to the dichotomous, intensity-dependent nature of the inflammatory response.

1.4.5.2 Role of microglia in neuroinflammatory response

Microglia are derived from immune cell lines (Del-Rio Hortega, 1932) and are effectively specialist macrophages that function as immune cells in the CNS (Nimmerjahn et al, 2005), forming the front line defence of the innate immune system (Glass et al, 2010). There are very few CNS pathologies in which a major role for microglia has not been proposed (Perry et al, 1993). Resident microglial cells in the healthy brain rest in a dormant state, characterised by a stellate shape, with numerous thin and highly ramified processes reaching out into the parenchyma.

Microglia are distributed in a highly organised manner, with fairly homogenous distances between cells and each cell responsible for a territorial domain of consistent size (Nimmerjahn et al, 2005). The morphology and distribution of microglia in the CNS is well adapted for the efficient surveillance of the paranchyma, allowing for the detection of foreign bodies, cell injury or infection (Kreutzberg, 1996).

Microglia are activated in response to cell stress, such as excitotoxicity, largely through the detection of inflammatory cytokines and chemokines (von Zahn et al, 1997) and through ATP-signalling (Davalos et al, 2005). Activation of microglia involves a profound morphological change, with the withdrawal of appendages and a switch to a rod-like morphology. Activated microglia migrate to the site of injury (Nimmerjahn et al, 2005) where they can play a role in a variety of processes of importance to epileptogenesis, including the amplification of inflammatory effects or the induction of neuronal degeneration.

1.4.5.3 Role of astrocytes in neuroinflammatory response

Astrocytes outnumber neurons in the CNS by a ratio of approximately 10:1 and play many roles in support of the normal functioning of neuronal assemblies. Traditionally, astrocytes have been viewed simply as the ‘glue’, providing a physical scaffold in order to hold neurons in place (Volterra & Meldolesi, 2005). In time, an increasingly broad palette of physiological functions for astrocytes have been ascribed, including the maintenance of ionic balance in the extracellular space, the provision of

metabolic support for neurons and the taking up of extracellular glutamate. They have, however, still been viewed primarily in a housekeeping, support role; ‘enablers’ of neuronal signalling, without a direct role in information processing. Evidence for the extent of astrocyte-astrocyte and astrocyte-neuronal communication, however, including the expression of receptors, the release of gliotransmitters and the ability for fast communication through gap junctions has led to a reappraisal of basic concepts and the growing inclusion of astrocytes in our understanding of information processing in the CNS (Volterra & Meldolesi, 2005).

Besides their important role in normal physiological function, astrocytes are heavily involved in mediating responses to pathology. The activation of astrocytes is implicated in almost all pathologies of the CNS including TLE, where they act in tandem with microglia to mediate inflammation (Vezzani, 2008). Astrogliosis initially involves reversible changes in astrocytic gene expression profiles, including the upregulation of intermediate filament proteins such as glial fibrillary acidic protein (GFAP), vimentin, and nestin, followed by hypertrophic and hyperplastic changes (Ravizza et al, 2008; Borges et al, 2006). Finally, proliferation and migration of astrocytes to the site of insult, in tandem with other cell types, the rearrangement of tissue structure and the deposition of dense collagenous extracellular matrix leads to the formation of a glial scar.

Many functions of reactive astrocytes are likely to be important in determining the tissue response to seizures. Steele & Robinson (2012) suggest a loss of function phenomena, where activated astrocytes have a reduced ability to perform their

supporting role, meaning a decreased uptake of glutamate and a greater exposure of neurons to excitotoxicity. Reactive astrocytes also have a gain of function effect, with the release of factors encouraging neuronal apoptosis (Haneka et al, 2010), the direct modulation of the electrochemical properties of neurons through the release of gliotransmitters, both at the synapse and at extrasynaptic sites and their role in mediating the permeability of the BBB (De Vries et al, 1997) and the release of both pro- and anti-inflammatory factors (Haneka et al, 2009). The net effect of the complex contribution of astrocytes to epileptogenesis is not well understood, however, it is likely that it is dependent on the severity and duration of the inflammatory response.

1.4.5.4 Role of inflammatory cytokines

While it was previously assumed that cytokines were involved only in modulating inflammation in response to pathology, the constitutive expression in the brain of a wide variety of cytokines and their receptors suggests they may contribute to normal physiological functions of the CNS (Lucas et al, 2006). Many Inflammatory cytokines, notably IL-1β and TNF-α, have been shown to play a role in CNS development (Stolp, 2012) and in neuronal function through the modulation of synaptic plasticity, neural transmission and Ca^{2+} signalling (Vitkovic et al, 2000). This indicates that increased expression of these signalling molecules in response to pathology is likely to have a direct effect on the behaviour of neural assemblies, independently of the role of cytokines in promoting or subduing inflammation.

A range of different brain insults can induce an increased transcription of cytokines and cytokine receptors, including traumatic brain injury, pathogens and seizures. Following a period of status epilepticus, the expression of both cytokine and cytokine receptors increases in response to excitotoxic stress. While astrocytes and microglia provide the major source of cytokines following seizures (Vezzani et al, 2008), an increased expression is also seen in neurons and endothelial cells. Seizures trigger a rapid-onset inflammatory response in glia, consisting of an increase in prototypical pro-inflammatory cytokines, such as lnterleukin-1β 1 (IL-1β), IL-6 and tumour necrosis factor –α (TNF-α) (Vezzani et al, 2008) while the IL-1 receptor is expressed at greatly increased levels in neurons (Ravizza et al., 2006).

While IL-1β, IL-6 and TNF-α are all expressed at elevated levels in epileptic tissue, the role they play in promoting or subduing epileptogenesis is not entirely clear. The role that IL-1β plays may be dependent on concentration and the specifics of the tissue microenvironment that are currently insufficiently understood. IL-1β signalling functions with the IL-1R and the endogenous antagonist IL-1Ra which are also upregulated during seizures. Evidence for a proconvulsive role of IL-1b is compelling, but it has also been shown to have anticonvulsive properties. In a rodent amygdala kindling model of epilepsy, fully kindled seizures are inhibited by IL-1b, and daily injection of IL-1b during kindling slows the rate of kindling (Lucas et al, 2006). The ratio between IL-1β and IL-1Ra is more important than IL-1β levels per se, and the location of IL-1R expression is important in mediating the outcome. While the role of IL-6 in the brain is fairly straightforwardly neurotoxic and pro-convulsive

(Li et al, 2011), the role of TNF-α is more complex. There is strong evidence indicating a dichotomous role for this cytokie, dependent on downstream signals and concentration (Li et al, 2011). Generally, high concentrations of TNF-α are pro-convulsive, while lower concentrations inhibit seizures.

In addition, overexpression of inflammatory cytokines can have long-term effects on brain excitability by inducing structural and functional changes in glial and neuronal networks. For example, IL-1β can activate mitogen-activated protein kinases (MAPK) and nuclear factor-κB (NF-κB) - dependent pathways. The resultant transcription of genes can lead to the modification of ion channels and contribute to long-term hyperexcitability and epileptogenesis (Bialer & White, 2010).

1.4.5.5 The blood-brain barrier and peripheral mediators

The BBB acts as a filter, functioning to maintain the integrity of the CNS and restrict access from systemic proteins, antibodies, immune cells and inflammatory mediators. As already discussed, following an insult, such as a seizure, the resultant neuroinflammatory response, cytokine signalling and glial cell activity can lead to an increase in BBB permeability and an influx of systemic immune cells such as macrophages and leukocytes into the brain paranchyma, exacerbating the neuroinflammatory response. The influx of immunoglobulin G and albumin into the brain paranchyma through a compromised BBB can also exacerbate the immune response. Serum albumin, when taken up, can impair astrocyte function and lead to

a decrease in their ability to clear extracellular glutamate and regulate extracellular ion homeostasis (Ralay Ranaivo & Wainwright, 2010).

1.4.6 Structural changes following seizures

Epileptiform firing is not just dependent on the excitibility of neurons, but also on the specifics of the interconnectivity between neurons. As already discussed, the CA3 region of the hippocampus has a high level of interconnectivity, while the dentate granule cells have a relatively sparse interconnectivity, allowing this region to act like a ‘filter’ for synchronised activity. Following seizures, the structure of neuronal networks in the hippocampal formation can be altered to increase the possibility of seizures.

The loss of principal cells in the CA3 region of the hippocampus removes the target for the axons of dentate granule cells, leading to the aberrant connections between these cells. Following neuonal cell loss in CA3, synapses form between dentate granule cells in the molecular layer of the dentate gyrus. This increased interconnectivity between dentate granule cells decreases the efficiency of the filter mechanism and leads to an increased susceptability to seizures. Following seizures in human patients, mossy fibres, the axons of dentate granule cells that form synapses in the hilus and on CA3 pyramidal cells in stratum lucidum, ‘sprout’ and form aberrant connections, notable in the molecular layer of the dentate gyrus (Sutula et al, 1989; Houser, 1990).

1.5 Reseach methods – Historical overview

1.5.1 Summary

Here, a brief historical perspective of the development of the methods used in this project is presented, including animal models of seizure and epilepsy with a particular focus on KA.

1.5.2 Models of seizure and epilepsy

1.5.2.1 Overview

In order to understand epilepsy and find new treatments, model systems must be employed. For this purpose, the use of animal models has disclosed much of what has been learnt about epilepsy and seizures. There are many rodent models of epilepsy, using both Rats and Mice. The variety of models stems from the lack of reliability with which any particular model faithfully recreates the syndrome observed in humans. Important findings are best replicated between models in order to increase reliability. Further, the sheer breadth of different epilepsy symptoms necessitates a similar variation in animal models (Fisher, 1989).

Models of seizures and epilepsy include both genetic models, where susceptabiliity to seizures has either been selected for during breeding, or specific genes are overexpressed or knocked out (Mita et al, 2001) and the induction of seizures in normal animals (Ben-Ari & Cossart, 2000). Genetic models can be further divided into animals showing spontaneously seizures (Sarkisova & van Luijtelaar, 2011) and those susceptable to seizures induced by a cue (i.e animals sensitive to audiogenic or photogenic seizures) under the control of an experimenter (Meldrum, 1984). Seizures can be induced in normal animals either electrically or chemically and either by directly inducing a seizure (Ben-Ari & Cossart, 2000), or by 'kindling'; the process of giving multiple subconvulsive electrical stimulations or chemical doses until a spontaneous convulsion occurs (Lothman et al, 1985).

Sarkisian (2001) lists six criteria by which the value of an animal model can be judged: 1. Similar electrophysiological patterns observed to human condition. 2. Similar etiology- human condition arising from underlying genetic predisposition should be modelled genetically, etc. 3. Animal model should reflect human condition in age of onset. 4. Animal model should replicate specific pathological changes observed in human conditions. 5. Animal model should respond to AEDs in similar way to human condition. 6. Behavioural characteristics should reflect those seen in human condition. Some animal models are used to investigate the generation of acute seizures, while others are used to investigate the development of chronic epilepsy. By either the induction of an IPI (usually a period of status epilepticus) or by electrical or chemical kindling, a chronically epileptic animal can be produced, acting as a model of temporal lobe epilepsy (Loescher, 2011).

1.5.2.2 Models of acute seizure

Models of acute seizure are widely used to explore the neurophysiological mechanisms underlying the generation of seizures. A popular model of simple partial seizures is the topical application of penicillin (Fisher, 1989). By placing electrodes close to the site of application, and applying other pharmacological agents, information regarding neuronal process during seizure generation can be obtained. Other chemical convusants, such as bicucculine, picrotoxin and strychnine are also used in a similar way. Simple partial seizures can also be induced electrically by directly stimulating cortical tissue (Adrian, 1936) with electrical pulses through ball electrodes cortex. Infusion of GABA via micro-syringe can also induce seizure activity upon removal (Brailowsky et al, 1987).

Models of acute seizures can also be used for assaying the efficacy of antiepileptic drugs. In the maximal electroshock test (MES), transcorneal or transauricular applications of suprathreshold electrical stimuli are given to normal mice or rats and the latency to hindlimb extension is recorded (Loescher, 2011). An alternative test is the administration of Pentylenetrazole (PTZ), in which the latency from drug treatment to seizure is recorded (Krall et al, 1978). The timepoint at which 97% of animals have undergone a tonic-clonic seizure of at least 5 seconds duration is the usual measure used. Other popular models of complex partial seizures include injections of pilocarpine, tetanus toxin or KA.

1.5.2.3 Diversity of in vivo epilepsy models

Following the guidelines for animal models articulated by Sarkisian (2001), many preparations exist for modelling specific syndromes. Some of these include infant febrile seizures can be modelled by exposing neonatal rats and mice to hyperthermic shock (Baram et al, 1997), exposure of neonates to global hypoxia as a model for perinatal hypoxic encephalopathy (Ohshima et al, 2012), childhood absence seizures, modelled using mutant mice, susceptable to spontaneous seizures which largely mimic the features of petit mal events (Puranam & McNamara, 1999) and epileptogenesis associated with a traumatic brain injury IPI, modelled in rodents using a controlled cortical impact or fluid percussion injury (Bolkvadze & Pitkanen, 2012).

1.5.2.4 Models of temporal lobe epilepsy

Models of TLE usually involve either the induction of an IPI, or kindling. Unless the research is concerned with seizures resulting from a particular type of insult, such as anoxic shock or traumatic brain injury (Kharatishvili et al, 2006), the IPI is usually a period of chemically or electrically induced SE. The most common chemical agents used to model TLE in rodents is pilocarpine, a cholinergic agonist, and KA (Sarkasian, 2001).

Kindling is a process by which the duration and behavioural involvement of induced seizures increases after seizures are induced repeatedly until a plateau is reached and so repeated stimulation lowers the threshold for more seizures to occur (Racine, 1972). Kindling is usually carried out by focal electrical stimulation in the brain. The term ‘seizures beget seizures’ is often used to study this phenomenon, whereby a seizure may increase the likelihood that more seizures will occur. In the kindling model, seizures begin to occur spontaneously after repeated subconvulsive stimuli leading to self-sustaining status epilepticus (SSSE). However, the relevance of the kindling model in animals compared to epileptogenesis in humans is still widely debated and although there are a number of well-described anatomical changes associated with kindling (glial activation, decreased neuronal density, mossy fiber sprouting), the changes are much less pronounced and widespread than those seen in epilepsy in humans (Cavazos and Sutula, 1990).

1.5.3 Kainic acid models

KA, an excitatory amino acid and an analog of the endogenous excitatory neurotransmitter, glutamate (McGeer et al, 1978) naturally occurs in the seaweed, *Digenea simplex*, or red seabroom. The purplish-red plant from the family *Rhodomelaceae* has a wide global distribution and is typically found in coastal areas, growing on rocks at depths of around 1.5 – 7 metres, where it has traditionally been harvested by divers and sold for use as an anthelmic, particularly in Japan. It was in Japan that KA was first extracted from *D. simplex* (Murakami et al, 1953), its structure described (Nitta et al, 1958) and its excitotoxic effects on the mammalian

central nervous system (CNS) discovered. Twenty years later, two studies (Ben-Ari et al, 1978; Nadler et al, 1978) independently showed that intraamygdaloid or intraventricular injections of KA respectively, could induce repetitive seizures and a pattern of neuronal damage reminiscent of that associated with TLE in humans.

Following the discoveries in 1978, KA has been widely used to induce seizures, particularly in rodents, providing useful models for both acute seizures and TLE. Local or systemic injections of kainate first activate CA3 pyramidal neurons via high-affinity receptors present in mossy fiber synapses. The activation of CA3 recurrent collateral synapses generates synchronized network-driven glutamatergic currents that propagate to other hippocampal regions (Ben-Ari & Cossart, 2000). Grabenstatter et al (2005) describe three major stages for a KA-induced SE model of epilepsy: 1. A period of SE, typically lasting several hours, 2. A seizure free latent period, typically lasting several days or weeks and 3. the gradual emergence and progressive increase in the frequency of spontaneous recurrent seizures (SRS).

For both ethical and scientific reasons it is often common practice to administer diazepam after inducing seizures with KA to reduce mortality and SE. Terminating SE with diazepam can allow for the experimental control over the duration of the insult, decreasing variability between animals. Diazepam and related compounds are routinely used in the treatment of epilepsy and are members of the benzodiazepine family (see section 1.6 of this chapter). The mechanism of action is via the potentiation of inhibitory drive via gamma-aminobutyric acid (GABA).

1.6 Pharmacological interventions in epilepsy

1.6.1 Overview

Because our understanding of the complex processes underlying the generation of both individual seizures and epileptogenesis is currently limited (Engel Jr, J, 2008), available treatments largely tackle the symptoms rather than underlying causes. Pharmacological agents that increase the threshold for seizures invariably have significant side-effects on normal brain activity, contributing to mood and cognitive disorders (Martin et al, 1999). Conditions that are well controlled often become refractory to treatment, while even when a treatment programme is effective, the reason for the success is often unclear. Antiepileptic drugs (AEDs) typically target ion channels, neurotransmitter transporters, neurotransmitter metabolic enzymes, modulate voltage-gated ion channels, enhance synaptic inhibition or inhibit synaptic excitation.

Continued development of AEDs is driven by two main goals: the need to develop drugs for use in patients refractory to currently available pharmacological treatment and the development of drugs with better side-effects and pharmacokinetic profiles than currently available AEDs (Walker & Sander, 1996). Alternatives, or

complements to pharmacological intervention include the adoption of a ketogenic diet, implantable electroshock devices or the surgical removal of parts of the brain. although there is little understanding of how the ketogenic is effective.

1.6.2 Phenobarbitol

Following on from the use of bromide salts, which were the first drugs to legitimately claim success in seizure suppression (Tunnicliff, 1996), barbiturates, such as Phenobarbitol (PB) became popular treatments for grand mal epilepsy. The big drawback of this type of therapy is the pronounced ancillary sedative actions (Tunnicliff, 1996). It is mainly used in the clinic in emergencies for the control of SE rather than the control of chronic epilepsy conditions. PB, like all barbiturates is a GABA agonist, with a high affinity for the $GABA_A$ receptor. The binding site is distinct from the binding site of GABA itself and from the benzodiazepine binding site. Although Barbiturates can halt seizures, they are not suitable for chronic control of epilepsy because of their general somnolescent effect and the strong danger of overdose

1.6.3 Diazepam

Diazepam and other benzodiazapines are also GABA agonists and enhance inhibitory drive by binding to the $GABA_A$ receptor at a different site from barbiturates. They have largely replaced barbiturates because they are safer drugs with less risk of dangerous overdose. Like phenobarbitol, Diazepam is often administered in in the clinic to halt SE in emergency situations, rather than to control chronic epilepsy.

1.6.4 Phenytion

Phenytoin, 5,5-diphenylhydantoin has been shown to be non-specific for sodium channels: it antagonises calcium dependent action potentials, calcium currents and calcium fluxes, delays or reduces voltage gated K^+ currents and augments post-synaptic responses to GABA (Lees & Leach, 1993). The introduction of phenytoin was important because it was the first effective anticonvulsant not to possess significant sedative side effects (Tunnicliff, 1996). Despite the large numbers of AEDs subsequently developed, Phenytoin is still widely used to control all epilepsy types other than absence seizures. It can also be used as emergency treatment to halt SE.

1.6.5 Carbamazepine

Carbamazapine (CBZ) is a tricyclic iminostilbene derivative related structurally to the antidepressant imipramine (Marangos et al, 1983). The primary mechanism of action of CBZ is the blocking of voltage-gated Na+ channels and the subsequent decreased Na+ influx into neurons (Willow et al, 1985), however, it also has other effects in the CNS, including interactions with adenosine receptors (Marangos et al, 1983). While it can subdue secondarily generalized seizures, CBZ can exacerbate the symptoms of absence epilepsy. It has a short half-life and therefore must be administered regularly (4 times daily) or administered in a controlled release formulation (Bonneto et al, 1993).

1.6.6 Oxcarbazepine

Oxcarbazepine (OXC) is an analog of CBZ, but with a much less complex pharmacokinetic profile (Kalis & Huff, 2001). The mechanism of action is similar to that of CBZ, however, the blocking of Na^+ channels occurs at much lower

concentrations (McLean, 2002) and there is a variation between the two drugs in their affinities for L-, N-, P-, R- and T-type Ca^{2+} channels (Schmidt & Elger, 2004). OXC can be more effectively combined with other AEDs than can CBZ and because of the difference in the way the drug is metabolised, OXC is associated with less adverse side effects.

1.6.7 Felbamate

Felbamate (FBM), 2-phenyl-1,3-propanediol dicarbamate is an orally active compound that exhibits anticonvulsant and neuroprotective properties (Faught et al, 1992). Its mechanism of action is poorly understood, however, it seems to function both by enhancing GABAergic transmission and inhibiting the excitatory effects of aspartate (Rho et al, 1994). Because it has severe side effect in the liver and bone marrow, FBM is used as a therapy of last resort for patients exhibiting refractory partial epilepsy and to control the severe Lennox-Gestaut syndrome. FBM is more commonly used as a monotherapy, because of the side effects related to its interaction with other AEDs, such as vomiting, insomnia, nausea and headache (Leppik et al, 1991). Side effects are particularly severe when FBM is combined with CBZ.

1.6.8 Gabapentin

Gabapentin (GBP), 1-(aminoethyl)cyclohexaneactic acid, is widely used as an adjunctive therapy for refractory partial epilepsy (Heilbroner & Devinsky, 1997). Although it has structural similarities with GABA, it is not believed to function as a GABA agonist. Its mechanism of action is not fully understood, however it is believed that it plays a role in modulating the metabolism of GABA as well as excitatory amino

acids in the CNS (Errante et al, 2003). GBP is an effective treatment against partial and secondarily generalized seizures in many patients, however, it is ineffective in generalized seizures and absence seizures. The use of GBP in epilepsy therapy is associated with a low incidence of serious adverse effects and, unlike many alternative therapeutic options, has not been associated with toxicity in the liver or bone marrow (Ojemann et al, 1992).

1.6.9 Lamotrigine

Lamotrigine (LTG), 3,5-diamino-6-(2,3-dichlorophenyl)-1,2,4-triazine, is chemically unrelated to other AEDs, but has a pharmacological profile similar to phenytoin and CBZ (Leach et al, 1991). LTG acts by perturbing voltage-gated cation channels, with a higher affinity for Na^+ channels than Ca^{2+} channels (Lees & Leach, 1993). When used as a monotherapy, LTG has a similar efficacy as CBZ or phenetoin against partial and generalised tonic-clonic seizures, however, it is generally much better tolerated and associated with fewer adversive side-effects, such as asthenia, dizziness and somnolence (Kaminow et al, 2003). It is also not associated with the weight-gain seen in patients taking valproate (Biton et al, 2001). Lamotrigine is effective against both partial and generalised seizures.

1.6.10 Topiramate

Topiramate (2,3;4,5-bis-O-(1-methylidene)-beta-D-fractopyranose sulphamate) is a sulphamate-substituted monosaccharide (Walker & Sander, 1996). It has a complex mechanism of action with five separate actions at the cellular level reported, including inhibition of kainate evoked currents, enhancement of GABA-evoked currents, blockage of voltage-gated N^+ channels, blockage of voltage-gated Ca^{2+}

channels, and inhibition of carbonic anhydrase isoenzymes. It is used in as an adjunctive to monotherapy in patients with partial epilepsy who are refractory to other pharmacological treatment regimes (Bensalam & Fakhoury, 2003). The multiple mechanisms of action confer broad spectrum efficacy against different seizure types and make topiramate an attractive choice in the treatment of both partial and generalized status epilepticus (SE) (Bensalem Fakhoury, 2003).

1.6.11 Tiagabine

Tiagabine (TGB), (R)-N-[4,4-di-(3-methylthien-2-yl)but-3-enyl] nipecotic acid hydrochloride, is a GABA reuptake inhibitor (Giardina, 1994), which increases extracellular concentrations of GABA, increasing the seizure threshold (Fink-Jensen et al, 1992). TGB can be used to supplement treatments in patients aged over 12 suffering recurrent partial seizures with or without secondary generalization which cannot be satisfactorily controlled with other antiepileptic drugs (Schmidt et al, 2000). TGB is effective in conjunction with other AEDs, such as CBZ and LTG (McKee, 2004) and has limited adverse side effects, generally limited to the CNS.

1.6.12 Levetiracetam

Levetiracetam (LEV), (S)-α-ethyl-2-oxo-1-pyrrolidine acetamide is used as an adjunctive therapy for patients refractive to other therapeutic treatment regimes, suffering from partial seizures with or without secondary generalization (Betts et al, 2000). The mechanism of action of LEV is not well understood. Unlike the majority of AEDs, it does not appear to function through the mediation of GABAergic inhibition, or by acting at voltage-gated Na^{+} or T-type Ca^{2+} channels (Rigo et al, 2002). However, there is some evidence to support the idea that it works by mediating

intacellular Ca^{2+} concentrations through effects at ryanodine and IP3 receptors (Nagarkatti et al, 2008) and at ROMK1 channels via the modulation of phosphorylation by protein kinase A (Lee et al, 2008). Adverse side-effects of LEV have been shown to lead to much lower levels of treatment discontinuity than in TPM (Bootsma et al, 2008).

1.6.13 Valproic Acid

Valproic Acid or valproate (VPA) is the most commonly used AED in the treatment of generalised epilepsy and also used against partial epilepsy absence seizures and myoclonic seizures (Johannessen, 2000). VPA has a pleiotropic mechanism of action, with a combination of effects of the drug in the CNS mediating its anticonvulsant function (Price, 1989). Similarly to GBP, it has a simultaneous effect of upregulating GABA synthesis, whilst downregulating the synthesis of asparate (Johannsessen, 2000), but it can also inhibit high-frequency firing of neurons by blocking voltage-gated Na^{+} channels and act by decreasing the potentiation of excitatory transmission at the NMDA receptor (Griffith & Taylor, 1988). Adverse effects of VPA include weight gain (Gidal et al, 1996) and relatively mild cognitive deficits which are reversible upon removal of the drug (Gallassi et al, 1990).

1.6.14 Vigabatrin

Vigabatrin (VGB), γ-vinyl GABA, is a selective inhibitor of GABA transaminase, having the effect of decreasing the enzymatic breakdown of GABA and increasing brain concentrations of the inhibitory neurotransmitter. VGB can be used to control a range of epilepsy conditions, though it has been found to be most effective against partial seizures (Mumford & Dam, 1989). Because of the severe adversive side

effects associated with it, such as the destruction of peripheral vision (Sergott et al, 2010), it is used mainly as a therapy of last resort and is banned in several countries including the United States. It is however, a useful option, because of its unique mechanism of action, it can be effective where other, less aversive treatment regimens have failed.

1.7 Nitric oxide

1.7.1 History of Nitric oxide research

NO was first discovered by the English chemist, Joseph Priestly (1775) and described by him as ‘nitrous air’. The biological importance of NO is testified by its ubiquity across taxa and in the diversity of physiological functions in which it is involved. The ancient evolutionary heritage of nitric oxide synthase enzymes (NOS) suggest that control over its release conferred a strong advantage in early organisms (Kream & Stefano, 2009), but despite its importance, the biological role of the molecule was not recognized until the 1980s. Prior to this discovery, a molecule of unknown identity, referred to as Endothelial Derived Relaxation Factor (EDRF) (Furchgott & Zawadzki, 1980) was described in many reports, until Ignarro et al (1987) discovered that NO and EDRF were one and the same.

NO does not have the features of a typical signalling molecule. It is a free radical and a highly reactive oxidizing agent capable of causing damage to the cellular machinery; indeed, in the concentrations typically studied by chemists, it is highly poisonous (Priestly, 1775). As a gaseous molecule, it freely crosses lipid bilayers and has a very short half-life meaning that it can therefore not be stored in vesicles, but diffuses from the site of synthesis according to the laws of Brownian motion. NO does not conform to any of the features of signalling molecules studied prior to its discovery.

Following the discovery of this important, ubiquitous signalling molecule, however, a number of gaseous molecules sharing similar features have been discovered to play important roles in mediating physiological processes, including carbon monoxide (CO) (Kim et al, 2006) and Hydrogen sulphide (H2S) (Lefer, 2007). It is now becoming clear that, far from disqualifying NO from a role in cell signalling, the very features of gaseous molecules that make them appear so unsuitable must confer advantages, however, this is currently poorly understood.

1.7.2 Nitric oxide and Nitric oxide synthase

Because of its ability to cross lipid bilayers, NO cannot be stored in vesicles and diffuses from the point of synthesis as an active molecule. It is produced by the conversion of L-arginine to L-citrulline by NOS enzymes, which exist in three isoforms: neuronal (nNOS), expressed mainly in neurons; endothelial (eNOS), expressed mainly in endothelial cells and inducible (iNOS), expressed mainly in immune cells, or microglia in the CNS. The isoforms are alternatively referred to as NOS-1, NOS-2 and NOS-3, respectively. A fourth isoform, mitochondrial NOS (Bates et al, 1995) has also been reported, however, it is currently unclear whether this molecule represents a novel isoform, or is simply nNOS with post-translational modifications (Finocchietto et al, 2009) and will not be further discussed here.

nNOS and eNOS are expressed constitutively and are activated by the binding of two NOS monomers with two calmodulin (CaM) molecules to form a tetramer (Knowles & Moncada, 1994) in the presence of Ca^{2+}. In contrast, iNOS expression is induced in response to inflammation, under the control of the transcription factor NF-κB, is permanently tightly bound to CaM and, thereby, synthesizes NO in a Ca^{2+}-independent manner. Each isoform is encoded by a separate gene and, while showing high levels of homology in the catalytic domains greater variability is found in their membrane anchor points (Meyer & Andrew, 1998).

NO is an extremely simple molecule made up of a single nitrogen atom, with 5 electrons in the outer shell and a single oxygen atom with 6 valence electrons. The two atoms form the simplest, stable 'odd electron' molecule possible (Stamler et al, 1992), with the unpaired electron classifying NO as a free radical. NO is synthesised by NOS, in the presence of the co-factor nicotinamide diphosphonucleotide (NADPH) alongside L-cittruline, from the substrates L-arginine and molecular oxygen (0_2). NOS enzymes have a reductase domain at the C-terminal and an oxygenase domain at the N-terminal, with the reductase domain passing an electron via NADPH to the oxygenase domain of the opposing NOS molecule in the tetramer as shown in Figure 1.7.1.

Oxygenase domain: L-arginine + O_2 → N^{ω}-OH-L-arginine → L-citrulline + NO

Reductase domain: NADPH → $NADP^+ + H^+$

Figure 1.7.1 Reaction catalysed by activated nitric oxide synthase

1.7.3 Molecular targets of Nitric oxide

Because of the highly diffusible nature of NO, the nature of the target is probably more important for defining the physiological function of NO signalling than the origin of the signal). The ‘classical’ target for NO signalling is soluble Guanyl cyclase (sGC), an enzyme which catalyses the production of the secondary messanger, cyclic guanosine monophosphate (cGMP) (Ignarro et al., 1991). cGMP production via activated sGC activates a wide array of signalling pathways which can involve translocation to the nucleus and the modulation in gene expression.

Downstream effectors of cGMP include c-GMP-dependent protein kinase (PKG), which can activate AP-1 transcription factors, mitogen-activated protein (MAP) kinase p38 and p42/p44 extracellular signal -related kinase (Erk-1/2) (Lamas et al, 2007). cGMP signalling can also exert an effect on physiological function independently of gene expression. cGMP-regulated phosphodiesterases such as can modulate intracellular signalling pathways and and cyclic nucleotide-gated (CNG) cation channels (Denninger and Marletta, 1999) can modulate neurotransmission.

Beyond the classical signalling via sGC, NO is involved in cellular signalling in a bewilderingly diverse number of ways. NO can exert post-translational modification of proteins via S-nitrosylation, altering their physiological function in a similar way to the addition of a phosphate by kinases (Stamler et al, 1992). Wink & Mitchell (1998) list mechanisms by which NO can interact with molecules in the cell: Interactions with metal-containing substrates such as haemoglobin, interactions with high energy radicals, such as peroxynitrite, nitration of tyrosine residues to form nitrotyrosine, and oxidation.

1.7.4 Nitric oxide signalling in the central nervous system

NO was first reported to have a role in the central nervous system by Garthwaite, et al (1989) and has since been ascribed a broad range of functions, including the modulation of synaptic plasticity (Yang, et al, 2007) and cerebral blood flow (CBF) (Pereira de Vasconcelos, 2005). In the vertebrate central nervous system (CNS), NO is associated with many different behaviours, including learning and memory formation, feeding, sleeping and male and female reproductive behaviour, as well as in sensory and motor function (Garthwaite, 2008).

1.7.5 Nitric oxide in epilepsy

Using a broad range of models, general NOS antagonism has been shown to have a proconvulsive effect (Takei, 2001; Hagioka, 2005). Pereira de Vasconcelos, et al (2005) report a major role for eNOS in the modulation of local CBF during seizures and the restriction of this mechanism may account for the pro-convulsive effect of general NOS inhibition. Evidence for the role of nNOS in seizure generation is less clear, with questionable specificity of available drugs targeting nNOS, such as 7-nitroindazole (7NI) and 3-bromo-7-nitroindazole (3-Br-7NI) and conflicting reports on the extent of nNOS involvement in CBF regulation (Santizo, et al, 2000; Pereira de Vasconcelos, 2005). Recently, Kovacs, et al (2009) have reported an anticonvulsant affect of nNOS antagonism using an *in vitro* approach; however, this is yet to be replicated *in vivo*.

2. GENERAL MATERIALS AND METHODS

2.1 Animals

Experiments were performed in 10-12 week old male C57BL/6J mice. All animals were purchased from Charles River (UK) and maintained in the Biomedical Services Unit, University of Liverpool under controlled environmental conditions ($19^{o}C$ – $23^{o}C$, 12h light: 12h dark), with food and water available *ad libitum*. All experiments were carried out according to Animals (Scientific Procedures) Act 1986 approved by the Secretary of State, Home Office, UK and University's Ethical Review Committee.

2.2 Reagents

KA (Ascent, UK) was prepared in distilled water (DW) at concentrations of 5mg/ml and (apart from in the incremental dosing protocol, described in chapter 5), administered at a dose of 20mg/kg via intraperitoneal injection. An equivalent volume of DW alone was used as a vehicle control. Rabbit anti-c-Fos (1:2000) was purchased from Calbiochem (UK), mouse anti-NeuN (1:400) from Chemicon (UK), and rabbit anti-synaptophysin (1:1000) was a gift from Dr P Greengard, Rockefeller University, USA. Mouse anti-GFAP (1:400) and biotinylated tomato lectin (1:500) were purchased from Sigma Aldrich (UK), CY3-conjugated streptavidin (1:300), donkey anti-rabbit IgG - CY3/FITC (1:200) and donkey anti-mouse IgG - CY3/FITC (1:200) were all purchased from Jackson ImmunoResearch Laboratories, UK. All antibodies were prepared in a diluting solution (PBS, 0.1% Triton X-100, 2.5%

donkey serum and 0.25% sodium azide). Streptavidin conjugates were diluted in PBS alone.

2.3 Drug treatments

Following initial pilot studies in our laboratory, A dose of 20mg/kg was considered suitable for inducing convulsive motor seizures without leading to high levels of mortality. While there was considerable inter-batch variation in response to KA, responses were largely consistent within batches. Batches were initially screened and were rejected if the behavioural response was either subconvulsive or fatal. Following the injection with KA, mice were monitored and their behaviour scored for a two hour time period. At the two hour point, mice were either sacrificed for immunohistochemical analysis of early markers of excitotoxicity, such as c-Fos, or seizures were terminated with diazepam (10mg/kg, i.m).

2.4 Behavioural scoring

The induced period of SE was videotaped and scored blind in 5 minute epochs for 2h following KA administration, with the most severe behaviour in each five-minute epoch recorded using a modified Racine scale (Racine, 1972): Stage 1 – absence-like immobility, Stage 2 – hunching with facial or manual automatisms, Stage 3 - rearing with facial or manual automatisms, Stage 4 – rearing with forelimb clonus and falling, and Stage 5 – generalised clonic convulsions with loss of the righting reflex. Scores 1 to 2 were defined as non-convulsive seizures (NCS) and scores 3 to 5 as convulsive motor seizures (CMS) (Williams *et al.,* 2009). Mann-Whitney U tests

were performed to compare the maximum severity score between treatment and vehicle treated animals.

2.5 Tissue processing and immunohistochemical analysis

Mice employed for immunohistochemistry were sacrificed at 2h, 24h 72h, 7d or 14d timepoints after KA administration by overdose of pentobarbitone (60mg/kg, i.p.). Animals were fixed by trans-cardial perfusion with 0.1M phosphate buffered saline (PBS), followed by 4% paraformaldehyde in PBS (PBS-PFA). Brains were dissected immediately, post-fixed for 4h in 4% PBS-PFA, then cryopreserved in 20% sucrose in PBS and stored at 4^{o}C. Thereafter, brains were gelatin-embedded (15% porcine gelatin, 7.5% sucrose, 0.1% sodium azide in PBS), incubated for 3h at 38^{o}C and chilled overnight at 4^{o}C in Saran wrap to avoid desiccation. Tissue blocks were then mounted on 10 mm corks with optimum cutting temperature embedding medium (TissueTek, Qiagen, UK), rapidly frozen by immersion in liquid nitrogen-cooled isopentane, and stored at -80^{o}C prior to sectioning. Coronal sections (15µm) were cut on a cryostat (Leica, UK) at an ambient temperature of -20^{o}C and a block temperature of -23^{o}C, thaw-mounted sequentially onto chrome-alum-gelatin coated slides as described previously for rat (Cosgrave *et al.,* 2010), and stored at -20^{o}C prior to immunohistochemical analysis.

Brain sections were washed several times in PBS to remove traces of fixative. Non-specific binding sites were blocked with 10% donkey serum in PBS for 1h at room temperature. Double-staining was performed on brain sections from vehicle or L-

NPA treated and untreated animals simultaneously, using the same reagents and antibodies. All antibodies were prepared in a diluting solution (PBS, 0.1% Triton X-100, 2.5% donkey serum and 0.25% sodium azide). Sections were incubated at 4^{o}C overnight with primary antibodies. Primary antibody omission was used as a negative control, while other brain regions served as known positive controls (e.g. thalamic nuclei for c-Fos). After overnight incubation, sections were again washed in PBS before being incubated with appropriate secondary antibodies (CY3/FITC conjugated) for 1h at room temperature. Following further washes, sections that had been incubated with biotinylated anti-species were subsequently treated with streptavidin-FITC (1:80, Vector Laboratories, UK) for 1h, washed thoroughly in PBS, rinsed in DW and cover-slipped with Vectashield® (Vector Laboratories, UK).

2.6 Microscopy and cell counting

Immunostained brain sections representing three different cortical regions [septal (cranial/rostral), middle and temporal (caudal)] were used for cell counts as described previously (Cosgrave *et al.,* 2008, 2010). Sections were viewed using a Nikon inverted microscope (Eclipse TE2000, Nikon, UK), photographed (Hamamatsu C-4742-95) and handled using IPL software (Nikon, UK). All photographs were taken following a 2 second exposure. ImageJ software (Rasband, 1997-2011) was used to measure the counting area (mm^2) and performed blind cell counts. Bilateral counts were made from a minimum of three sections per animal, each representing a different cortical region (15 sections per treatment group). *NeuN* was used to mark neurons.

Microglia and astrocytes, stained with Biotinylated tomato lectin and GFAP respectively were counterstained with 4',6-diamidino-2-phenylindole (DAPI) and only those cells positive for either tomato lectin or GFAP and with a visible nucleus were counted. An Abercrombie correction was used (Abercrombie et al., 1946), based on the width of the mean of 20 randomly selected DAPI-stained nuclei in each section, with the formula: $P = A \times [M \div (L+M)]$, where P = corrected cell count, A = crude cell count, M = section thickness (µm) and L = average width of nuclei (µm). This correction allows for a closer approximation of the number of cells in a section, correcting for the overcounting bias caused by the counting of fractions of cells as whole cells. Synaptophysin immunoreactivity was analysed by measuring the mean intensity of a given area using ImageJ and normalizing against unstained regions. c-Fos^{+} cell counts were analysed using a Student's t-test, while synaptophysin and glial immunoreactivity were analysed using a one-way ANOVA with post-hoc tests.

2.7 Surgical procedure – transmitter implant

In each study, a number of mice were implanted with a telemetry device (Physiotel® transmitter TA10ETA-F20, 3.8 g, 1.75cc, Data Science International, Amsterdam, The Netherlands) for remote EEG recording. Pre-operative antibiotics (Baytril®, Bayer Health group, Germany, 5mg/kg, s.c) and buprenorphine (Vetergesic, Reckitt Benckiser Healthcare, UK, 0.3mg/kg, i.m) were administered prior to anaesthetisia with gaseous isoflourane. The surgical site was shaved and Videne® surgical scrub applied. Mice were placed on a sterile drape on a heating pad and surgery was performed in sterile conditions. An incision was made through the skin, muscle and connective tissue over the skull. Bilateral burr holes (0.7 mm) were drilled,

approximately 5 mm cranial to lambda and 2 mm lateral to midline over each hemisphere.

A subcutaneous pocket was created over the spine and flank, irrigated with sterile saline solution and the telemetry device inserted. Insulation was removed from the electrode tips, a 'V-shape' bend was made and inserted into the burr holes, in contact with the *dura mater*. Electrodes were secured using dental cement (Alphacryl Rapid Repair, National Dental Supplies, UK), taking care to insulate electrode terminals from surrounding tissues in order to eliminate signal interference. The incision was sutured using size 4.0 absorbable sutures and reinforced with Vetbond^{TM} Tissue adhesive (3M Animal Care Products, USA). Claws were trimmed to prevent scratching and removal of stitches. Animals were given soft food, and their eating, drinking, behaviour and bodyweight monitored for 10 days post-surgery. After post-operative recovery, animals were subjected to experiments, as described in the methods sections of individual research chapters.

2.8 EEG recording

EEG recording commenced 2h prior to the first drug treatment. In animals receiving a pre-treatment, this meant 2h 30m prior to the KA administration. Recording continued for 7 days throughout SE and the subsequent early epileptogenic phase. Data was transmitted to a RPC-1 receiver pad (Data Science International, Amsterdam, The Netherlands) placed under each cage, forwarded to a data exchange matrix, and from there to a PC via a Micro1401-3 data acquisition unit.

Electrographic data was captured using Spike2 software (Cambridge Electronic Design, UK). Distinctive patterns in the EEG trace were described qualitatively and quantitative analysis was performed offline in Matlab 7 (Mathworks, UK) as described below.

2.9 Quantification of electrographic status epilepticus and electrographic changes during 'latent period'

Two independent methods were used to quantify electrographic SE; spike-frequency analysis and quantification of power in the γ-frequency band. In order to count spike events, raw EEG data was band-pass filtered between 1 and 100Hz. Artifacts were removed manually. A standard deviation was calculated from the baseline EEG (i.e., prior to any treatment) for each animal in order to produce a threshold at mean +/- 3 x SD. These thresholds were applied to the post-KA data and each threshold-crossing event was counted. Total counts were halved in order to calculate a spike rate. Spike rate was calculated from the time of KA injection for 7 days. The temporal change of spike rate was displayed graphically and Student's t-tests were performed, with a Bonferroni correction for multiple samples, to compare mean spike rates between treatment and vehicle mice for the time periods 0-30mins, 30 – 60 mins, 60 – 90 mins and 90 – 120 mins. A similar method was applied to the EEG trace following the termination of SE with diazepam. The temporal progression of spike frequency was displayed graphically and the frequency of spikes was binned into wider time periods for statistical analysis, including: 3 – 12h post-SE, 12 – 48h post-SE and 48 – 168h post-SE.

The power distributed in the γ-frequency band is a reliable indicator of the severity of electrographic SE (Lehmuke et al., 2008). In order to quantify the power in the gamma band, raw data was band-pass filtered between 20 and 70 Hz. Power was calculated in 5 minute epochs and normalised to artifact-free epochs of baseline data. The temporal change in the power distributed in the γ-frequency band and mean γ-band power was presented for each 30 minutes of SE.

2.10 Statistical analysis

All statistical analysis was carried out using SPSS v16 (IBM, USA). Student's t-tests were performed to analyse the effect of treatment versus vehicle on γ-frequency band power, with a Bonferroni correction for multiple samples. c-Fos^{+} cell counts were analysed using a Student's t-test, while synaptophysin and glial immunoreactivity were analysed using a one-way ANOVA with post-hoc tests. A Student's t-test was applied for the latency to the onset of CMS (Racine score ≥ 3) and duration of CMS i.e., summation of epochs in which epileptic behaviour (Racine score ≥ 3) was observed. The median maximum seizure severity was compared between treatment groups using Mann-Whitney U tests.

Chapter 3. Neurobiological, electrographic and behavioural characterisation of a kainic acid-induced status epilepticus model of epileptogenesis in the C57BL/6J mouse

3.1 ABSTRACT

In this chapter, the anatomical distribution of GABAergic, GAD-67 immunopositive interneurons in the hippocampal formations of two strains of mice was compared: an outbred strain, CD-1 and an inbred strain: C57BL/6J. The anatomical distribution of neurons expressing a neuropeptide, somatostatin, an enzyme, nNOS and a calcium binding protein, Calbindin-D28K, was also compared; all considered important modulators of hippocampal network dynamics. A period of status epilepticus was induced in both strains using intraperitoneal injections of the excitotoxic glutamate analog, kainic acid and quantified the emergence of epileptiform behaviour and analysed the anatomical distribution of c-Fos expression in the hippocampal formation 2 hours post KA.

In C57BL/6J mice, the emergence of electrographic changes during the period of status epilepticus and in the 7 days was investigated following the termination of seizures with diazepam, using implantable electrodes to record directly from the surface of the brain. Indicators of epileptogenesis, including reactive gliosis and synaptogenesis were investigated using immunohistochemistry at 24 and 72 hours.

We report that C57BL/6J mice generally have a lower tolerance to kainic acid than CD-1, however c-Fos expression in the CD-1 mice is more widespread in the hippocampal formation following status epilepticus. 4 patterns of EEG associated with status epilepepticus in the C57BL/6J mouse are described and he frequency of epileptiform discharges quantified. The power distributed in the gamma frequency band is quantified, following the methods described in Lehmuke et al (2009). Further, it is reported that epileptiform spiking continues for at least 7 days following kainic acid injection, in the absence of any behavioural indicators and that reactive gliosis in the CA3 region and reactive synaptogenesis in the outer molecular layer of the dentate gyrus occur 72 hours after induction of SE with diazepam.

3.2 INTRODUCTION

Kainic acid has been used as an agent for modelling seizures and the development of chronic epilepsy for many years (Ben-Ari & Cossart, 2000) (See introduction for more information on the development of Kainic acid as a research tool). A wide variety of approaches have been used, including in vitro models investigating excitotoxicity in culture (Rothman, 1985), acute (Alici et al, 1996) and organotypic hippocampal slices (Gahwiler, 1981, Bruce et al, 1995) and in vivo studies, where the drug is administred via intracerebral (Cavalheiro et al, 1982) or systemic (Lothman et al, 1981) injections. For a review of the contribution kainic acid models to the understanding of epilepsy, see Laursen (1984).

Studies performed in the 1980s have shown that systemic or intracerebral injections of kainic acid produce epileptiform seizures in the CA3 region of the hippocampus. These seizures propagate to other limbic structures and are followed by a pattern of cell loss that is similar to that seen in patients suffering TLE (Nadler, 1981). The induction of a period of SE in rodents has served as a useful model for investigating the progression of epileptogenesis and the emergence of chronic epilepsy and spontaneous seizures. SE models of TLE have offered insights into molecular and cellular changes underlying epileptogenesis, such as neuroinflammation (Vezzani, 2008) gliosis (Riban et al, 2002), selective neuronal loss (Sperk et al, 1983) and mossy fibre sprouting (Tauck & Nadler, 1985).

For a number of reasons historically, the majority of in vivo studies have been performed in rats. Rats show a consistent response to KA and a spatiotemporal pattern of neurobiological changes that closely replicates that seen in human TLE (Sperk, 1994). With the development of transgenic technology, however, the use of mice has quickly outstripped rats as the priniciple animal model for the majority of neurological conditions. The reduced cost of housing and quicker breeding speed make mice a preferable species for developing techniques in genetic manipulation. As a result, an understanding of the genetics and developmental biology of mice is far more advanced than in rats, however, neurobiological and electrophysiological changes in models of disease requires greater characterisation in this species.

Both outbred and inbred strains of mice are commonly used to model neurological diseases, including TLE. While inbred strains offer the advantage of isogenicity, especially valuable to geneticists, they also often exhibit strong strain-specific behaviour, physiology or responses to pharmacological treatment (Crawley, 2008). The CD-1 outbred strain is widely used in biomedical research, particularly in studies of drug toxicology, whereas the C57BL/6J is the most widely used background strain for the generation of mutants and is therefore of particular interest for the development of genetic studies in epilepsy.

While outbred strains, such as CD-1 show significant neuronal loss and spontaneous seizures comparable to rats following a period of drug-induced SE, the hallmarks of TLE have proven harder to model in inbred strains. C57BL/6J mice have proved to be particularly resistant to induced TLE. C57/BL6J mice have widely been reported

as having a high tolerance for kainic acid (Engstrom & Woodbury, 1986; 1988) and a resistance to neuronal loss and the development of spontaneous seizures following temporal lobe epilepsy (McKhann et al, 2003).

Other studies, however have found that C57BL/6J mice are not as resistant to kainic acid-induce epileptogenesis as widely reported. A variety of studies have reported that sensitive methods for the detection of neuronal cell loss, such as a Flourojade B stain indicate that a period of KA-induced SE does indeed cause lasting and progressive damage to neurons in the hippocampal formation in this strain (Hu et al, 1998; Shikhanov et al, 2005) comparable to the cell loss found in TLE. The emergence of spontaneous seizures in C57BL/6J mice, however, is yet to be reported.

Neurons in the hippocampal formation can be roughly divided into excitatory, principal cells and inhibitory interneurons. Excitatory cells are largely restricted to the granule cell layer of the dentate gyrus and pyramidal cell layer of the hippocampus, however, small numbers of specialised excitatory neurons, such as mossy cells exist in other lamina (Anderson et al, 2006). Inhibitory interneurons represent approximately 10% of the neurons in the hippocampal formation, are heterogenous and express varieties of neuropeptides and calcium binding proteins, however it is assumed that the majority of them are GABAergic (Freund & Buzsaki, 1996).

Despite their low numbers, GABAergic interneurons play an important role in keeping the hippocampal network in balance. Differences in the anatomical distribution of particular populations of interneurons is likely to have an effect on the network response to excitotoxins, such as kainic acid. GABA is synthesised by the enzyme glutamic acid decarboxylase (GAD), of which there are 2 varieties: GAD-65 and GAD-67. A study by Jinno et al (1998) showed that markers of GABA and markers of GAD-67 co-expressed to such an extent that GAD-67 can be cautiously used as a marker for all GABAergic neurons in the hippocampus. The anatomical distribution of GAD-67 immunopositive cells in the hippocampal formation of CD-1 and C57BL/6J mice is investigated and the distribution of the neuropeptide somatostatin (SST), the enzyme nNOS and the calcium binding protein, calbindin D28K (CB).

Activator protein 1 (AP-1) is a heterodimeric transcription factor composed of proteins which can include both c-Fos and c-Jun. The exact composition of the transcription factor determines the nature of transcription catalysed. Transcription of AP-1 subunits is regulated in a given cell by a broad range of physiological and pathological stimuli, including cytokines, growth factors and excitotoxic stress (Karin et al, 1995). The expression of c-Fos in particular is rapidly elevated in response to neuronal firing, which has meant that this subunit is often used in studies of the CNS, as a marker of neurons undergoing high levels of activity (Dragunow & Faull, 1989). The distribution of a range of markers of distinct populations of inhibitory interneurons in the hippocampus between CD-1 and C57BL/6J mice is compared, and characterised the progression of epileptiform behaviour during a 2 hour period of

KA-induced SE. Further, the spatiotemporal expression of c-Fos in the hippocampal formation in both strains from 2 – 12h following the induction of SE is analysed.

Despite the consistent presence of gliosis in post-mortem sections from TLE patients, the likely importance of gliosis to the progression of the disease and potential opportunity afforded for treatment of the latent period, time-course studies of the onset of gliosis in mouse SE-models are fairly limited in number and suffer from a lack of temporal resolution. The development of electrographic status epilepticus and electrographic activity for 7 days following seizure in C57BL/6J mice is characterised using implantable electrodes and analysed glial activation and reactive synaptogenesis at 24 and 72 hours following KA in this strain.

During seizure, higher frequency oscillations show an increase in power, representing the combined effect of hyperactivity and hypersynchronisation. Lehmuke et al (2009) demonstrated that the dynamic power of oscillations in the gamma frequency (20 – 70Hz) was a good correlate of seizure severity during a period of KA-induced SE in rats. Following seizure, the frequency of IED's is a good indicator of the progression of epileptogenesis. In C57BL/6J mice only, EEG was recorded during a period of KA-induced SE and for 7 subsequent days and described qualitatively and quantitatively the changes observed in the trace associated with seizure and epileptogenesis.

3.3 MATERIALS AND METHODS

3.3.1 Overview

Information regarding materials and methods described in this chapter refer only to that which is specific to this particular study. For general materials and methods, see chapter 2 where detailed protocols of methods performed throughout all chapters are described, including: KA administration and behavioural scoring of SE, basic protocols used for immunohistochemistry, microscopy and quantification of immunohistochemistry, surgical procedures for the implantation of electrodes and transmitters and EEG data collection and analysis. For ease of understanding, however, some information is duplicated.

3.3.2 Animals

Experiments were performed in 10-12 week old male C57BL/6J and CD-1 mice. All animals were purchased from Charles River (UK) and maintained in the Biomedical Services Unit, University of Liverpool under controlled environmental conditions ($19^{o}C$ – $23^{o}C$, 12h light: 12h dark), with food and water available *ad libitum*. All experiments were carried out according to Animals (Scientific Procedures) Act 1986 approved by the Secretary of State, Home Office, UK and University's Ethical Review Committee.

A total of 54 mice were used for studies reported in this chapter, including 18 CD-1 and 36 C57BL/6J. 5 mice from each strain were used as control animals for free-floating immunohistochemistry, while SE was induced with KA (20mg/kg, i.p) in 13 CD-1 mice and 11 C57BL/6J mice. Behavioural seizures in these mice were scored for 2 hours. Of these mice, 5 CD-1 and 4 C57BL/6J were perfused 2 hours after KA injection for the analysis of c-Fos in the hippocampal formation in free floating sections. Of the remaining mice, seizures were terminated with an intramuscular (i.m) injection with diazepam (10mg/kg) and these mice were perfused at 6 hours (CD-1: n = 4, C57BL/6J: n = 4) and 12 hours (CD-1: n = 3, C57BL/6J: n = 3). 1 CD-1 mouse died during SE.

Following this comparison between strains, a further study was performed investigating histological and electrographic changes in the hippocampus of C57BL/6J mice only. Of the remaining 20 C57BL/6J mice, 5 were used as controls for thaw mounted immunohistochemistry, while SE was induced in 10 mice using KA (20mg/kg). In these mice, seizures were terminated 2 hours following injection with KA (diazepam, i.m, 10mg/kg) and these mice were perfused at 24 (n = 5) and 72 (n = 5) hours. A further 5 mice were implanted with telemetry device for the recording and transmitting of EEG. Following post-operative recovery, SE was induced in these mice with KA (20mg/kg, i.p), terminated with diazepam at 2 hours (10mg/kg, i.m) and EEG was recorded for 7 days post-SE.

3.3.3 Drugs, Reagents and antibodies

Mouse anti-GAD-67 (1:1000) was purchased from Chemicon (UK) and visualised using an FITC-conjugated donkey anti-mouse secondary antibody (1:200). Sheep anti-nNOS (1:2000) was a gift from Dr P.C. Emerson and visualised using a CY3-conjugated donkey anti-sheep antibody (1:200). Rabbit anti-CB D28K (1:2000) was purchase from Millipore (UK) and visualised using a CY3-conjugated donkey anti-rabbit antibody (1:200). Rabbit anti-SST (1:1000) was purchased from Chemicon (UK) and visualised using a CY3-conjugated donkey anti-rabbit antibody (1:200). Rabbit anti-c-Fos (1:2000) was purchased from Calbiochem (UK) and visualised using a CY3-conjugated donkey anti rabbit secondary antibody (1:200). Mouse anti-NeuN (1:400) was purchased from Chemicon (UK) and visualised using an FITC donkey anti-mouse secondary antibody (1:200). Rabbit anti-synaptophysin (1:1000) was a gift from Dr P Greengard, Rockefeller University, USA and visualised using a CY3-conjugated donkey anti-rabbit antibody (1:200). Mouse anti-GFAP (1:400) was purchased from Sigma Aldrich (UK) and visualised using an FITC-conjugated donkey anti-mouse secondary antibody (1:200) Biotinylated tomato lectin (1:500) was purchased from Sigma Aldrich (UK) and visualised using CY3-conjugated streptavidin (1:100). All flourochrome-conjugated secondary antibodies and streptavadin were purchased from Jackson Immunoresearch laboratories (UK). DAPI used for visualizing cell nuclei was in the Vectashield ® mounting medium (Vector Laboratories, UK).

3.3.4 Free-floating sections

Following transcardial perfusion with 4% PFA (as described in chapter 2), brains were put soaked in 4% PFA for 4 hours, before being transferred to a 20% sucrose (in PBS) solution for cryopreservation. Brains remained in the sucrose solution for at least 24 hours before being sectioned as soon as possible (brains remained in sucrose for no longer than 2 weeks). 80µm thick free floating sections were cut using a freeze-plate microtome, directly into PBS. Sections were washed several times in PBS to remove any traces of PFA, before incubation in 5% donkey serum for 1.5 hours to block non-specific binding. Following incubation in donkey serum, sections were incubated in primary antibodies for at least 12 hours. Sections were again washed in PBS several times, prior to incubation in secondary antibodies for 3 hours. Sections were again thoroughly washed in PBS, placed into distilled water to reduce the salt content and mounted on CAG-coated slides using a fine paintbrush. Finally, sections were mounted using a Vectashield ® wet mount medium (Vector Laboratories, UK).

3.3.5 Semi-quantitative analysis of c-Fos expression

Because c-Fos expression in the hippocampal formation was too dense for accurate cell counting in 80µm sections following KA-induced SE, a semi-quantitative method was employed to score the extent of c-Fos expression in different regions. This involved a scoring system from 0 – 5, as follows: 0: no c-Fos expression. 1: A minimum of 1 cell immunopositive for c-Fos, up to 10% of cells 2: between 10 and 20% of cells immunopositive 3: between 20 and 50% of cells immunopositive 4:

majority of neurons c-Fos immunopositive, but not expressed in all neurons5: c-Fos expressed in all neurons.

3.4 RESULTS

3.4.1 Inhibitory interneurons

GAD-47 immunopositve cell bodies were found in the highest density in the CA1 region, with a slightly higher density in the stratum oriens (around 16 immunopositive cells/section) than in the stratum radiatum (around 14 immunopositive cells/section) (Figure 3.1a - d). A dense band of fibre tracts were clearly marked in the deep layers of Stratum radiatum of CA1 and CA3. GAD-47 distribution in the hippocampal formation varied little between strains, however, C57BL/6J mice did show higher numbers of GAD-47 immunopositive cell bodies in the Stratum Oriens region of CA1 (t_8 = 2.7386, p = 0.026, Fig 3.1a – d).

In both strains of mice, the highest density of SST-positive somata were found in in the polymorphic layer of the dentate gyrus, with far fewer found in the molecular layer of either strain (Figure 3.1a, 3.1d). CD-1 mice showed higher concentrations of SST-positive cells in both Stratum radiatum (t_8 = 2.8415, p = 0.022) and Stratum oriens (t_8 = 2.5175, p = 0.036) of the CA3 region of the hippocampus (Figure 3.1a, d), while C57BL/6J mice had a higher distribution in the same layers of the CA1 region (Stratum radiatum: t_8 = 3.901, p = 0.005) Stratum oriens: : t_8 = 4.1712, p = 0.003, Figure 3.1a, d). In all mice, some SST-;like immunoreactivity was observerd in the pyramidal cell layer throughout the hippocampus, however this staining was of a much lower intensity than in other layers and cells with this lower intensity of staining

were not counted as SST-positive. This lower intensity staining may be an artefact, or evidence of some SST-staining in pyramidal neurons. The intensity of this staining was much higher in CD-1 mice (Figure 3.1a). SST-immunopositive fibres were found in the highest density in the polymorphic and molecular layers of the dentate gyrus.

In both strains, nNOS-immunopositive neuronal somata were found in high densities in the polymorphic layer of the dentate gyrus, with 30 – 40 neurons observed in each section and a heavy density of fibres was observed in the inner molecular layer, particularly in CD-1 mice (Figure 3.1b, 3.1d). nNOS-immunopositive somata were also observed at lower densities (5 – 15 cells/section) throughout the dentate gyrus molecular layer and the stratum radiatum and oriens throughout CA3 and CA1, however, no nNOS immunopositive neurons were observed in the dentate gyrus granule cell layer or the pyramidal layer of the hippocampus in any sections. C57BL/6J mice showed a slightly higher density of nNOS-immunopositive cell bodies throughout the hippocampal formation, however, this was most pronounced in the molecular layer of the dentate gyrus ($t_8 = 2.5976$, $p = 0.0317$) and Stratum oriens of the CA3 region ($t_8 = 2.400$, $p = 0.043$).

CB-immunopositive cells were found in the highest denstity in thin band in the Stratum lacunosum-moleculare and were also dispersed in the stratum radiatum of the CA3 region (Figure 3.1c, d). Although cell bodies were found at a lower density than GAD-47, SST or nNOS, a very high intensity staining of fibre tracts was observed throughout the dentate gyrus and a distinctive high density band of CBD-

postive fibres could be clearly seen in every section in the stratum lucidum of CA3 (Figure 3.1c).

3.4.2 Behavioural scoring

C57BL/6J mice could be divided into three distinct populations based on their response to KA. While the majority of mice (approximately 80%) showed tonic-clonic seizures between 30 minutes and one hour following KA administration, followed by recovery, some mice exhibited either an enhanced resistance or an enhanced sensitivity to KA. Animals in the resistant group failed to show CMS in response to 20mg/kg KA, while animals in the hypersensitive group showed full tonic clonic seizures within 10 minutes of KA administration, which were lethal. This variability was at the level of the batch, with relatively consistent responses seen between individuals from the same home cage. Consequently, when an animal was found to show an 'aberrant' response to KA, the entire batch was excluded. From here in, only C57BL/6J mice from 'normal' batches are considered.

Shortly after KA administration, all mice (excluding aberrant C57BL/6J populations showed similar behaviour, with pronounced hypoactivity (Racine stage 1, lasted approximately 5 to 10 minutes), CD-1 mice showed a greater tolerance to KA than C57BL/6J mice (Figure 3.2). CD-1 mice reached a lower maximum severity, with a median of Racine 4, compared with Racine 5 in C57BL/6J mice (Mann Whitney U test: $U = 1915$, $p < 0.001$, Figure 3.2b). The latency to complex motor seizures

(≥Racine 3) was approximately 20% longer than in C57BL/6J mice (t_{22} = 2.212, p = 0.019, Figure 3.2c), whilst the duration was approximately 30% lower in the outbred strain (t_{22} = 2.632, p = 0.008, Figure 3.2d).

3.4.3 Expression of immediate early gene products in the hippocampal formation

In control mice of both strains, c-Fos expression was completely absent from the the principal excitatory neurons, including both granule cells in the granule cell layer of the dentate gyrus and pyramidal cells in the pyramidal cell layer of the CA1, CA2 and CA3 regions of the hippocampus. In both strains, cFos was constitutively expressed in a number of neurons in the polymorphic zone of the dentate gyrus. In C57BL./6J mice, this constitutive expression extended into the stratum radiatum and stratum oriens regions of areas CA1, CA2 and CA3(Figure 3.3a, e).

2 hours following KA administration, c-Fos expression was strongly elevated in in the granule cell layer of the dentate gyrus in both strains (Figure 3.3b, e). This elevated expression was also found throughout the pyramidal cell layer of the all hippocampal regions in CD-1 mice, however, in C57/BL6 mice, although there was some c-Fos expression in pyramidal cells of all mice investigated, expression was generally lower, sporadic, with greater variation between animals (U = , p = 0.032, Figure 3.3b, e). c-Fos expression was also elevated more strongly in neurons found in the dentate hilus of CD-1 mice than the C57/BL6 strain (Figure 3b, e).

At 6 hours following KA administration, there is a greater variability in c-Fos expression between individual animals than between strains. c-Fos is observed throughout the dentate gyrus and hippocampus, both in the main excitatory circuitry (dentate granule cells and pyramidal cells) and in interneurons in the hilus, dentate gyrus molecular layer, stratum radiatum and stratum oriens (Figure 3.3c, e). at this timepoint, c-Fos expression was found in higher densities in the granule cell layer of C57BL/6J mice than in CD-1 mice. 12 hours following KA administration, c-Fos expression is largely indistinguishable from naive controls. In some CD-1 mice, some low density c-Fos immunoreactivity can be observed in the granule cell layer, however, this was completely absent in all sections taken from C57BL/6J mice (Figure 3.3d, e).

In both strains of mice, there was high-intensity c-Jun immunoreactivity in the granule cell layer of the dentate gyrus, suggesting that this protein is constitutively expressed (Figure 3.3f). c-Jun is absent in the pyramidal cell layer throughout the hippocampus and was not found to be induced in any region following KA-induced Status epilepticus, suggesting that it was not suitable as an indicator of seizure severity.

3.4.4 Electrographic status epilepticus

C57/BL6J mice implanted with telemetry devices exhibited normal behavioral patterns following post-operative recovery period, with no obvious effect on eating, drinking, activity levels, alertness, aggression or signs of discomfort. Baseline EEG activity was also normal, with occasional changes in amplitude and frequency that correlated with activity levels and state of alertness (Figure 3.4a, b). SE began with discrete electrographic seizures (figure 3.4c), correlating with hypoactivity (Racine Class I) As these electrographic seizures become more regular, they began to merged into each other, evolving into continuous, high amplitude spiking (figure 3.4e) with intervening flat periods. The spiking interrupted by flat periods gradually became more regular (figure 3.4f) until the pattern observed resembled regular high-amplitude discharges (figure 3.4d).

Following the administration of KA, the rate of epileptiform spikes increased over the initial 20 minutes to a peak of approximately 65 spikes min^{-1} (Figure 3.5a), and from this point, decreased to around 30 spikes min^{-1} by approximately 35 minutes. Over the period from 20 minutes to 80 minutes, the spike rate fluctuated in regular cycles of approximately 25 minutes duration, with a general trend downwards. By 80 minutes, the spike rate had decreased to approximately 50 spikes min^{-1}. From around 100 minutes, the spike rate decreased towards the 2 hour point to approximately 40 spikes min^{-1}. In contrast to the spike rate, the power distributed in the γ-band increased steadily from the point of KA administration to a peak of 5dB around 90 minutes post injection. From this point, it gradually declined to approximately 3.5 at 120 minutes.

3.4.5 Gliosis

24h after KA administration, there were no qualitative differences in morphology, distribution, or quantitative differences in cell numbers in either astrocytes or microglia than seen in sections taken from control mice (Figure 3.6e, f). In region CA3, astroglial distribution was largely restricted to stratum radiatum and stratum oriens and this pattern was largely replicated by microglia (Figure 3.6a, b). By 72h, however, there was an approximately two-fold increase in GFAP immunopositive astrocytes and a three-fold increase in microglia in the CA3 region compared to control mice. A one-way analysis of variance with a Tukey's honestly significant difference criterion was performed and found that this was significant (Astroctyes: $F_{12} = 122.0$, $p < 0.001$ Microglia: $F_{12} = 53.77$, $p < 0.001$).

Qualitative analysis revealed evidence of significant invasion of stratum lucidum and the pyramidal cell layer by both cell types (Figure 3.6a, b, d, e) and an increased number of microglial cells and GFAP immunopositive astrocytes possessing an 'activated' phenotype with hypertrophic cell bodies and thick processes (Figure 3.6c).

3.4.6 Reactive synaptogenesis

High levels of Synaptophysin immunoreactivity was constitutively expressed in the dentate hilus and stratum lucidum of the CA3 region C57BL/6J mice (Figure 3.7a). Initial changes in the spatial distribution of synaptophysin following KA induced status epilepticus were witnessed at 72h. At this timepoint, synaptophysin

immunoreactivity was elevated in the outer molecular layer of the dentate gyrus (F_{12} = 92.55 = , p < 0.001 . Figure 3.7a, b), suggesting an increase in synaptogenesis in this region.

3.4.7 EEG analysis for 7 days following kainic acid administration

Following termination of SE with diazepam and subsequent recovery, no behavioural seizures were observed in any animals during the first 7 days. However, despite diazepam treatment and the absence of behavioural seizures, epileptiform activity was still evident in all animals throughout the post-SE or early epileptogenic period. This was dominated by the regular epileptiform spikes (Figure 3.4d) Spike frequency was initially high (>5 spikes per minute), declining to close to 1 spike/minute at 52h, before re-emerging and remaining at approximately 4-5 spikes per minute for the remainder of the 7 day recording period (Figure 3.8).

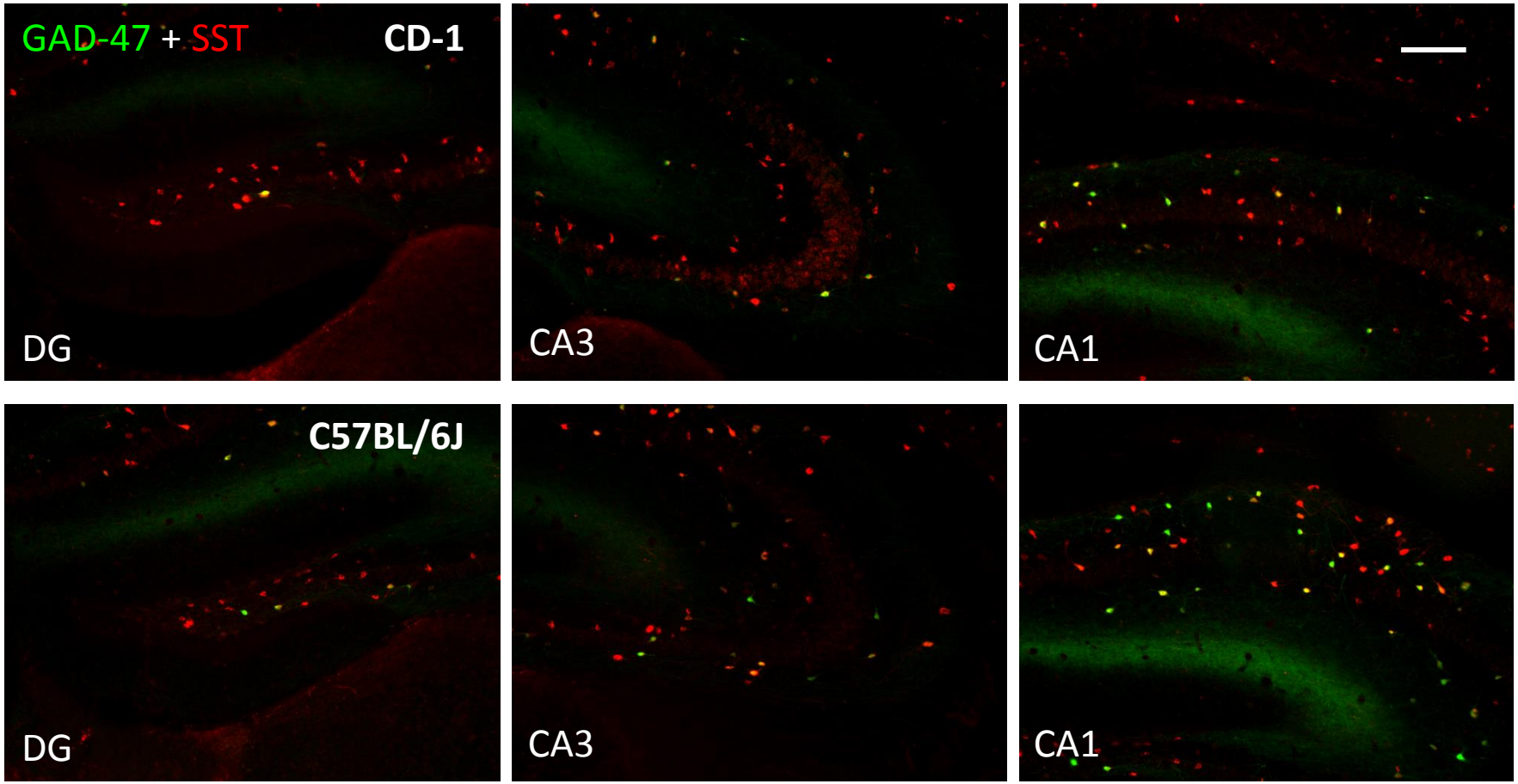

Figure 3.1a. GAD-47 and Somatostatin expression in the hippocampal formation: comparison between CD-1 and C57BL/6J mice. Magnification: x20. Scale bar = 100µm.

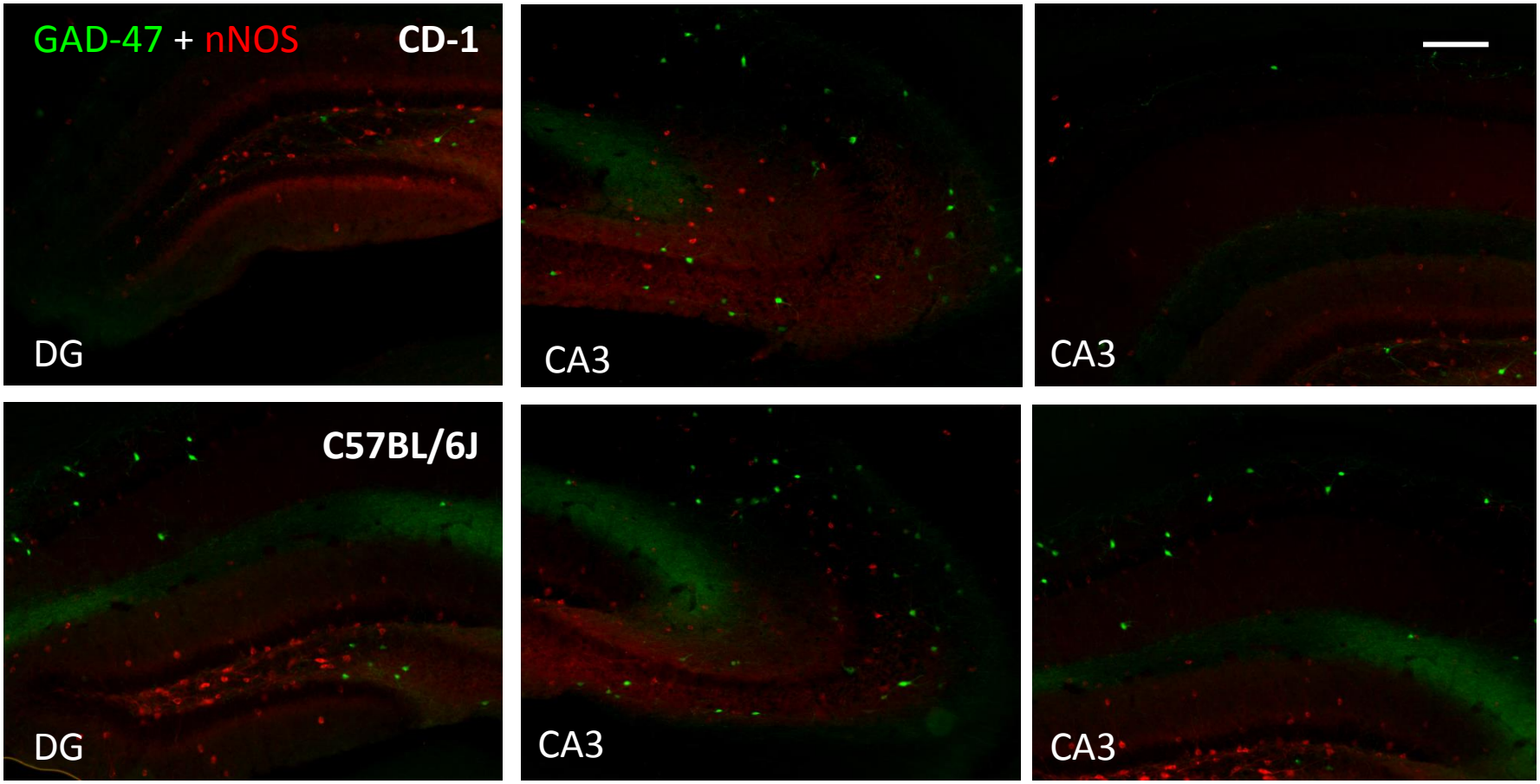

Figure 3.1b. GAD-47 and nNOS expression in the hippocampal formation: comparison between CD-1 and C57BL/6J mice. Magnification: x20. Scale bar = 100µm.

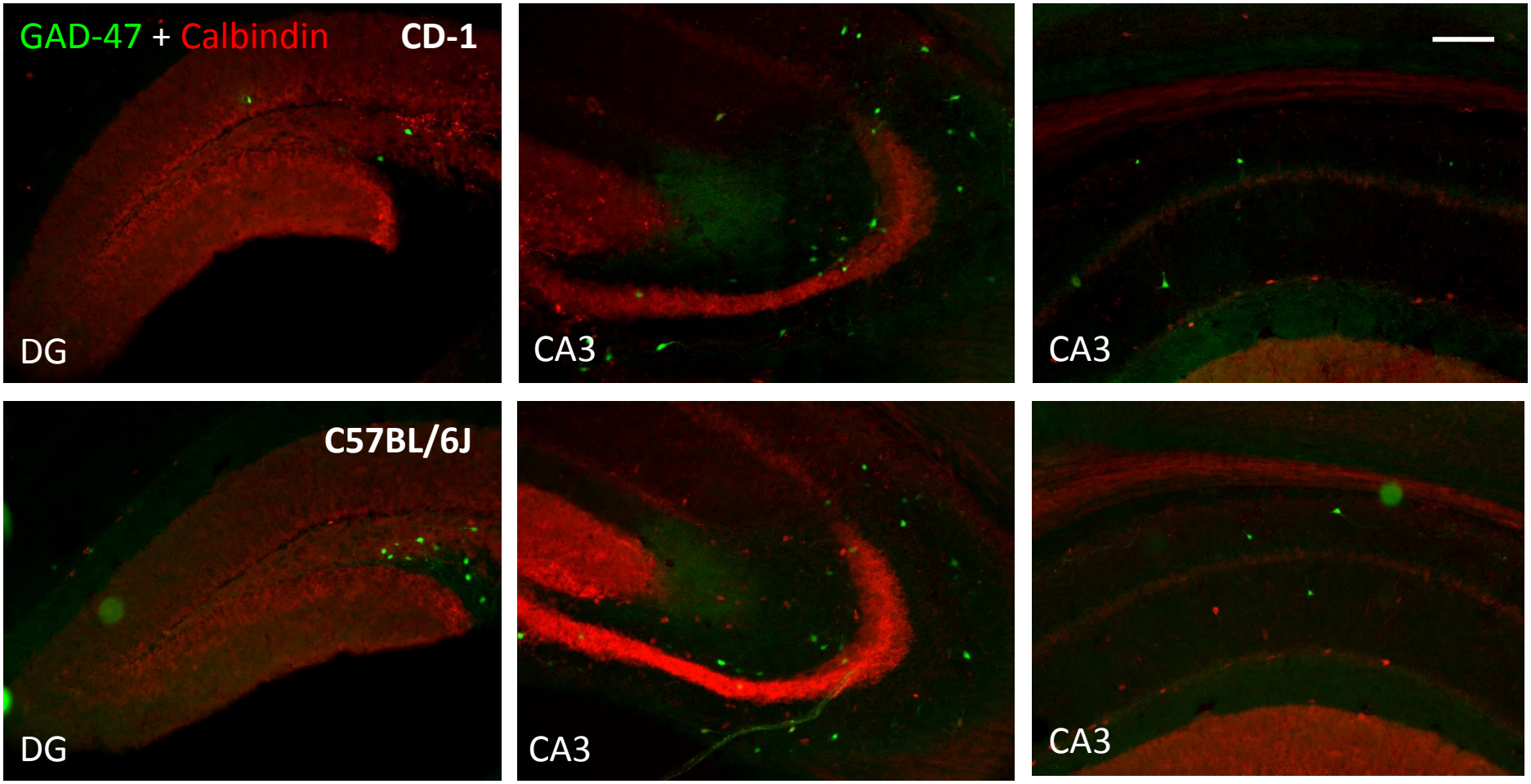

Figure 3.1c. GAD-47 and Calbindin expression in the hippocampal formation: comparison between CD-1 and C57BL/6J mice. Magnification: x20. Scale bar = 100µm.

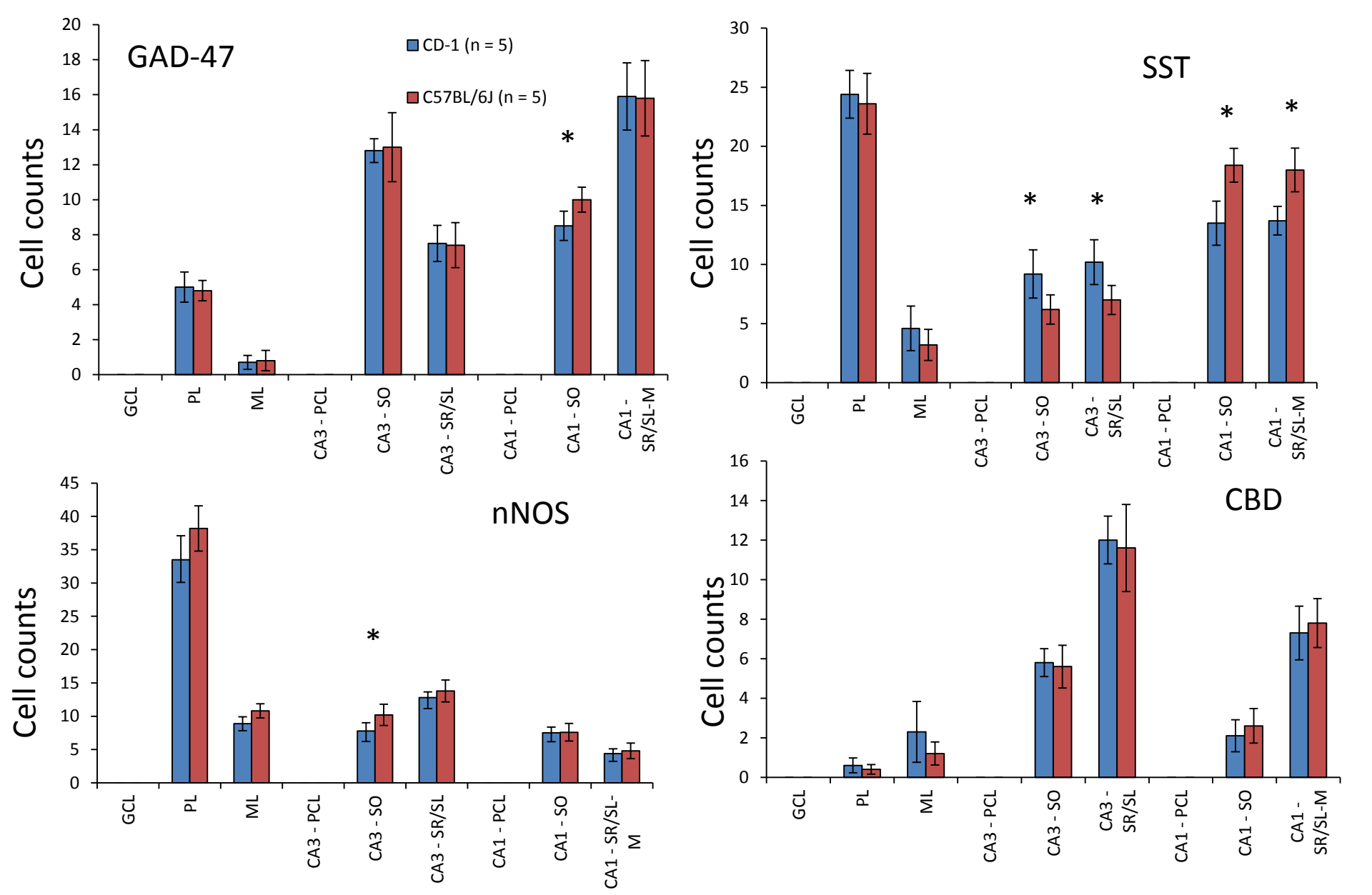

Figure 3.1d. Cell counts of GAD-47, Somatostatin, nNOS and Calbindin in hippocampal formation of CD-1 and C57BL/6J mice. GCL: granule cell layer; PL: polymorphic layer; ML: molecular layer; PCL: pyramidal cell layer; SO: stratum oriens; SR: stratum radiatum; SL: stratum Lucidum; SL-M: stratum lacunosum-moleculare (* $p < 0.05$).

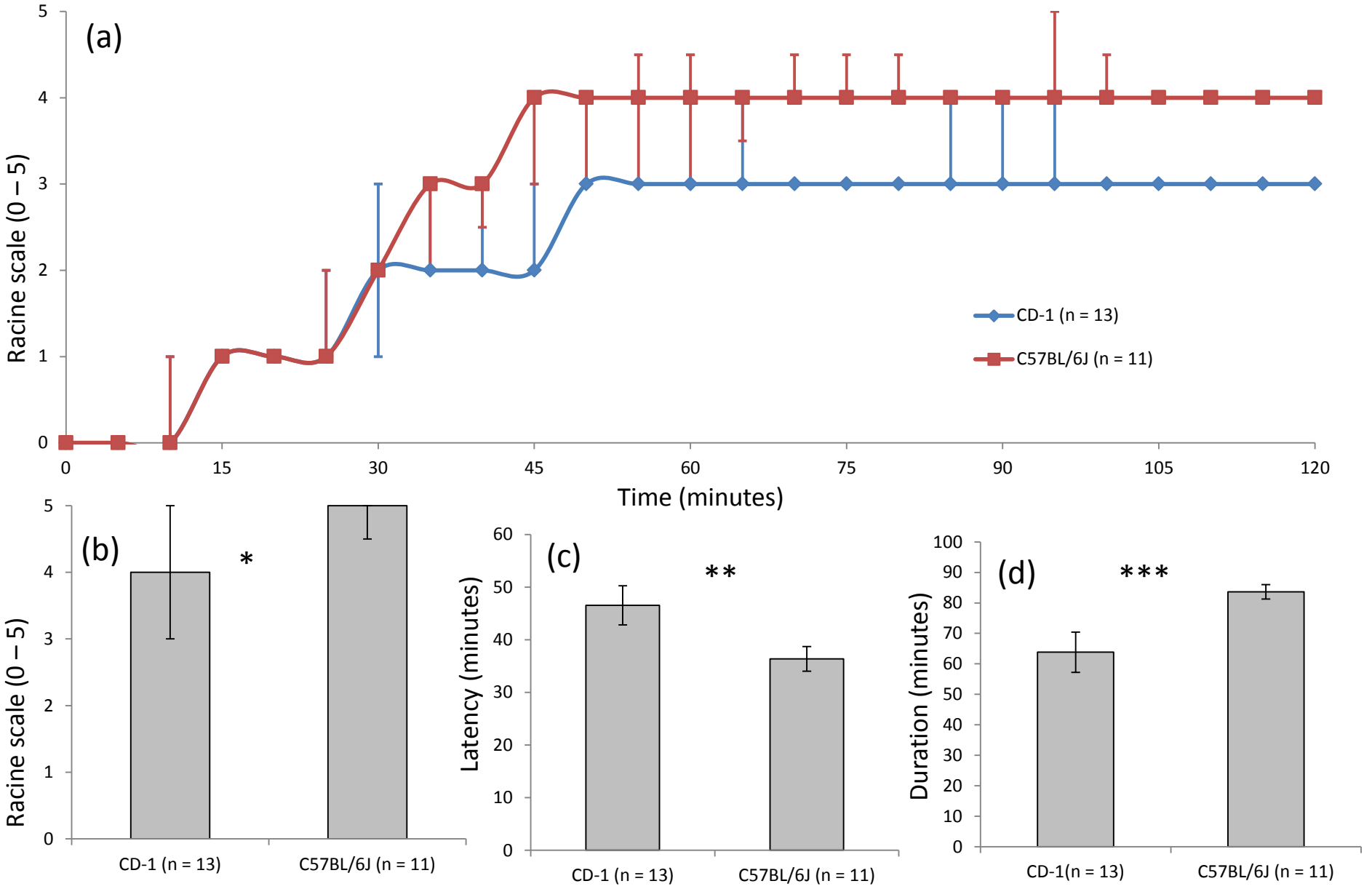

Figure 3.2. CD-1 mice have a higher tolerance for kainic acid than C57BL/6J. (a) Timecourse of seizure severity over 120 minutes following injection with 20 mg/kg KA. **(b)** Maximum seizure severity reached (Median +/- IQ range) *p <0.001. **(c)** Latency to onset of CMS (≥Racine 3) seizures. **p = 0.019. **(d)** Duration of CMS . ***p = 0.008.

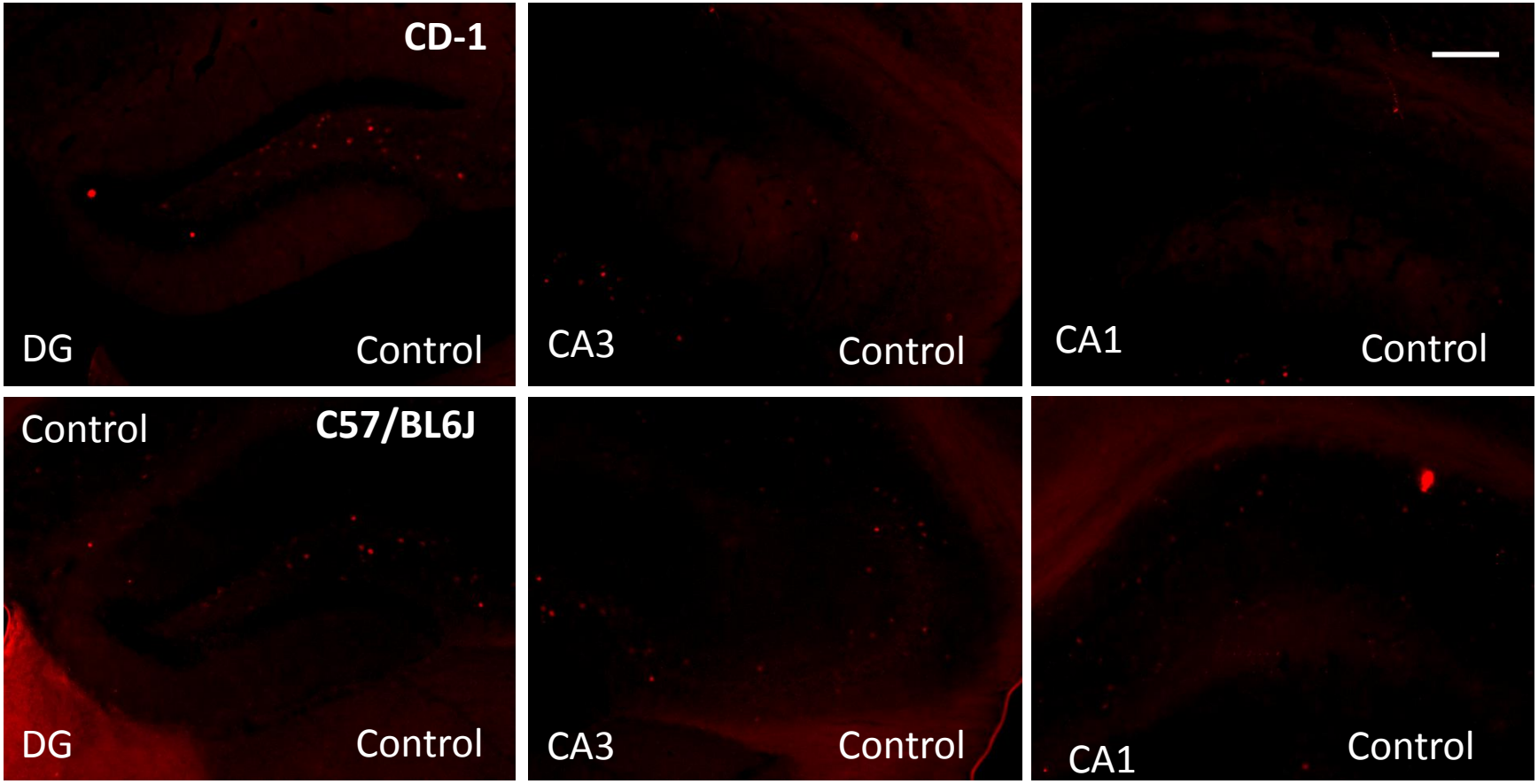

Figure 3.3a. c-Fos expression in hippocampal formation of CD-1 and C57BL/6J control mice. Magnification: x20. Scale bar = 100µm. *p = 0.032 (CD-1, n = 5, C57BL/6J, n = 4).

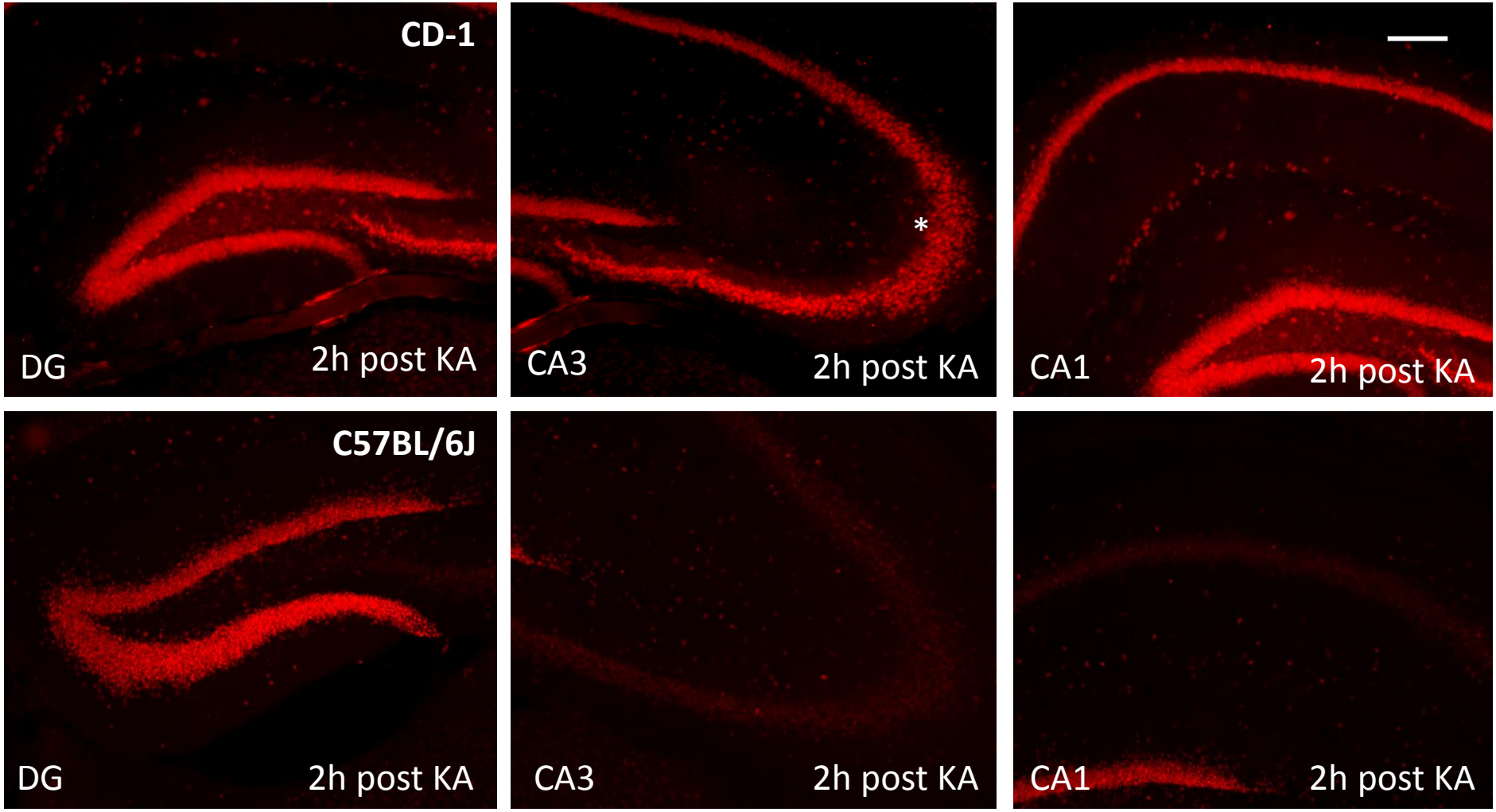

Figure 3.3b. c-Fos in hippocampal formation of CD-1 and C57BL/6J mice 2h following injection with Kainic acid.
Magnification: x20. Scale bar = 100µm. *p = 0.032 (CD-1, n = 5, C57BL/6J, n = 4).

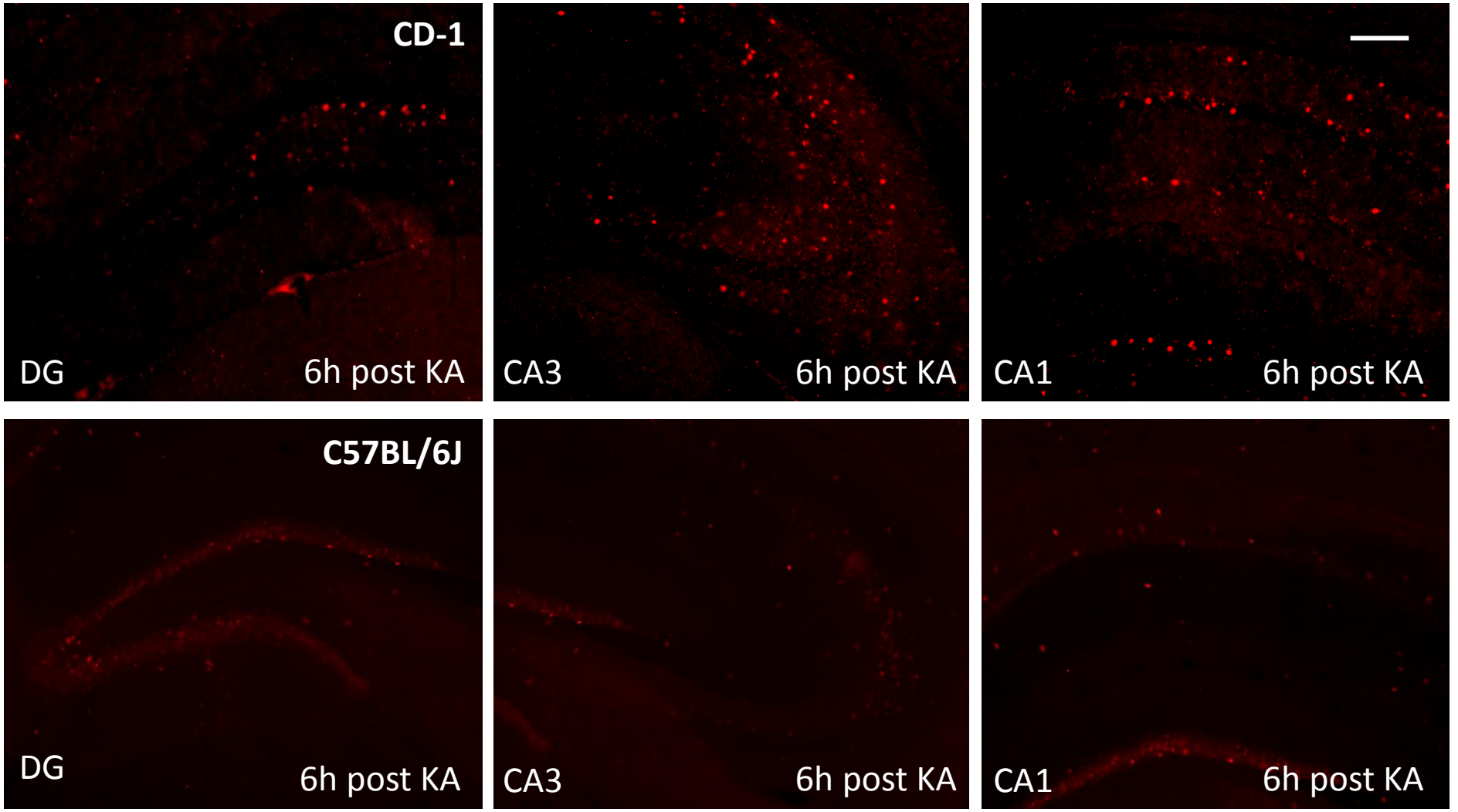

Figure 3.3c. c-Fos in hippocampal formation of CD-1 and C57BL/6J mice 6h following injection with Kainic acid.
Magnification: x20. Scale bar = 100µm.

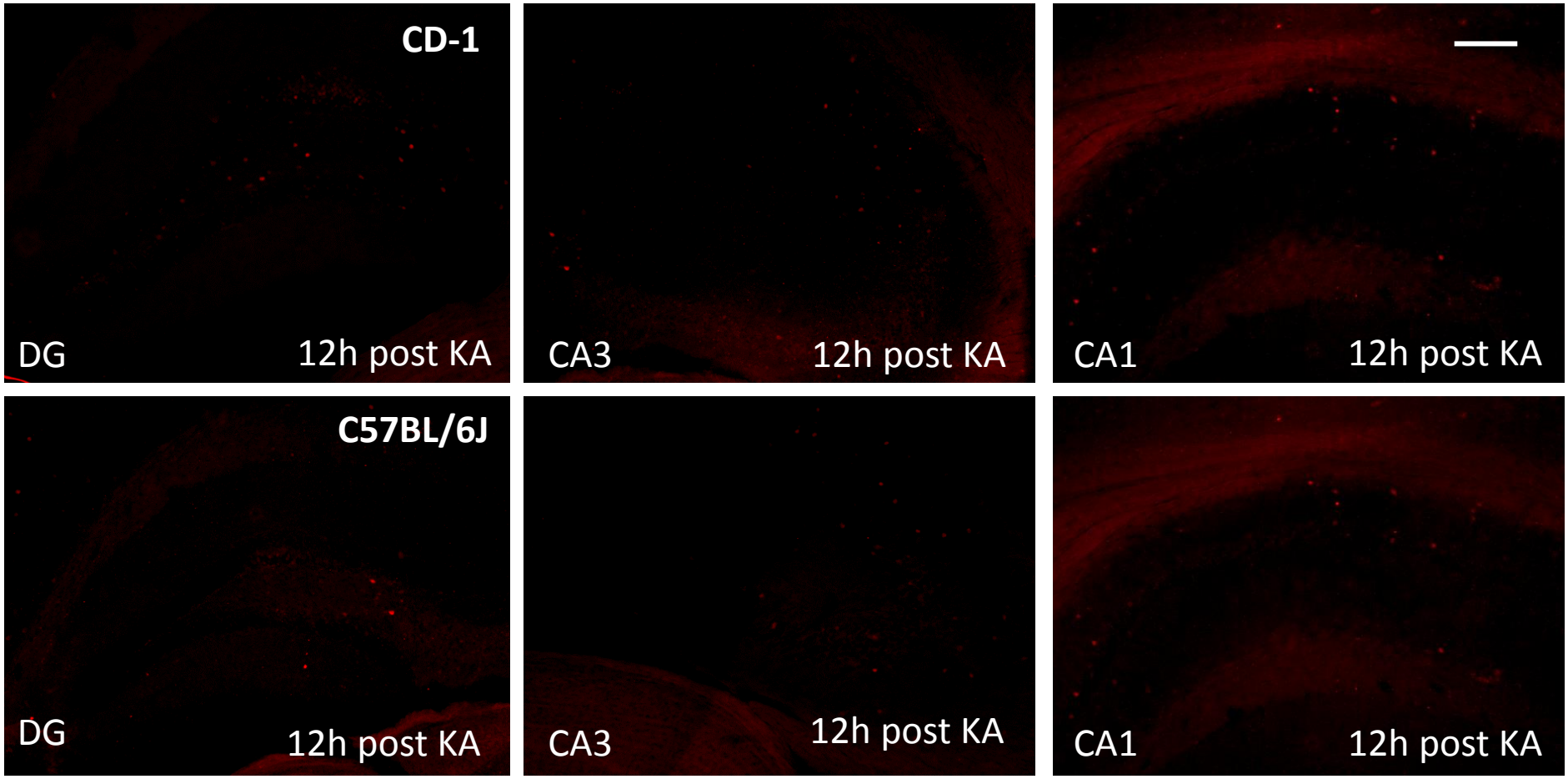

Figure 3.3d. c-Fos expression in hippocampal formation of CD-1 and C57BL/6J mice 12h following injection with Kainic acid. Magnification: x20. Scale bar = 100µm.

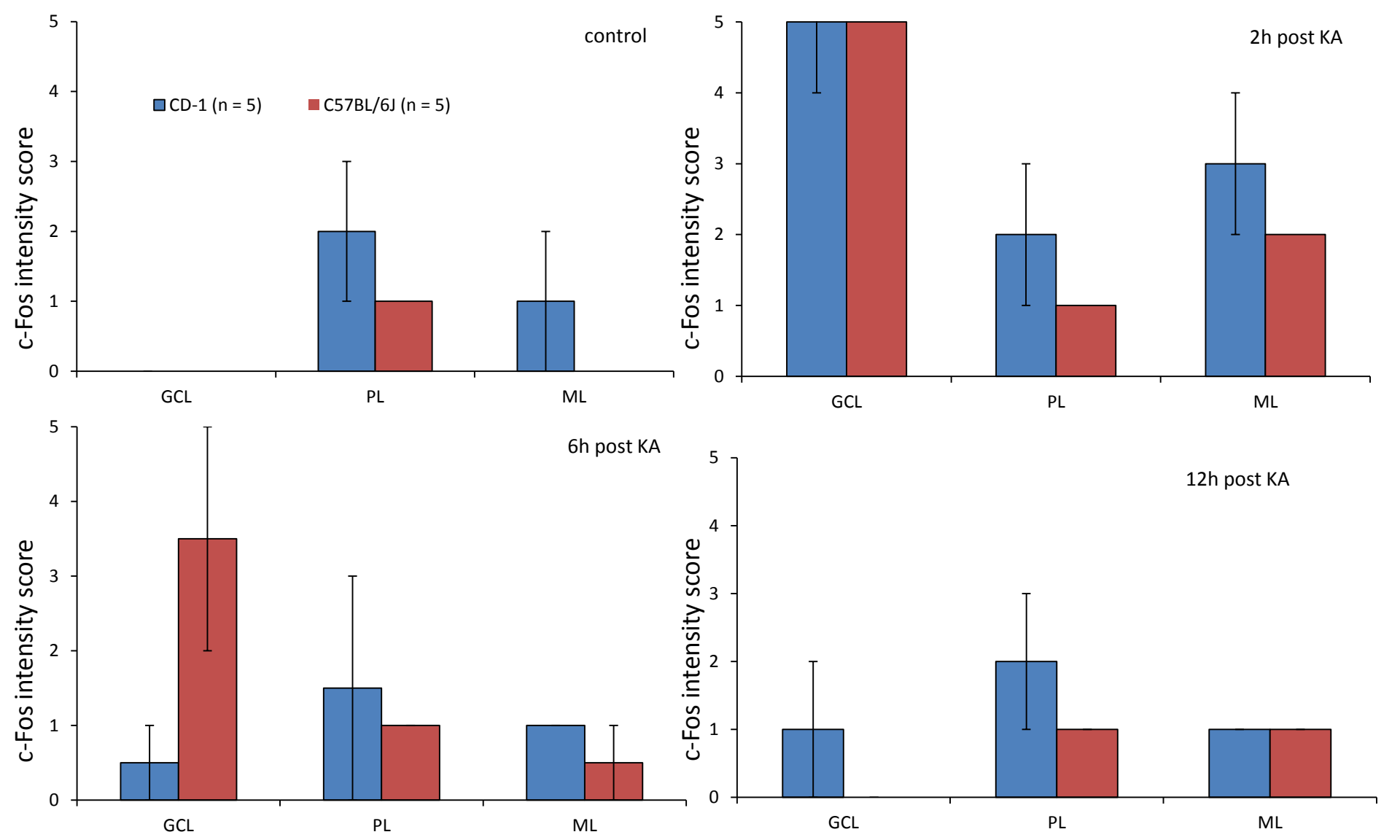

Figure 3.3e. c-Fos expression in dentate gyrus of CD-1 and C57BL/6J mice up to 12 hours following kainic acid administration. c-Fos intensity score: score 0 – 5, described in 3.35 materials and methods. GCL: granule cell layer, PL: polymorphic layer, ML: molecular layer

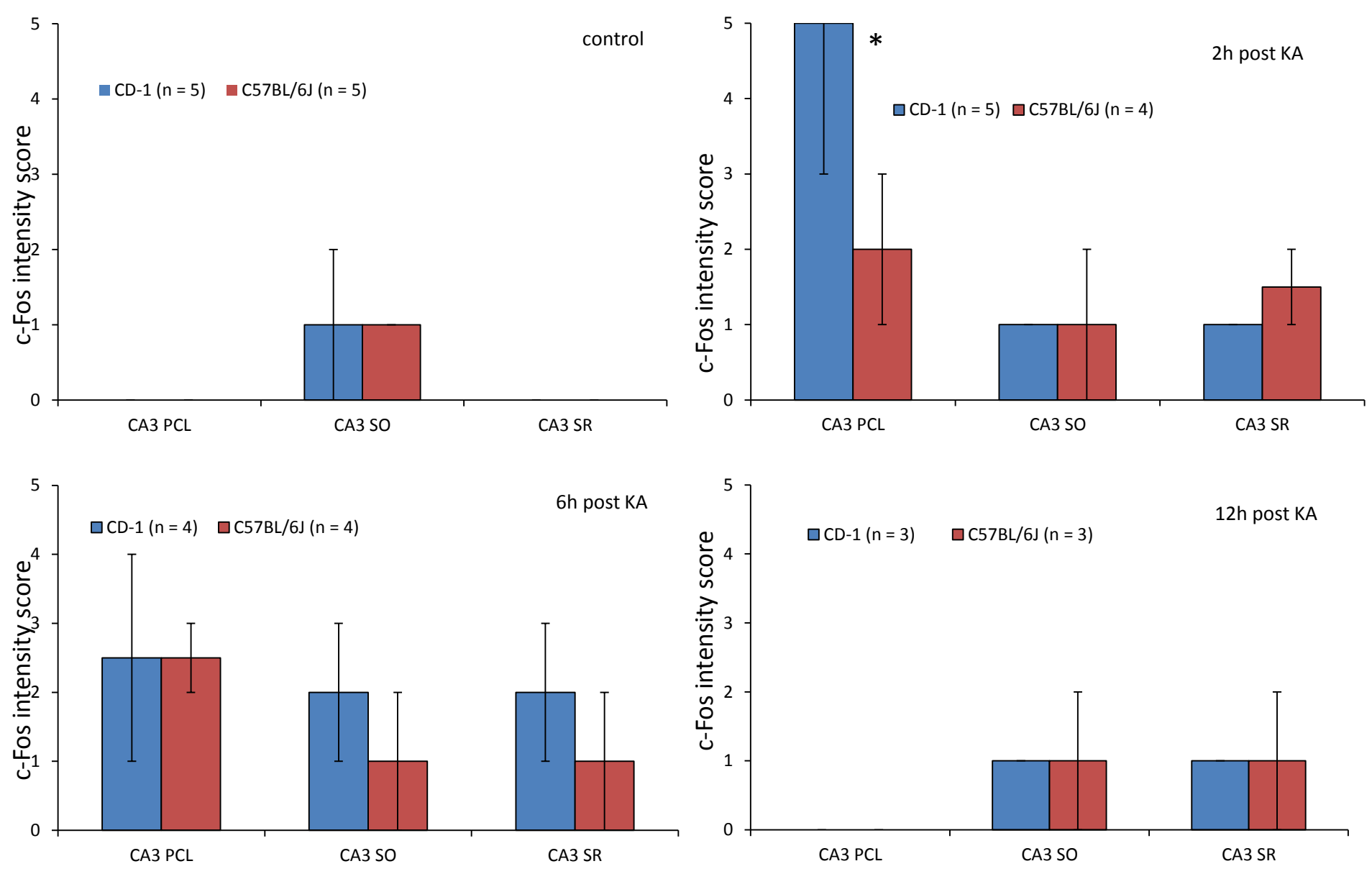

Figure 3.2e. c-Fos expression in CA3 region of hippocampus up to 12h following kainic acid administration. c-Fos intensity score: score 0 – 5, described in 3.35 materials and methods . PCL: pyramidal cell layer, SO: Stratum oriens, SR: Stratum radiatum. * U = 10.5, p = 0.032

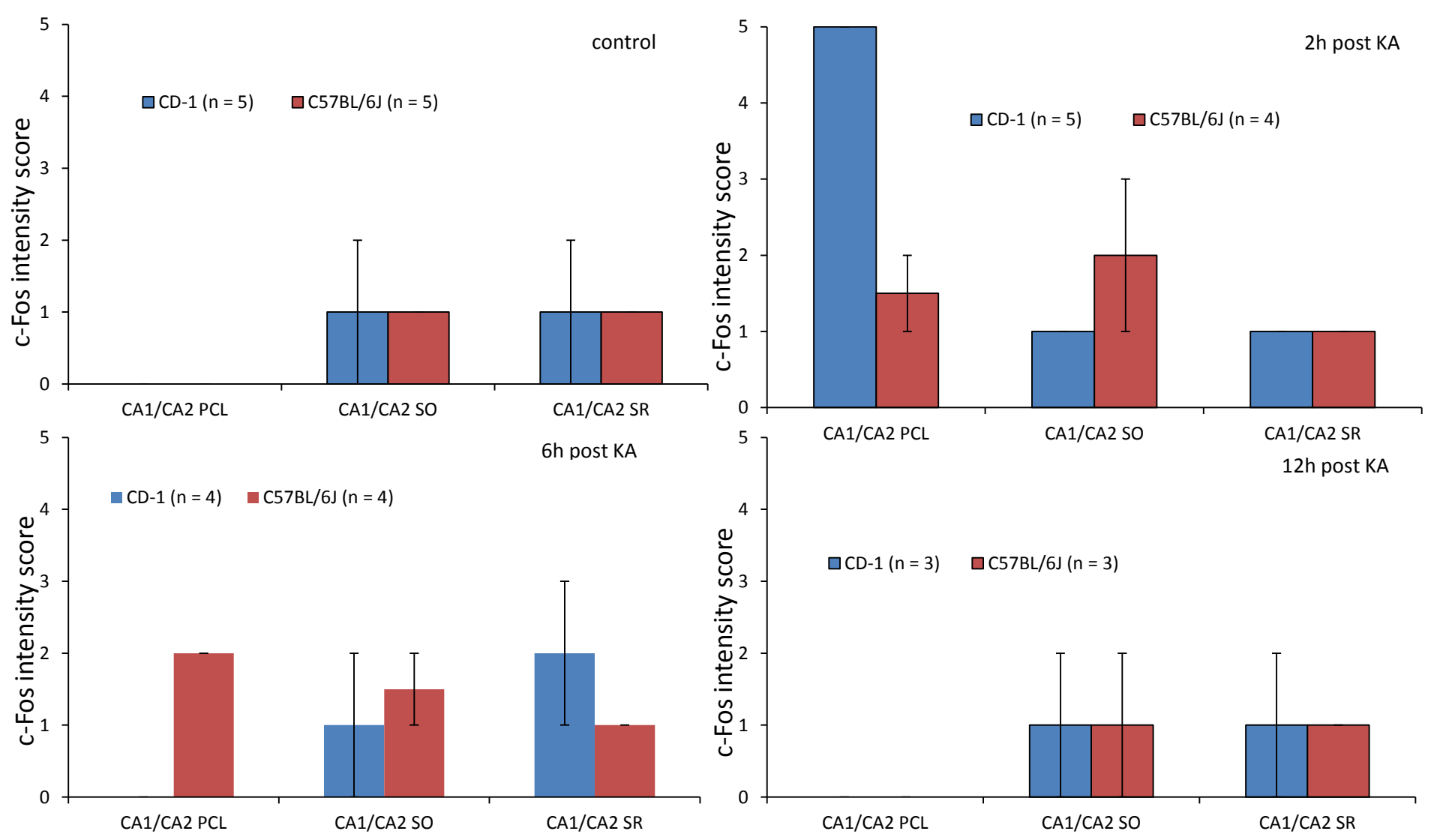

Figure 3.3e. c-Fos expression in CA1 and CA2 region of hippocampus up to 12 hours following kainic acid administration. c-Fos intensity score: score 0 – 5, described in 3.35 materials and methods . PCL: pyramidal cell layer, SO: Stratum oriens, SR: Stratum radiatum.

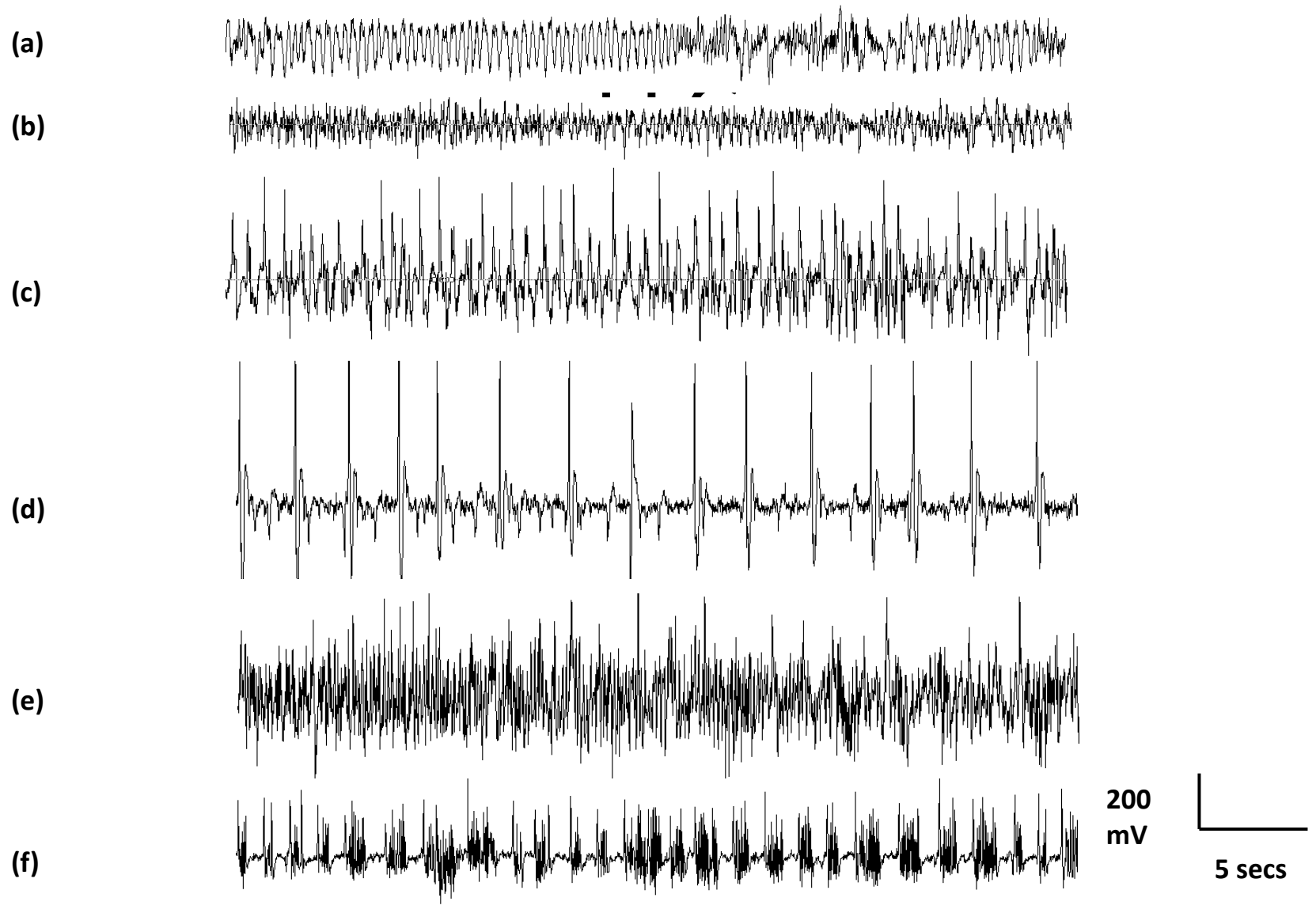

Figure 3.4. Typical EEG patterns associated with Kainic acid-induced Status epilepticus in C57BL/6J mouse. **(a & b)** Typical EEG pattern from control mice. (c) irregular high amplitude epileptiform discharges. (d) regular high amplitude spikes. (e) High frequency epileptiform discharges. (f) Burst firing.

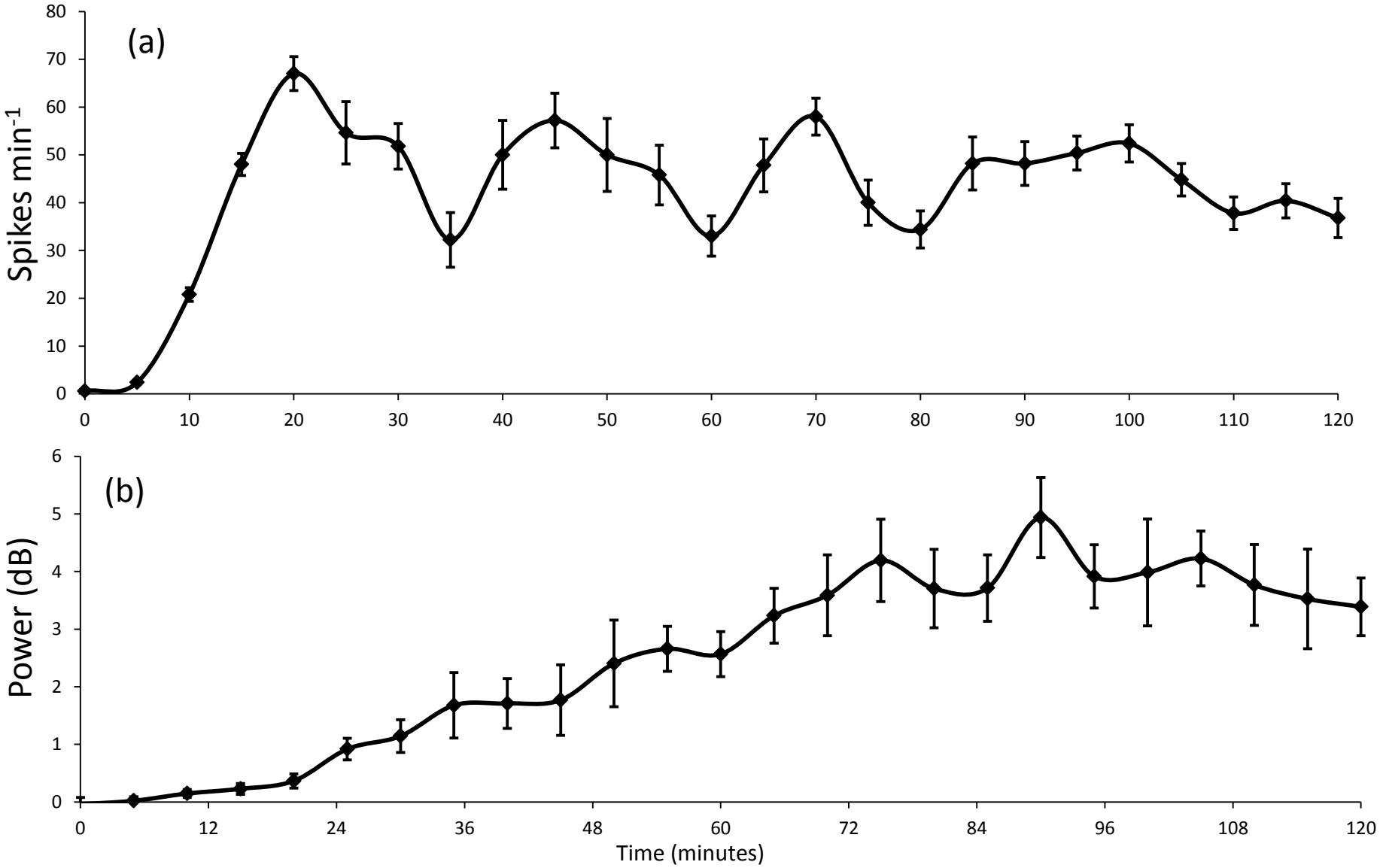

Figure 3.5. Timecourse of status epilepticus in C57BL/6J mice over 2 hour period from injection with kainic acid. (a) Spike rate (spikes min-1) with resolution of 5 minutes. **(b)** Power distributed in Gamma-band (dB). n = 5.

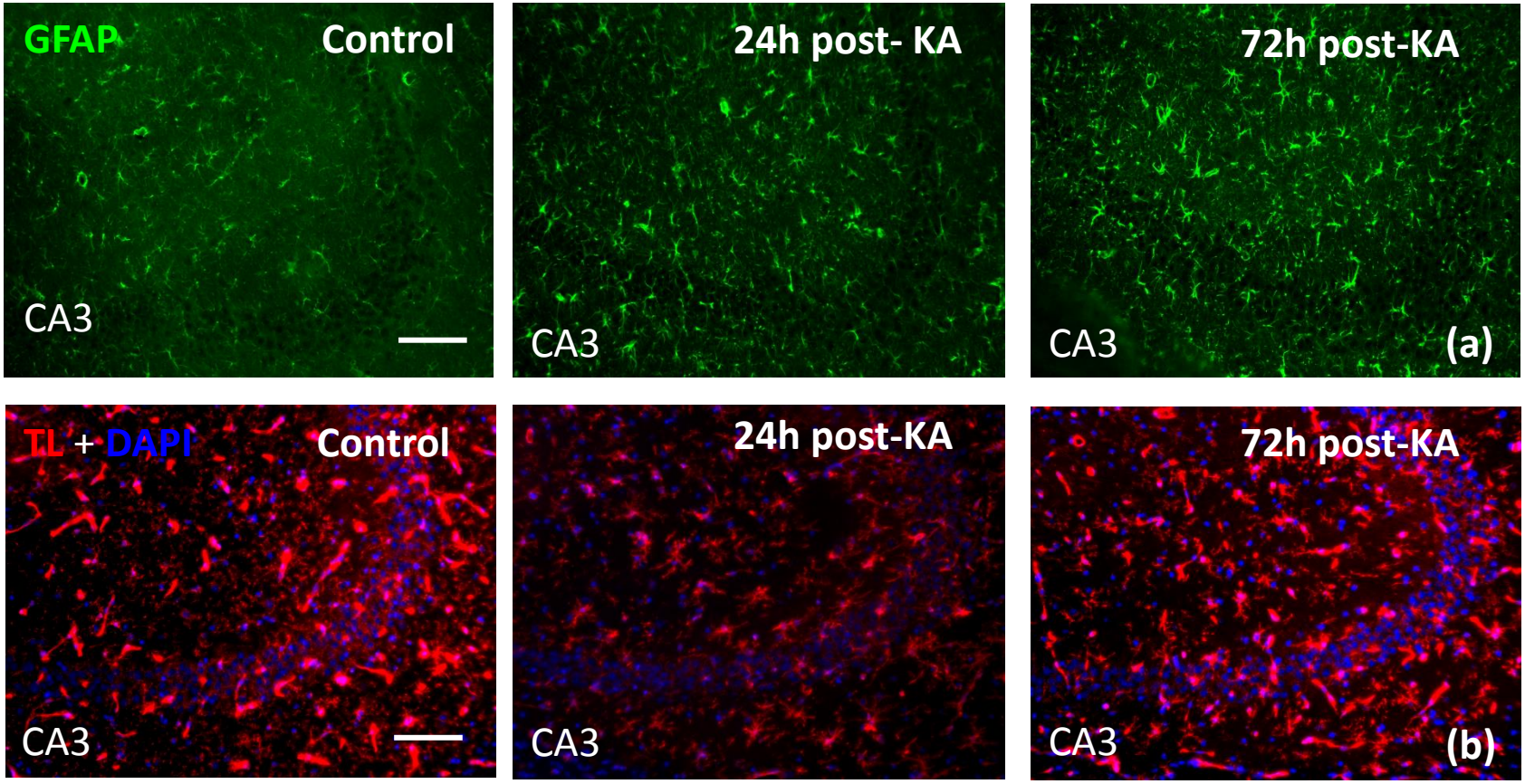

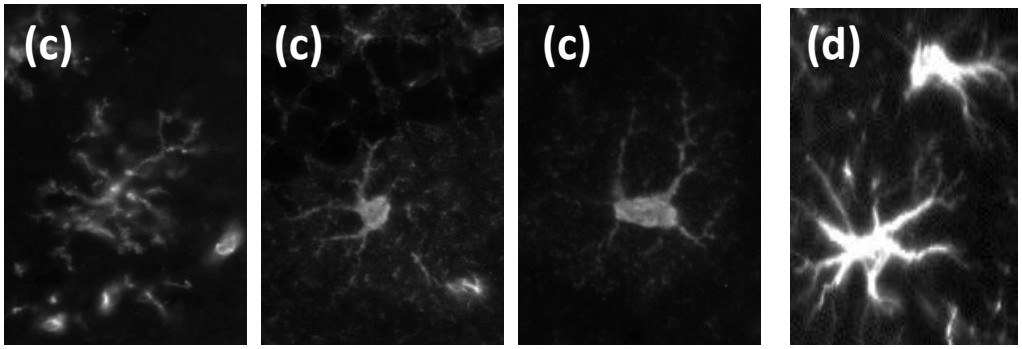

'resting' microglia

'activated' microglia

'activated' microglia

'activated' astrocyte

Figure 3.6. Gliosis in CA3 at 1 – 3 days post Kainic acid-administration. (a) GFAP-positive cells in CA3 **(b)** Tomato lectin positive cells in CA3 region of hippocampus **(c)** Close up images of Tomato lectin-positive microglia demonstrating morphological changes during activation. **(d)** Close up image of activated astrocyte

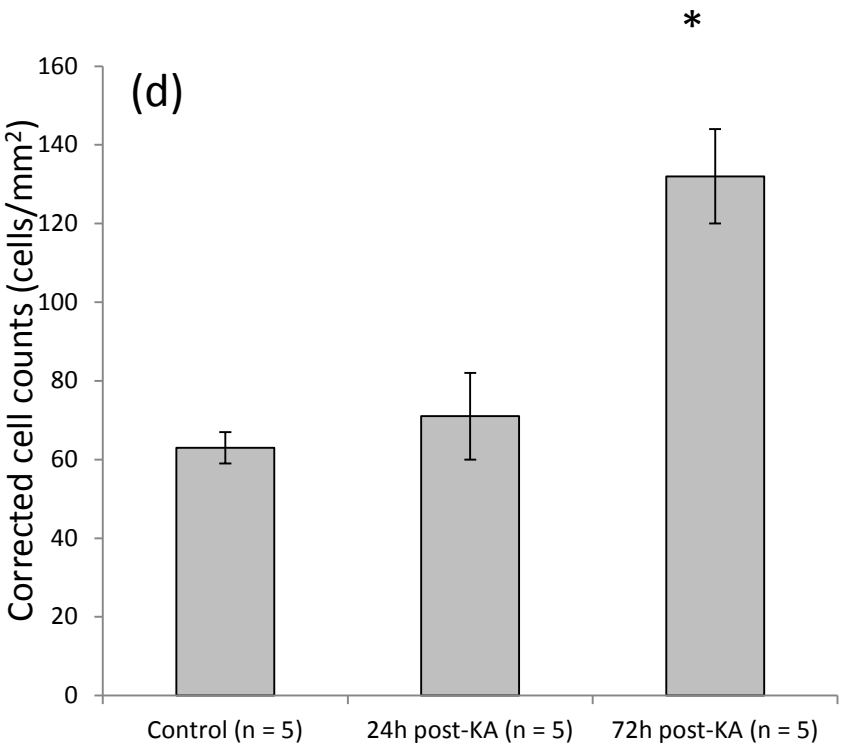

Astrocytes in CA3 region of hippocampus

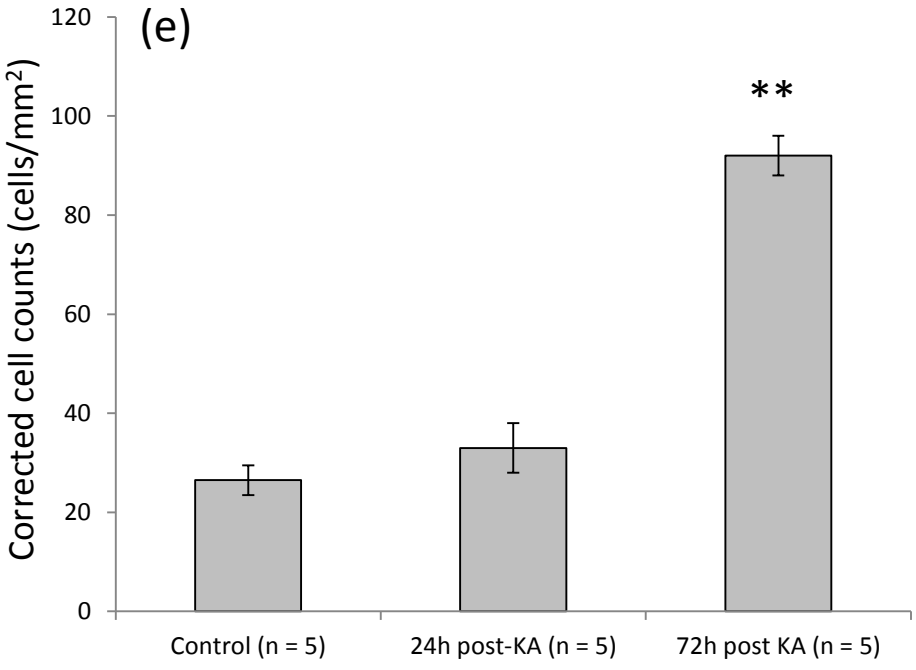

Microglia in CA3 region of hippocampus

Figure 3.6c. Gliosis in CA3 region of hippocampus during latent period following KA-induced status epilepticus. (d) Corrected astrocyte cell numbers in CA3 region . *F_{12} = 122.0, $p < 0.001$ **(e)** Corrected microglia cell numbers in CA3 region. **F_{12} = 53.22, $p < 0.001$

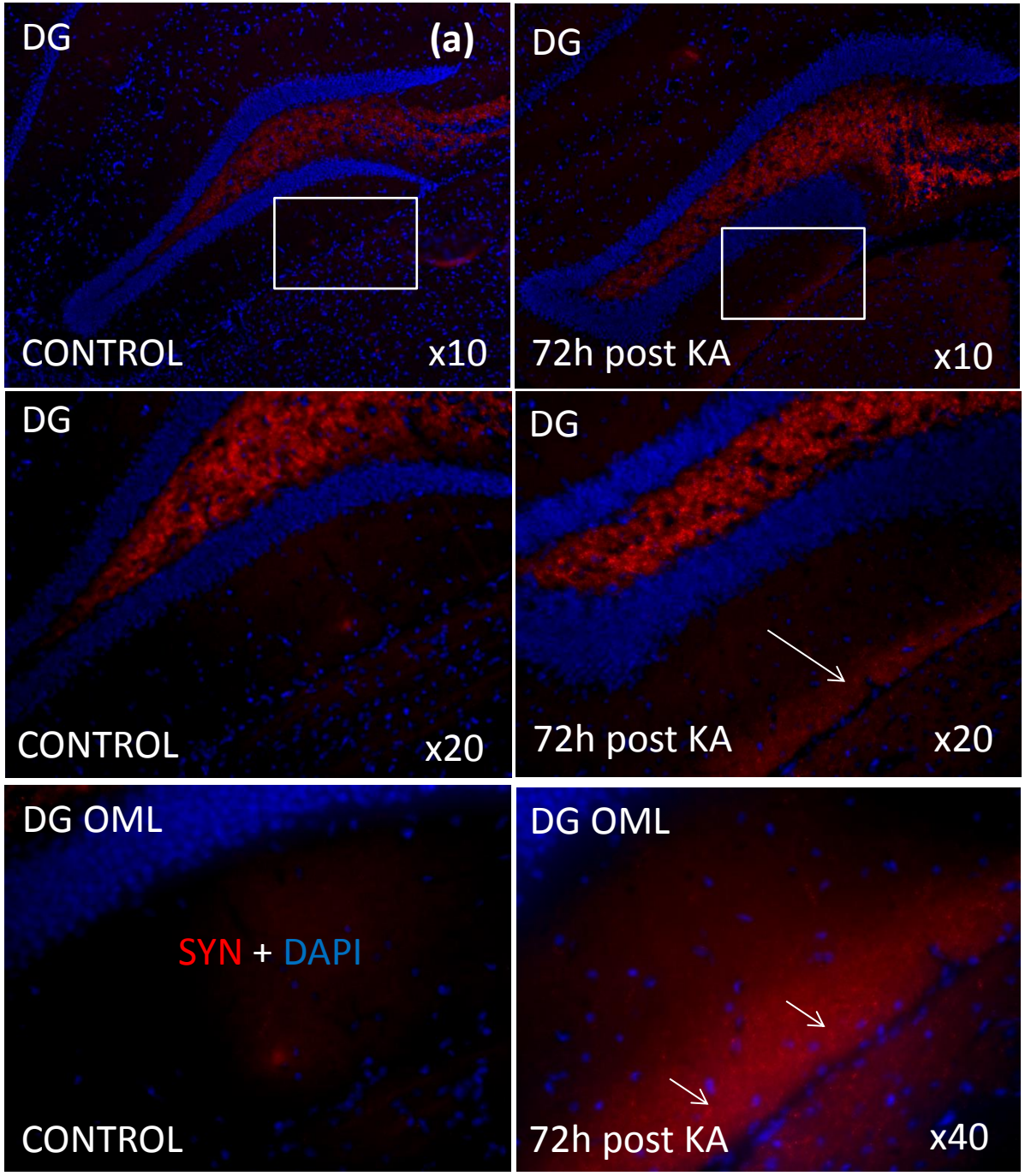

Figure 3.7. Kainic acid-induced status epilepticus increases Synpatophysin immunoreactivity in molecular layer of Dentate gyrus 3 days following injection. (a) photomicrographs. Magnification: x20, scale bar: 100 µm. DG: Dentate gyrus
(b) Quantitative analysis of staining intensity. *F_{12} = 92.55, $p < 0.001$.

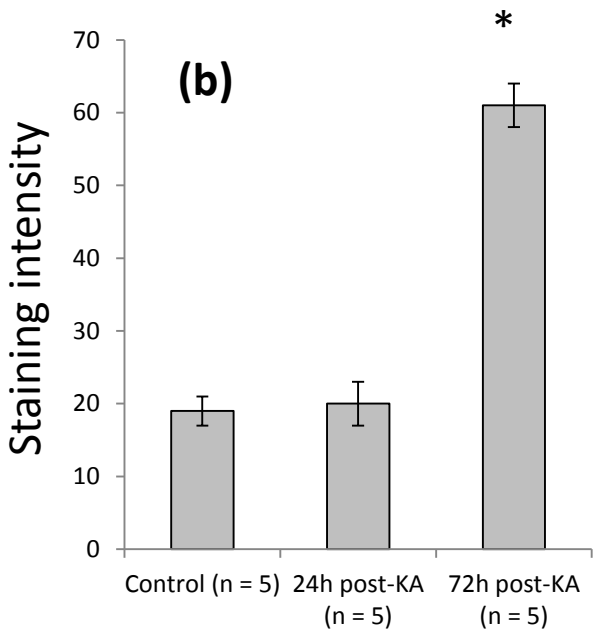

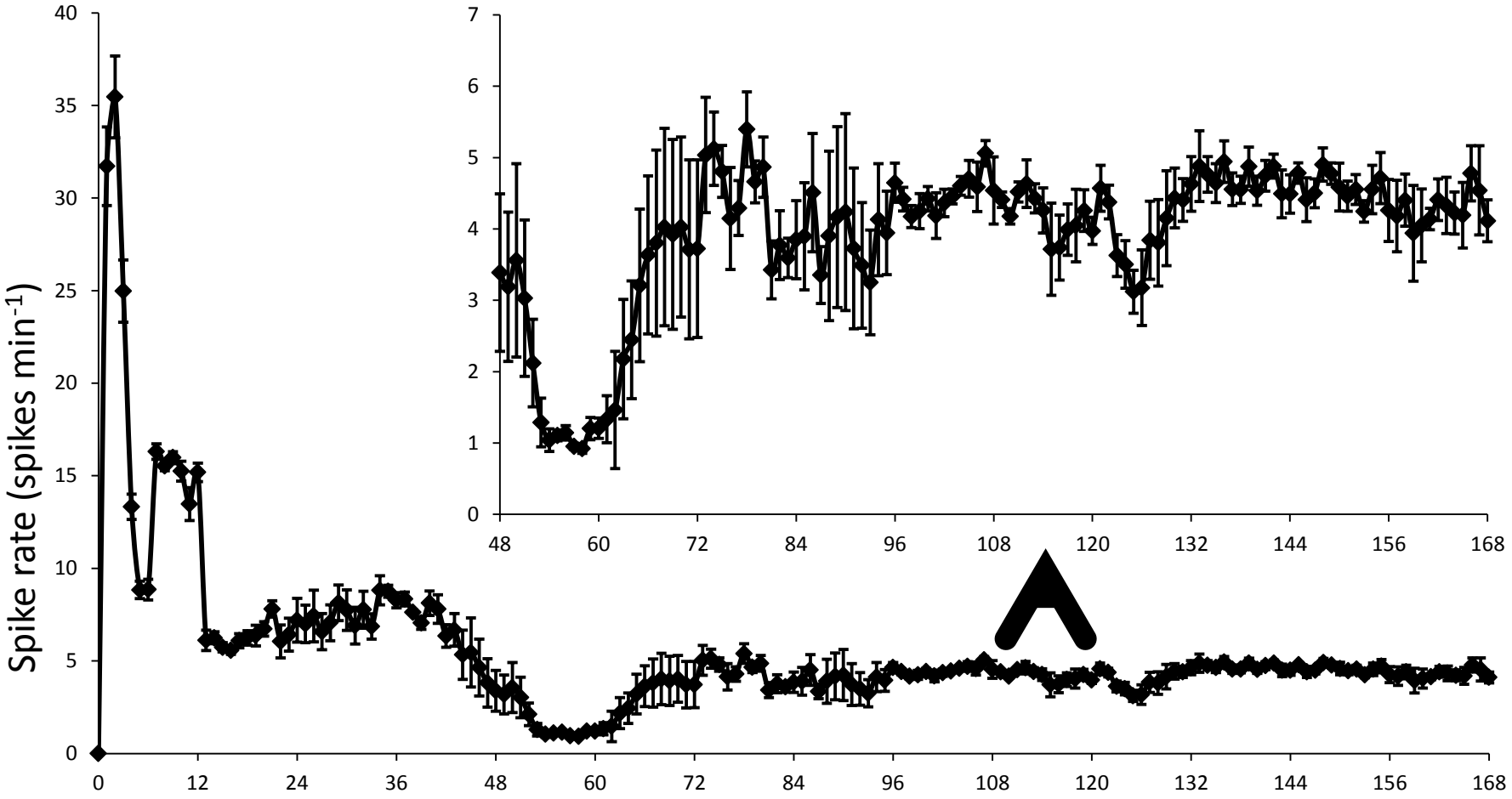

Figure 3.8. Interictal spike frequency for 7 days following injection with kainic acid. Inset: 48h – 168h at higher spike rate resolution.

3.5 DISCUSSION

3.5.1 Overview

Minor differences were found between strains in the anatomical distribution of GAD-67, SST, nNOS and CB. C57BL/6J mice generally have a lower tolerance to kainic acid than CD-1, however c-Fos expression in CD-1 mice is more widespread in the hippocampal formation following status epilepticus. 4 patterns of EEG associated with status epilepepticus in the C57BL/6J mouse are described and the frequency of epileptiform discharges and power distributed in the gamma frequency band quantified. Further, epileptiform spiking continues for at least 7 days following kainic acid injection, in the absence of any behavioural indicators and that reactive gliosis in the CA3 region and reactive synaptogenesis in the outer molecular layer of the dentate gyrus occur 72 hours after induction of SE with diazepam.

3.5.2 Inhibitory interneurons in the hippocampus

The distribution of GAD-67 immunopositive neurons in the hippocampal formation of C57BL/6J mice largely corresponded to the numerical densities found by Jinno et al (1998) using optical dissection with a confocal laser scanning microscope. Reduced numbers of neurons immunopositive for GAD-67 have been linked with an increased susceptability to seizures in a number of animal models, including in hyperbaric oxygen exposure, where a reduction in GAD-67 content occured shortly prior to convulsions (Li et al, 2008), cathepsin-D deficient mice, where a reduction of GAD-67 increased disinhibition (Shimizu et al, 2005) and the use of an antisense GAD

oligodeoxynucleotide (Wang et al, 2002) to expirmentally decrease expression of GAD67 protein. A small but sigificant difference between strains in the number of GAD-67 immunopositive neurons in the stratum oriens of the CA1 region of the hippocampus was found. However, the C57BL/6J strain which showed a slightly higher density of GAD-67 neurons in this region was also slightly more sensitive to kainic acid, suggesting that this difference was not of principal importance.

It has been reported that SST suppresses epiletiform activity in the CA1 and CA3 subfields of the hippocampus, is released in greater concentrations during seizures and that the selective loss of SST neurons may contribute to the neurobiological causes of epileptogenesis (Tallent & Siggins, 1999). A crude analysis of this information would suggest that seizure susceptability may be considered inversely proportional to SST expression in the hippocampal formation. Because SST expression was not found to be uniformly higher in either strain, but, rather, showed a slightly different anatomical distribution, with CD-1 mice showing higher numbers of SST-immunopositive neurons in the CA3 region and C57BL/6J mice showing higher numbers in CA1, it is difficult to interpret whether this is likely to have contributed to the sensitivity to kainic acid.

The anatomical distribution of nNOS in the hippocampal formation is consistent with that found by other authors in mice (Cork et al, 1998; Kovacs et al, 2009) and other mammalian species (Chung et al, 2004), with the highest density of nNOS-positive cells, with immunoreactivity in both soma and neurites, is found in the polymorphic layer of the dentate gyrus. nNOS expression has been tentatively linked to an increased susceptibility to seizures, for example Kovacs et al (2009) have reported

that nNOS inhibition reduces seizure-like events in an *in vitro* hippocampal slice model and Kim (2010) reported that an up-regulation of nNOS in the rat hippocampus in response to early-life seizures was followed by an nNOS-dependent elevation in seizure susceptibility in adulthood (Kim, 2010). It is likely that large differences between strains in hippocampal nNOS expression would lead to similar difference is sensitivity to kainic acid. Our study showed a slightly increased number of nNOS-immunopositive neurons in C57BL/6J mice, particularly in the stratum oriens of the CA3 region. This could be considered a potential contributor to the increased sensitivity to kainic acid in this strain.

Data for the distribution of CB largely concurred with that reported in C57BL/6J mice by Maskey et al (2012). Decreased CB immunoreactivity in the hippocampal formation has been linked with temporal lobe epilepsy in humans (Magloczky et al, 1997) and in genetically epilepsy-prone rats (Montpied et al, 1995) and there is evidence to suggest that alterations in hippocampal expression of CB may be one potential mechanism for the mechanism for seizure control exerted by the ketogenic diet (Kim & Rho, 2008). No significant difference was found however, in the anatomical distribution of CB-immunopositive neuronal cell bodies. Neither were any qualitative differences in the distribution of fibres observed, suggesting that CB expression was unlikely to be an important difference between the two strains.

Although minor differences in the anatomical distributions of neuropeptides in the hippocampal formation were found between the two strains and the clear importance of the network dynamics of inhibitory interneurons in modulating susceptability to seizures, it is not possible, from our data to make any strong connection between

differences in interneuron distribution and seizure susceptabiilty. Differences that were found were small and did not always correlate with seizure severity in the way predicted from the literature. From intraperitoneal injection to the expression of status epilepticus, there are myriad variables, such as the rate of adsorption of the drug into the blood stream, the permeability to the drug of the BBB, fine network dynamics in the hippocampus, or expression of glutamate receptors and ion channels which went untested, but may differ between strains.

3.5.3 Behaviour comparison between strains

The outbred CD-1 strain is not widely used in studies of seizure and epilepsy and so little data exists regarding sensitivity to kainic acid. The C57BL/6J strain, however, as the principal background strain for genetic studies, has been widely investigated. Comparisons between the strains in response to convulsant drugs are limited, however, Shibley & Smith (2002) report an increased latency to seizure in C57BL/6J mice in comparison with CD-1 mice, induced with pilocarpine, contrasting with our findings with KA-induced status epilepticus.

The dose of kainic acid administered via i.p injection necessary for inducing convulsive motor seizures in mice varies considerably across strains. More surprisingly, however, it also varies within the same strain across studies. Hu et al (1998) report only 2 out of 6 mice displaying manual automatisms at a dose of 20mg/kg, with 4 out of 6 mice not even showing any rearing behaviour. Indeed, at 40mg/kg, there was still no mortality. Ferraro et al (1995) report that 25mg/kg KA was sufficient to induce tonic-clonic seizures in only 25% of C57BL/6J mice.

Schauewecker & Steward (1997), in a study investigating response to KA across a range of inbred strains report a dose of 25mg/kg as being sufficient for inducing tonic-clonic seizures whilst limiting mortality in C57BL/6J and this dose seems to be fairly standard in other studies.

C57/Bl6 mice have often been contrasted with DBA strains as seizure resistent vs. seizure-prone, respectively (Engstrom & Woodbury, 1986; 1988; Wang & Chow, 1994; Kurschner et al, 1998). In contrast, our studies indicated that 20mg/kg was sufficient a dose to induce tonic-clonic seizures in of C57BL/6J mice, while increasing the dose to 25mg/kg induced mortality in almost 50% of animals (data not shown), suggesting a higher sensitivity to KA in C57BL/6J mice than previously reported.

While a fairly consistent response between animals caged together was found, between cages, there was greater variation. It is possible that this is due to an increased sensitivity to environmental factors resulting from isogenicity. Subtle differences between laboratory can manifest themselves in different behavioural responses in inbred mouse strains. It may be that the same is true for responses to KA, perhaps accounting for the variation in responses reported across laboratories and between studies. While no similar issues are typically reported in the literature, Benkovic et al (2004) report a biphasic response to systemic KA in C57BL/6J mice, with a hypersensitive population showing high mortality in response to KA administration.

3.5.4 Immediate early gene expression in hippocampus between strains

Expression of c-Fos is triggered by excessive levels of intracellular Ca^{2+} and has been widely used as a marker for excitotoxic glutamatergic neurotransmission (Gall *et al.,* 1998). c-Fos immunoreactivity is considered a hallmark of neuronal network activation and the spatiotemporal pattern of expression in the hippocampal formation is a reliable and sensitive indicator of seizure severity (Samoriski *et al.,* 1997; Willoughby *et al.,* 1997; Vezzani *et al.,* 2000). In mice, c-Fos is expressed in dentate granule cells within 30 to 90 minutes of a seizure and in pyramidal cells of CA1, CA3 and the subiculum at between 2 to 6 hours.

Our data indicates that at 2 hours following KA administration, in C57/BL6J mice, c-Fos in excitatory circuits is largely restricted to dentate granule cells, whereas in CD-1 mice, c-Fos expression extends in the pyramidal cell layers of CA3, CA2 and CA1 of the hippocampus. This is indicative of neurons in these regions being exposed to high levels of excitotoxic stress. However, it may not be entirely appropriate to infer information about the spatial evolution of epileptiform activity from c-Fos distribution. Rather, the anatomical distribution of c-Fos proceeds according to the severity of the seizure and the time interval. Rather than an anatomical distinction between the two strains in epileptiform activity, this is more likely to represent an increased severity of epileptiform activity per se in the hippocampi in CD-1 mice in comparison with C57BL/6J, in contrast to behavioural observations of motor seizures.

3.5.5 Electrographic status epilepticus in C57BL/6J mice

For various reasons, the vast majority of electrographic data recorded in experimental seizure models has come from rats. With the increasing use of mice as a model organism and the development of microtechnology, however, an increasing number of studies are being performed in mice. Data that is consistent between species and strains and has correlates in human patients is of greatest significance. Typically, in animal models of TLE, the actual period of SE has attacted less interest for analysis than subsequent electrographic changes. This is partly because of the challenge of making meaningful interpretations of such chaotic data and because SE has been generally considered merely as a method of induction. Our qualitative observations of epileptiform activity in the EEG trace corresponds strongly with that observed by Treiman et al (1990) and Medvedev et al (2000) following KA-induced SE in rats. The gradually increasing power of γ-frequency over the 2 hour period of analysis conforms to the findings of Lehmuke et al (2009) using a similar model and method of analysis in rats.

3.5.6 Gliosis during 'latent period' in C57BL/6J mice

Reactive gliosis in the hippocampal formation has long been considered a hallmark of TLE. Evidence of gliosis associated with neuronal loss in resected hippocami from TLE patients has been reported numourous times (e.g. Crespel et al, 2002; Cohen-Gadol et al, 2006), however the role that gliosis plays in disease progression is impossible to dissect from correlations with disease state in human sections alone. Evidence from animal studies indicates that the effect of gliosis on neuronal loss or survival and in modulating network dynamics is strongly dependent on the extent and duration of the gliosis and on tissue specific microenvironmental factors.

While low levels of astrocyte proliferation may contribute to protecting neurons with the release of trophic factors and reduce the excitability of neuronal assemblies by taking up glutamate from the extracellular space, higher levels of gliosis are associated with molecular changes in astrocytes, including the suppressed expression of glutamate transporter-1 (Tanaka et al, 1997) and glutamate-aspartate transporter (Watanabe et al, 1999) and enzymes involved in glutamate metabolism, such as glutamine synthatase and glutamate dehydrogenase (Eid et al, 2004). These changes reduce the capacity of astrocytes to manage extracellular levels of glutamate in the extracellular space (Coulter & Eid, 2012) and may contribute to the increased excitability of neuronal networks.

Reactive astrocytes may also provide a source of glutamate. Because they release glutamate through a regulated Ca^{2+}-dependent mechanisms, high densities of reactive astrocytes may play a causal role in synchronous firing of large populations of neurons. Ortinski et al (2010), however found an alternative mechanism for the increased excitability of neuronal circuits in the hippocampus following reactive gliosis. By virally inducing astrogliosis, this grou found a reduction in inhibitory drive, while excitatory neurotransmission remained intact.

Regardless of the extent to which gliosis plays a pro- or anti- epileptogenic role, the activation and proliferation of glial cells is a well characterised feature of the early stages of epileptogenesis and strongly predictive of neuronal loss and the development of spontaneous seizures (Vezzani *et al.,* 2000; 2009; Foresti *et al.,* 2009). The increased number of both astrocytes and microglia, the morphological

changes described and the invasion of these cells into stratum lucidum and the pyramidal cell layer of CA3 at 72 hours (figure 3.6) is predictive of both neuronal loss in this region and a decreased threshold for seizure generation.

Other authors have found similar results in different models. Do Nascimento et al (2012) report a slight increase reactive astrogliosis in the CA3 region of the mouse hippocamus at 24 hours and a peak in astrogliosis in this region one week following the induction of status epilepticus in a pilocarpine induced SE model, however, they did not investigate intervening timepoints. A greater number of these studies have been performed in rats. Hendrikson et al (2001) report extensive gliosis in the hippocampus, with upregulation of markers for both microglia and astrocytes 8 days following the induction of SE in rats, however, again, their study offers no data regarding the latency to onset of gliosis as earlier timepoints were not investigated. Our data suggest that, in the case of KA-induced SE in mice at least, the initiation of reactive gliosis occurs far earlier than 1 week. Strong evidence was found of astro- and microgliosis in areas CA3 and CA1 from 72h onwards, correlating with the sites where neuronal loss has been reported in the hippocampus, both of TLE patients (Wieser, 2004) and in rodents following a period of status epilepticus (Nitecka et al, 1984).

The extent to which the increase in GFAP+ve astrocytes and microglia in the CA3 region of the hippocampus post seizure is the result of cell proliferation or migration of existing cells into the site of insult from other anatomical regions is unclear. Work done in culture has shown that astrocytes both proliferate and migrate to the site of injury when challenged. Under these experiments, it is easier to track cell fate by

tagging cells, or using BrdU to mark newly formed cells. This is more difficult to study in vivo and the methods that we have used do not tackle this issue.

3.5.7 Synaptophysin

SYN is effectively a marker of activity-dependent synaptogenesis, rather than of synapse density per se. The high density of SYN immunoreactivity constitutively expressed in the stratum lucidum of CA3 and dentate hilus is indicative of a high turnover of synapses in these regions, possibly relating to their role in the consolidation of spatial memory. Our studies show that at 72h post KA, these areas of high SYN immunoreactivity remain unchanged, while a modest increase in SYN immunoreactivity occurs in the OML of the dentate hilus within 72h of KA administration, indicating reactive synaptogenesis in this region (figure 3.7).

Neosynapse formation in the molecular layers of the dentate gyrus is strongly predictive of the emergence of chronic epilepsy (Wenzel et al, 2000) and is usually associated with the aberrant sprouting of mossy fibres, creating recurrent connections between dentate granule cells. In SE rodent models, however, while varying depending on species, strain and method of induction, mossy fibre sprouting is typically reported no sooner than from around 4 - 8 weeks following SE (Cantallops & Routtenberg, 2000). Our data suggests the formation of new synapses precedes this by a significant time margin.

Hendrikson et al (2001) also found evidence of neosynapse formation in the molecular layer of the dentate gyrus 8 days following the induction of SE in rats,

however, the progression of epileptogenesis is more rapid in mice and the authors did not investigate earlier timepoints. Both our data and that of the Hendrikson group indicates that reactive synaptogenesis in the molecular layer of the dentate gyrus long precedes the sprouting of mossy fibres. The vast majority of inputs to the outer molecular layer are from by neurons originating in layer II of the entorhinal cortex via the perforant path, suggesting that the increase in synaptophysin immunoreactivity may indicate a strengthening of this perforant path input. It may be that the molecular cues involved in synaptogenesis in the early 'latent phase' are also involved in the formation of aberrant synapses formed between dentate granule cells in later stages of the development of chronic epilepsy.

3.5.8 EEG recorded during 'latent period'

The causative role of IEDs in the progression of epilepsy is not at all clear (Gotman, 1991; Janszky et al, 2001). While it was previously assumed that a seizure developed from an IED (Ralston, 1958), more recent research has revealed that the two phenomena are characterised by different EEG patterns are are, in part mediated by different neuronal mechanisms. Katz et al (1991) demonstrated a decrease in IED activity prior to seizures, while numerous studies have suggested that IED activity actually inhibits seizures (Engel & Ackermann, 1980; Barbarosie & Avoli, 1997).

Long-term potentiation (LTP) induced by spikes in vitro can increase the strength of recurrent collateral synapses in a network, thereby increasing positive feedback and the propensity for synchronous activity (Staley et al 2001). Staley et al (2011)

suggest that IEDs play the role of maintaining and expanding recurrent networks by inducing synaptic changes, and thereby drive epileptogenesis. Regardless of the causative role of IEDs, however, they are strongly predictive for the development of chronic epilepsy. In a SE model in rats, Chauviere et al (2012) report that IEDs preceed spontaneous seizures by several days and that shortly before spontaneous seizures, IED with a spike and wave shape lose the wave.

3.5.9 Conclusions

C57BL/6J were more sensitive to KA-induced SE, however, this was unlikely to be related to the minor differences between the two strains in the distribution of GAD-67, SST, nNOS and CB in the hippocampal formation. Interestingly, despite their greater tolerance of KA, c-Fos expression in CD-1 mice was more widespread in the hippocampal formation following status epilepticus, suggesting that our understanding of the mechanisms underlying the expression of immediate early genes in response to excitotoxicity is insufficient. The patterns of EEG observed during status epilepticus the C57BL/6J mouse had correlates with observations in rats and in human patients. Epileptiform spiking continues for at least 7 days following kainic acid injection, in the absence of any behavioural indicators. Reactive gliosis occured in the CA3 region of the hippocampus at an earlier timepoint following SE than has previously been reported and that reactive synaptogenesis in the molecular layer of the dentate gyrus precedes mossy fibre sprouting by a significant period of time.

Chapter 4. Effects of an NR2B antagonist, [R-(R,S)]-α-(4-hydroxyphenyl)-β-methyl-4-phenyl-methyl)-1-piperidine-propanol (Ro 25-6981), and an nNOS inhibitor, N^w-propyl-L-arginine (L-NPA), on acute KA-induced status epilepticus and neurobiological and electrographic changes in the early latent period in C57BL/6J mice.

4.1 ABSTRACT

In this chapter, the anticonvulsant effects of a specific antagonist of the NR2B subunit of the NMDA receptor, Ro 25-6981 and a highly selective neuronal nitric oxide synthase inhibitor, L-NPA, was investigated on kainic acid induced status epilepticus using behavioural scoring and analysis of c-Fos distribution in the dentate gyrus 2 hours following injection with kainic acid. Further, the effect of L-NPA on modulating electrographic status epilepticus and electrographic changes during the 'latent period' was investigated, using an implantable telemetry device for the recording and transmission of EEG signals. Neurobiological changes, such as gliosis and reactive synaptogenesis during the 'latent period' were also investigated

Status epilepticus was induced with 20mg/kg kainic acid and seizures terminated after 2h with diazepam (10mg/kg, i.m). Pharmacological interventions, or appropriate vehicles were delivered 30 minutes prior to kainic acid. Behavioural seizure severity was scored using a modified Racine score and c-Fos immunoreactivity in the dentate

gyrus was investigated using immunohistochemistry. Reactive gliosis and synaptogenesis were investigated using astrocyte and microglial markers and a marker of activity dependent synaptogenesis, synaptophysin, respectively. R 25-6981 was found to have little effect on status epilepticus or c-Fos expression, however, L-NPA treatment reduced the severity and duration of convulsive motor seizures, the power of EEG in the gamma band, and the frequency of epileptiform IEDs during status epilepticus, reduced c-Fos expression in dentate granule cells 2h post kainic acid injection. Furthermore, L-NPA pretreatment reduced electrographic indicators of epileptogenesis during the 'latent period', including the frequency of epileptiform discharges over the first 7 days and reactive gliosis and synaptogenesis at 3 days following status epilepticus. These results suggest that nNOS facilitates seizure generation during SE and may be important for the neurobiological changes associated with the development of chronic epilepsy, especially in the early stages of epileptogenesis. As such, it might represent a novel target for disease modification in epilepsy.

4.2 INTRODUCTION

4.2.1 Overview of NMDA receptor and NMDAR-mediated excitotoxicity

The NMDAR acts as a coincidence detector, activated only when the membrane is simultaneously depolarized and activated by glutamate, allowing it to reinforce signals that are close in space or time. NMDAR, in the open state allows for the influx of Ca^{2+} into the neuron, which can activate numerous downstream targets, modulating ion channel kinetics (Derkach et al, 1999), transcription (Malenka & Bear, 2004) or the trafficking of AMPA receptors to the cell surface (Bredt & Nicoll, 2003). The NMDA receptor is a powerful modulator of synaptic plasticity, underlying mechanisms of memory. Under pathophysiological conditions however, Ca^{2+} influx through the NMDA receptor has been heavily implicated in mediating excitotoxic cell death (Duchen, 2000). NMDAR kinetics can also be modulated by a ligand binding site for the amino acid neurotransmitter, glycine, which can act as a co-agonist (Danysz & Parsons, 1998)

High levels of glutamate signalling associated with seizures, and particularly, the excessive stimulation of NMDA receptors, can lead to a series of potentially neurotoxic events (Hellier et al, 2009). The Ca^{2+} influx, vital to normal signalling, when in excessive quantities, can lead to neurodegeneration, the perturbation of neural networks, leading to a chronic state of seizure susceptibility (Mody & Macdonald, 1995). The clinical utility of general NMDA antagonists, however, is reduced by the severe associated side-effects, including psychotropic effects, similar

to schizophrenia (Newcomer et al, 1999). Any neuroprotective strategy of potential clinical importance must leave physiological NMDA signalling largely intact.

Although general NMDA receptor antagonists, such as ketamine and MK801 have proven extremely problematic in the clinic, the increasing understanding of the extent of NMDA receptor heterogeneity has reinvigorated research into potential methods for restricting its pathophysiological role. The NR2 subunit content of the NMDA receptor defines the receptors' location on the cell membrane and its pharmacological and functional properties (Moyner et al, 1992). Antagonists which are subunit selective have been developed and their efficacy in suppressing disease progression in a range of CNS pathologies is being explored.

An alternative approach is to target downstream effectors of Ca^{2+} influx through the NMDA receptor. In neurons, Ca^{2+} influx through NMDARs promotes cell death more efficiently than through other Ca^{2+} channels (Aarts et al, 2002), suggesting that the most important proteins responsible for Ca^{2+}-dependent excitotoxicity reside within the NMDAR signaling complex (NSC) (Soriano et al, 2008). Two potential pharmacological interventions following KA-induced SE in C57BL/6J mice were investigated, targetting NMDA receptors containing the NR2B subunit with a selective antagonist, (αR,βs)-α-(4-Hydroxyphenyl)-β-methyl-4-(phenylmethyl)–1-piperidinepropanol maleate (Ro25-6981) and use a selective inhibitor of nNOS, N^{w}-propyl-L-arginine to reduce Ca^{2+} induced NO signalling at excitatory synapses..

4.2.2 NMDAR subunits

NMDARs are tetrameric (some reports have indicated pentomeric) complexes made up of a combination of subunits from the groups NR1, NR2 and NR3 (Malherbe et al, 2003). Of these different groups, there are eight different NR1 subunits, four NR2 and 2 NR3 subunits. Whereas all NR1 subunits are encoded in a single gene, with the diversity stemming from alternative splicing, each NR2 and NR3 subunit is independently encoded in the DNA. The rules of subunit composition in functioning NMDARs is incompletely understood, however, it seems that at least one NR1 and one NR2 subunit is required. The NR1 subunit provides the glycine binding site and the NR2 subunit provides the site for glutamate binding. Data regarding NR3 is limited, however, Nishi et al (2001) reported that it can act in a dominant negative fashion, while it has also been demonstrated that it can form excitatory channels with NR1, activated by glycine (Chatterton et al, 2002).

NMDAR subunits all share a common membrane topology, characterized by a large extracellular N-terminus, three transmembrane segments (TM1, 3 and 4), a re-entrant pore loop (M2), an extracellular loop between TM3 and TM4 and a cytoplasmic C-terminus. While the extracellular loop determines the affinity for neurotransmitters, the C-terminal is the site of the majority of variation between subunits, conferring differences between differently composed receptors in distribution, kinetics, interaction with intracellular proteins and physiological function (Danysz & Parsons, 1998). The NR1 subunit forms a substrate for the folding of other subunits for the formation of the complete receptor, however little is known regarding functional differences in NR1 subunit diversity. Of the three subunit families, the most completely understood is the NR2 subunit.

4.2.3 NR2B and Ro 25-6981

NMDA receptors modulate a wide array of physiological processes through Ca^{2+} signalling. In order for a single molecule to modulate such a diversity of signalling pathways within the cell, requires spatiotemporal division. At excitatory synapses, a collection of Ca^{2+}-sensitive effector molecules are held in close apposition to the NMDAR Ca^{2+} channel (Soriano et al, 2008) where highly localized Ca^{2+} IEDs exert physiological effects dependent on the identity of effector molecules in the microdomain. Ca^{2+} influx through other routes, such as extrasynaptic NMDA receptors effects an entirely different set of signalling pathways with divergent physiological functions (Dumas, 2005).

The pharmacology, functionality and location of NMDA receptors is largely determined by their NR2 subunit content. NMDA receptors containing NR2B subunits are expressed extrasynaptically in adults (Kudryashova, 2007), where they mediate neuronal responses to excessive glutamate in the extracellular space as a result of 'spill over' from the synaptic cleft or release from astrocytes (Pasti et al, 2001). A role for NR2B-containing extrasynaptic NMDA receptors in mediating neuronal death has been reported (Poddar et al, 2010) and NR2B subunit specific antagonists have been developed in order to intervene in this pathway without disrupting the normal functioning of synaptic NMDA receptors.

Ro25-6981 is a moderate-affinity, uncompetitive and NR2B-selective NMDAR antagonist that shared a structural similarity with ifenprodil (Lynch et al, 2001), and binds to the allosteric modulatory site on the NR2B leucine/isoleucine/valine binding

site (LIVBP) (Malberbe et al, 2003). Positive outcomes have been reported when used in animal models of, amongst others migraine (Peeters et al, 2007), Alzheimer's disease and ischemic brain injury (Wang & Schaib, 2005). The efficacy of Ro 25-6981 in modulating the severity of a period of epileptiform behaviour was investigated when administered prior to the induction of KA-induced SE. The severity of epileptiform behaviour was scored using the Racine scale and the anatomical distribution of c-Fos was quantified in the dentate gyrus 2 hours following injection with KA.

4.2.4 nNOS and L-NPA

Nitric oxide (NO), a gaseous signaling molecule, was first reported to have a role in neurotransmission in the central nervous system (CNS) by Garthwaite *et al* (1989). It has since been ascribed a wide range of neurophysiological functions, including the modulation of synaptic plasticity (Yang & Cox, 2007). Importantly, NO is also implicated in the pathogenesis of a variety of CNS disorders, including epilepsy (Takei, *et al.,* 2001; Pereira de Vasconcelos *et al.,* 2005; Hagioka *et al.,* 2005; Kovacs *et al.,* 2009; Kim, 2010; Arhan *et al.,* 2011). NO is catalysed by three isoforms of NO synthase (NOS); endothelial (eNOS), inducible (iNOS) and neuronal (nNOS), and plays a pleiotropic role in the nervous system which is determined by the site of catalysis, NOS isoform and cell type involved. NO, produced by nNOS associated with the NSC may mediate much of the neurotoxic effects of excessive NMDAR signalling (Bonfoco, et al, 1995). As discussed in Chapter 1, high levels of NO production, coupled with the generation of the superoxide anion, O^{2-}, can react to form peroxynitrite, (ONOO-) resulting in neuronal damage (Heales et al, 1999).

Using a broad range of *in vivo* and in vitro models, non-specific NOS inhibition has been shown to have a pro-convulsive effect (Takei, 2001; Hagioka, 2005), which may be largely attributed to the inhibition of eNOS modulation of local cerebral blood flow (CBF) (Pereira de Vasconcelos et al., 2005). Evidence for the role of nNOS in seizure generation and/or modulation is less clear, with questionable specificity of available inhibitors, (such as 7-nitroindazole and 3-bromo-7-nitroindazole) and conflicting reports on the extent of nNOS involvement in CBF regulation (Santizo et al., 2000; Pereira de Vasconcelos, 2005).

A recent study has reported an up-regulation of nNOS in the rat hippocampus in response to early-life seizures, followed by an nNOS-dependent elevation in seizure susceptibility in adulthood (Kim, 2010). This suggests a role for nNOS in the epileptogenic process. Kovacs et al (2009) have reported that nNOS inhibition reduces seizure-like events in an *in vitro* hippocampal slice model, although this is yet to be tested *in vivo*. A highly selective nNOS inhibitor would offer an opportunity to address this issue. N^{w}-propyl-L-arginine (L-NPA) has been reported by Zhang et al (1997) to have a149- and 3,158-fold greater selectivity (Zhang *et al.,* 1997) over eNOS and iNOS, respectively. While various studies have suggested a more modest level of selectivity (Boer et al, 2000), used at the correct dose, it nevertheless offers a promising method for dissecting the contribution of neuronal NO from other sources. This has been exploited in a wide-range of studies of nitric oxide signaling pathways (e.g. Romero et al, 2012), but, to our knowledge has not yet been applied to an in vivo model of SE.

Using a period of KA-induced SE, the effects of L-NPA pre-treatment on epileptiform activity in C57BL/6J mice was investigated, in order to elucidate the role of nNOS signalling in modulating seizures. Three complementary approaches were employed to characterise the severity of SE. Behavioural seizures during SE were scored using a modified Racine score (Racine, 1972) and electrographic seizures detected using electroencephalography (EEG) recorded with an implanted telemetry device. In addition, neuronal activity, activity-dependent synaptogenesis and hippocampal gliosis were investigated immunohistochemically, using c-Fos (Samoriski *et al.,* 1997), synaptophysin, tomato lectin (microglia marker) and glial fibrillary acidic protein (GFAP, astrocyte marker) and analysed both qualitatively and semi-quantitatively.

4.3 MATERIALS AND METHODS

4.3.1 Overview

Information regarding materials and methods described in this chapter refer only to that which is specific to this particular study. For general materials and methods, see chapter 2 where detailed protocols of methods performed throughout all chapters are described, including: KA administration and behavioural scoring of SE, basic protocols used for immunohistochemistry, microscopy and quantification of immunohistochemistry, surgical procedures for the implantation of electrodes and transmitters and EEG data collection and analysis. For ease of understanding, however, some information is duplicated.

4.3.2 Animals

Experiments were performed in 10-12 week old male C57BL/6J mice. All animals were purchased from Charles River (UK) and maintained in the Biomedical Services Unit, University of Liverpool under controlled environmental conditions ($19^{o}C$ – $23^{o}C$, 12h light: 12h dark), with food and water available *ad libitum*. All experiments were carried out according to Animals (Scientific Procedures) Act 1986 approved by the Secretary of State, Home Office, UK and University's Ethical Review Committee.

A total of 60 mice were used in this study. 15 mice were used to test the effects of RO 25-6981, in the following treatment groups: dimethyl sulphide (DMSO) only (control, n = 5), DMSO + KA (vehicle, n = 5), RO-25 6981 + KA (n = 5) (see below for a more detailed description of this protocol). In these mice, epileptiform behaviour

was scored using a modified Racine scale for 2 hours after KA injection, before they transcardial perfusion for immunohistological analysis of c-Fos expression in the dentate gyrus.

Of the remaining 45 mice, 5 mice were used as naïve control animals and 30 mice were used for behavioural and immunohistological analysis. In all of these animals, pre-treatment of either 20mg/kg L-NPA or an equivalent volume of distilled water (DW, vehicle) was administered via i.p injection 30 minutes prior to 20mg/kg KA. Mice were perfused at 2 hours post-KA (Vehicle, n = 5, L-NPA, n = 5) or SE was terminated with diazepam and mice perfused at 24 (Vehicle, n = 5, L-NPA, n = 5) or 72 (Vehicle, n = 5, L-NPA, n = 5) hours following KA injection. Of the 10 remaining mice, telemetry devices were implanted (as described in chapter 2) and following post-operative recovery, were treated in the following groups: L-NPA + KA (n = 5), vehicle + KA (n= 5). In implanted mice, seizures were terminated with diazepam 2 hours following KA injection and EEG was recorded for 7 days.

4.3.3 Drugs, reagents and antibodies

L-NPA (Tocris, UK) was prepared in distilled water (DW) at a concentration of 5mg/ml and administered i.p at a dose of 20mg/kg. An equivalent volume of DW alone was used as a vehicle control. RO 25-6981 (Tocris, UK) was prepared in DMSO at a concentration of 2.5mg/ml and administered i.p at a dose of 10mg/kg. An equivalent volume of DMSO was used as a vehicle control.

Rabbit anti-c-Fos (1:2000) was purchased from Calbiochem (UK) and visualised using a CY3-conjugated donkey anti rabbit secondary antibody (1:200). Mouse anti-NeuN (1:400) was purchased from Chemicon (UK) and visualised using an FITC donkey anti-mouse secondary antibody (1:200). Rabbit anti-synaptophysin (1:1000) was a gift from Dr P Greengard, Rockefeller University, USA and visualised using a CY3-conjugated donkey anti-rabbit antibody (1:200). Mouse anti-GFAP (1:400) was purchased from Sigma Aldrich (UK) and visualised using an FITC-conjugated donkey anti-mouse secondary antibody (1:200) Biotinylated tomato lectin (1:500) was purchased from Sigma Aldrich (UK) and visualised using CY3-conjugated streptavidin (1:100). All flourochrome-conjugated secondary antibodies and streptavadin were purchased from Jackson Immunoresearch laboratories (UK). DAPI used for visualizing cell nuclei was in the Vectashield ® mounting medium (Vector Laboratories, UK).

4.3.4 Drug treatment and experimental groups

In the RO 25-6981 study, 10mg/kg RO 25-6981 diluted in DMSO (n = 5) or an equivalent volume of DMSO vehicle control (n = 5) was administered, i.p 30 minutes prior to i.p injection with KA. Behavioural seizures were scored for 2 hours and mice were sacrificed at this timepoint and perfused for immunohistochemical analysis. In the L-NPA study, 20mg/kg L-NPA or an equivalent volume of DW was administered 30 minutes prior to induction of SE with 20mg/kg KA. Again, seizures were scored for 2 hours and mice were either sacrificed at 2 hours (vehicle, n = 5; L-NPA, n = 5), or seizures were terminated with diazepam (i.m, 10mg/kg) and mice sacrificed at 24 (vehicle, n = 5; L-NPA, n = 5) or 72 (vehicle, n = 5; L-NPA, n = 5) hours post KA.

Mice implanted with telemetry devices for the recording of EEG (vehicle, n = 5; L-NPA, n = 5) were treated in the same way. Behaviour was assessed in all animals (vehicle, n = 20; L-NPA, n = 20).

4.4 RESULTS

4.4.1 Ro 25-6981 effect on kainic acid induced epileptiform behaviour

Ro 25-6981 administration prior to KA injection had little discernible effect on the severity of KA-induced status epilepticus when compared with mice treated with vehicle DMSO (Figure 4.1). The median peak seizure severity in both treatment groups was Racine 5 (Figure 4.1a, b), the latency to CMS was slightly reduced with Ro 25-6981 treatment, from 45 to 35 minutes (Figure 4.1c), while the duration of CMS was slightly increased, from 70 to 90 minutes, suggesting that, if anything, Ro 25-6981 had a facilitatory effect on seizures. Neither of these effects, however, was statistically significant.

4.4.2 Ro 25-6981 effect on SE-induced c-Fos expression

As with behaviour, Ro 25-6981 administration had little or no effect on SE-induced c-Fos expression in the dentate gyrus (Figure 4.2). c-Fos was expressed in between 60 and 75% of neurons in the granule cell layer of the dentate gyrus in both treatment groups and between 40 and 50% of neurons in the polymorphic and molecular layers. Ro 25-6981 treated animals showed a trend towards a decrease in c-Fos expression in granule cells and an increase in expression in neurons of the polymorphic and molecular layers, however this effect was small and insignificant.

4.4.3 L-NPA has anticonvulsant effect on kainic acid-induced epileptiform behaviour

Pre-treatment with L-NPA 30 minutes prior to KA-induced SE delayed and reduced the severity and duration of epileptiform behaviour (Figure 4.3). The peak severity score reached during the two hour period of observation was significantly reduced by L-NPA pre-treatment ($U = 294.0$ $p<0.001$, Figure 4.3a, b), the latency to onset of CMS was increased ($t_{38} = 2.130$, $p = 0.040$, Figure 4.3a, c) and the duration of CMS was decreased ($t_{38} = 4.303$, $p < 0.001$, Fig 4.3a, d).

4.4.4 L-NPA pretreatment suppresses SE-induced c-Fos immunoreactivity

In both groups, c-Fos immunoreactivity was largely restricted to dentate granule cells, however there was also lower levels of expression in neurons of the polymorphic and molecular layers (Figure 4.4a). Expression in the hippocampus, subiculum or entorhinal cortex was minimal (data not shown). L-NPA pre-treatment reduced the percentage of neurons expressing c-Fos in the DG as a whole by approximately 65% ($t_8 = 10.653$, $p < 0.001$, Fig. 4.4c) at 2h post-KA. This reduction was most pronounced in dentate granule cells (~70%) ($t_8 = 9.273$, $p < 0.001$), however, expression was also suppressed in the molecular layer, although no effect of L-NPA was found on c-Fos expression in the polymorphic layer. c-Fos expression was entirely restricted to neuronal nuclei at this timepoint, with no expression in the cytoplasm of either cell bodies, axons or dentrites (Figure 4.4c).

4.4.5 L-NPA reduces the severity of electrographic status epilepticus.

Following post-operative recovery, mice behaved normally, with no obvious effect on eating, drinking, activity levels, alertness, aggression or signs of discomfort. EEG activity was regular, with some changes in amplitude and frequency dependent on activity levels (Figure 3.4). L-NPA alone had a mild behavioural effect, with mice showing increased alertness, aggression and resistance to handling, in comparison with vehicle treated animals; however, this was not accompanied by any discernible effect in the EEG (data not shown).

Following the administration of KA, the frequencies of epileptiform discharges in vehicle pre-treated mice increased over the initial 20 minutes to a peak of approximately 65 epileptiform discharges min^{-1}. In L-NPA pre-treated mice, this slope was shallower, with an initial peak reached at approximately 25 minutes, of just below 35 epileptiform discharges min^{-1} (Figure 4.5a). Throughout the entire duration of the 2 hour period of induced status epilepticus, L-NPA pre-treated animals had a reduced frequency of epileptiform discharges in comparison with animals in the vehicle pre-treated group (Figure 4.5a). When split into 30 minute bins, the frequency of epileptiform discharges was significantly reduced by L-NPA pre-treatment for all time points (0 – 30 mins: $t_8 = 5.946$, $p < 0.001$, 30 – 60 mins: $t_8 = 4.480$, $p = 0.002$, 60 – 90 mins: $t_8 = 5.420$, $p < 0.001$, 90 – 120 mins: $t_8 = 7.400$, $p < 0.001$, Figure 4.5b).

From the initial peak, 20 minutes following KA injection, spike frequency in vehicle pre-treated animals followed a cyclical pattern, with peaks ranging between 50 and 70 epileptiform discharges min-1, troughs ranging between 30 and 40 epileptiform discharges min-1 and a cycle length of approximately 20 minutes (Figure 4.5a). The

frequency of epileptiform discharges in L-NPA pre-treated animals followed a similar cyclical pattern, however, the difference between peaks and troughs was smaller (peaks: 30 – 40 epileptiform discharges min-1, troughs: 20 – 30 epileptiform discharges min-1) and the cycle lengths were shorter (~10 mins) (Figure 4.6a). While in vehicle pre-treated animals, the frequency of epileptiform discharges began to decline from around 100 minutes, in L-NPA pre-treated animals, this occurred approximately 15 minutes earlier.

In contrast to the frequency of epileptiform dischages, the power distributed in the γ-band increased steadily in vehicle pre-treated animals from the point of KA administration to a peak of 5dB around 90 minutes post injection (Figure 4.6a). In L-NPA pre-treated animals, a similar pattern was seen, with a peak in γ-band also around 90 minutes, however, the peak was considerably lower at around 2dB and throughout the entire the 2 hour period, γ-band power was less than 50% of that seen in the vehicle pre-treated group. When divided into 30 minute bins, the power distributed in the γ-band was significantly lower in L-NPA pre-treated animals for every timepoint apart from the first 30 minutes (30 – 60 mins: $t_8 = 3.135$, $p = 0.014$, 60 – 90 mins: $t_8 = 3.664$, $p = 0.006$, 90 – 120 mins, $t_8 = 4.540$, $p = 0.002$, Figure 4.6b).

4.4.1 The effects of L-NPA pre-treatment on electrographic seizures during early latent period

Following the termination of SE with diazepam and subsequent recovery, no epileptic behaviour was observed in any animals during the first 7 days. Diazepam

administration 2 hours following KA injection, terminated behavioural indicators of epileptic activity, however, although epileptiform spiking was dramatically reduced, it was not completely stopped, but reached a nadir of approximately 8 IEDs min^{-1} in vehicle pre-treated mice and 6 IEDs min^{-1} in L-NPA pre-treated mice (Figure 4.7a, b). In both treatment groups, following the initial diazepam-induced sharp decline in IED frequency, the IED rate increased approximately 6 hours following diazepam injection, presumably as an effect of the reduction in the concentration of the drug (Figure 4.7a, black arrow) to approximately 17 IEDs min^{-1} in vehicle pre-treated animals and 12 IEDs min^{-1} in L-NPA pretreated animals.

During the period from 6 – 12 hours, the frequency of epileptiform spiking was between two and three-fold higher in vehicle pre-treated animals than in animals pre-treated with L-NPA (Figure 4.7a). From 12 hours, the IED frequency in the two treatment groups diverged, with Vehicle pre-treated animals showing a steady, or slightly increasing rate of firing between 5 and 10 IEDs min^{-1} between 12 and 40 hours before declining, while IED frequency in L-NPA pretreated animals continued to decline steadily from 12 hours onwards. This period showed the most marked difference between the treatment groups throughout the entire 7 day period observed following the termination of seizures with diazepam (Figure 5.1a, black horizontal line).

IED frequency was lowest in Vehicle pre-treated animals by around 52h post KA injection. In L-NPA pretreated animals, this low point occurred around 36h. From between 50 and 65h, the IED frequency in both treatment groups began to increase again, with a local peak in vehicle pre-treated animals at approximately 5 IEDs min^{-1}

and in L-NPA pre-treated animals at approximately 3 IEDs min^{-1} (Figure 4.7a). From approximately 80h post KA until the termination of the experiment at 7d, IED frequency remained relatively consistent, with Vehicle pre-treated animals showing between 4 and 5 IEDs min-1 and L-NPA pre-treatment suppressing this by approximately 2 - 2.5 fold. No obvious circadian effects were observed in the IED rate of either treatment group (Figure 4.7a). For all time periods quantified, L-NPA reduced the frequency of IEDs (3 – 12 h: $t_8 = 6.788$, $p < 0.001$. 12 – 48h: $t_8 = 14.45$, $p < 0.001$. 48 – 168h: $t_8 = 3.907$, $p = .0045$, figure 4.7a).

In summary, L-NPA treatment, prior to KA administration, increased the effectiveness of diazepam at reducing the IED rate more quickly in comparison with vehicle pre-treated mice (Figure 5.1a). It reduced the subsequent increase in IEDs around 6h following the reduced control of epileptiform activity by diazepam (Figure 5.1b). It decreased the latency for the IED frequency to reduce below 5 IEDs min-1 by approximately 16 hours (Figure 5.1a) Most importantly, in comparison with Vehicle pre-treated mice, L-NPA pre-treatment reduced the IED frequency between 3 and 7 days post KA injection by 2 – 2.5 fold.

4.4.2 L-NPA pre-treatment reduces gliosis during early latent period.

In view of assertaining L-NPA's effect beyond acute SE period and to understand whether seizure modulation by L-NPA during SE will have an effect on epileptogenic events during the early latent period, glial cells and synaptophysin immunostaining was examined. At 24h post-KA period, there was no significant difference in microglia or astrocyte cell counts in any treatment groups (Figure 4.8f – i), nor was

there any qualitative differences in astrocyte or microglial morphology that would associate them with an activated state. This suggests, that in the kainic acid model, 24h is too early to see changes in glial activation associated with seizures.

By 72h, however, qualitative changes in morphology of both astrocytes and microglia could be observed in sections from animals of both treatment groups. Astrocytes expressed higher densities of GFAP and were hypertrophic (Figure 4.8b, c) and many microglia were observed to assume the rod-like 'activated' morphology (Figure 4.8d, e) as described by Kreutzburg (1996). These changes could be seen in stratum radiatum and stratum oriens throughout the hippocampus, however the activated morphology was not increased in any region of the dentate gyrus (Figure 4.8a). L-NPA pre-treatment had the effect of suppressing these morphological changes, with fewer cells showing an activated morphology (Figure 4.8b, c, d, e). As well as qualitative changed in morphology, changes in cell numbers and distribution, associated with reactive gliosis were also observed.

72h after KA injection, both astrocytes (Figure 4.8b) and microglia (Figure 4.8d) showed a propensity to invade the stratum lucidum and pyramidal cell layer of the CA3 region. Further to this, the density of both types of glial cells increased throughout the CA3 region, with GFAP-immunopositive cell numbers increasing approximately 2-fold (Figure 4.8b, f) and tomato lectin-immunopositive cell numbers increasing approximately 3-fold (Figure 4.8d, i). The number of tomato lectin immunopositive cells in the CA1 region also increased by approximately 2-fold. L-NPA pre-treatment suppressed both the tendancy for cell migration to stratum lucidum and the pyramidal cell layer of CA3 and the increased number of glia in this

region, with astrocyte proliferation reduced by close to 50% (t_8 = 6.534, $p < 0.001$. Figure 4.8b, f) and microglial proliferation reduced by approximately 30% (t_8 = 5.674, $p < 0.001$. Figure 4.8d, i). L-NPA had only a minor suppressing effect on microglia proliferation in the CA1 region at this timepoint, which was not found to be significant with a 95% confidence interval.

4.4.3 Synaptogenesis

High levels of SYN immunoreactivity was constitutively expressed in the polymorphic layer of the dentate gyrus and stratum lucidum of the CA3 region of C57BL/6J mice (figure 4.9a). 24h following KA administration, no changes in SYN immunoreactivity were observed (figure 4.9b). Initial changes in the spatial distribution of SYN following KA induced status epilepticus were witnessed at the 72h timepoint. At this timepoint, SYN immunoreactivity was elevated in the outer molecular layer of the dentate gyrus (t_8 = 3.748, $p = 0.006$. Figure 4.9a, c), suggesting an increase in synaptogenesis in this region. This increase was suppressed in animals pre-treated with L-NPA. No change in synaptophysin immunoreactivity was observed in the stratum lucidum of CA3 or the polymorphic layer of the dentate gyrus in any treatment group at this timepoint.

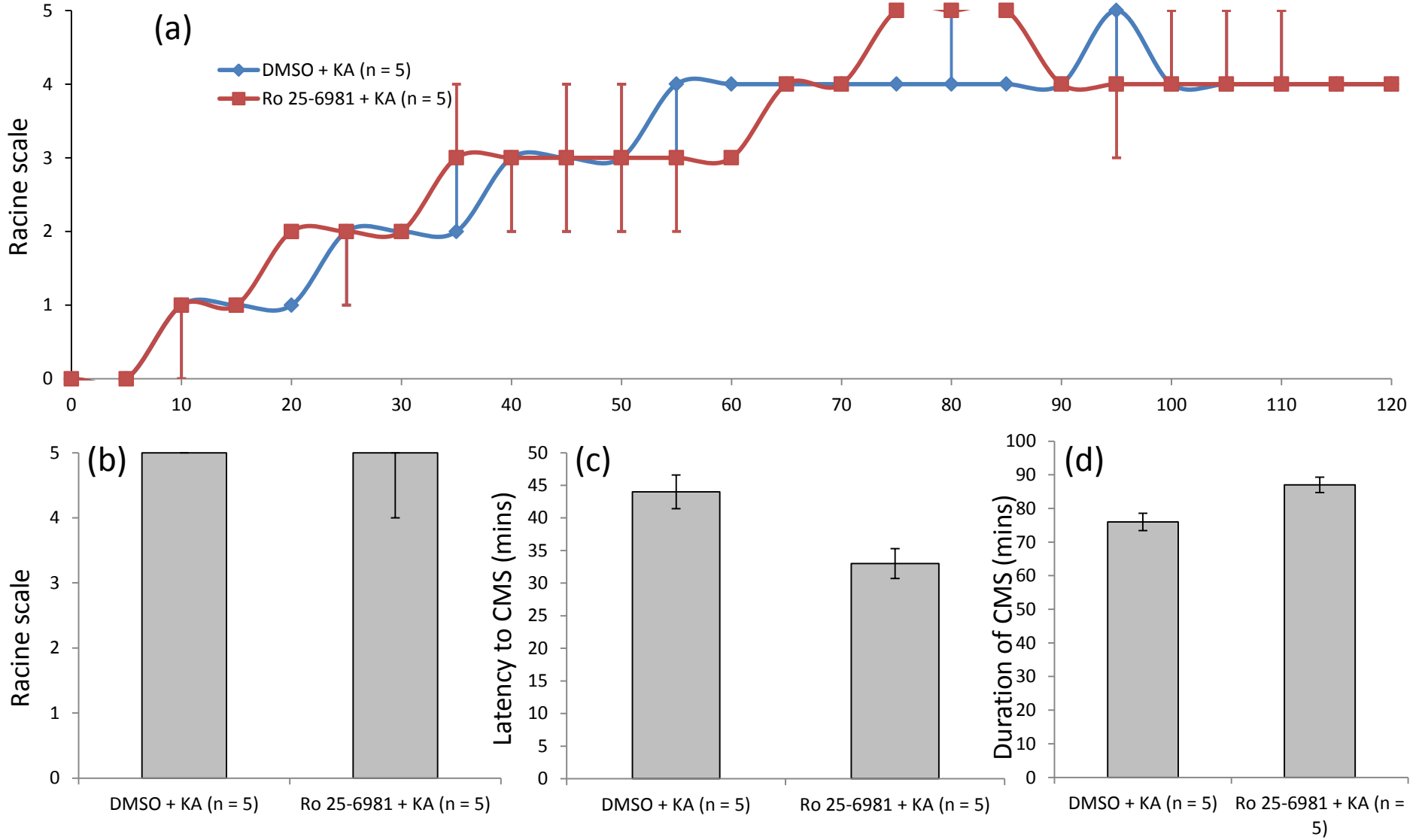

Figure 4.1. NR2B antagonist, Ro 25-6981 shows no effect on severity of Kainic acid-induced status epilepticus. (a) Timecourse of behavioural seizure progression over 120 minutes following kainic acid injection **(b)** Maximum seizure severity reached (Median +/- IQ range . **(c)** Latency to onset of CMS (≥Racine 3) **(d)** Duration of CMS.

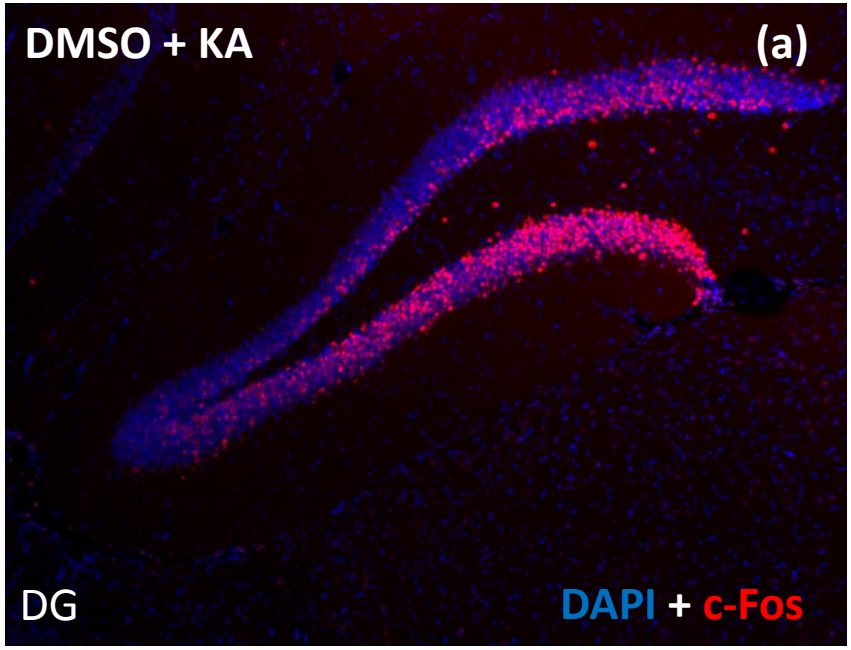

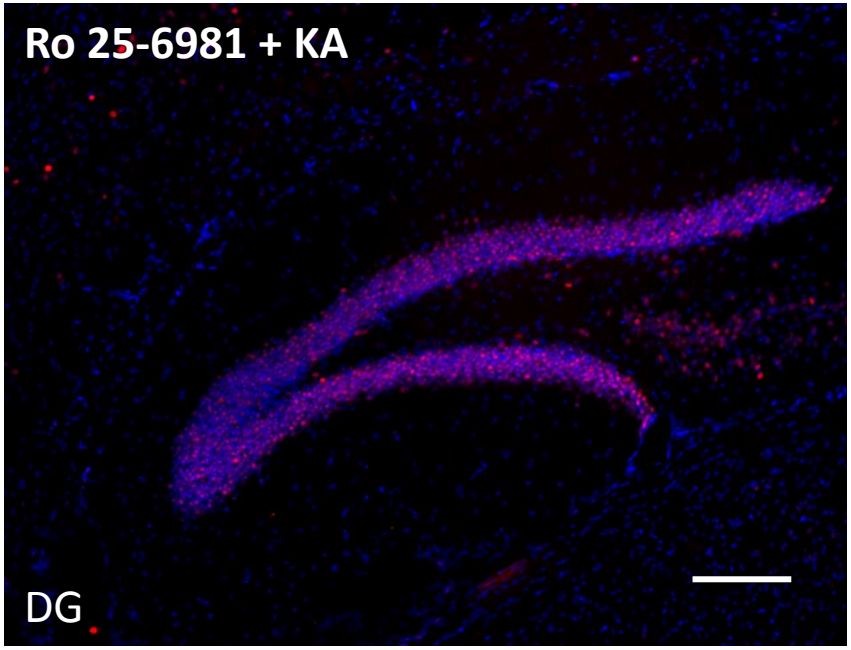

Figure 4.2. NR2B antagonist, Ro 25-6981 has no effect on c-Fos expression in the Dentate gyrus 2 hours following systemic administration of Kainic acid. (a) Photomicrographs displaying c-Fos expression in Dentate gyrus 2h post KA administration with pre-treatment of DMSO vehicle control or Ro 25-6981**.** Magnification: x20. Scale bar: **(b)** Counts of c-Fos immunopositive neurons in dentate gyrus displayed as neurons/10 (+/- S.E.M). GCL: Granule cell layer; PL: Polymorphic layer; ML: Molecular layer.

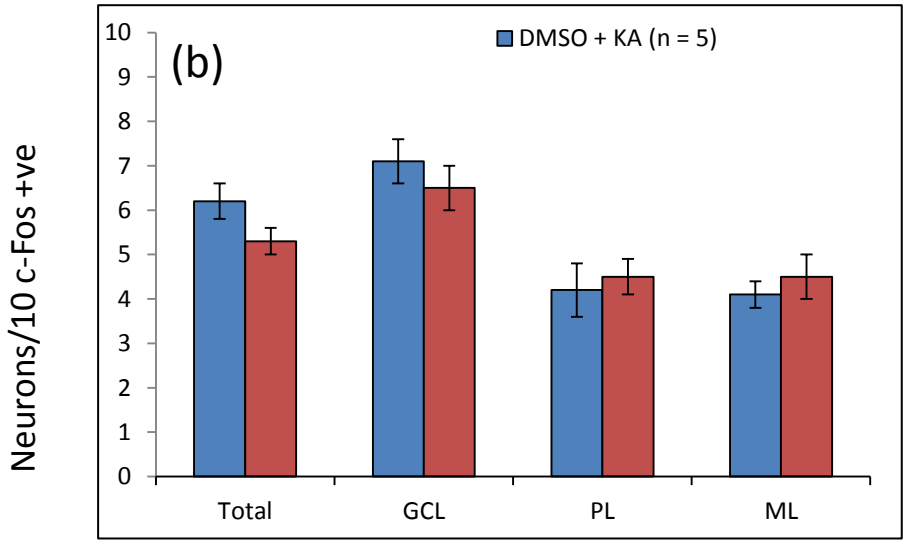

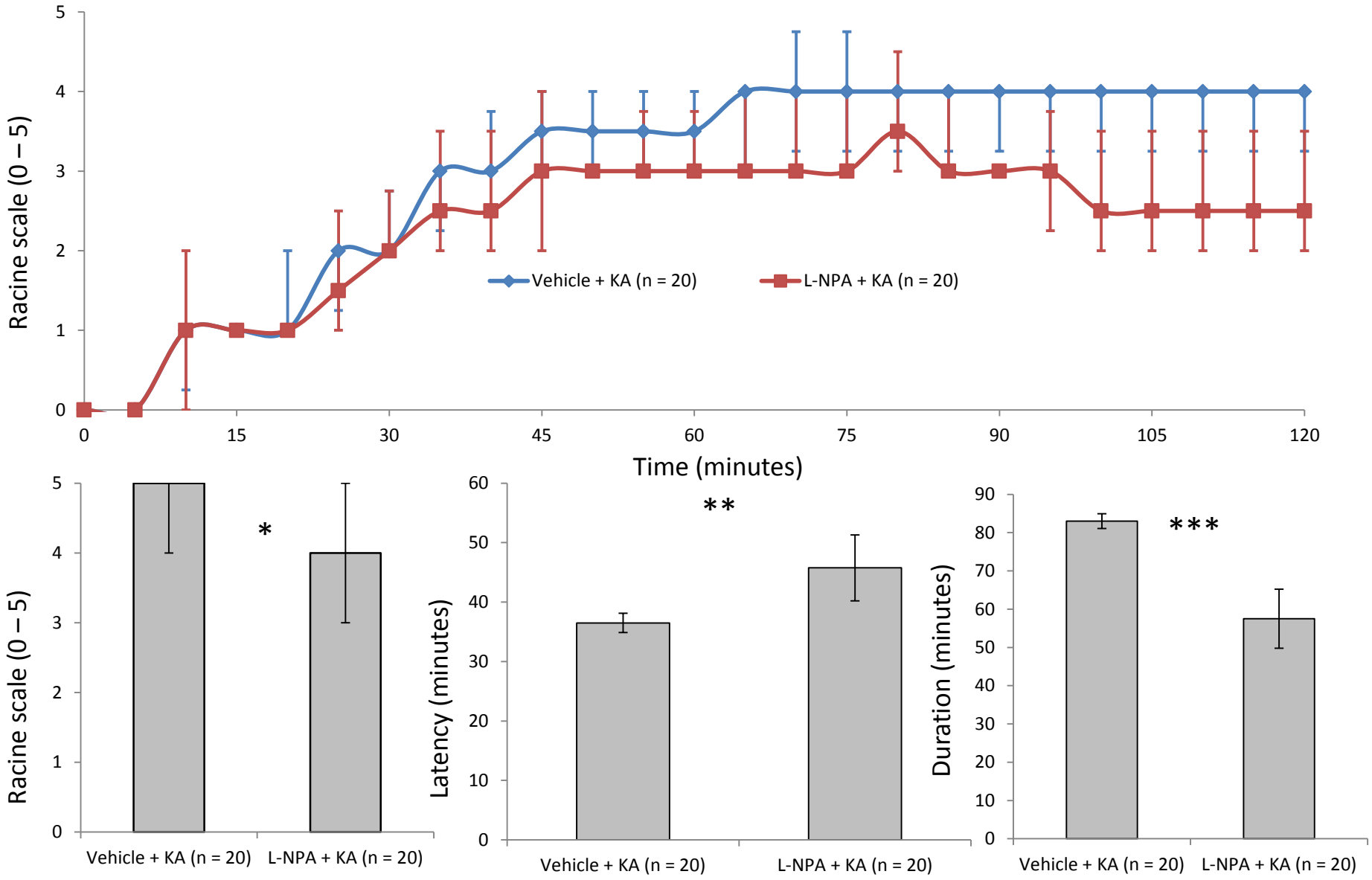

Figure 4.3. L-NPA reduces severity of kainic acid-induced Status epilepticus in C57BL/6J mice (a) Timecourse of behavioural seizure progression over 120 minutes following kainic acid injection **(b)** Maximum seizure severity reached (Median +/- IQ range . *p <0.001 (c) Latency to onset of CMS. **p = 0.040. (d) Duration of CMS. ***p = 0.008

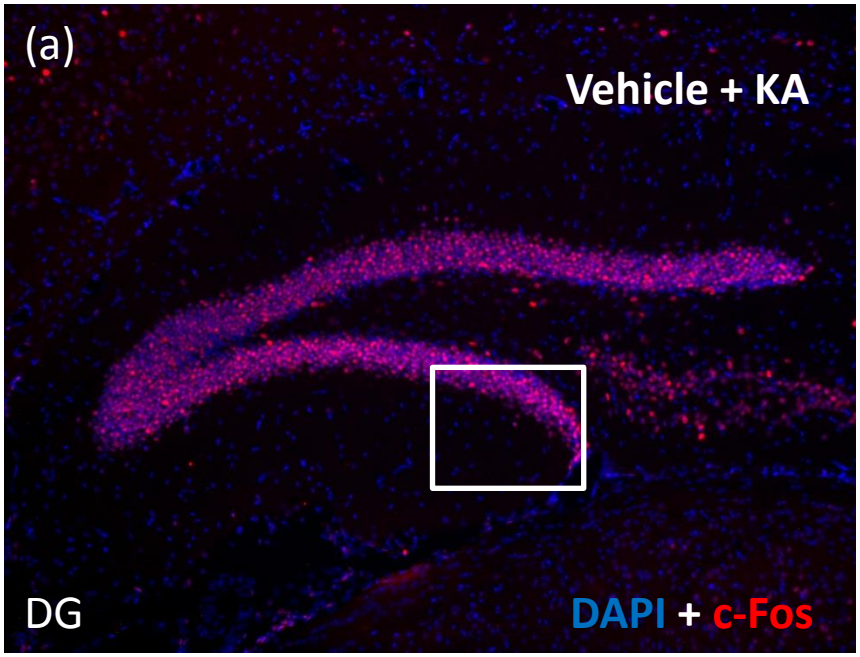

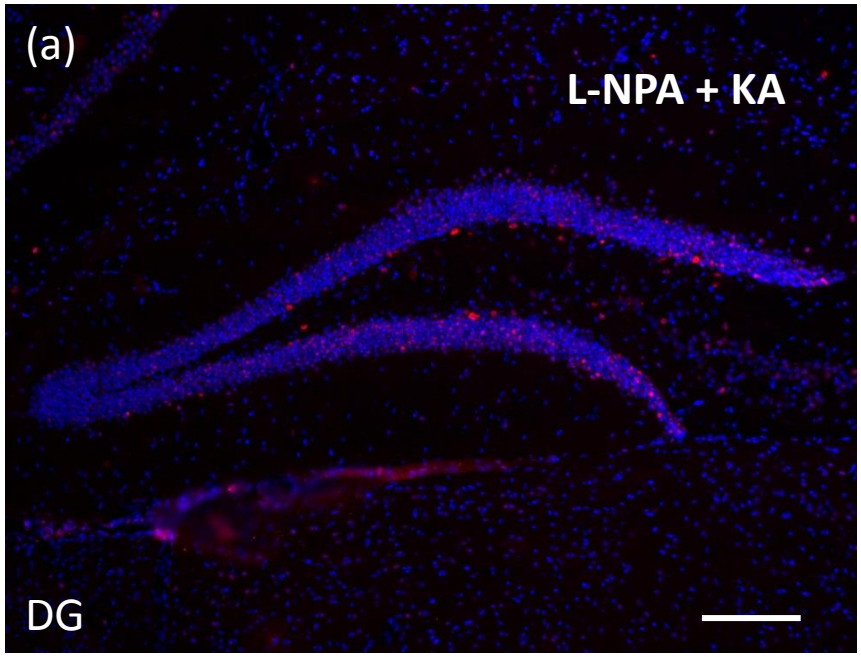

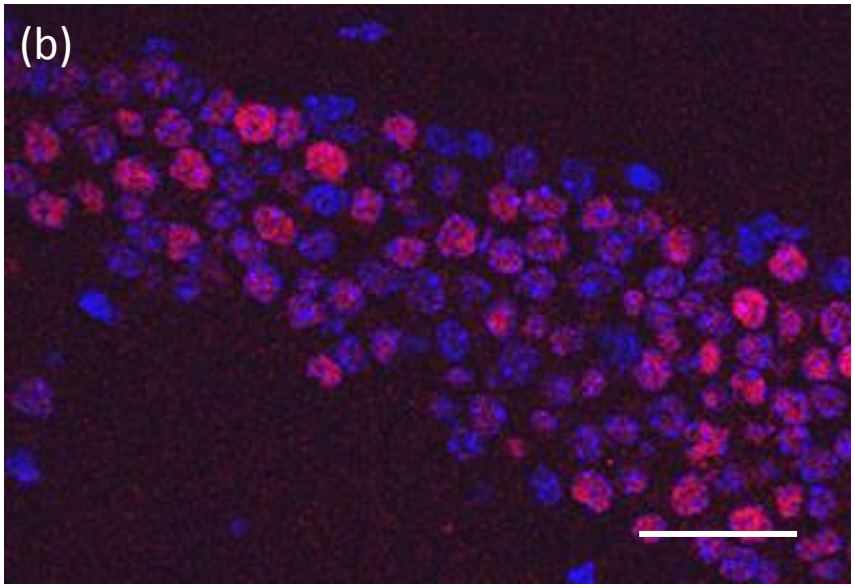

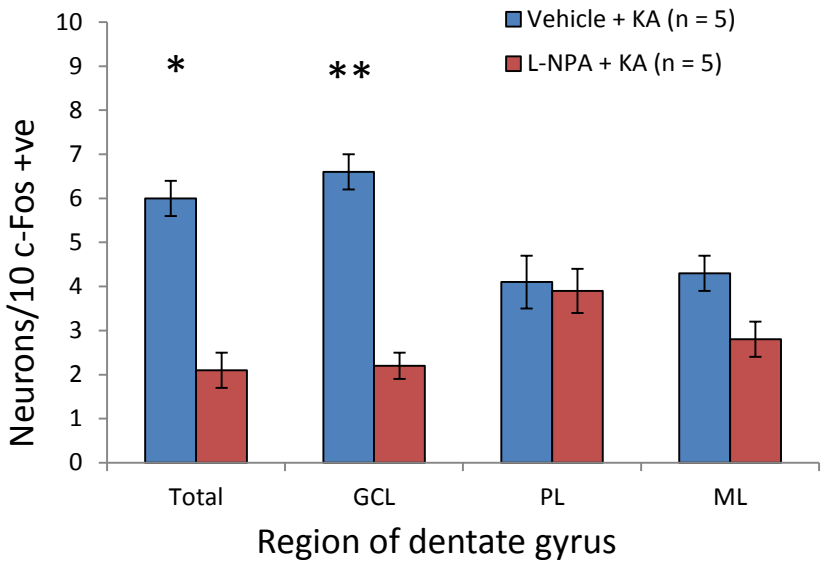

Figure 4.4. L-NPA reduces seizure-induced c-Fos expression in dentate granule cells. (a) DAPI and c-Fos in Dentate gyrus. Magnification: x20. Scale bar: **(b)** c-Fos clearly restricted to neuronal nuclei. Number of cells +ve for c-Fos/10. Magnification: x 63. Scale bar: **(c)** cell counts. *t_8 = 10.653, $p < 0.001$, **t_8 = 9.273, $p < 0.001$.

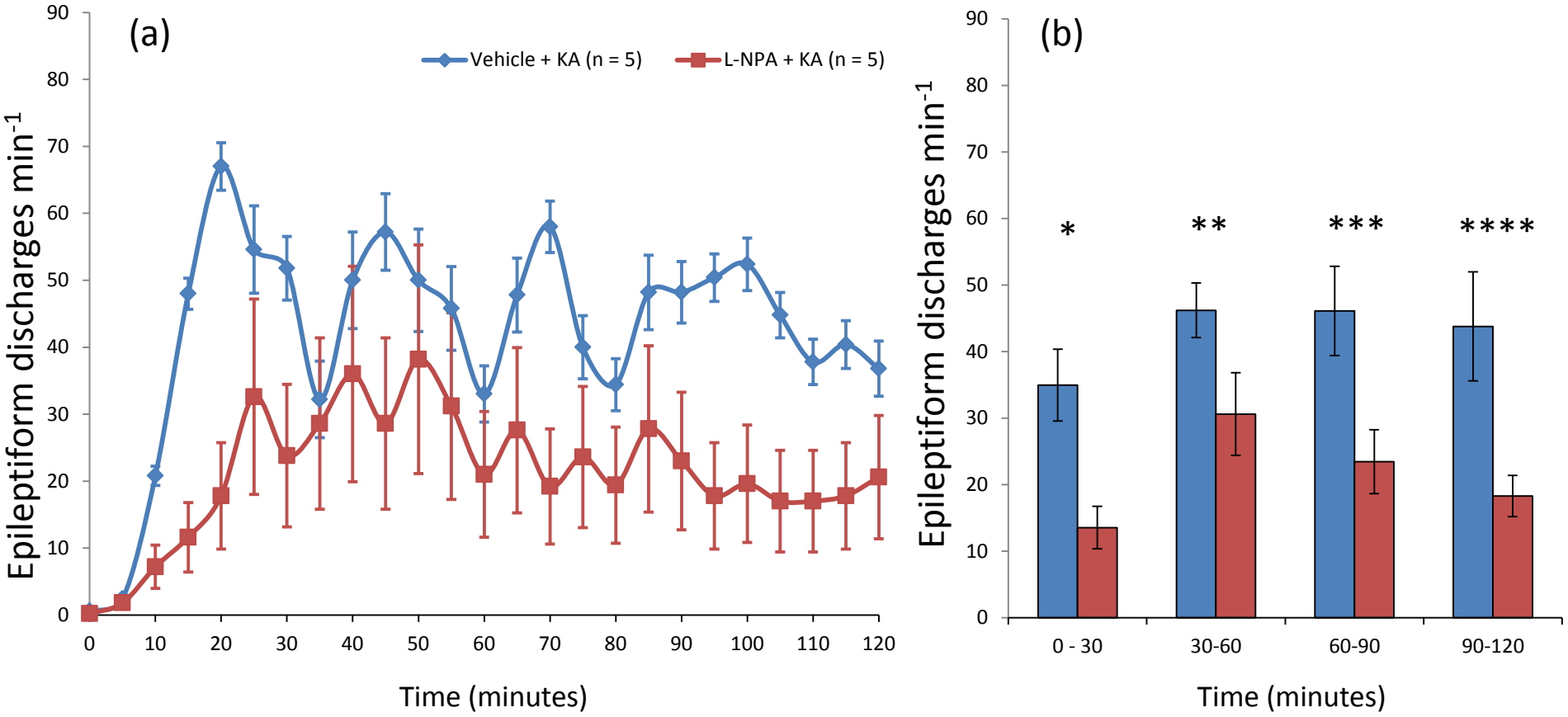

Figure 4.5 L-NPA reduces frequency of epileptiform discharges in C57BL/6J mice during 2 hour period of Status epilepticus following injection with kainic acid. (a) Spikes min-1 over initial 2 hours with resolution of 5 minutes. **(b)** Spikes min^{-1} in 30 minute bins. * $t_8 = 5.946$, $p < 0.001$, ** $t_8 = 4.480$, $p = 0.002$, *** $t_8 = 5.420$, $p < 0.001$, **** $t_8 = 7.400$, $p < 0.001$

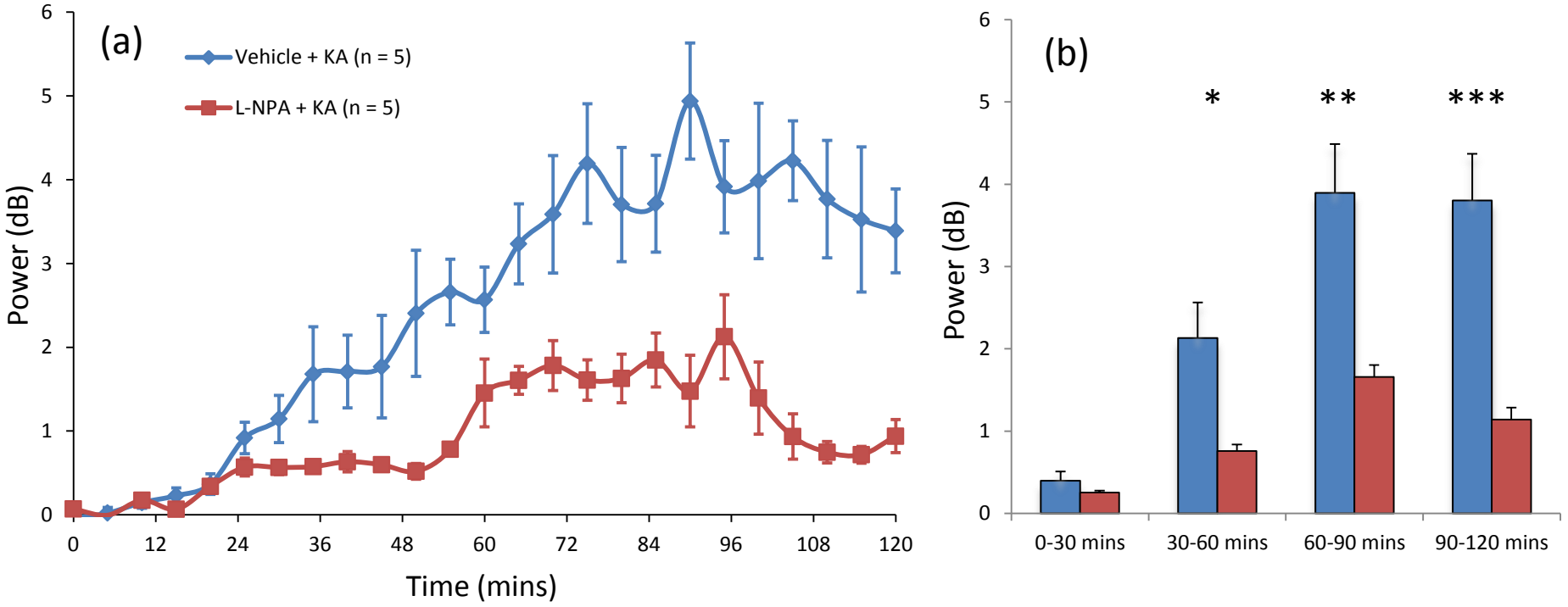

Figure 4.6. L-NPA decreases power (dB) in γ –frequency band during status epilepticus. (a) Timecourse over 2 hours **(b)** Quantified data in 30 minute bins. *t_8 = 3.135, p = 0.014. **t_8 = 3.664, p = 0.006., ***t_8 = 4.540, p = 0.002

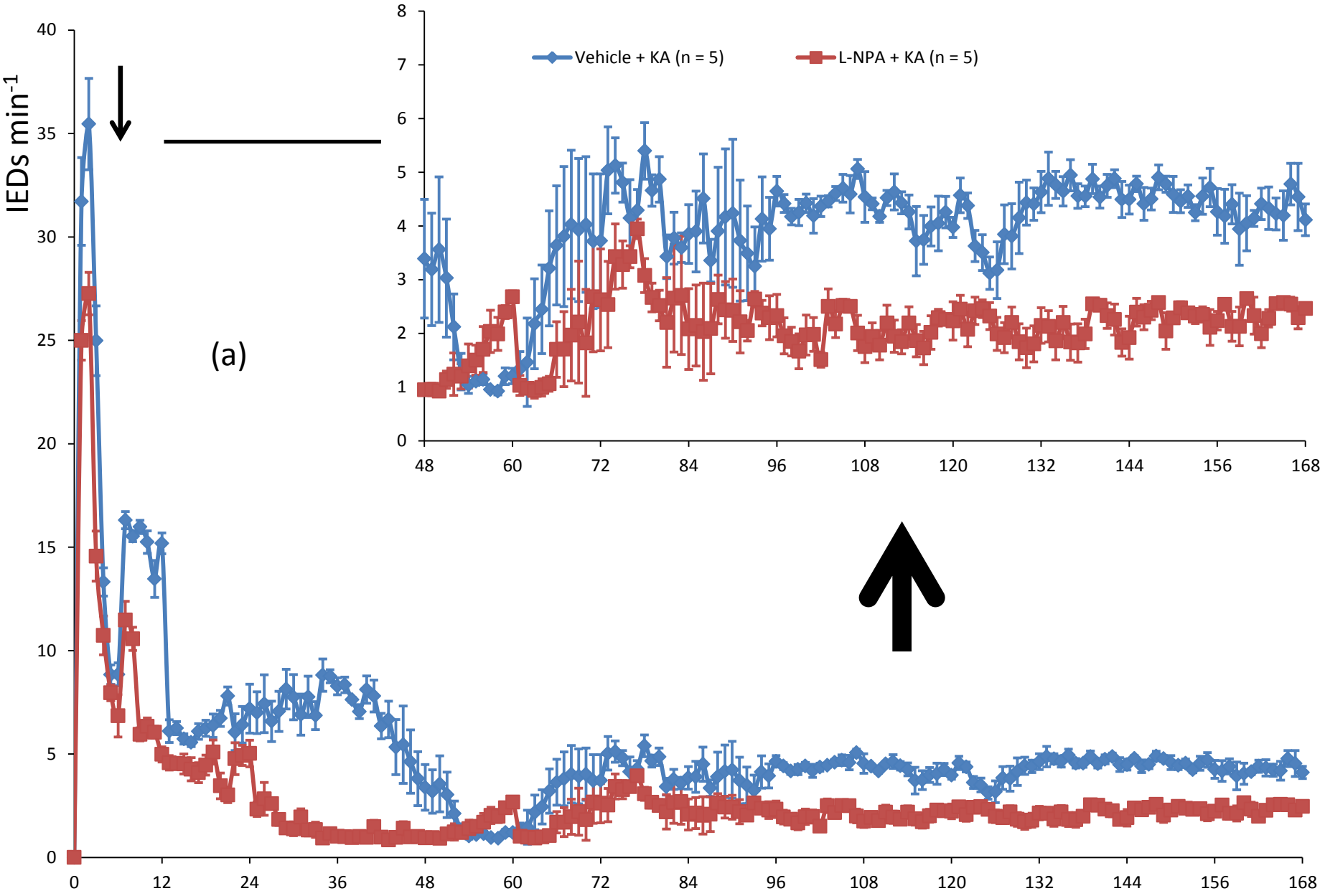
IEDs min-1
(a)
Vehicle + KA (n = 5)
L-NPA + KA (n = 5)
0
5
10
15
20
25
30
35
40
0
12
24
36
48
60
72
84
96
108
120
132
144
156
168
0
1
2
3
4
5
6
7
8
48
60
72
84
96
108
120
132
144
156
168

(b)

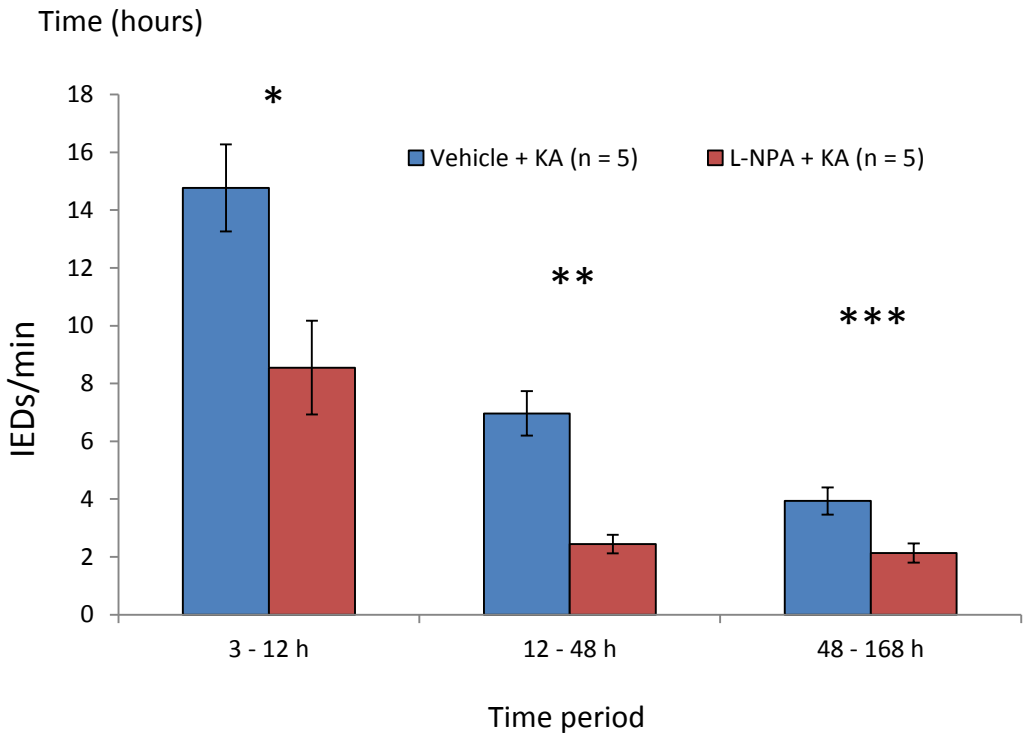

Figure 4.7. L-NPA pre-treatment reduces frequency of IEDs recorded during first 7 days post kainic acid injection. (a) Timecourse of IED frequency for 7 days following KA injection. Inset: 48 – 168h at higher spike frequency resolution **(b)** Quantified data for. *t_8 = 6.788, $p < 0.001$. **t_8 = 14.45, $p < 0.001$. ***t_8 = 3.907, $p = .0045$.

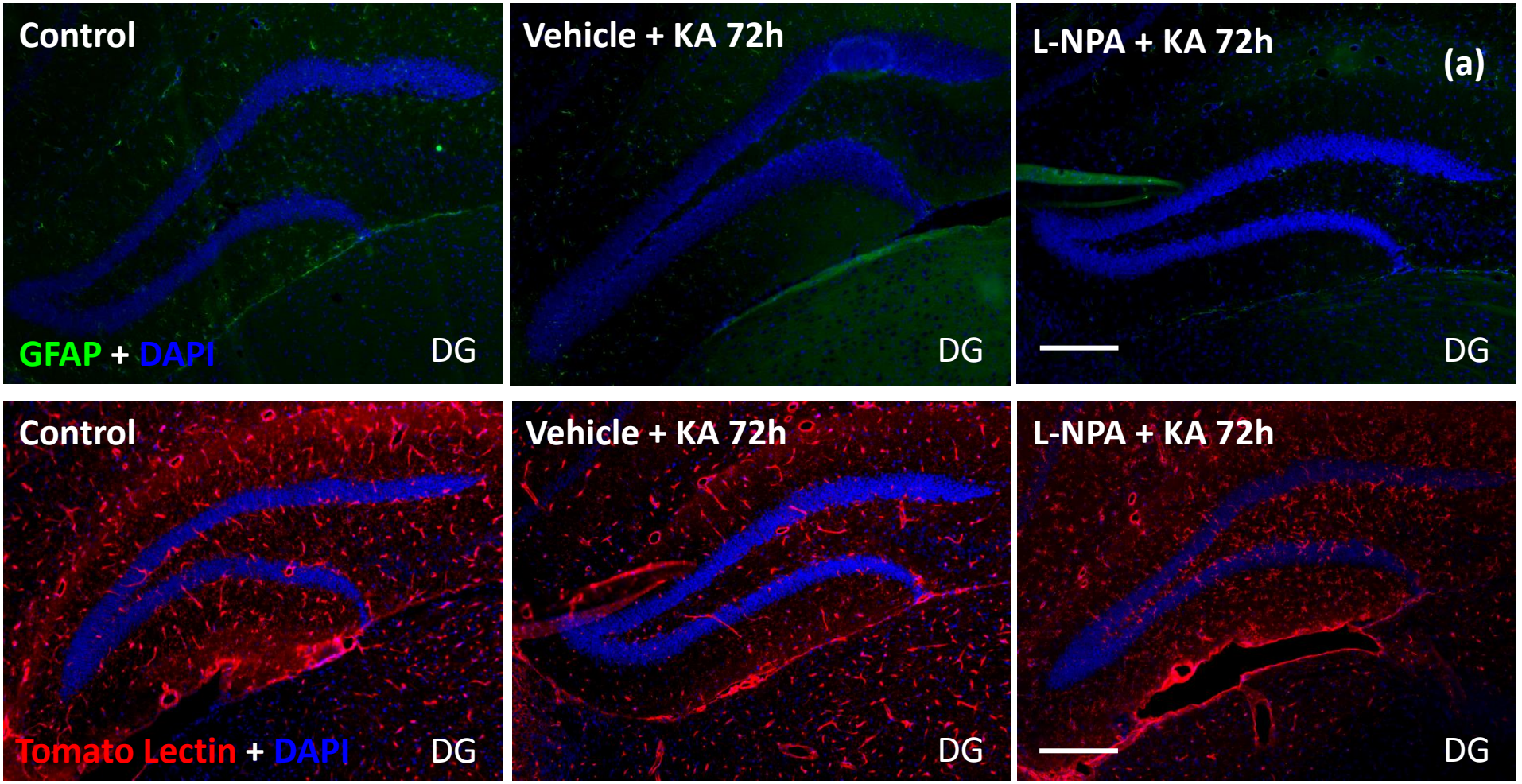

Figure 4.8. L-NPA supresses gliosis in CA3 region of hippocampus. (a) Astrocytes and microglia in dentate gyrus. Magnification 10X, scale bar: 100µm **(b)** Astrocytes in CA3 region of the hippocampus .Magnification 10X (scale bar: 100µm), Magnification 20X (scale bar: µm), Magnification 40X (scale bar: µm)**(c)** Astrocytes in CA1 region of hippocampus. Magnification 10X (scale bar: 100µm), Magnification 20X (scale bar: µm), Magnification 40X (scale bar: µm) **(d)** Microglia in CA3 region of the hippocampus . Magnification 10X (scale bar: 100µm), Magnification 20X (scale bar: µm), Magnification 40X (scale bar: µm)**(e)** Microglia in CA1 region of the hippocampus. Magnification 10X (scale bar: 100µm), Magnification 20X (scale bar: µm), Magnification 40X (scale bar: µm) **(f)** Astrocyte cell counts in dentate gyrus, CA3 and CA1, 24h post-KA. **(g)** Astrocyte cell counts in dentate gyrus, CA3 and CA1 72h post-KA. $*t_8 = 6.534$, $p < 0.001$. **(h)** Microglia cell counts in dentate gyrus, CA3 and CA1, 24h post-KA. **(i)** Microglia cell counts in dentate gyrus, CA3 and CA1, 72h post-KA. $**t_8 = 5.674$, $p < 0.001$.

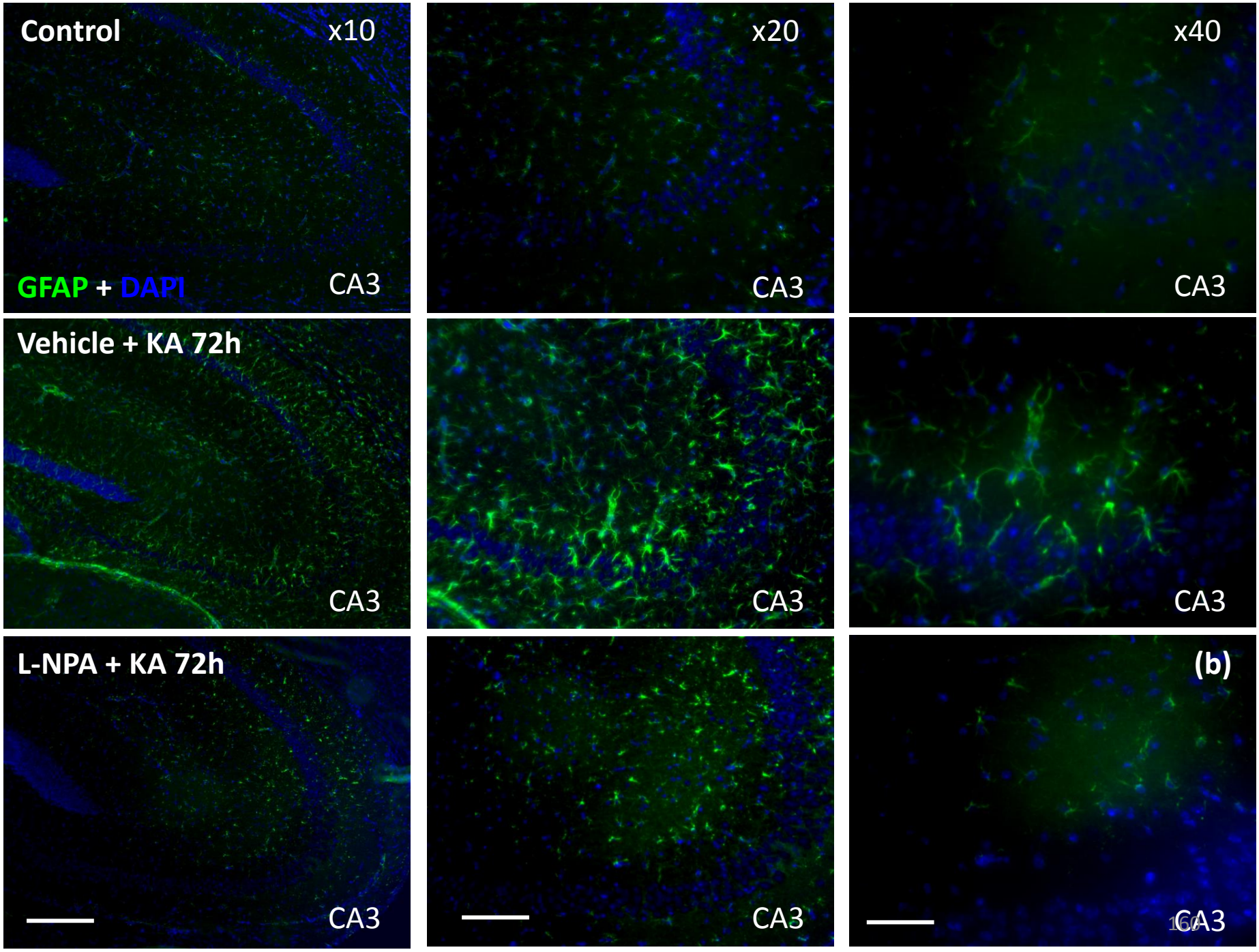
Control
x10
GFAP + DAPI
CA3
x20
CA3
x40
CA3
Vehicle + KA 72h
CA3
CA3
CA3
L-NPA + KA 72h
CA3
CA3
(b)
CA3

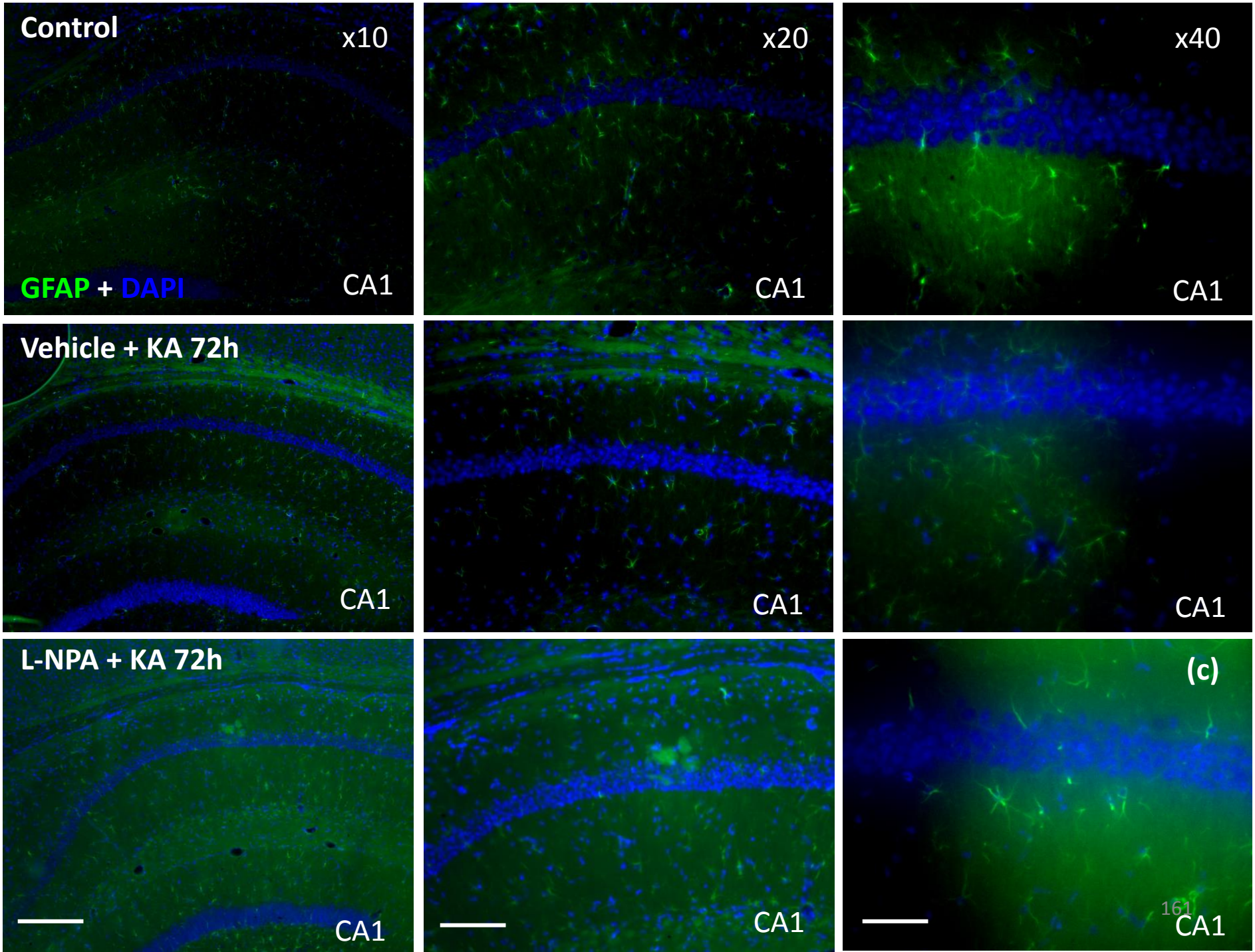
Control
x10
GFAP + DAPI
CA1
x20
CA1
x40
CA1
Vehicle + KA 72h
CA1
CA1
CA1
L-NPA + KA 72h
CA1
CA1
(c)
CA1

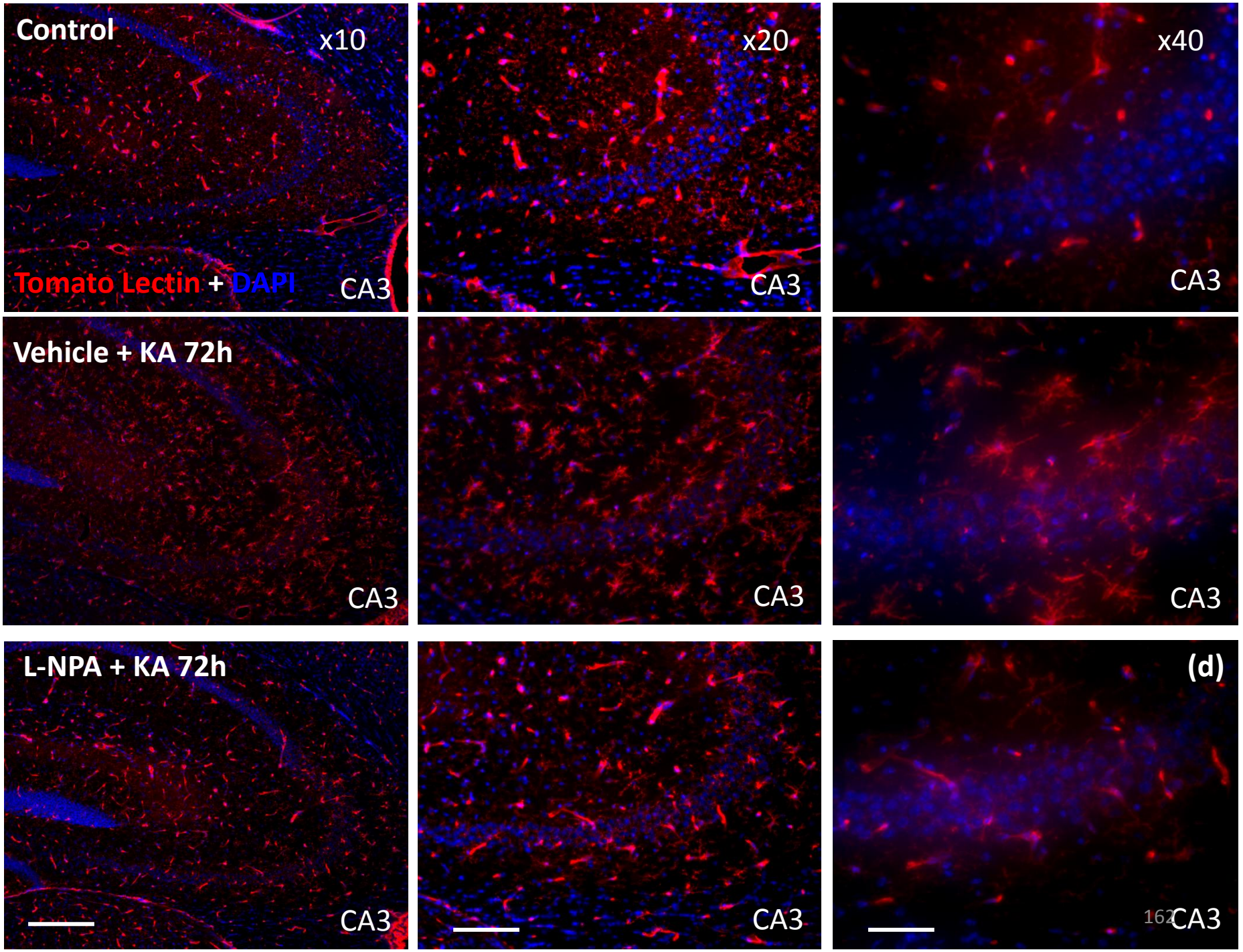
Control
x10
x20
x40
Tomato Lectin + DAPI
CA3
CA3
CA3
Vehicle + KA 72h
CA3
CA3
CA3
L-NPA + KA 72h
CA3
CA3
(d)
CA3

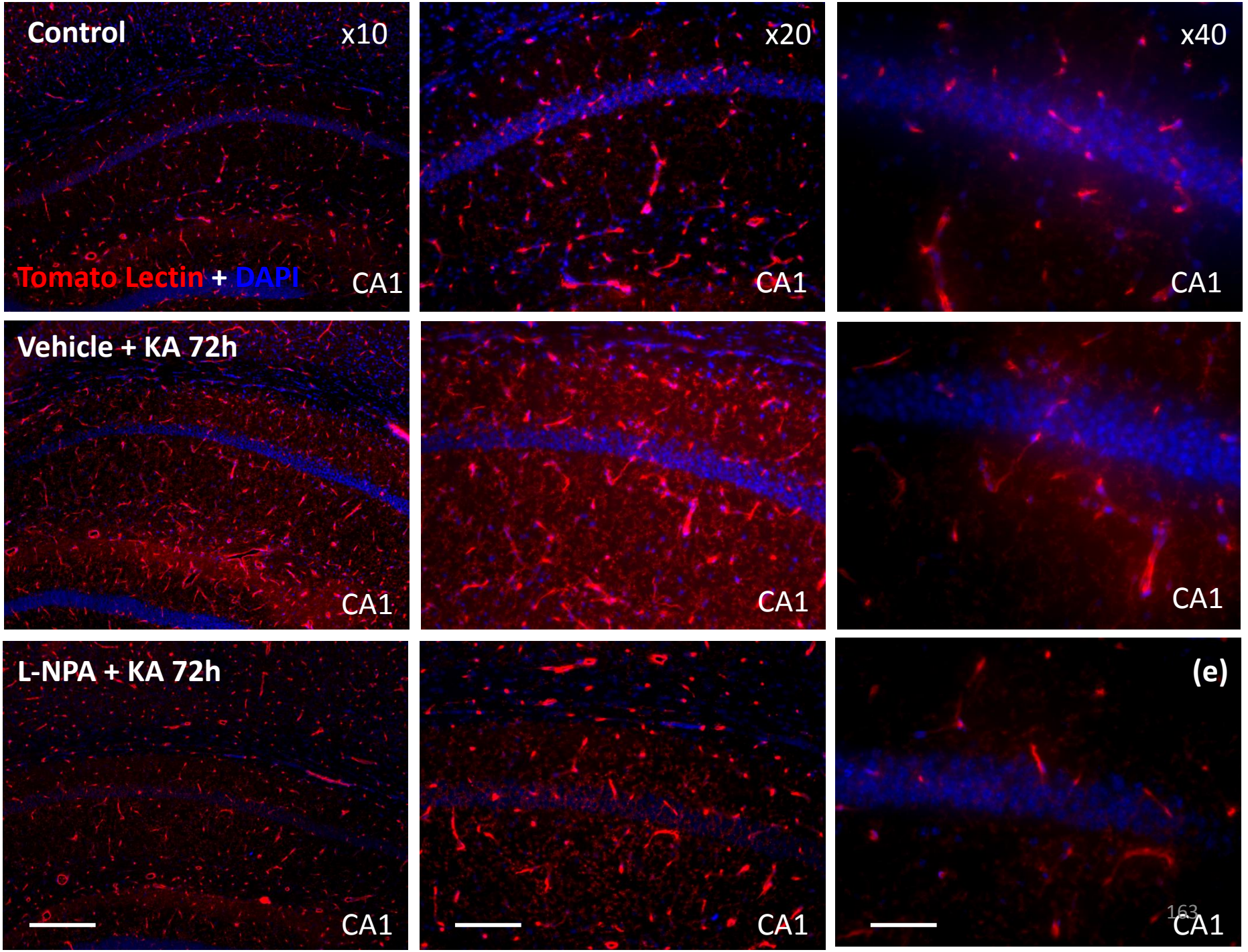
Control
x10
x20
x40
Tomato Lectin + DAPI
CA1
CA1
CA1
Vehicle + KA 72h
CA1
CA1
CA1
L-NPA + KA 72h
CA1
CA1
(e)
CA1

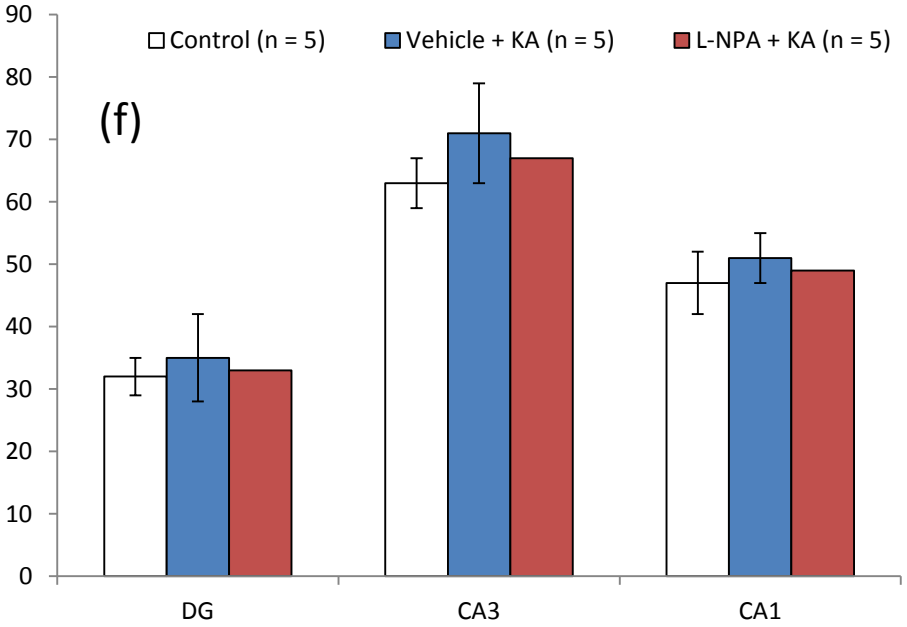

Astrocytes 24 post-KA

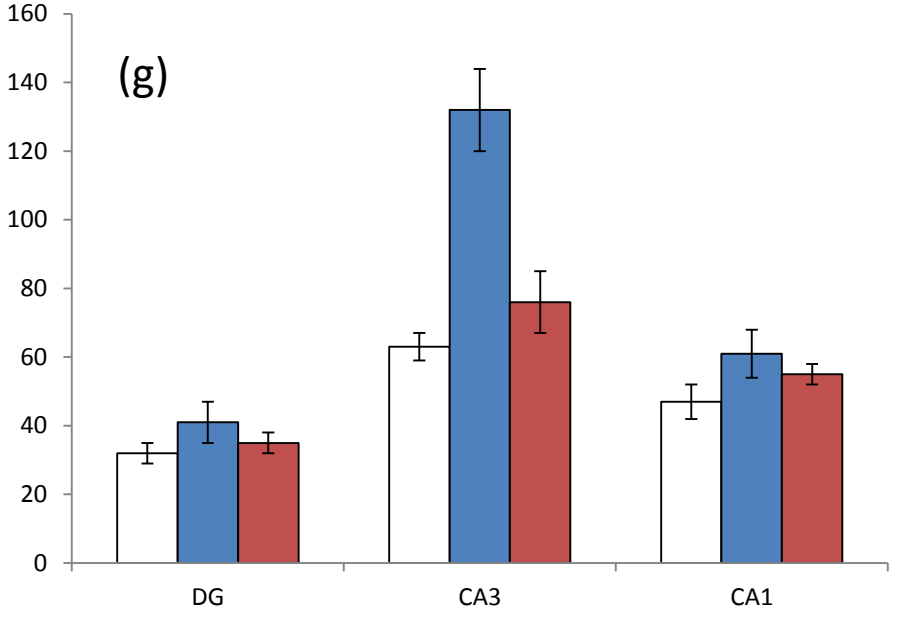

Astrocytes 72h post-KA

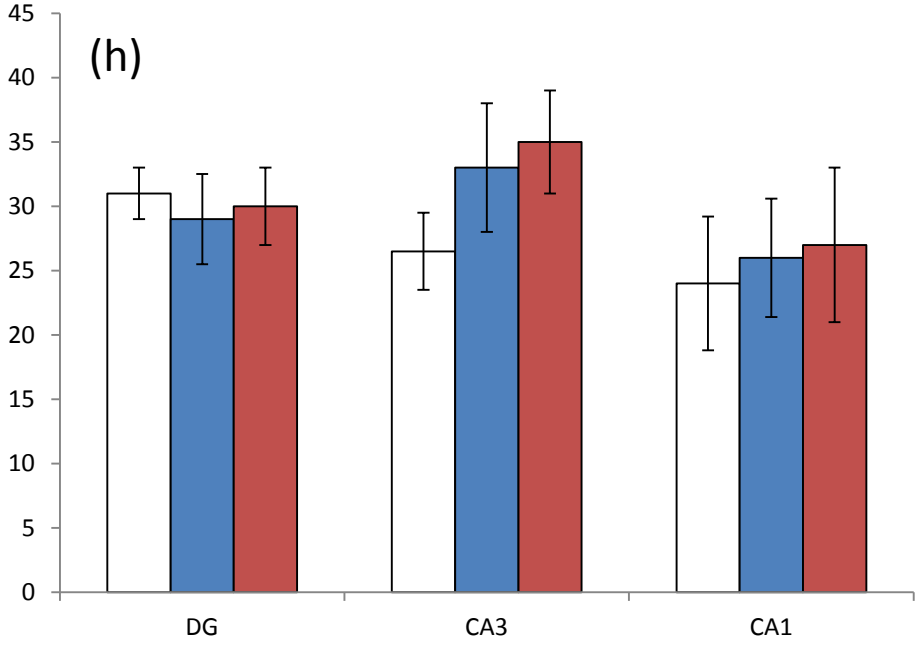

Microglia 24 post-KA

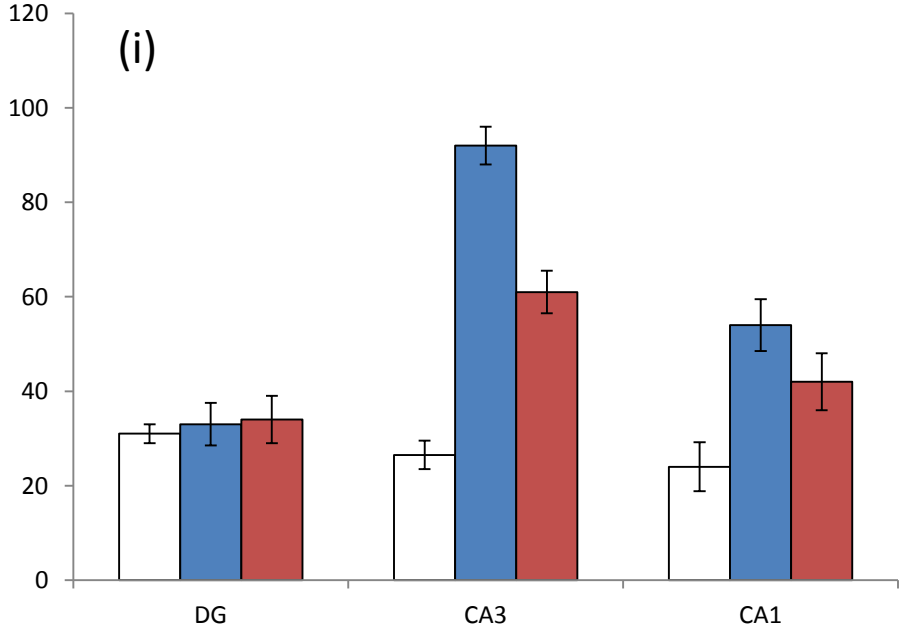

Microglia 72h post-KA

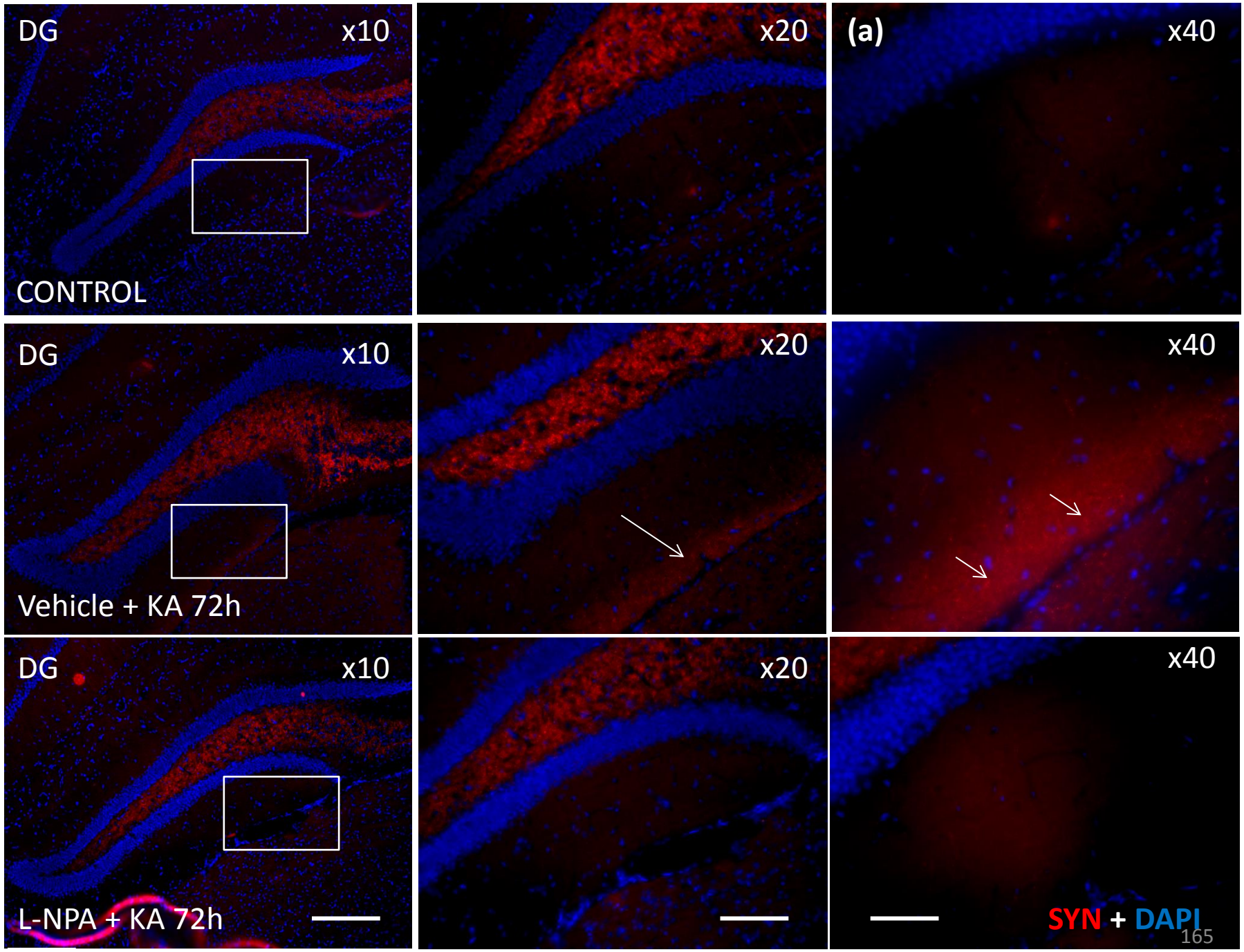
DG
x10
x20
(a)
x40
CONTROL
DG
x10
x20
x40
Vehicle + KA 72h
DG
x10
x20
x40
L-NPA + KA 72h
SYN + DAPI

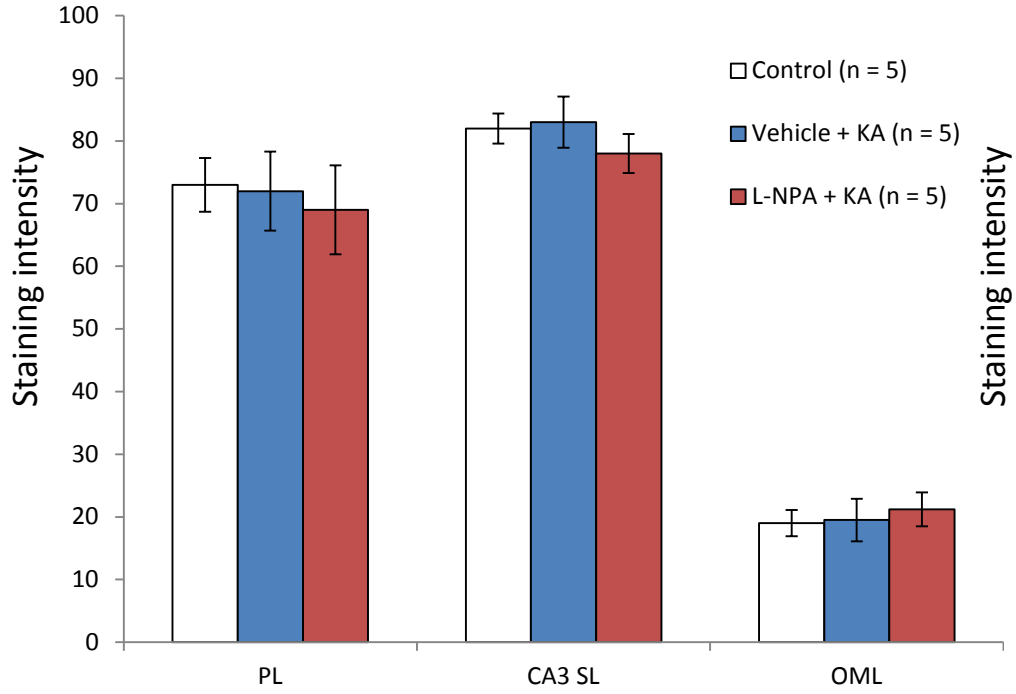

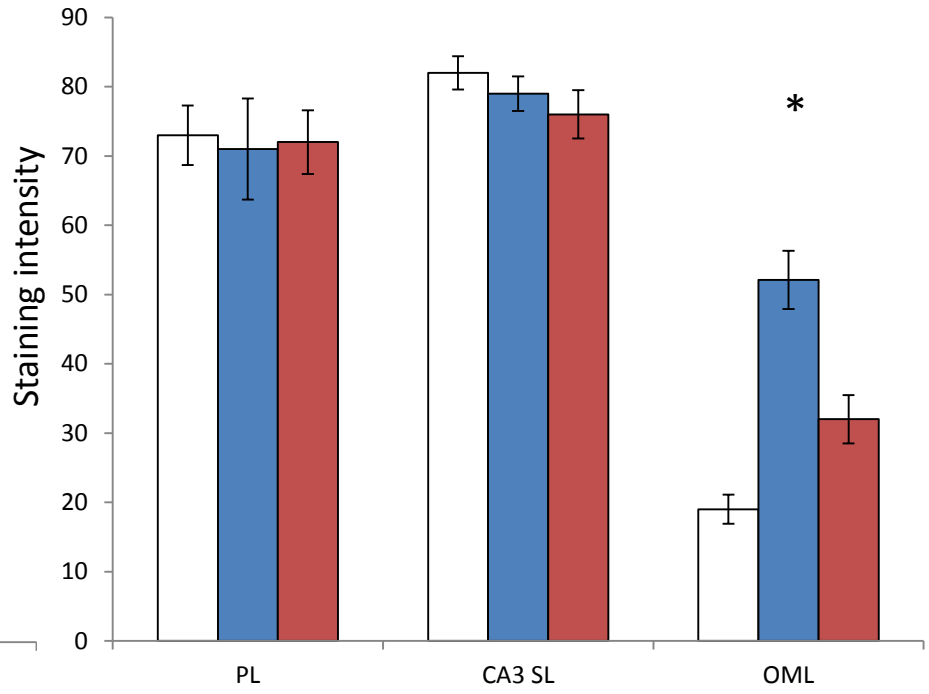

Figure 4.9 L-NPA supresses reactive synaptogenesis in molecular layer of dentate gyrus 72h post KA. (a) Photomicrographs of dentate gyrus at 3 levels of magnification: Dentate gyrus 10X (scale bar = 100µm), 20X (scale bar =) and molecular layer of dentate gyrus 40X (scale bar =) Boxes indicate regions viewed at increased magnification **(b)** Quantification of SYN staining intensity 24h post-KA **(c)** Quantification of SYN staining intensity 72h post-KA. *t_8 = 3.748, p = 0.006.

4.5 DISCUSSION

4.5.1 Overview

In this chapter, the effects of an NR2B specific antagonist, Ro 25-6981 and a highly selective nNOS inhibitor, L-NPA were tested on SE and the effects of L-NPA on early neurobiological and electrographic indicators of early epileptogenesis. Targetting the NR2B subunit with the antagonist Ro 25-6981 had no effect, or perhaps even a slightly pro-convulsive effect on behavioural SE (figure 4.1) and had no effect on the anatomical distribution of c-Fos expression in the dentate gyrus (figure 4.2) post SE. L-NPA treatment, meanwhile, delayed the onset and reduced the severity of KA-induced SE (figure 4.3), suppressed c-Fos expression in the dentate gyrus (figure 4.4), reduced electrographic indicators of severe SE (figures 4.5, 4.6) and reduced the extent of electrographic and neurobiological indicators of epileptogenesis in the hippocampus during the 'latent period' following KA-induced SE (figures 4.7 – 4.9).

The acute effects of L-NPA on SE were characterised by a reduction in; the duration of CMS (figure 4.3), the power of the γ-frequency band (20 - 70Hz) EEG (figure 4.6) associated with seizure severity, the frequency of epileptiform discharges (figure 4.5), and a decrease in the expression of c-Fos (figure 4.4), suggesting that nNOS is involved in seizure susceptibility and in the manifestation of CMS in the KA model. In the early epileptogenic period, L-NPA treatment reduced the frequency of IEDs (figure 4.7), suppressed reactive gliosis in the CA3 region (figure 4.8) and reactive

synaptogenesis in the OML and MML of the dentate gyrus (figure 4.9) These observations might suggest a potential disease-modifying action of L-NPA on the epileptogenic process by modulation of the initiating event.

4.5.2 Effect of specific NR2B antagonist, Ro 25-6981 on SE

Pharmacological agents targetting the NMDA receptor have been widely tested for their role in controlling seizures and processes underlying epileptogenesis. Although numerous agents have proved effective as anticonvulsants, their aberrant side effects are too severe for the drugs to be clinically useful (Newcomer et al, 1999). Targetting pathophysiological NMDAR signalling, while not disrupting normal function could be the key to addressing numerous CNS disorders that involve excitotoxicity and neuronal death, such as ischemic or traumatic brain injury and temporal lobe epilepsy.

While RO 25-6981 has previously been reported to have a protective effect against spontaneous seizures in animal models after a period of epileptogenesis (Wang et al, 2004), no effect of the drug was found on epileptiform behaviour during a period of KA-induced SE, nor on the subsequent expression of c-Fos in the dentate gyrus. NMDA receptors with NR2B subunits have been heavily implicated in excitotoxic cell death, making them potential key players in progressive diseases, involving neuronal loss, such as chronic epilepsy (Moddel et al, 2005), however, the role of NR2B in mediating network excitation directly is not so straight forward. This means that while targetting the NR2B subunit may be effective in chronic models of epilepsy, the effect prior to an acutely induced seizure is negligible.

4.5.3 Hippocampal nNOS and seizures

NO production in the hippocampus increases during seizures as a result of Ca^{2+}-dependent activation of nNOS in neurons and eNOS in the vascular endothelium (Al-Ghoul *et al.,* 1995; Kaneko *et al.,* 2002; Cosgrave *et al.,* 2008; Kovacs *et al*., 2009). Conflicting roles for NO in the generation of seizures have been reported, with both pro- and anti-convulsant effects described. Periera de Vasconcelos *et al* (2005) reported a reduction in seizure susceptibility due to eNOS-mediated effects on blood flow to the epileptic focus, whereas Kovacs et al (2009) reported an exacerbation of seizure-like events through nNOS-mediated modulation of synaptic plasticity in a hippocampal slice model.

It has been widely reported that membrane-associated nNOS plays a significant role in the signal transduction through glutamate receptors (Garthwaite, 1985; Garthwaite *et al.,* 1988). Hopper and Garthwaite (2006) showed that phasic NO-signalling mediated by nNOS is necessary, in conjunction with a tonic, paracrine NO signal from eNOS, for long-term potentiation, a phenomenon that is largely dependent on NMDA-receptors. Kovacs *et al* (2009), eliminating the role of CBF changes by using organotypic slices, showed that the same mechanism is involved in the initiation of seizure-like events in the hippocampus.

The scaffolding protein, PSD95, associates nNOS with glutamate receptors via PDZ domains (Burette et al, 2002) coupling glutamatergic neuronal activity and Ca^{2+}-

dependent NO formation, allowing transient, autocrine and synaptic NO signaling (Namiki et al, 2005). This is important in modulating synaptic transmission, excitatory post-synaptic potentials (EPSPs) and LTP. (Hopper & Garthwaite, 2006; Kovacs, et al, 2009). Wang et al (2002) reported that NMDA receptors on dentate granule cells are involved in regulating synaptic plasticity via perforant path inputs from the entorhinal cortex, suggesting the DG granule cell layer as a possible site of action for the NMDA-PSD95-nNOS complex.

nNOS, activated during seizures by high levels of Ca^{2+} influx, may influence seizure severity through paracrine, autocrine and synaptic signaling from nNOS anchored at the PSD, or all three mechanisms. These results support the findings of Rajesekaran (2005), who suggested abnormal nNOS activity as a major trigger for seizure generation. Recently, an increase in nNOS expression following early-life seizures has been reported (Kim, 2010), which increased susceptibility to spontaneous seizures later in life in an nNOS-dependent manner, giving further evidence for how nNOS may play a role in the development of chronic epilepsy from a precipitating event.

Robust *in vivo* evidence to support the proconvulsant effect of nNOS-derived NO, however, is lacking. *In vivo* studies reported thus far have been undermined by the use of nNOS inhibitors of questionable specificity, such as 7-nitroindazole, 3-bromo-7-nitroindazole and 1-[2-(trifluoromethyl)phenyl] imidazole (kaneko et al., 2002)**.** The use of L-NPA, which has 149- and 3,158-fold greater selectivity (Zhang *et al.,* 1997) for nNOS over eNOS and iNOS, respectively, has allowed us to undertake a more reliable characterization of the role of nNOS in both icto- and epilepto- genesis.

4.5.4 L-NPA suppresses KA-induced SE reduces epileptogenic changes

Triggered by excessive intracellular Ca^{2+} and widely used as a marker for excitotoxic glutamatergic neurotransmission (Gall et al, 1998), c-Fos expression is considered a hallmark of neuronal network activation. The spatiotemporal pattern of expression in the hippocampal formation is a reliable and sensitive indicator of seizure severity (Samoriski *et al.,* 1997; Willoughby *et al.,* 1997; Vezzani *et al.,* 2000). Our data indicates that, in the C57BL/6J strain, c-Fos expression in excitatory circuits is largely restricted to dentate granule cells 2h post-SE. The significant reduction of c-Fos expression in this region associated with L-NPA treatment is consistent with the view that our intervention reduced the severity of SE and profoundly reduced the exposure of neurons in the region to excitotoxic stress.

Electrographic markers of epileptogenesis include the re-emergence of IEDs following an initial post-SE decline in IED frequency (Williams *et al.,* 2009). The reduced frequency of IEDs in L-NPA pretreated mice, when compared with vehicle pre-treated controls provides evidence that the suppression of neurobiological changes associated with epileptogenesis is accompanied by changes in the pattern of neuronal network activity. Further work is necessary in order to establish the extent to which IED frequency in the first week following KA administration is predictive of the onset and pattern of spontaneous recurrent seizures.

Reactive gliosis is a well characterised feature of the early stages of epileptogenesis and strongly predictive of neuronal loss and the development of spontaneous seizures (Vezzani *et al.,* 2000; 2009; Foresti *et al.,* 2009). The suppression of gliosis

in L-NPA treated animals provides strong evidence that the seizure-modulating effect is sufficient to prevent pathological neurobiological changes associated with neuronal loss and the development of chronic epilepsy. SYN was used as a marker of activity-dependent synaptic formation to explore synaptic events occurring in the hippocampus and dentate gyrus during the early epileptogenic period. As described in the previous chapter; following a period of KA-induced SE, C57BL/6J mice show signs of reactive synaptogenesis in the molecular layer of the dentate gyrus. This appears to long precede the aberrant sprouting of mossy fibres and presumably indicates a strengthening of inputs from the perforant path. The suppression of early synaptogenesis in this region in L-NPA pretreated animals is further evidence of the drug's considerable disease-modifying effect.

4.5.5 Conclusions

We present data demonstrating a strong disease modifying effect of L-NPA when administered as a pre-treatment prior to KA-induced SE. To our knowledge, this is the first study to have investigated the effect of an nNOS inhibitor on ictogenesis and charted the subsequent effect of the initial intervention on neurobiological and neurophysiological indicators of subsequent disease progression. The severity of SE was dramatically reduced, leading, in turn, to a reduced expression of a wide range of biomarkers of epileptogenesis at 2h, 24h, 72h and for the first 7 days following KA administration. Our data support the hypothesis that nNOS plays a facilitatory role in seizure generation and may represent a target for novel disease-modifying therapies.

Chapter 5. Incremental dosing of kainic acid and pharmacological interventions in the post-synaptic density and iNOS

5.1 ABSTRACT

In this chapter, the development of an incremental dosing regimen for kainic acid administration is reported in order to induce status epilepticus with a greater inter-animal uniformity and increase the duration of severe status epilepticus without increasing the mortality rate. By comparing the effects on status epilepticus and the early 'latent period' this method was found to be preferable to the administration of a single dose of KA for modeling TLE in inbred mouse strains commonly used as background for genetic manipulations. In particular, C57BL/6J.

We then used this incremental dosing regimen to carry out pilot studies to investigate the value of two separate potential interventions of the progression of epileptogenesis and the development of chronic epilepsy, using indicators of disease progression during the 'latent period'. A cell permeable peptide, Tat-NR2B9c was injected intravenously directly after the termination of status epilepticus with diazepam and the effects on gliosis at 3 days post-status epilepticus were investigated. 1400W, a specific inhibitor of the inducible isoform of nitric oxide synthase was administered and neuronal cell loss and the anatomical distribution of nNOS were investigated at 7 and 14 days post-status epilepticus. In both studies,

the frequency of epileptiform discharges was also analysed for 7 days following the induction of status epilepticus.

We report that Tat-NR2B9c reduced the frequency of epileptiform discharges during the ‘latent period’, possibly as a result of modulating network activity directly following the termination of behavioural seizures with diazepam. Tat-NR2B9c also had a minor effect of reducing gliosis at 3 days post-SE. 1400W slightly reduced the frequency of epileptiform discharges between 3 and 7 days post-SE and reduced the proliferation of nNOS immunopositive neurons 14 days post-SE.

5.2 INTRODUCTION

5.2.1 Incremental dosing regimen

The presence of a latent period between the first manifestations of seizures and the emergence of chronic epilepsy offers a potential window for therapy. While it is informative to investigate the effects of potential disease-modifying pharmacological agents administered prior to the induction of SE, treatments that are effective in suppressing disease progression when administered after an IPI could be of far greater clinical value. The control of epilepsy in the clinic suffers from a shortage of tools for suppressing disease progression, with the majority of effective interventions targeted the symptoms of epilepsy, rather than disease progression (see chapter 1.6).

In order to investigate the efficacy of treatments administered post-seizure, pharmacological agents used in animal models must be shown to be effective in controlling the progression of epileptogenesis when administered after an IPI. In order to achieve this, the variability in the severity of epileptiform behaviour must be reduced as much as possible in SE models. Further, the severity of the initial insult should be maximized in order to increase the potential for suppression without increasing mortality. While the dose of kainic acid, per se, may be important in determining the outcome, it is likely that the severity and duration of the period of status epilepticus is of greater importance.

For this reason, an incremental dosing regimen was developed in order to titrate the dose of kainic acid by behavioural response. In this way, the severity of seizure can be standardised, maximized, while at the same time the mortality of animals can be minimized. The effects on behavioural indicators of seizure severity were compared, hippocampal c-Fos expression post-SE and EEG both during the period of KA-induced SE and for a 7-day period following. This model was then used in two pilot studies to test the efficacy of pharmacological agents administered following the termination of status epilepticus with diazepam. Two separate molecular signalling pathways that may be involved in mediating epileptogenesis were investigated.

5.2.2 PSD-95 and Tat-NR2B9c

The NMDA receptor is heavily implicated in mediating excitotoxic and inflammatory processes post-seizure and though treatments that target this molecule have proven effective at suppressing seizures, the side effects associated with NMDA antagonism have meant that the drugs are largely unsuitable for disease control (Newcomer et al, 1999). A range of pharmacological therapies that target specific subunits of the NMDA receptor (see chapter 4) or signalling pathways downstream of the NMDA receptor have been investigated (Koponen et al, 2000). The NMDA receptor exists within a multiprotein signalling complex known as the post synaptic density (PSD). There is considerable interest in elucidating the molecular mechanisms that controls synaptic targeting and trafficking of glutamate receptors, particularly because of their role in the induction and expression of various forms of synaptic plasticity underlying myriad functions in the CNS, including memory formation and also important in the pathogenesis of epilepsy (Malenka & Nicholl, 1999).

Most populous amongst the myriad proteins involved with organising the structure of the PSD is the post-synaptic density protein 95 (PSD-95), with between 200 and 300 molecules of PSD-95 present at in an average PSD (Chen et al, 2005). Alternatively referred to as synapse-associated protein-90, PSD-95 is a member of the membrane-associated guanlylate kinase (MAGUK) family (Oliva et al, 2012), encoded by the disks large homolog 4 (DLG4) gene (Cho, et al, 1992). PSD-95 couples the NMDA receptor to intracellular proteins and signaling enzymes, including nNOS. This spatial coupling is a vital component of signalling cascades, but is also important for the signalling pathways underlying excitotoxicity. It therefore represents an opportunity to disrupt potentially pathophysiological aspects of NMDAR-signalling.

NMDARs are anchored in the PSD by interactions between the cytoplasmic C-terminal tails of their NR2 subunits and the PDZ domains of PSD-95, an abundant PSD protein that forms a two-dimensional lattice immediately under the postsynaptic membrane. The PDZ domains of PSD-95 bind to other postsynaptic membrane proteins, including potassium channels, tyrosine kinases, cell adhesion molecules, stargazin, which is involved in AMPAR trafficking (Tomita et al, 2005), shank, which forms a polymeric network structure with homer and regulates the maturation of dendritic spines (Hayashi et al, 2009), nNOS, as discussed in previous chapters, and many other proteins involved in both the maintenance of structural integrity of the synapse, trafficking receptors to and from the post-synaptic membrane and transducing signals from the synapse into the cell body. PSD-95 functions as a scaffold to assemble a specific set of signaling proteins around the NMDAR, with multiple domains that bind to a variety of cytoplasmic proteins.

PSD-95 forms multimers, mediated by N-terminal interactions (Hsueh & Sheng, 1999). The multimerization of the PDZ scaffolds enhances clustering of specific assemblies of proteins in the PSD. The role that PSD-95 plays in clustering scaffolding and signalling proteins in the PSD is important in the maturation and strengthening of excitatory synapses (Kim et al, 2007). Of particular importance to epilepsy is the role that PSD-95 plays in facilitating the function of various proteins involved in transducing the molecular signalling pathways from Ca^{2+} influx through the NMDAR. Of particular note, PSD-95 holds nNOS in close apposition to the NMDAR pore, coupling NMDAR activation with NO production. Further, PSD-95 plays an important role in recruiting AMPA receptors to the synapse.

The use of pharmacological antagonsits is of limited clinical benefit because of the severity of side effects, while PSD-95 knockout mice show a severe phenotype, due to the disordered nature of excitatory synapses (Chen et al, 2011), specifically targetting subsets of NMDARs selected by subunit composition has proved to have greater potential. Another route to tackling NMDAR-mediated excitotoxicity associated with TLE is by disrupting the interaction between NMDARs and PSD-95, and thereby weakening the cellular response to Ca^{2+} influx though the NMDAR channel.

Aarts et al (2002) developed a cell permeable peptide that targets the PDZ domain of PSD-95 and dissociates it from NR2 subunits of the NMDA receptor, thereby decoupling signalling pathways that link Ca^{2+} influx through the receptor with enactors of neuronal death, whilst largely preserving other functionalities of the

NMDA receptor in modulating synaptic plasticity. This cell permeable peptide, Tat-NR2B9c has been used by Aarts et al (2002) and other authors (Cook et al, 2012) in models of neurodegenerative diseases and has proven to be strongly neuroprotective in a range of animal models of CNS pathology without exhibiting the aversive side effects associated with NMDA antagonists. In this study, the effects of post-SE administration with Tat-NR2B9c on epileptogenesis was investigated, investigating the frequency of IEDs during the 'latent period' (0 – 7 days post-SE) and on gliosis at three days post-SE.

5.2.3 iNOS and 1400W

NO acts via multiple downstream signalling mechanisms, depending on the concentration, with low concentrations being neuroprotective and mediating physiological signalling (e.g., neurotransmission or vasodilatation), whereas higher concentrations mediate immune/inflammatory actions and are neurotoxic. Nanomolar concentrations of NO are generated by eNOS and nNOS, whereas iNOS can produce micromolar levels in response to proinflammatory stimuli. Because iNOS production of NO is more clearly correlated with the progression of neuroinflammatory diseases and its expression is delayed following insult, the specific targetting of this isoform represents an attractive target for therapeutic intervention in the disease progression of chronic epilepsy.

While the role of Ca^{2+}/Calmodulin-dependent nitric oxide signalling has been extensively studied in epilepsy (Takei, et al., 2001; Pereira de Vasconcelos et al., 2005; Hagioka et al., 2005; Kovacs et al., 2009; Kim, 2010; Arhan et al., 2011), the

inducible isoform has been largely neglected. Strong evidence exists for a huge upregulation of iNOS expression following seizures (Zheng, et al, 2010). There is also strong evidence that iNOS inhibition can significantly improve the pathological outcomes in animal models of a range of CNS pathologies (Parmentier et al, 1999; Sennlaub et al, 2002; Jafarian-Tehrani et al, 2005; Montezuma et al, 2012).

Most NOS inhibitors described to date have been analogs of the NOS substrate, L-arginine (Garvey, 1997), such as N-(G)-L-arginine methyl ester (L-NAME), L-N^G-Nitro arginine (L-NOARG) (Moore et al, 1990) or L-NPA, as already discussed in previous chapters. iNOS specific inhibitors also include L-arginine analogs such as N^6-(1-iminoethyl)-L-lysine (L-NIL) (Moore et al, 1994). Other specific iNOS inhibitors include S- substituted isothioureas, such as S-methylisothiourea (SMT) (Southan et al, 1995), cyclic amidine derivatives, such as (1S,5S,6R,7R)-7-Chloro-3-imino-5-methyl-2-azabicyclo[4.1.0]heptane hydrochloride (ONO-1714) (Naka et al, 2000), aminoguanidine (AG) (Griffiths et al, 1993) and 2-amino-5,6-dihydro-6-methyl-4H-1,3-thiazine (AMT) (Nakane et al, 1995).

N-[3-(aminomethyl)benzyl]acetamide (1400W) dihydrochloride is a potent, slow, tight-binding, inhibitor of inducible isoform of NOS and is described by Garvey, et al (1997) as the most selective discovered, with 5000- and 200- fold selectivity over endothelial and neuronal isoforms, respectively. 1400W is the iNOS inhibitor most widely used as an experimental tool and has previously been shown to ameliorate the pathogenesis associated with traumatic brain injury (Jafarian-Tehrani, et al, 2005), ischaemic brain injury (Parmentier, et al, 1999), depression (Montezuma, et al, 2012) and ischaemic proliferative retinopathy (Sennlaub, et al, 2002) in in vivo animal models.

Despite the promise of this potential intervention, to our knowledge, no similar studies have been carried out using a kainic acid model of epileptogenesis in mice. 1400W was administered after the termination of SE with diazepam, with regular treatments given over the first three days post-SE. The effect of inhibiting iNOS on electrographic indicators of epileptogenesis over the first 7 days post-SE was investigated and on neuronal loss and nNOS proliferation at 7 and 14 days.

5.3 MATERIALS AND METHODS

5.3.1 Overview

Information regarding materials and methods described in this chapter refer only to that which is specific to this particular study. For general materials and methods, see chapter 2 where detailed protocols of methods performed throughout all chapters are described, including: KA administration and behavioural scoring of SE, basic protocols used for immunohistochemistry, microscopy and quantification of immunohistochemistry, surgical procedures for the implantation of electrodes and transmitters and EEG data collection and analysis. For ease of understanding, however, some information is duplicated.

5.3.2 Animals

Experiments were performed in 10-12 week old male C57BL/6J mice. All animals were purchased from Charles River (UK) and maintained in the Biomedical Services Unit, University of Liverpool under controlled environmental conditions ($19^{o}C$ – $23^{o}C$, 12h light: 12h dark), with food and water available *ad libitum*. All experiments were carried out according to Animals (Scientific Procedures) Act 1986 approved by the Secretary of State, Home Office, UK and University's Ethical Review Committee.

A total of 47 mice were used for studies reported in this chapter. 20 mice were implanted with telemetry devices for the recording and transmitting of EEG from electrodes placed below the skull. Of these, 5 were given a single dose of 20mg/kg

KA and the remaining 15 subjected to an incremental KA dosing schedule, titrated according to behaviour and described below. Following the termination of seizures with diazepam, the 15 incrementally dosed mice were put into one of four treatment groups: Tat-NR2B9c (n = 4), Tat-NR2B9c placebo (n = 3), 1400W (n = 4) or DW vehicle (n = 4). Specifics of the treatment regimen for these mice is described below.

The remaining 27 mice were used for immunohistochemistry. Of these, 5 were used as naïve controls, and did not receive KA. The other 22 mice were given incremental doses of KA according to the protocol described below, and then treated accordingly: Tat-NR2B9c, sacrificed at 3 days (n = 4), Tat-NR2B9c-placebo, sacrificed at 3 days (n = 4), 1400W, sacrificed at 7 days (n = 3), DW vehicle sacrificed at 7 days (n = 3), 1400W, sacrificed at 14 days (n = 4), DW vehicle sacrificed at 14 days (n = 4).

5.3.3 Drugs, reagents and antibodies

Tat-NR2B9c (gift from Dr M. Tymianski, University of Toronto) was prepared in saline at a concentration of 5mg/ml and delivered by intravenous injection into a tail vein at a dose of 7.8mg/kg. An inert peptide with structural similarities was administered via the same route and employed as a vehicle control. 1400W (Tocris, UK) was diluted in distilled water at a concentration of 20mg/ml and administered via i.p injection at a dose of 50mg/kg.

Sheep anti-nNOS (1:2000) was a gift from Dr P.C. Emerson and visualised using a CY3-conjugated donkey anti-sheep antibody (1:200). Mouse anti-NeuN (1:400) was purchased from Chemicon (UK) and visualised using an FITC donkey anti-mouse

secondary antibody (1:200). Mouse anti-GFAP (1:400) was purchased from Sigma Aldrich (UK) and visualised using an FITC-conjugated donkey anti-mouse secondary antibody (1:200) Biotinylated tomato lectin (1:500) was purchased from Sigma Aldrich (UK) and visualised using CY3-conjugated streptavidin (1:100). All flourochrome-conjugated secondary antibodies and streptavadin were purchased from Jackson Immunoresearch laboratories (UK). DAPI used for visualizing cell nuclei was in the Vectashield ® mounting medium (Vector Laboratories, UK).

5.3.4 Incremental dosing protocol

Mice were given repeated doses of KA and behaviour closely monitored. An initial dose of 10mg/kg KA was administered. 30 minutes later, a further 5mg/ml was given. This dose was repeated at 30 minute intervals until the first class II seizure. Behaviour was scored for a 2 hour period from this point. 2 hours from the first class III seizure, SE was terminated with diazepam (10mg/kg, i.m).

5.3.5 Tat-NR2B9c & 1400W administration

Tat-NR2B9c is a peptide comprising the nine COOH-terminal residues of NR2B (Lys-Leu-Ser-Ser-Ile- Glu-Ser-Asp-Val, fused to the cell-membrane transduction domain of the human immunodifficiency virus-type 1 (HIV-1) Tat protein (Tyr- Gly-Arg-Lys-Lys-Arg-Arg-Gln-Arg-Arg- Arg) (Aarts et al, 2002). Tat-NR2B9c (or Tat-NR2B9c-placebo) was administered in our studies immediately following the termination of SE with diazepam, with a dose of 7.8mg/kg being injected directly into the tail vein. 50mg/kg 1400W (or equivalent volume of DW in vehicle controls) was

administered immediately following the termination of SE with diazepam. A further dose of 50mg/kg was administered every 24 hours for 3 days.

5.4 RESULTS

5.4.1 Behaviour following incremental dosing of kainic acid

Mice were given a dose of 10mg/kg KA, followed by a further 5mg/kg every 30 minutes until convulsive motor seizures were observed (Racine 3), at which point treatment did not continue. Of all the mice given this treatment, 100% showed full tonic-clonic seizures, while there was 0% mortality. The median dose given was 25mg/kg, with a range between 15 and 35mg/kg, meaning that, while all animals had an identical duration of complex motor seizures, the duration from the administration of the initial dose of KA to the termination of status epilepticus with diazepam ranged from 150 minutes to 240 minutes.

5.4.2 c-Fos expression following status epilepticus induced by incremental doses of kainic acid

In both animals treated with 20mg/kg KA and animals given an incremental dosing regimen to titrate dose according to behaviour, c-Fos expression was highest in the granule cell layer of the dentate gyrus. Expression in this region was moderately higher in animals given a single dose (figure 5.1a, b), however, the most notable difference in the distribution of c-Fos between the two treatment groups was in the excitatory circuitry of the hippocampus. While animals given a single injection showed low and variable expression of c-Fos in the pyramidal cell layer of CA3 and CA1, with between 5 and 10% of pyramidal neurons c-Fos positive in CA3 and around 10% in CA1, animals undergoing an incremental dosing regimen showed c-

Fos expression in between 30 and 35% of pyramidal neurons in CA3 and between 35 and 40% in CA1 (pyramidal cells in CA3: $t_8 = 5.782$, $p < 0.001$, pyramidal cells in CA1: $t_8 = 5.431$, $p < 0.001$, figure 6.1a, c, d). In the stratum radiatum and stratum oriens of the CA1 region of both treatment groups, c-Fos expression was observed in around 10% of neurons, while in the CA3 region, incrementally dosed animals showed an approximately 25% increase in the percentage of neurons expressing c-Fos in stratum oriens and a 75% increase in stratum radiatum (Figure 6.1a, d).

5.4.3 Comparison between electrographic status epilepticus induced with bolus injection and incremental dosing regimen of kainic acid

In animals given an incremental dosing regimen, the analysis of status epilepticus began at the point at which complex motor seizures were first observed. Spike frequency was initially around 40 spikes min^{-1}, increasing to a peak of between 65 and 75 spikes min^{-1}, which was similar to the initial peak observed in animals given a single injection (figure 5.2a). While the spike frequency during status epilepticus in mice given a single injection followed a cyclical pattern with peaks and troughs, incrementally dosed animals showed a steadier spike rate, remaining between 50 and 70 spikes min^{-1} from around the 20 minute mark to 80 minutes when the spike rate began to decrease (figure 5.2a). In each 30 minute bin for the first 90 minutes post-KA, incrementally dosed mice showed a spike frequency significantly higher than mice receiving a single injection (0 – 30mins: $t_{18} = 3.811$, $p = 0.005$; 30 – 60 mins: $t_{18} = 2.525$, $p = 0.035$; 60 – 90 mins: $t_{18} = 3.144$, $p = 0.014$, figure 5.2b).

While mice receiving a single injection of kainic acid showed a steadily increasing power distributed in the γ-frequency band, reaching a peak at around 90 minutes, incrementally dosed animals showed a greater level of power in the γ-frequency band power throughout the two first 90 minutes of observation (0 – 30 mins: t_{18} = 10.889, $p < 0.001$; 30 – 60 mins: t_{18} = 7.769, $p < 0.001$, 60 – 90 mins: t_{18} = 4.237, $p < 0.001$). This variation suggests that γ-frequency power is more strongly related to the time since the initial dose of kainic acid, rather than the severity of seizures, as these animals showed a fairly pattern of behaviour (figure 1.1a).

5.4.4 Comparison of EEG during latent phase between animals receiving bolus injection and incremental dosing regimen of kainic acid

Following termination of SE with diazepam, no behavioural seizures were observed either in animals receiving a single dose of kainic acid or in animals given an incremental dosing regimen over the first 7 days. Animals undergoing an incremental dosing regimen had a higher frequency of epileptiform spikes throughout the first 36 hours of recording post KA injection and from around 3 days to the end of the 7th day period of recording. Between 36 and 72 hours, the frequency of epileptiform spiking between the two treatment groups converged (figure 5.3a).

The timecourse of spike frequency over the first 7 days in mice treated with a single dose of kainic acid has been described in previous chapters. In incrementally dosed animals, the spike frequency at the point of diazepam administration was approximately 2-fold higher (figure 5.3a), and the suppression of epileptiform spikes by diazepam was less effective. While in mice treated with a single dose,

epileptiform spikes had decreased to around 10 spikes min^{-1}, 2 hours after diazepam injection, in incrementally dosed animals, the spike rate was still around 80 spikes min^{-1} at this timepoint (figure 5.3a).

While at around 6 hours following diazepam injection, mice treated with a single dose of kainic acid showed an increase in spike rate, up to around 15 spikes min^{-1}, (presumably as a consequence of decreasing brain concentrations of diazepam), at this timepoint, the frequency of epileptiform spiking in incrementally dosed mice plateaued at around 60 spikes min^{-1}. From around 8 hours post injection, the spike rate continued to decline steeply before plateauing again at around 20-25 spikes min^{-1} at approximately 15 hours post kainic acid injection (figure 5.3a). From approximately 20 hours post injection, the spike rate in incrementally dosed mice decreased steadily and the spike rate of mice from both treatment groups converged at around 40 hours at approximately 10 spikes min^{-1}.

The frequency of epileptiform spikes both decreased from 40 hours post injection to approximately 58 hours post injection, where it dropped to around 1 spike min^{-1} in both treatment regimen. At this timepoint, the frequency of epileptiform spikes in incrementally dosed animals increased sharply to approximately 6 spikes min-1 at 60 hours, dropped to around 4 spikes min-1 at around 60 hours, before increasing again reaching approximately 8 spikes min-1 at around 72 hours. In contrast, in animals receiving a single dose of kainic acid, the spike frequency gradually increased from around 1 spike min^{-1} at 60 hours to approximately 4 spikes min^{-1} at 72 hours.

In both treatment groups, the spike frequency between 72 hours and 7 days remained relatively constant, at approximately 8 spikes min^{-1} in incrementally dosed animals and 4 spikes min^{-1} in animals receiving a single dose of kainic acid (figure 5.3a). When the 7 day period of recording was split into bins of 3 – 12 hours, 12 – 48 hours and 48 – 168 hours, incrementally dosed animals showed a higher spike frequency than animals receiving a single dose at between 3 and 48 hours (3 – 12h: $t_7 = 7.109$, p 0.002, 12 – 48h: $t_7 = 3.614$, p = 0.009, figure 5.3a), however, though spike frequency was higher in incrementally dosed animals from 48h – 168h, the difference was not statistically significant at the 0.05 level.

5.4.5 Effect of Tat-NR2B9c treatment on epileptiform spike frequency in 7 day period following kainic acid induced status epilepticus

Following the termination of status epilepticus with diazepam and the administration of either placebo or Tat-NR2B9c, mice in both treatment groups showed no behavioural seizures for the first 7 days. In animals treated with Tat-NR2B9c, the decline in spike frequency associated with diazepam administration was steeper, suggesting that Tat-NR2B9c had a facilitatory or complementary effect on the action of diazepam (figure 5.4a). While in placebo treated animals, Rather than sharp reduction in spike rate, followed by an increase as the drug concentration reduced, as seen in animals given a single dose, incrementally dosed animals showed a shallow decline in spike frequency, followed by a plateauing from around 6 hours at approximately 60 spikes min^{-1} (figure 5.4b).

From around 12 hours post-KA, spike frequency again decreased sharply to approximately 30 spikes min^{-1} by the 24 hour point. Spike frequency continued to steadily decline until it reached around 15 spikes min^{-1} at around 36 hours post-KA, from where it remained at approximately this frequency for remainder of the 7 day recording period (Figure 6.4b, c).Throughout the entire 7 day period recorded, Tat-NR2B9c treated mice had a reduced frequency of epileptiform spikes, in comparison with placebo-treated controls, however, this difference was only statistically significant at the level of 0.05 for the first 12 hours post KA: 3 – 12 hours: t5 = 3.438, p = 0.019 (figure 5.5b, e).

5.4.6 Effect of Tat-NR2B9c treatment on gliosis in hippocampal formation during latent phase

In view of assertaining L-NPA's effect beyond acute SE period and to understand whether seizure modulation by L-NPA during SE will have an effect on epileptogenic events during the early latent period, glial cells and synaptophysin immunostaining was examined. At 24h post-KA period, there was no significant difference in microglia or astrocyte cell counts in any treatment groups (Figure 5.5f – i), nor was there any qualitative differences in astrocyte or microglial morphology that would associate them with an activated state. This suggests, that in the kainic acid model, 24h is too early to see changes in glial activation associated with seizures.

By 72h, however, qualitative changes in morphology of both astrocytes and microglia could be observed in sections from animals of both treatment groups. Astrocytes expressed higher densities of GFAP and were hypertrophic (Figure 5.5a) and many

microglia were observed to assume the rod-like ‘activated’ morphology (Figure 5.5b) as described by Kreutzburg (1996). These changes could be seen in stratum radiatum and stratum oriens throughout the hippocampus, however the activated morphology was not increased in any region of the dentate gyrus (Figure 5.5a). L-NPA pre-treatment had the effect of suppressing these morphological changes, with fewer cells showing an activated morphology (Figure 5.5b, c, d, e). As well as qualitative changed in morphology, changes in cell numbers and distribution, associated with reactive gliosis were also observed.

72h after KA injection, both astrocytes (Figure 5.5b) and microglia (Figure 5.5d) showed a propensity to invade the stratum lucidum and pyramidal cell layer of the CA3 region. Further to this, the density of both types of glial cells increased throughout the CA3 region, with GFAP-immunopositive cell numbers increasing approximately 2-fold (Figure 5.5b, f) and tomato lectin-immunopositive cell numbers increasing approximately 3-fold (Figure 5.5d, i). The number of tomato lectin immunopositive cells in the CA1 region also increased by approximately 2-fold. Tat-NR2B9c had a small effect towards suppressing the proliferation of astrocytes and microglia, however, this effect was not significant in any region of the hippocampal formation investigated.

5.4.7 Effect of 1400W treatment on EEG recorded during latent phase

Following the termination of status epilepticus with diazepam and the administration of either DW or 1400W, mice in both treatment groups showed no behavioural seizures for the first 7 days. 1400W had no effect on the frequency of IEDs for the

first 48 hours following SE. When the spike rate increased again between the second and third day post-SE, 1400W appeared to suppress epileptiform spiking, reducing the frequency by approximately 50%, however this was not statistically significant at the 0.05 level.

5.4.7 Neurodegeneration at 7 and 14 days post-seizure

At 7 days post-seizure, no evidence of neuronal loss was found, however after 14 days, neurons in the pyramidal cell layer of the hippocampal CA3 region were sparser (figure 5.7a – c). Cell counts revealed a small drop in numbers of neurons stained with NeuN (figure 5.7d) and cresyl violet (figure 5.7e). 1400W administration, however, had no detectable neuroprotective properties in this model.

5.4.8 Distribution of nNOS immunopositive neurons at 7 and 14 days post-seizure

7 days following KA-induced SE, no detectable changes in the anatomical distribution of nNOS immunopositive neurons were found in the hippocampal formation. By 14 days post-SE, however, a notable proliferation of nNOS immunopositive neurons was observed (figure 5.8). nNOS positive neurons increased in numbers most strikingly in the polymorphic layer of the dentate gyrus (F_{10} = 7.0094, p = 0.0125, figure 5.8a, d) and the stratum radiatum of CA3 (figure 5.8a, d). Control regions of the brain with high densities of nNOS were photographed, including the thalamus and the arcuate nucleus. In these regions, no changes in nNOS distribution were witnessed, suggesting that the SE-induced increase is local and specific.

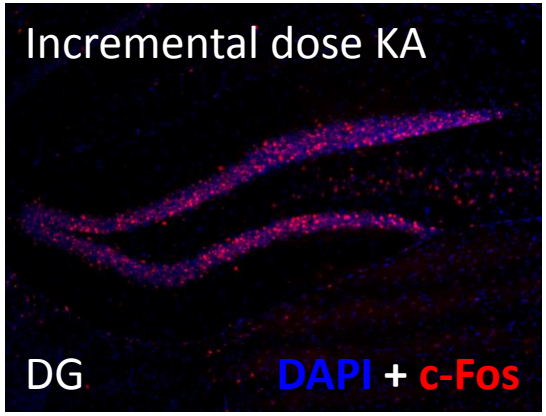

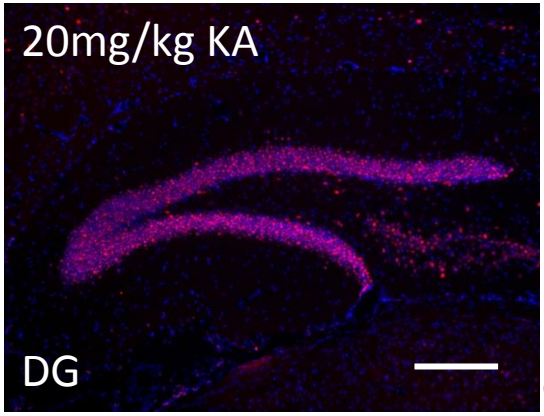

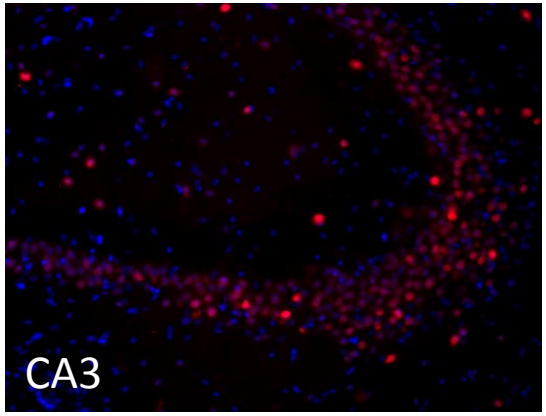

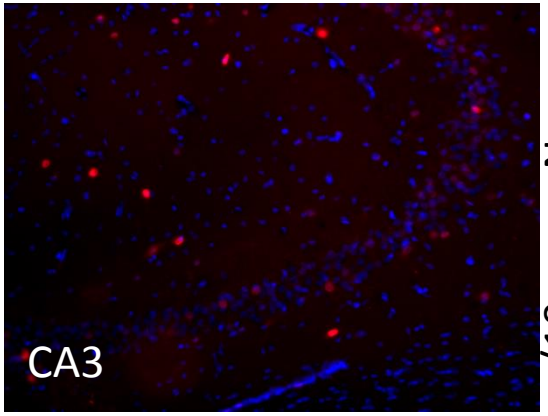

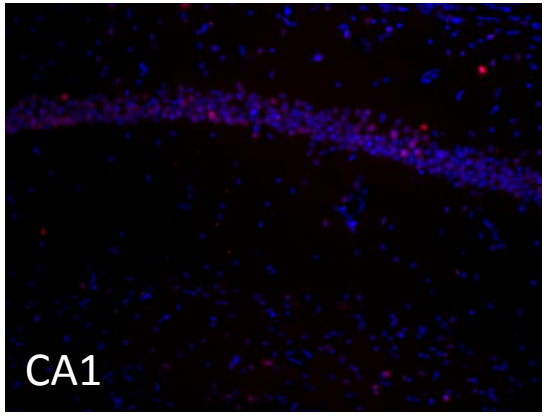

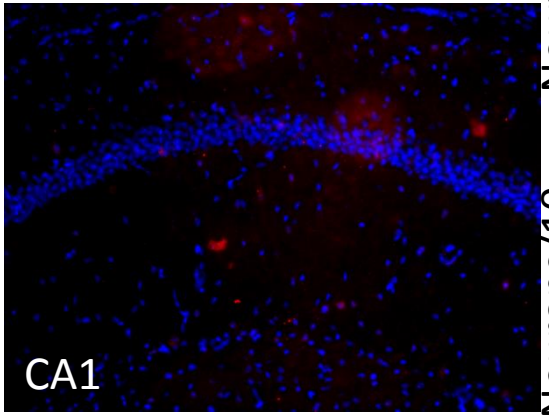

Figure 5.1. c-Fos expression is more widespread in hippocampal formation following incremtal dosing of KA (a) Photomicrographs. Magnification: 10X, scale bar: 100µm **(b)** Quantification of c-Fos immunopositive neurons. (neurons/10) *,**,***,****p<0.001

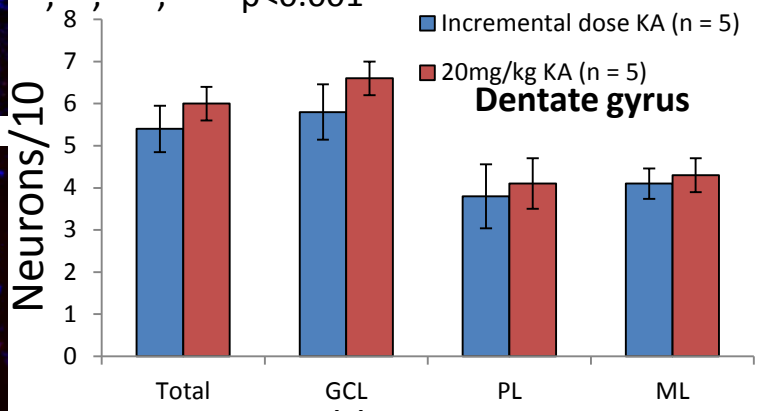

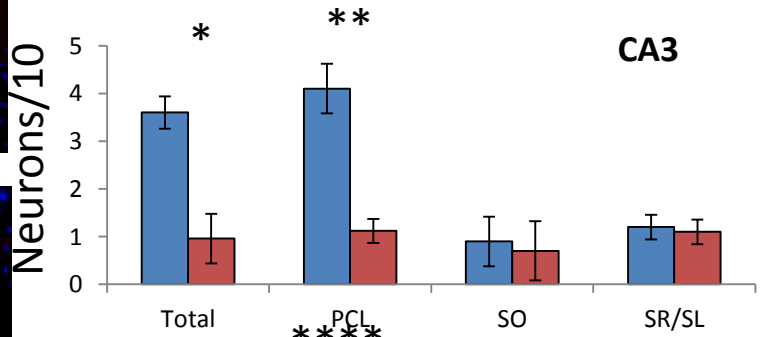

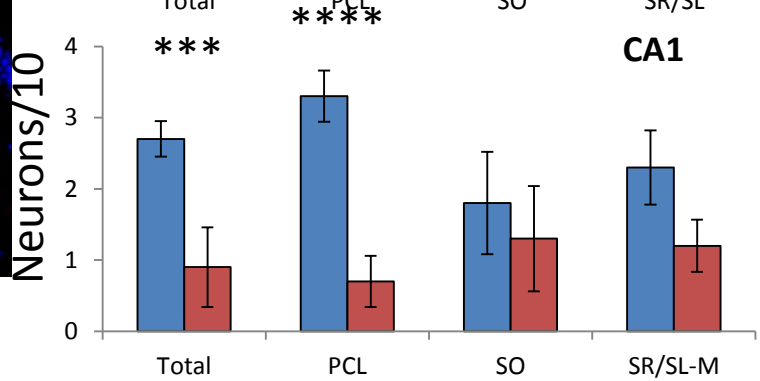

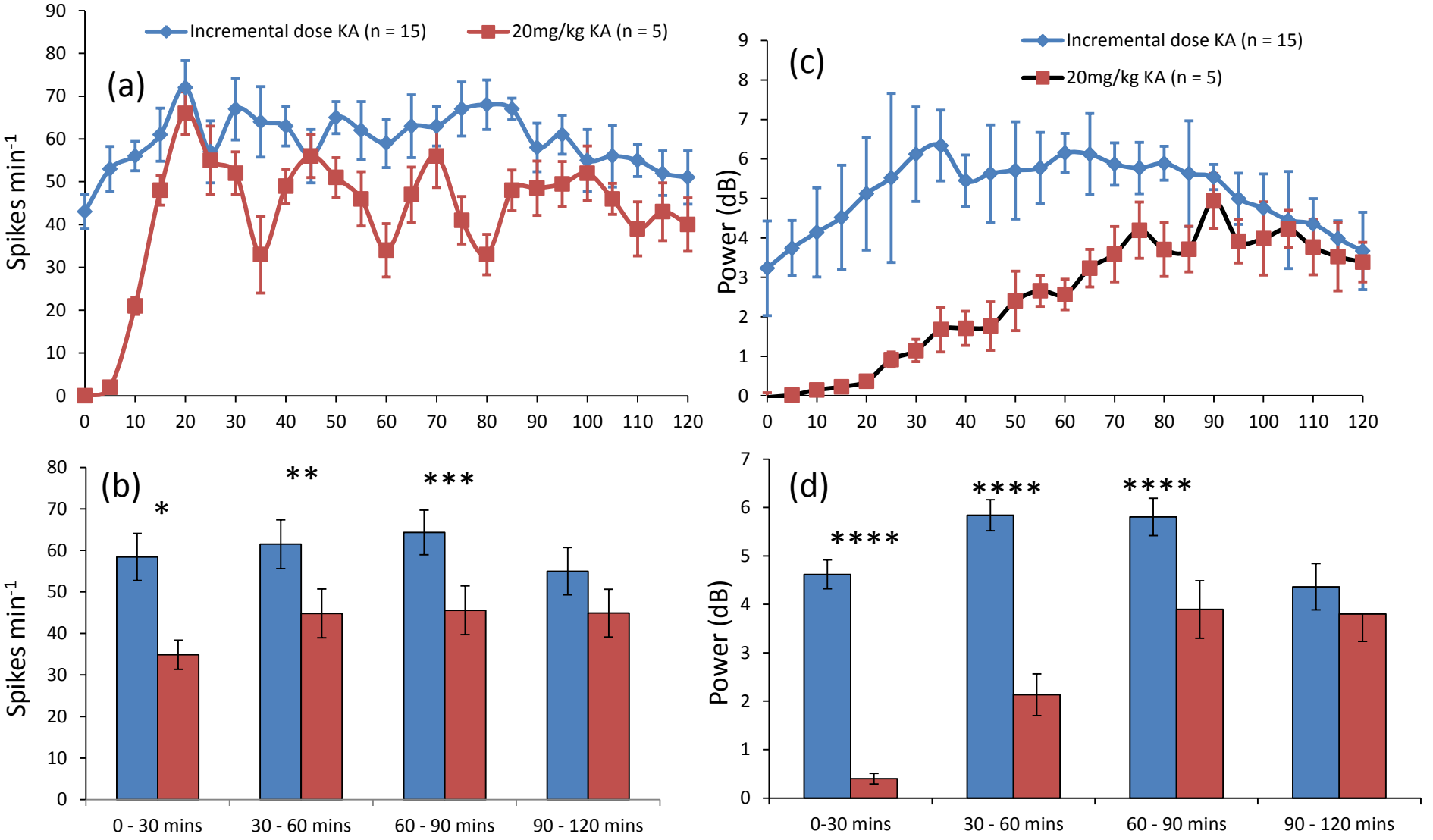

Figure 5.2. Comparison between bolus injection and incremental dosing regime in electrographic status epilepticus. (a) Epileptiform spike frequency **(b)** Epileptiform spike frequency *p = 0.005, **p = 0.035, ***p = 0.014 **(c)** Power distributed in γ-frequency band (dB) **(d)** Power distributed in γ-frequency band (dB). ****p < 0.001.

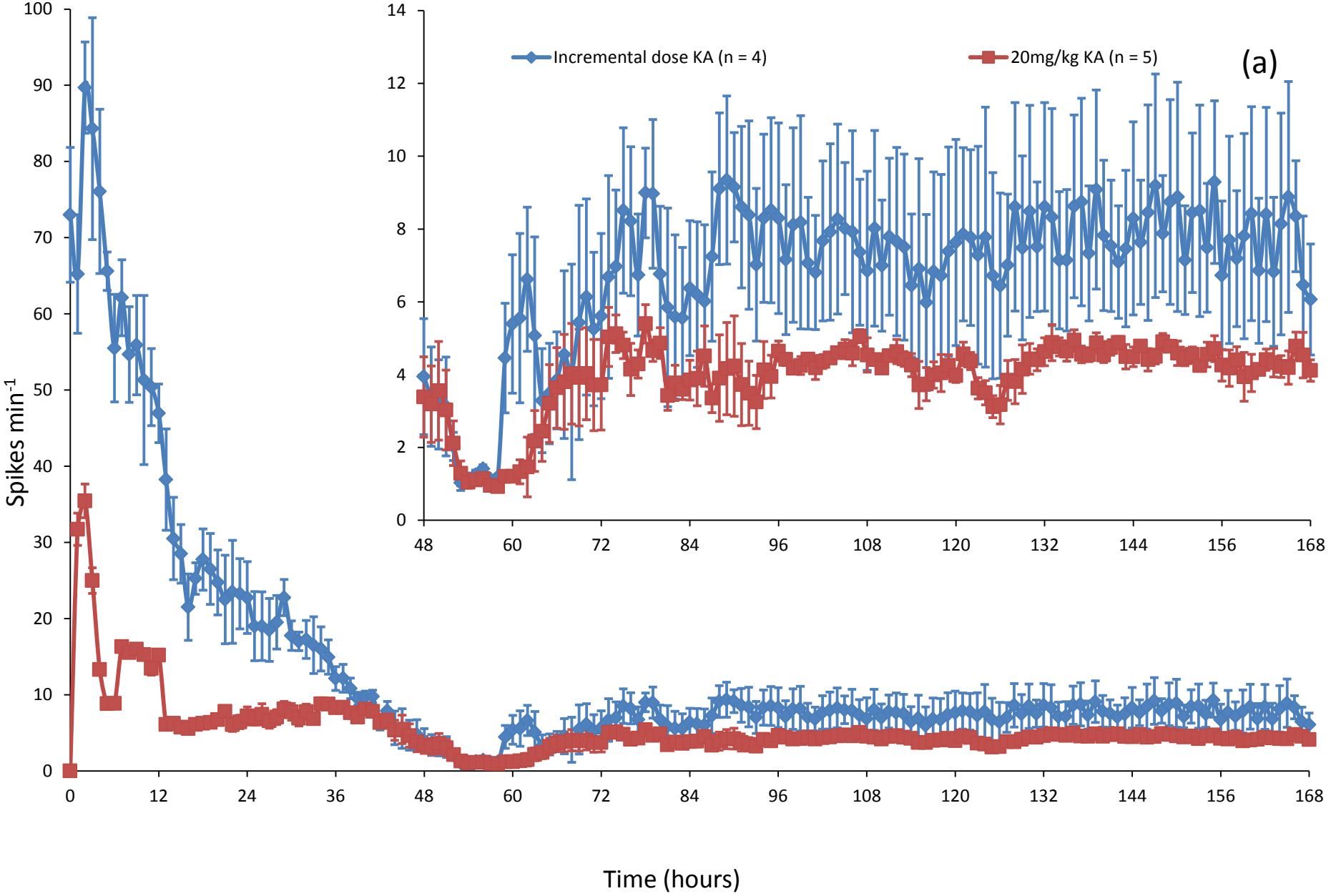
Incremental dose KA (n = 4)
20mg/kg KA (n = 5)
(a)
Spikes min-1
Time (hours)
0
10
20
30
40
50
60
70
80
90
100
0
12
24
36
48
60
72
84
96
108
120
132
144
156
168
0
2
4
6
8
10
12
14
48
60
72
84
96
108
120
132
144
156
168

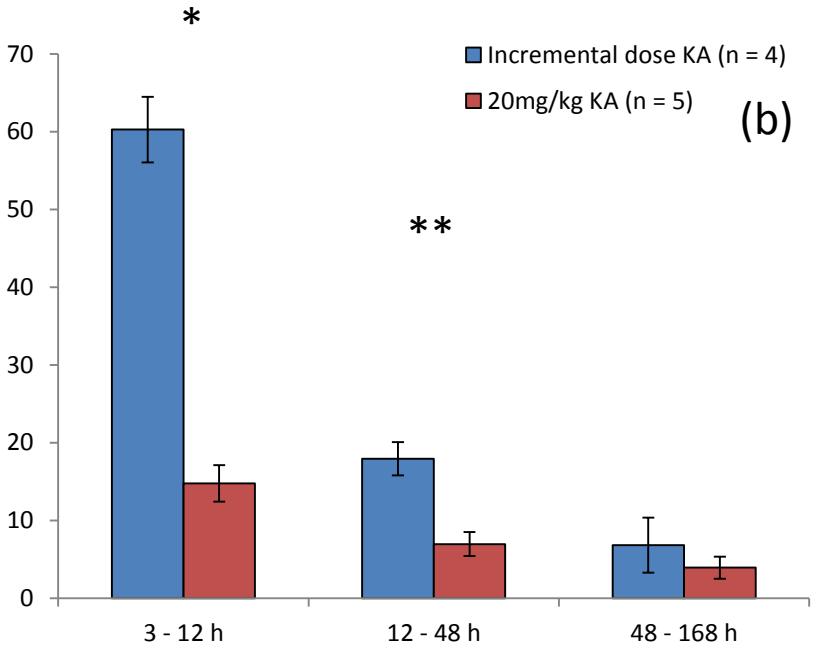

Figure 5.3. Comparison between single injection of KA and incremental dosing regime in first 7 days following seizure. **(a)** Frequency of epileptiform spikes for full 7 day period. Inset: 48 – 168h at higher spike rate resolution. **(b)** Spike frequency average over extended time periods. *t_7 = 7.109, p 0.002, ** t_7 = 3.614, p = 0.009

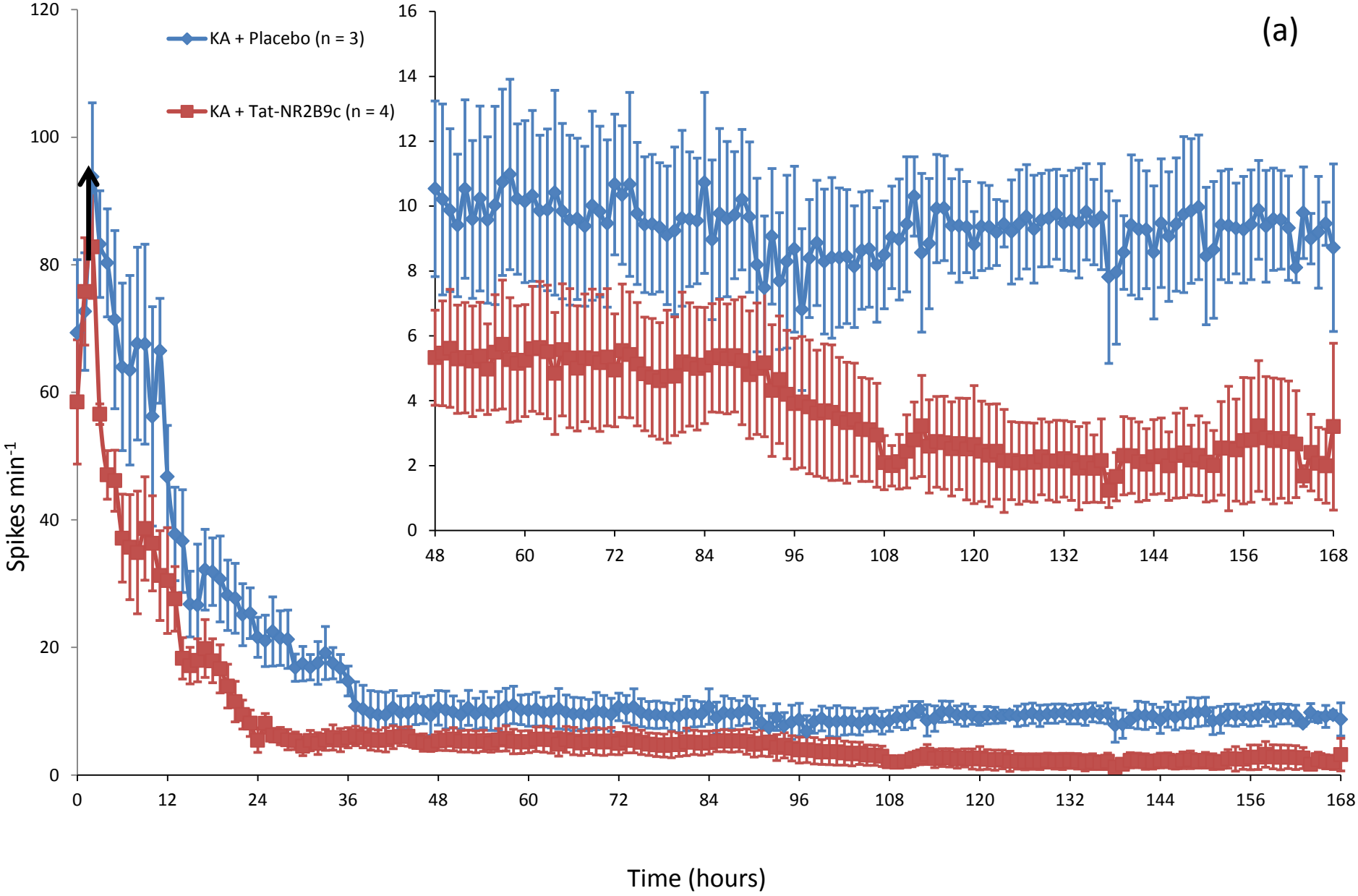
(a)
KA + Placebo (n = 3)
KA + Tat-NR2B9c (n = 4)
Spikes min-1
Time (hours)
0
20
40
60
80
100
120
0
12
24
36
48
60
72
84
96
108
120
132
144
156
168
0
2
4
6
8
10
12
14
16
48
60
72
84
96
108
120
132
144
156
168

Figure 5.4. Tat-NR2B9c administration post-Status epilepticus reduces frequency of epileptiform spikes **(a)** epileptiform spike frequency over full 7 days . Inset: 48 - 168h post-KA at higher spike frequency resolution **(b)** Spike frequency averaged over periods of longer duration. *t_5 = 3.438, p = 0.019. Arrow indicates tat-NR2B9c injection time.

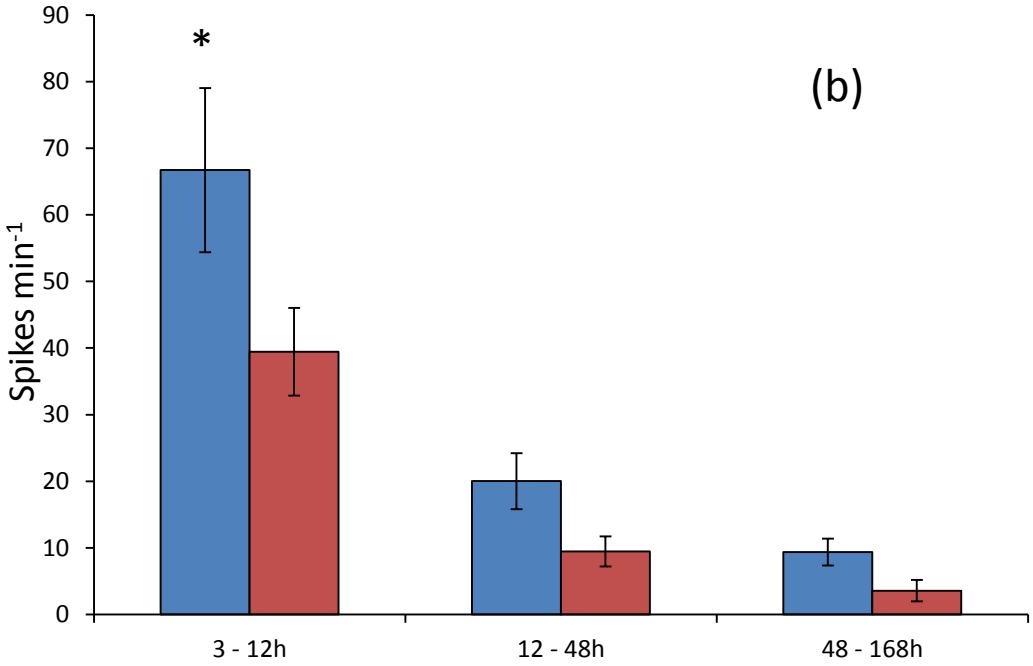

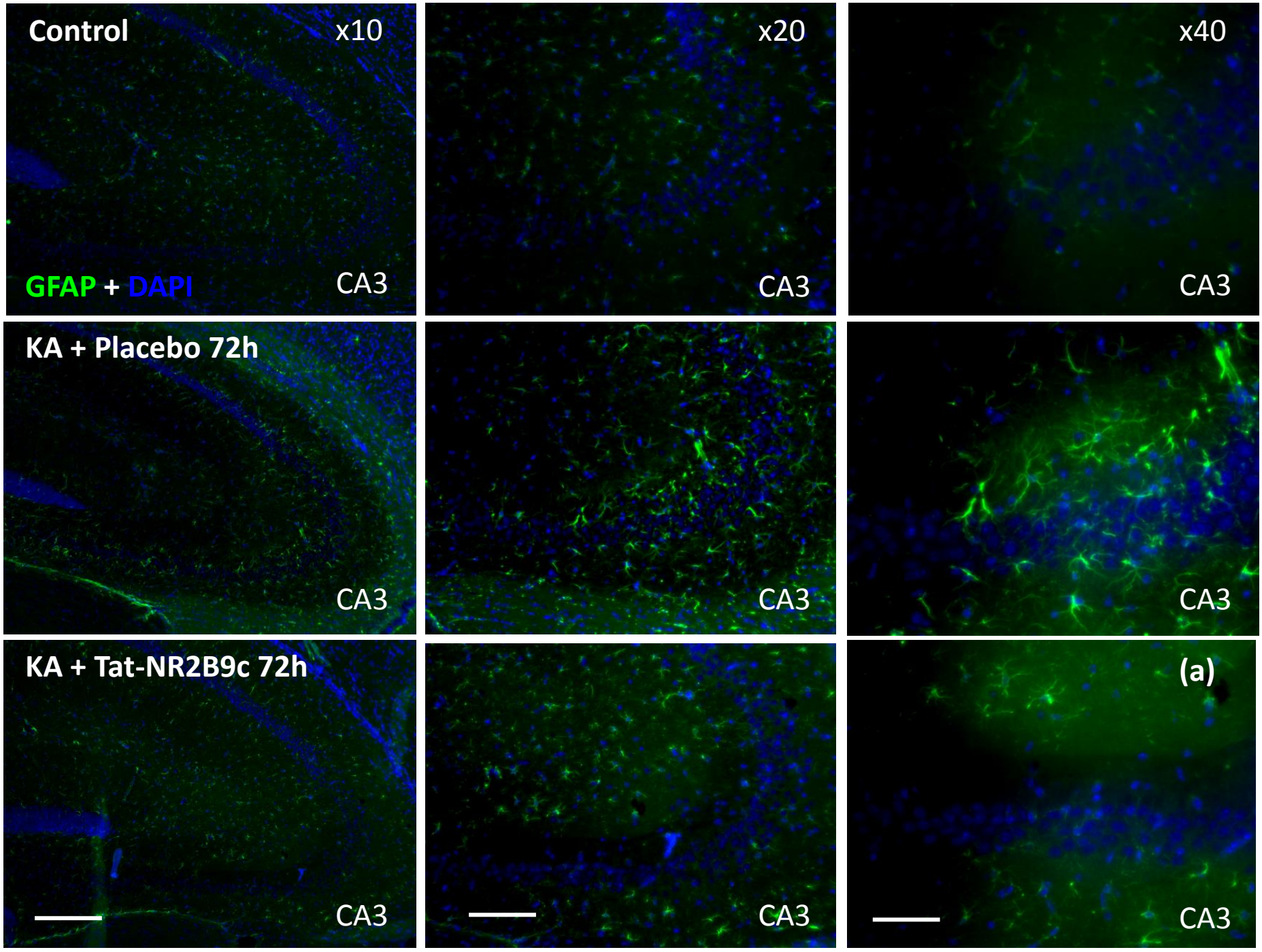
Control
x10
x20
x40
GFAP + DAPI
CA3
CA3
CA3
KA + Placebo 72h
CA3
CA3
CA3
KA + Tat-NR2B9c 72h
CA3
CA3
(a)
CA3

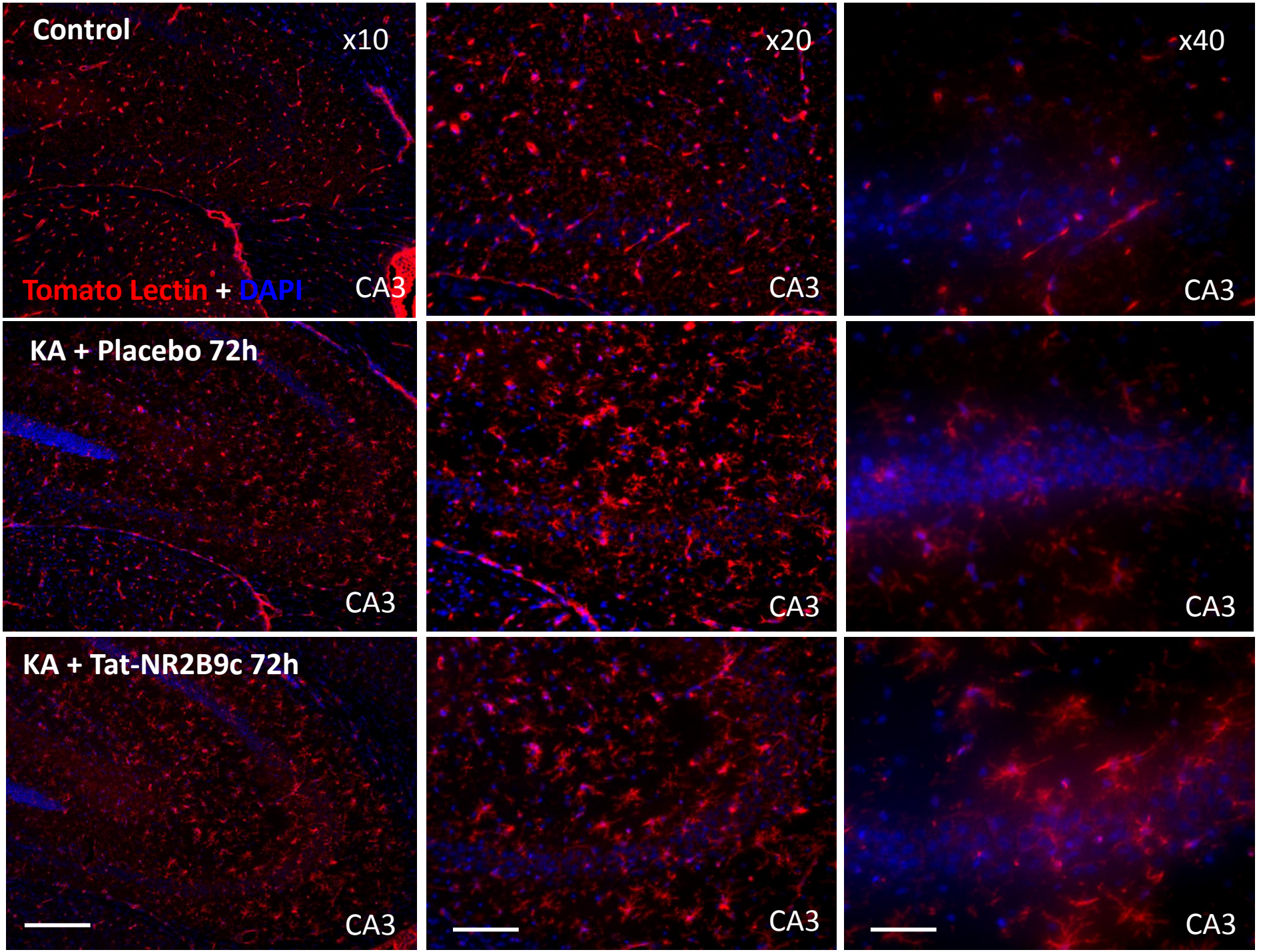
Control
x10
x20
x40
Tomato Lectin + DAPI
CA3
CA3
CA3
KA + Placebo 72h
CA3
CA3
CA3
KA + Tat-NR2B9c 72h
CA3
CA3
CA3

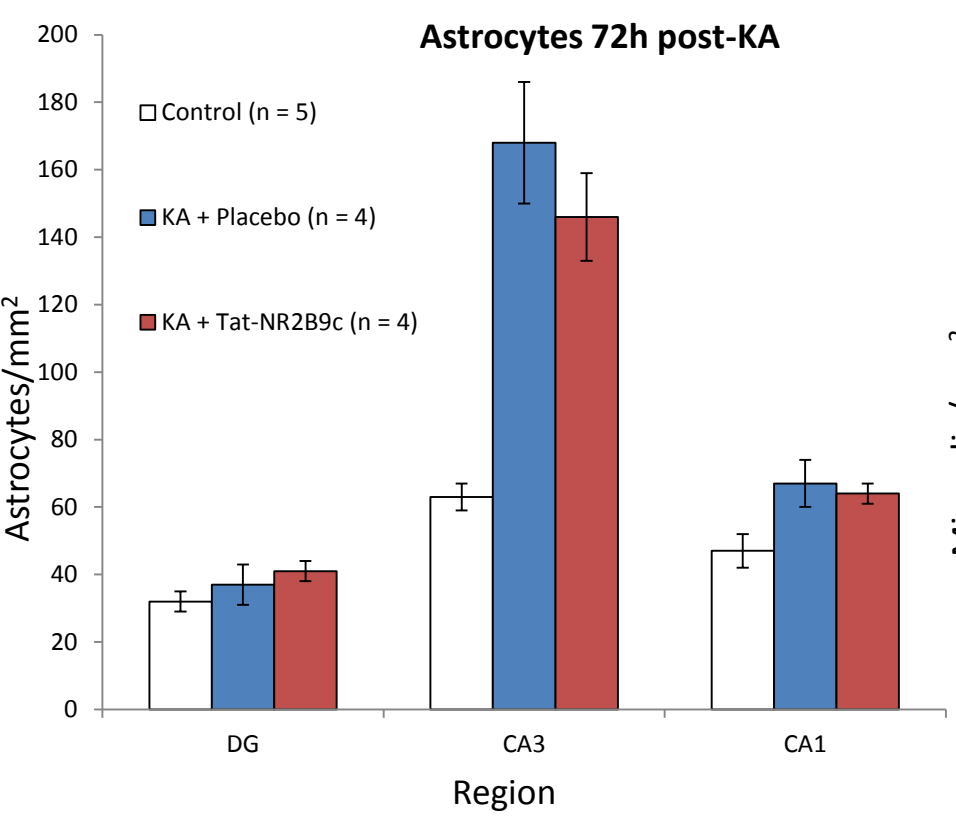

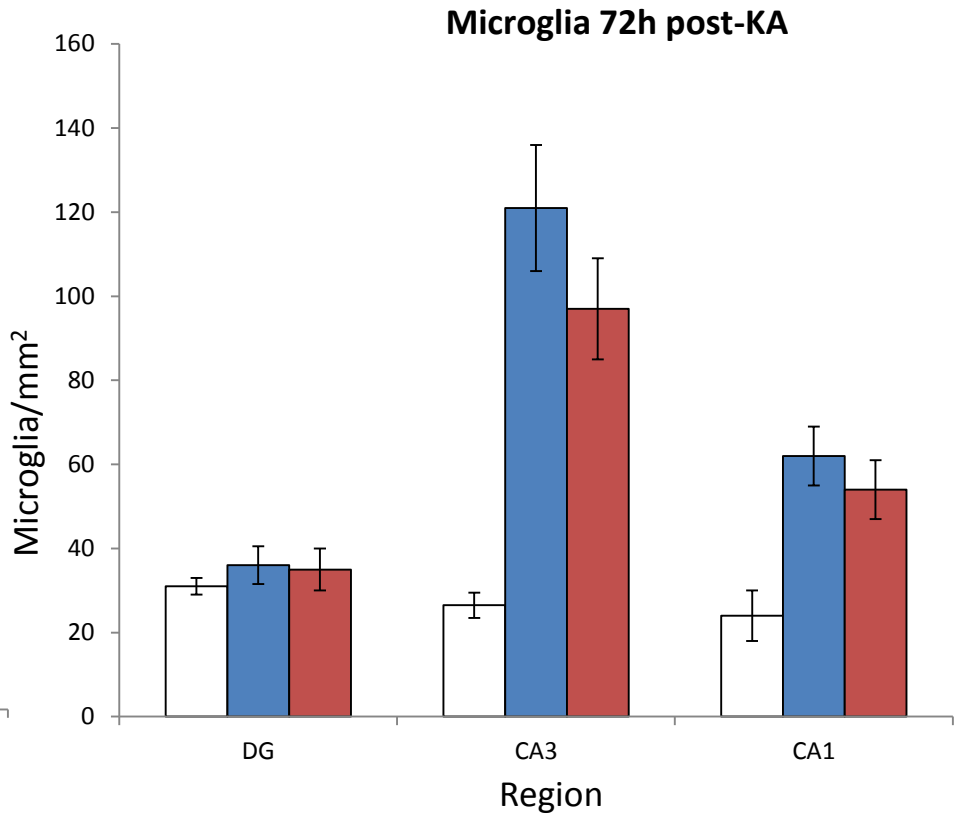

Figure 5.5. Reactive gliosis 3 days following KA-induced status epilepticus (a) Astrocytes in CA3 region. Magnification Magnification 10X (scale bar: 100µm), Magnification 20X (scale bar: µm), Magnification 40X (scale bar: µm) **(b)** Microglia in CA3 region. Magnification 10X (scale bar: 100µm), Magnification 20X (scale bar: µm), Magnification 40X (scale bar: µm) **(c)** Quantification of astrocytes in hippocampal formation 72 hours after KA injection **(d)** Quantification of microglia in hippocampal formation 72 hours after KA injection

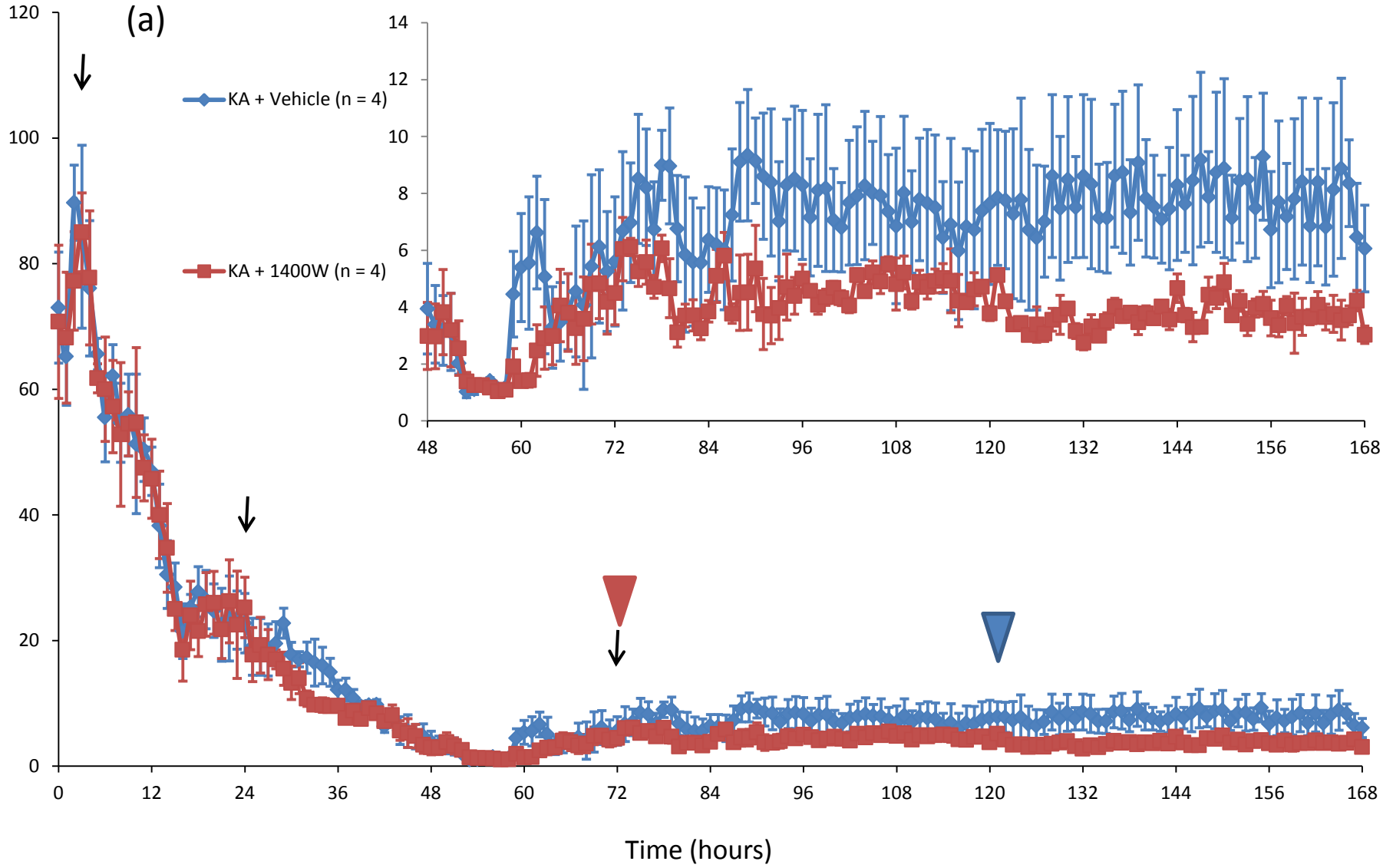
(a)
KA + Vehicle (n = 4)
KA + 1400W (n = 4)
120
100
80
60
40
20
0
0
12
24
36
48
60
72
84
96
108
120
132
144
156
168
14
12
10
8
6
4
2
0
48
60
72
84
96
108
120
132
144
156
168
Time (hours)

Figure 5.6. 1400W administration post-Status epilepticus reduces frequency of epileptiform spikes (a) frequency of epileptiform spikes for full 7 days post-SE. Inset: 48 – 168h at higher spike frequency resolution **(b)** frequency of epileptiform spike frequency averaged over 3 broader time periods.

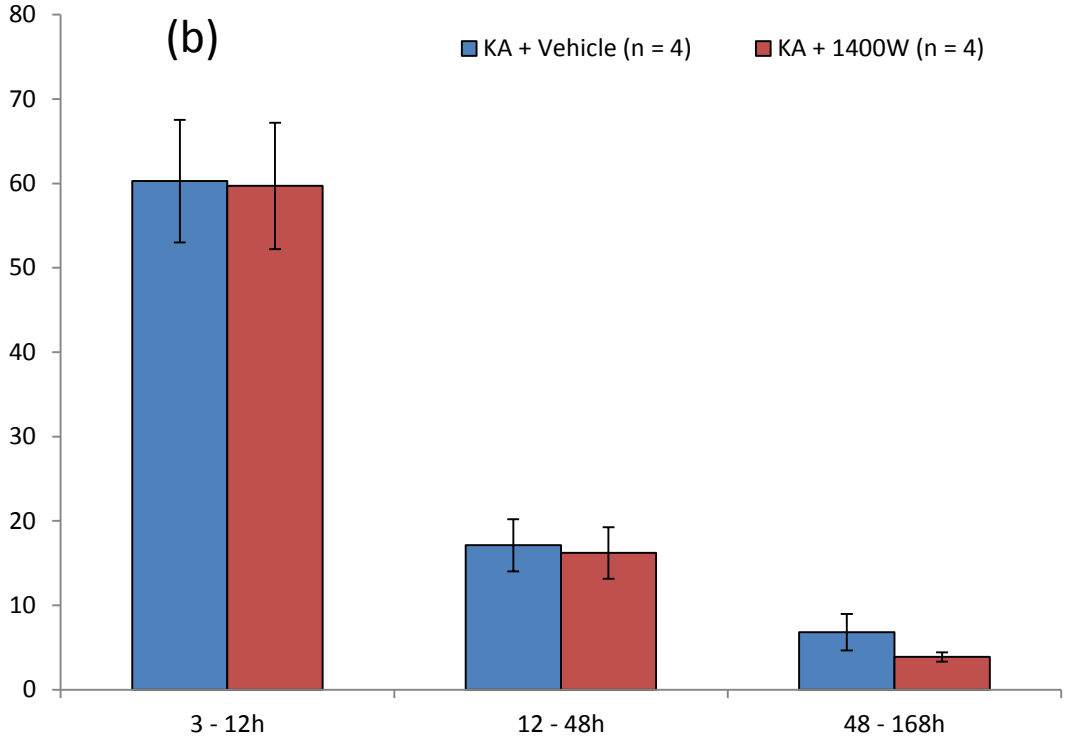

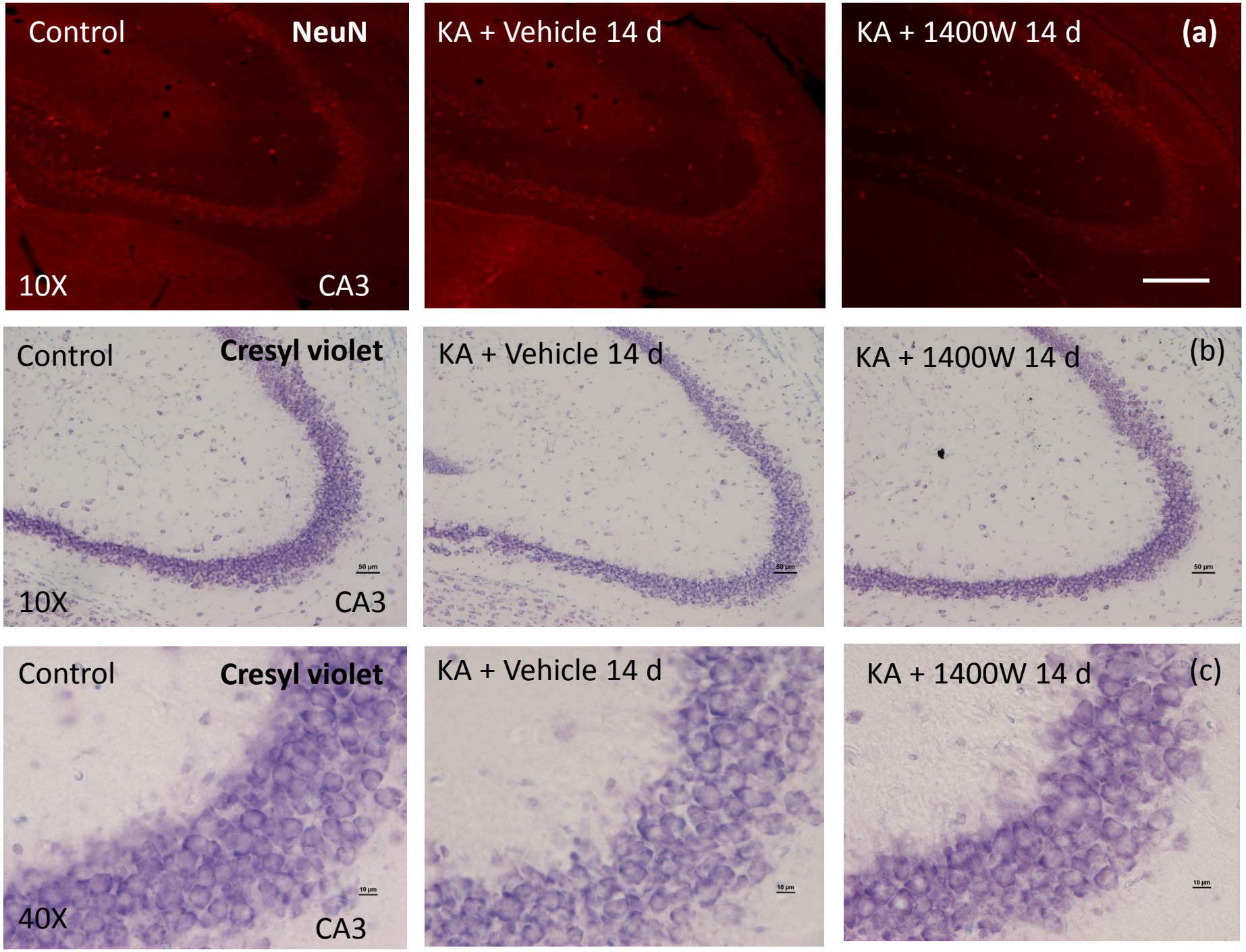
Control
NeuN
KA + Vehicle 14 d
KA + 1400W 14 d
(a)
10X
CA3
Control
Cresyl violet
KA + Vehicle 14 d
KA + 1400W 14 d
(b)
50 µm
10X
CA3
Control
Cresyl violet
KA + Vehicle 14 d
KA + 1400W 14 d
(c)
10 µm
40X
CA3

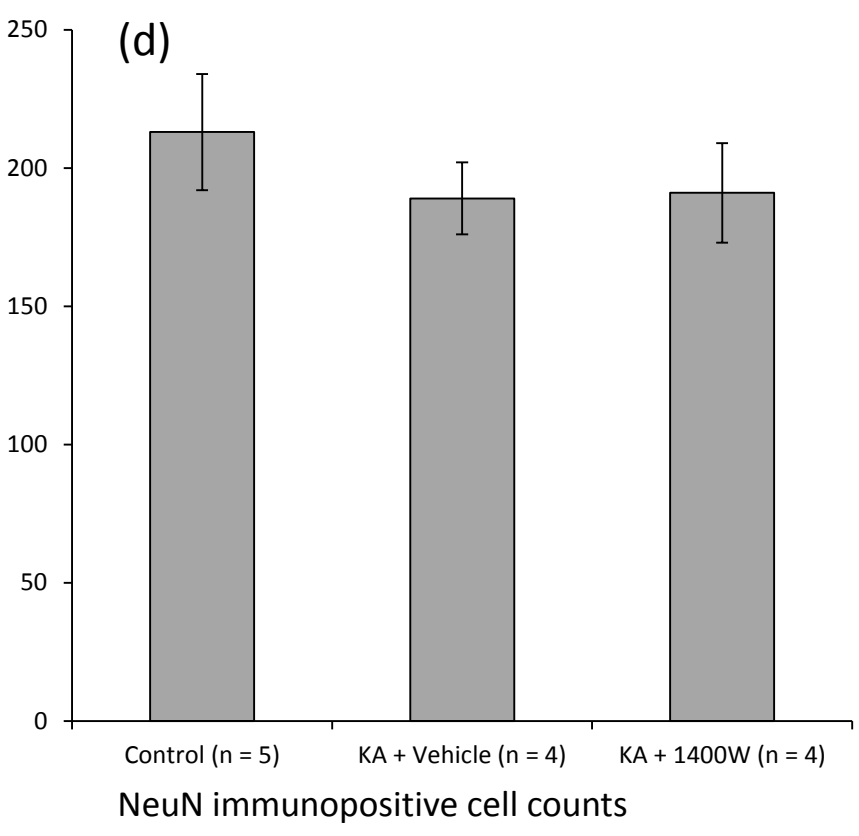

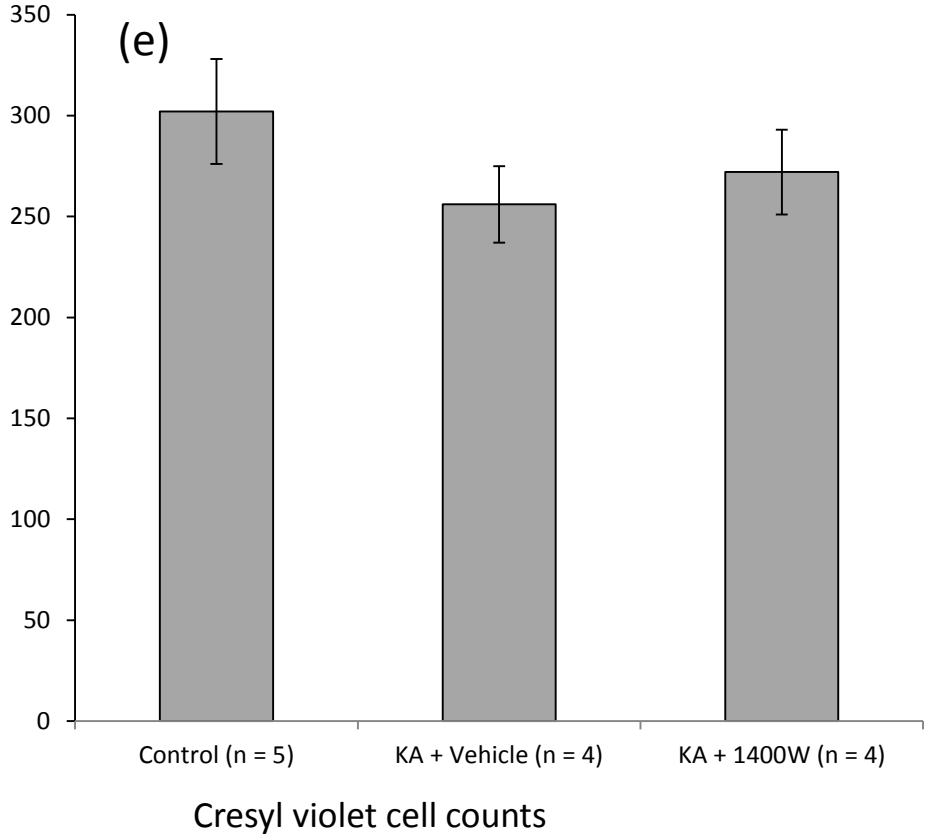

Figure 5.7. Neuronal cell loss in the CA3 region 14 days following KA-induced SE. 1400W has no effect. (a) Photomicrographs of NeuN-like immunoreactivity in the CA3 region of the hippocampus. Magnification: 10X, scale bar: 100µm **(b)** Photomicrographs of CA3 in cresyl violet stained sections. Magnification: 10X, scale bar 50µm. (c) Higher resolution micrographs of CA3 in cresyl violet stained sections. (d) Cell counts of NeuN immunopositive cells in CA3 region of hippocampus. (e) Cell counts of neurons stained with cresyl violet in CA3 region of hippocampus

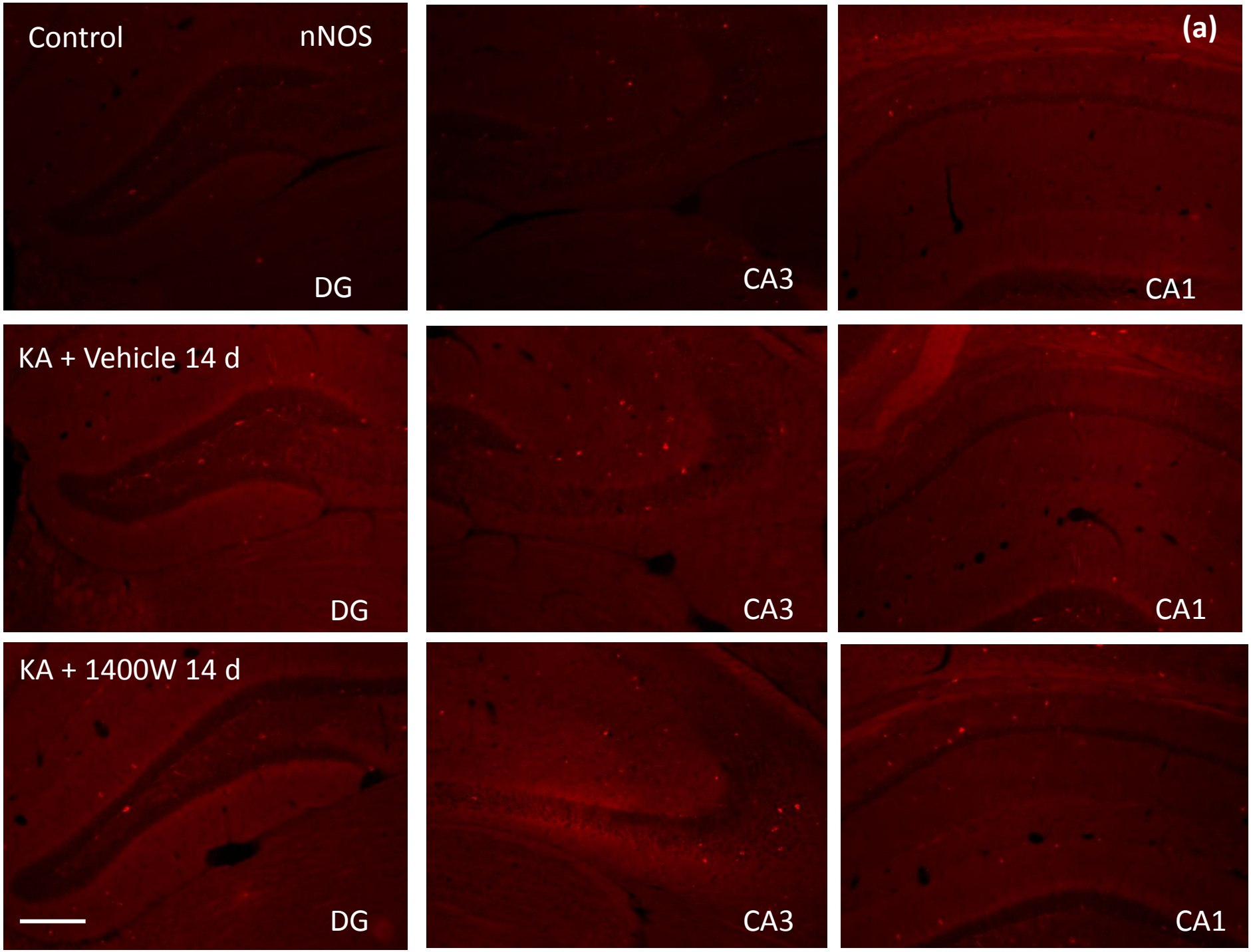
Control
nNOS
DG
CA3
(a)
CA1
KA + Vehicle 14 d
DG
CA3
CA1
KA + 1400W 14 d
DG
CA3
CA1

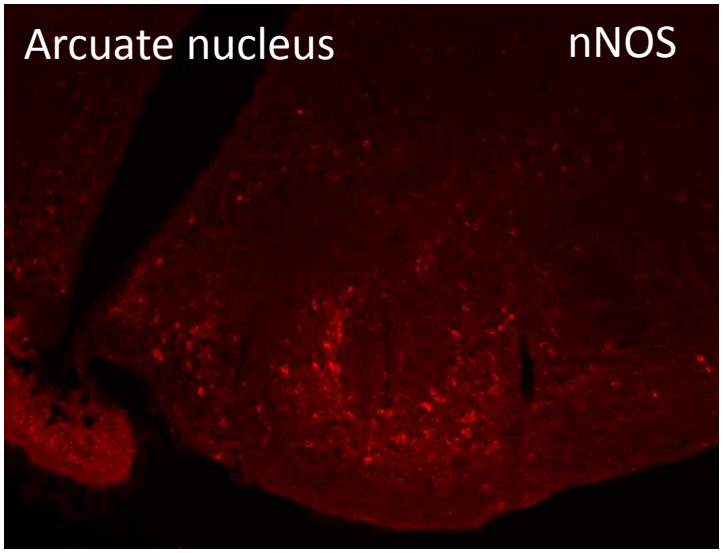

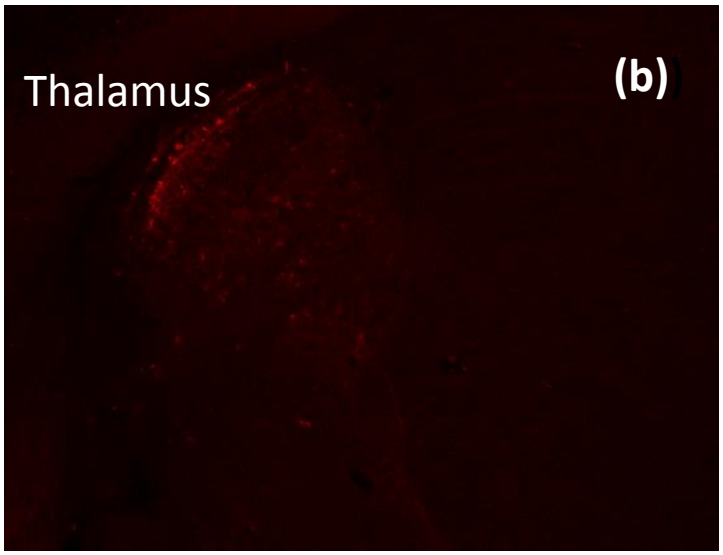

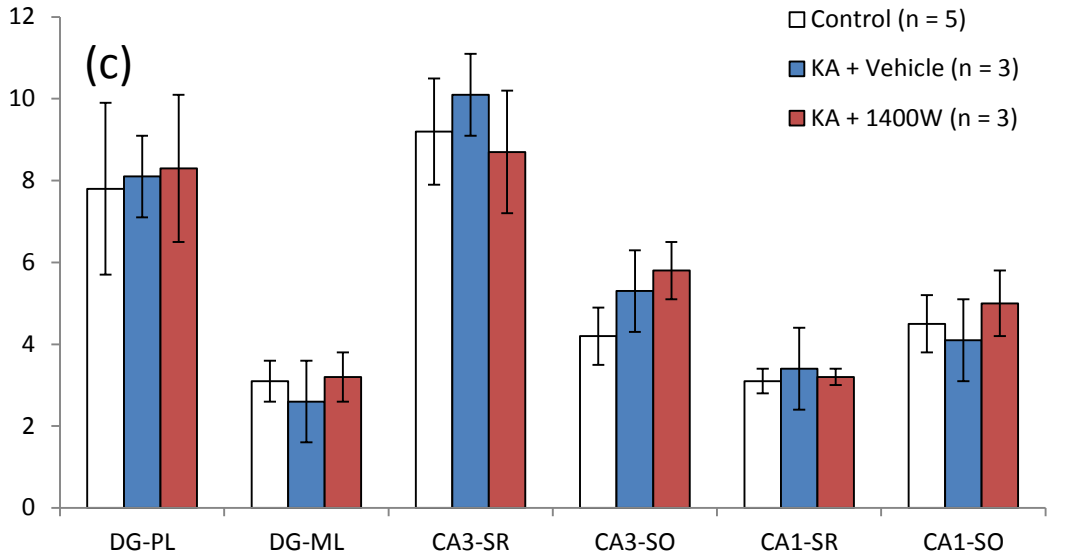

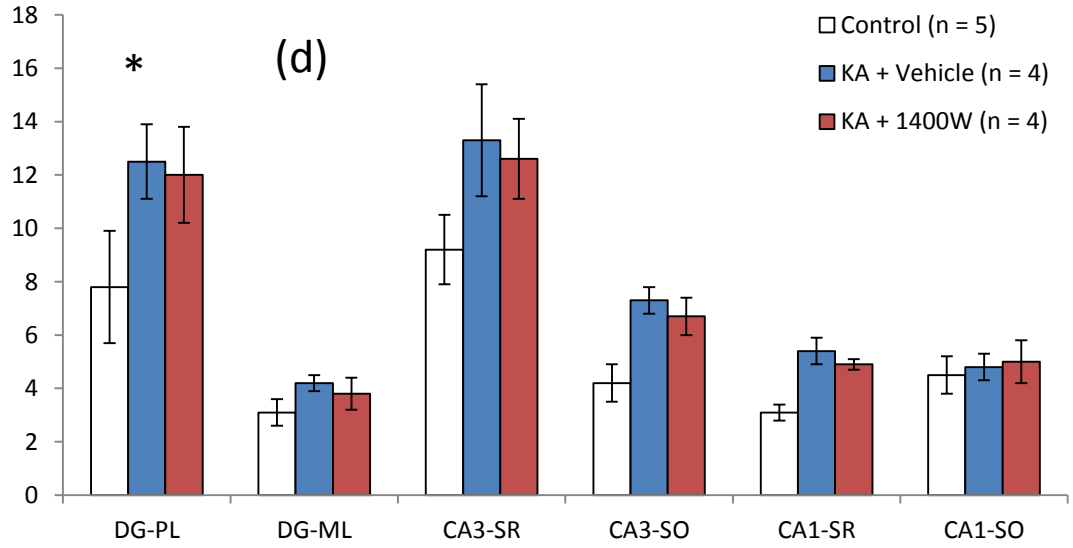

Figure 5.8. nNOS expression is increased in the hippocampal formation, but not elsewhere in the brain 14d post-SE. 1400W has no effect. (a) Photomicrographs of nNOS-like immunoreactivity in the dentate gyrus, CA3 and CA1. **(b)** Photomicrographs of nNOS in control regions of the brain: arcuate nucleus and thalamus. No change in expression induced by SE **(c)** Quantification of nNOS-immunopositive cells in different regions of the hippocampal formation. At 7 d post-SE. **(d)** Quantification of nNOS-immunopositive cells in different regions of the hippocampal formation. At 14d post-SE. *F_{10} = 7.0094, p = 0.013.

5.5 DISCUSSION

5.5.1 Overview

In this chapter a dosing regimen has been developed for the administration of KA to induce SE in mice, injecting the drug in incremental doses, titrated according to the development of epileptic behaviour and terminating SE with diazepam two hours after the first expression of class III seizures. This method was assessed by quantifying behavioural and electrographic indicators of SE severity and analyzing the distribution of hippocampal c-Fos expression. It is reported that the method could reliably induce SE with a prolonged period of repeated class IV and class V seizures, accompanied with an increased frequency of epileptiform spiking and an increased power of γ-frequency recorded by electrodes placed under the skull. Hippocampal c-Fos expression was also more widespread in the excitatory circuitry of the hippocampal formation than in seizures induced with a single dose of KA. The method was also associated with a zero mortality rate in the animals tested.

Analysis of electrographic and neurobiological changes post-SE revealed that this method of induction could more reliably induce indicators of epileptogenesis, including reactive gliosis, synaptogenesis, neurodegeneration and nNOS proliferation and could prove to be a superior model of temporal lobe epilepsy in

inbred mouse strains, such as C57BL/6J, which have previously been reported as being largely resistant to epileptogenesis.

Further, the incremental dosing regimen has been employed to perform pilot studies with low numbers of animals to investigate the potential of two pharmacological agents in suppressing disease progression, when administered after the period of KA-induced SE. A peptide, Tat-NR2B9c, targeted at the PDZ domains of PSD-95 and an iNOS inhibitor, 1400W were used to inhibit two signalling pathways thought to be key modulators of the inflammatory response. Tat-NR2B9c offered some limited suppression of gliosis at three days post-SE and suppressed the frequency of IEDs during the first 7 days post SE. 1400W, meanwhile, had little effect on either neuronal loss at 7 or 14 days, or on the distribution of nNOS at 14 days post SE.

5.5.2 Incremental dosing regimen

Two main reasons exist for developing an incremental dosing regimen for KA administration in favour of a single injection. Firstly, it affords the ability to maximize the severity of SE in animals, whilst simultaneously limiting associated mortality (Hellier et al, 1998; Glien et al, 2001). Secondly, the incremental dosing regimen, titrated according to behavioural response, allows for a reduction in variation between individuals in the severity of the SE, reducing error and the number of animals necessary for studies of the latent phase and of chronic

epilepsy; particularly important in highly invasive procedure that are expensive in cost and time, such as the implanting of electrodes for recording EEG. Similar approaches have previously been used in rats (Hellier et al, 1998; Glien, 2001) and while incremental dosing regimens have been used to induce SE in mice (McKhann et al, 2003), they have not been directly compared with animals receiving a single dose and the characterization of the development of SE and subsequent indicators of epileptogenesis have been limited.

We present evidence that by administering KA in incremental doses, titrated according to behaviour, a highly consistent period of SE, with a prolonged period of repeated class V tonic-clonic seizures can be achieved in C57BL/6J mice. These findings are similar to those reported using a repeated low-dose of KA in rats by Hellier et al (1998). This group administered systemic injections of KA at a concentration of 5mg/kg per hour until animals showed class IV Racine seizures, increasing the consistency of post-SE events and reducing the mortality observed in a single dose model. Glien et al (2001) also found similar results with a repeated low dose induction method using pilocarpine. Incremental KA dosing regimens have also been reported in mice. McKhann et al (2003) gave subcutaneous injections of 6 – 12mg/kg KA every 30 – 90 minutes until Class II seizures were observed. In all these studies, an increase in severity and inter-individual uniformity was reported along with a decrease in mortality.

We also provide evidence that the effect of prolonging the period of severe SE extends to an effect during the 'latent period'. It is reported that, following an incremental dosing regimen approximately doubles the frequency of IEDs between 3 and 7 days post-SE. The frequency of IEDs is a strong predictor of chronic epilepsy (Staley et al, 2001). Longitudinal studies investigating neuronal loss, mossy fibre sprouting and spontaneous seizures would offer confirmation of whether this method has the potential to offer a useful model of TLE in the C57BL/6J strain, in which current methods induce only mild epileptogenic indicators. Because this strain is the most popular background for genetic manipulations, the development of a more useful model of chronic epilepsy would be a major step forward.

A potential criticism of our approach is the variation between animals in the dose of KA received and duration in which animals have subconvulsive concentrations of KA in the brain. Although these concerns are valid, evidence suggests that the principal predictors of epileptogenesis are the duration and severity of epileptogenic activity, rather than specifics of the inducing agent per se and therefore, controlling these variables is of greatest concern. Many studies, using intracerebral administration of KA have indicated that neurobiological damage occurs distally to the site of injection, indicating that the induction of hyperexcitable networks is of greater significance than direct kainate toxicity (Schwob et al, 1980).

The effect of subconvulsive doses of KA prior to seizures is highly complex and likely to depend on drug concentrations and the exact timecourse. There is evidence that exposure to subconvulsive excitotoxic challenges can precondition the brain and increase the threshold for seizures and reduce neurobiological damage post-SE (Jiminez-Mateos & Henshall, 2009). There is, however, much evidence for the reverse effect, with the kindling model of seizure based on the premise that repeated sub-threshold stimulations eventually lead to a convulsion (Morimoto et al, 2004).

Currently the pharmacokinetics of KA are poorly understood (and likely to vary considerably across species and strain). In order to better understand exactly what is happening during the period of incremental dosing, data on KA concentrations in the brain with a high temporal resolution would be extremely useful. The best method for achieving this would be through intracerebral microdialysis. A better understanding of the pharmacological induction of SE would aid the interpretation of subsequent neurobiological and electrographic changes. Evidence is provided, however, that regardless of the mechanisms involved, the administration of KA in regular low doses in mice, as already reported in rats (Hellier et al, 1998) can maximize the severity of SE, whilst limiting associated mortality.

5.5.4 Tat-NR2B9a effect on electrographic and neurobiological changes during 'latent period'

We report that administration of Tat-NR2B9c post-SE reduces the frequency of IEDs during the 'latent period' in comparison with placebo treated controls and slightly reduces reactive gliosis, involving both astrocytes and microglia, in the CA3 region of the hippocampus associated with epileptogenesis three days after the induction of SE with an incremental dosing regimen of KA. This adds to the work of Dykstra et al (2009) who reported that Tat-NR2B9c administration could reduce neuronal loss in the rat hippocampus following a period of pilocarpine-induced SE and suggests that perturbing NMDA receptor-PSD-95 protein interactions can retard disease progression in animal models of TLE.

High levels of glutamate signalling associated with seizures, and particularly, the excessive stimulation of NMDA receptors, can lead to a series of potentially neurotoxic events (Hellier et al, 2009). The Ca^{2+} influx, vital to normal signalling, when in excessive quantities, can lead to neurodegeneration and the perturbation of neural networks, leading to a chronic state of seizure susceptibility (Mody & Macdonald, 1995). The clinical utility of general NMDA antagonists, however, is reduced by the severe associated side-effects, including psychotropic effects, similar to schizophrenia (Newcomer et al, 1999). Any antiepileptogenic strategy of potential clinical utility must leave physiological NMDA signalling largely intact.

Aarts, et al (2002) were the first group to target the PDZ domains of PSD-95, using Tat-NR2B9c in an effort to alleviate excitotoxic damage. They administered

the cell permeable peptide following transient middle cerebral artery occlusion in rats and found that when applied before or 1 hour following insult Tat-NR2B9c could reduce focal ischemic brain damage and improve neurological function. In our study, Tat-NR2B9c is administered directly following the termination of behavioural seizures with diazepam and was found to facilitate the effect of diazepam in reducing the frequency of IEDs. Our data suggest that targetting PSD-95 directly after a seizure or period of status epilepticus can potentially have an effect on the disease progression of TLE, with the frequency of IEDs reduced throughout the first 7 days post-SE and indicators of reactive gliosis in the CA3 region of the hippocampus reduced three days post SE.

By dissociating PSD-95 from the NR2B subunit of the NMDA receptor, the neurotoxic effects of Ca^{2+} influx can be reduced whilst largely retaining the normal functioning of the synapse. PSD-95 is linked to the C-terminal PDZ ligand of NR2B, and also binds to nNOS. When the interaction of NR2B and PSD-95 is disrupted, the NMDAR becomes uncoupled from nNOS activation. As reported in chapter 4, nNOS signalling is involved in modulating the severity of seizures. By uncoupling NMDAR signalling from nNOS, NMDAR-dependent excitotoxicity can be reduced (Doucet et al, 2012).

While targetting the NMDAR with a general antagonist, such as ketamine or MK801 creates severe side effects, it may be possible to reduce the excitotoxic effects of NMDA signalling, without disrupting the receptors general activity,

through the more specific targetting of receptors including the NR2B subunit. Alternatively, dissociating NMDAR from PSD-95 and, thereby, disrupting its close association with nNOS, may reduce the deleterious effects of excessive local NO production. NMDAR activity has been shown to be unaffected by the genetic disruption of PSD-95, or by the suppression of its expression in vitro (Lim et al, 2003). These approaches do, however, dissociate NMDAR activity from nNOS and suppress excitotoxicity (Cui et al, 2007).

5.5.5 1400W effect on electrographic changes during 'latent period' and neurobiological changes from 7 – 14 days

Post insult iNOS expression is one part of the complex inflammatory response which has a role to play in almost all CNS pathologies (discussed at length in the context of seizures and epilepsy in chapter 1). While this response is usually protective; removing debris and promoting tissue repair (Brown & Bal-Price, 2003), an inappropriately high or prolonged inflammatory response can contribute to disease progression. While inflammation is seldom the 'root cause' of pathology (something must initially induce the inflammation) the contributions to cell death, excitability and cerebral blood flow may often turn a relatively benign pathology into a dangerous one (Brown & Bal-Price, 2003).

Unlike neuronal and endothelial NOS, which are constitutively expressed in the CNS at relatively high levels, are Ca^{2+}/Calmodulin-dependent and are heavily involved in a wide array of physiological functions (such as synaptic transmission,

regulation of cerebral blood flow and development), the inducible isoform (iNOS) is constitutively expressed at very low levels, is thought to be largely uninvolved in physiological brain activeity and is regulated largely at the transcriptional level. iNOS expression is characteristic of the 'activated' state of microglia and astrocytes. As has been described, high levels of microglia activation are observed in our model from 72 hours (figure 5.4) and iNOS expression in similar models of epilepsy have been reported at similar time points (Zheng, et al, 2010).

The capability to generate NO at micromolar levels provides potent pathological potential. NO from iNOS can lead to the release of Ca^{2+} from intracellular stores in astrocytes, stimulating the exocytosis of vesicular glutamate. In this way, different cell types can combine to increase the excitatory potential of neuronal networks. High levels of NO can also induce glutamate release and cell death in neurons directly by inhibiting mitochondrial cytochrome C oxidase (Antunes et al, 2007).

Inhibition of iNOS has been reported to have positive outcome in rodent models of neurological disease including traumatic brain injury (Jafarian-Tehrani et al, 2005) and cerebral ischemia (Wang et al, 2004), however, to our knowledge, the effects of this drug on the progression of epileptogenesis following the induction of SE has not been investigated. It is found that systemic administration with 1400W decreased the frequency of IEDs between three and seven days post-SE, suggesting that the drug has some ability to modulate disease progression.

However, no effect was found on neuronal cell loss at either 7 or 14 days post SE, nor did 1400W administration have any effect on the epileptogenic proliferation in nNOS expression.

Almost everything that has been accepted about iNOS function in the CNS has been challenged. While it had been thought that it was not constitutively expressed, evidence has shown that low levels are expressed in the healthy brain (Chan et al. 2001; Starkey et al. 2001; Buskila, 2005). While it had been thought that its activity was controlled exclusively at the transcriptional level, Ratovitski, et al (1999) demonstrated that Kalarin could exert post-translational regulation by preventing the formation of functional dimers.

The view that there is no functional role for iNOS in the healthy brain has also been challenged. Kalinchuk, et al (2006) demonstrate an important role for iNOS in the basal forebrain for inducing non-REM 'recovery' sleep. Ikeda & Murase (2004) report a role for astrocytic iNOS in regulating synaptic LTP in the spinal cord and more recently, Buskila & Amitai (2010) have demonstrated that a similar function is performed by iNOS released by astrocytes in the neocortex. The importance of these physiological functions remains unclear, however, despite the ever emerging complexity, the general view of iNOS as an induced (as opposed to constitutive) actor, regulated largely at the transcriptional level and of particular importance in pathological brain states is still largely intact.

5.5.6 Conclusions

In this study, an alternative method of KA administration has been used in order to standardise the period of status epilepticus and have found that it increases the severity and inter-individual uniformity of SE. By inducing SE using this method, indicators of epileptogenesis, such as neuronal cell loss could be detected using fairly crude methods. The incremental dosing regimen is a promising model of TLE for inbred mouse strains that have proven relatively resistant to epileptogenesis. Of the two pharmacological agents tested, Tat-NR2B9c seems the most promising, however, it is not clear whether the effect of this drug is in mediating the duration of post-diazepam electrographic SE, which could be considered a part of the initiating event, or on processes involved in disease progression. In order to get a better picture of the effects of these drugs on epileptogenesis, studies with larger numbers of animals are needed and longitudinal studies of longer duration are needed in order to assess the potential development of chronic epilepsy.

Chapter 6. General Discussion

6.1 Overview

In this thesis, behavioral, electrographic and neurobiological indicators of seizure severity during a period of kainic acid-induced status epilepticus (SE) on the C57BL/6J inbred mouse strain was investigated. The severity of epileptic behaviour was recorded using the Racine scale (Racine, 1972); the anatomical distribution of c-Fos expression in the hippocampal formation post-seizure was quantified using immunohistochemistry, and electrographic indicators of seizure severity including a qualitative analysis of EEG and quantification of epileptiform spikes and the power of oscillations distributed in gamma frequencies (20 – 70Hz) were assessed using implanted electrodes. Further to assessing the severity of SE, subsequent changes in EEG activity associated with epileptogenesis was assessed for one week following KA-induced SE and neurobiological indicators of the emergence of chronic epilepsy, including reactive gliosis and synaptogenesis were assessed at 24 and 72 hours post seizure.

The effect of a range of pharmacological interventions on the severity of KA-induced SE and on the development of chronic epilepsy were investigated, including an nNOS inhibitor, L-NPA, an NR2B specific antagonist, Ro 25-6981,. An iNOS inhibitor, 1400W and a synthesised peptide targetted at disrupting PDZ

binding sites on PSD-95, Tat-NR2B9c were given as post-treatments after the induction of SE in order to investigate the potential for targetting iNOS and downstream signalling pathways from the NMDAR associated with excitotoxicity in order to reduce the development of chronic epilepsy following an initial precipitating event. An incremental KA dosing regimen was developed for studies investigating post-SE epileptogenesis, in order to standardise and maximise seizure severity whilst reducing mortality.

6.2 Strain comparison

Minor differences were found between strains in the anatomical distribution of GAD-67, SST, nNOS and CB. C57BL/6J mice generally have a lower tolerance to kainic acid than CD-1, however c-Fos expression in CD-1 mice is more widespread in the hippocampal formation following status epilepticus. Epileptiform spiking continues for at least 7 days following kainic acid injection, in the absence of any behavioural indicators and that reactive gliosis in the CA3 region and reactive synaptogenesis in the outer molecular layer of the dentate gyrus occur 72 hours after induction of SE with diazepam.

C57BL/6J mice were more sensitive to KA-induced SE, however, this was unlikely to be related to the minor differences between the two strains in the distribution of GAD-67, SST, nNOS and CB in the hippocampal formation. Despite their greater tolerance of KA, c-Fos expression in CD-1 mice was more

widespread in the hippocampal formation following status epilepticus, suggesting that our understanding of the mechanisms underlying the expression of immediate early genes in response to excitotoxicity is insufficient. Epileptiform spiking continues for at least 7 days following kainic acid injection, in the absence of any behavioural indicators. Reactive gliosis occured in the CA3 region of the hippocampus at an earlier timepoint following SE than has previously been reported and that reactive synaptogenesis in the molecular layer of the dentate gyrus precedes mossy fibre sprouting by a significant period of time.

While a fairly consistent response between animals caged together was found, between cages, there was greater variation. It is possible that this is due to an increased sensitivity to environmental factors resulting from isogenicity. Subtle differences between laboratory can manifest themselves in different behavioural responses in inbred mouse strains. It may be that the same is true for responses to KA, perhaps accounting for the variation in responses reported across laboratories and between studies.

Our data indicates that at 2 hours following KA administration, in C57/BL6J mice, c-Fos in excitatory circuits is largely restricted to dentate granule cells, whereas in CD-1 mice, c-Fos expression extends in the pyramidal cell layers of CA3, CA2 and CA1 of the hippocampus. This is indicative of neurons in these regions being exposed to high levels of excitotoxic stress. However, it may not be entirely appropriate to infer information about the spatial evolution of epileptiform activity from c-Fos distribution. Rather, the anatomical distribution of c-Fos proceeds

according to the severity of the seizure and the time interval. Rather than an anatomical distinction between the two strains in epileptiform activity, this is more likely to represent an increased severity of epileptiform activity per se in the hippocampi in CD-1 mice in comparison with C57BL/6J, in contrast to behavioural observations of motor seizures.

6.3 Status epilepticus

Our qualitative observations of epileptiform activity in the EEG trace corresponds strongly with that observed by Trieman et al (1990) and Medvedev et al (2000) following KA-induced SE in rats. The gradually increasing power of γ-frequency over the 2 hour period of analysis conforms to the findings of Lehmuke et al (2009) using a similar model and method of analysis in rats.

6.4 Epileptogenesis

Electrographic markers of epileptogenesis include the re-emergence of IEDs following an initial post-SE decline in IED frequency (Williams *et al.,* 2009). The reduced frequency of IEDs in L-NPA pre-treated mice, when compared with vehicle pre-treated controls provides evidence that the suppression of neurobiological changes associated with epileptogenesis is accompanied by changes in the pattern of neuronal network activity.

Regardless of the extent to which gliosis plays a pro- or anti- epileptogenic role, the activation and proliferation of glial cells is a well characterised feature of the early stages of epileptogenesis and strongly predictive of neuronal loss and the development of spontaneous seizures (Vezzani *et al.,* 2000; 2009; Foresti *et al.,* 2009). The increased number of both astrocytes and microglia, the morphological changes described and the invasion of these cells into stratum lucidum and the pyramidal cell layer of CA3 at 72 hours (figure 3.6) is predictive of both neuronal loss in this region and a decreased threshold for seizure generation. Strong evidence was found of astro- and microgliosis in areas CA3 and CA1 from 72h onwards, correlating with the sites where neuronal loss has been reported in the hippocampus, both of TLE patients (Wieser, 2004) and in rodents following a period of status epilepticus (Nitecka et al, 1984). Our studies show that at 72h post KA, these areas of high SYN immunoreactivity remain unchanged, while a modest increase in SYN immunoreactivity occurs in the OML of the dentate hilus within 72h of KA administration, indicating reactive synaptogenesis in this region (figure 3.7).

6.5 Status epilepticus – Pharmacological interventions

L-NPA, when administered prior to the induction of SE was found to profoundly suppress the emergence of epileptiform activity, including behavioural, electrographic and neurobiological indicators. Further, L-NPA's modulation of the precipitating event lead to a decrease in neurobiological changes associated with

epileptogenesis, such as reactive gliosis in the CA3 region of the hippocampus and elevated synaptogenesis in th molecular layer of the hippocampus. This correlated with a marked decrease in epileptiform discharges in the EEG trace.

The acute effects of L-NPA on SE were characterised by a reduction in; the duration of CMS (figure 4.3), the power of the γ-frequency band (20 - 70Hz) EEG (figure 4.6) associated with seizure severity, the frequency of epileptiform discharges (figure 4.5), and a decrease in the expression of c-Fos (figure 4.4), suggesting that nNOS is involved in seizure susceptibility and in the manifestation of CMS in the KA model. nNOS, activated during seizures by high levels of Ca^{2+} influx, may influence seizure severity through paracrine, autocrine and synaptic signaling from nNOS anchored at the PSD, or all three mechanisms. These results support the findings of Rajesekaran (2005), who suggested abnormal nNOS activity as a major trigger for seizure generation. While RO 25-6981 has previously been reported to have a protective effect against spontaneous seizures in animal models after a period of epileptogenesis (Wang et al, 2004), no effect of the drug was found on epileptiform behaviour during a period of KA-induced SE, nor on the subsequent expression of c-Fos in the dentate gyrus.

Our data indicates that, in the C57BL/6J strain, c-Fos expression in excitatory circuits is largely restricted to dentate granule cells 2h post-SE. The significant reduction of c-Fos expression in this region associated with L-NPA treatment is

consistent with the view that our intervention reduced the severity of SE and profoundly reduced the exposure of neurons in the region to excitotoxic stress.

6.6 Incremental dosing regimen

We present evidence that by administering KA in incremental doses, titrated according to behaviour, a highly consistent period of SE, with a prolonged period of repeated class V tonic-clonic seizures can be achieved in C57BL/6J mice. These findings are similar to those reported using a repeated low-dose of KA in rats by Hellier et al (1998). This group administered systemic injections of KA at a concentration of 5mg/kg per hour until animals showed class IV Racine seizures, increasing the consistency of post-SE events and reducing the mortality observed in a single dose model. Glien et al (2001) also found similar results with a repeated low dose induction method using pilocarpine. Incremental KA dosing regimens have also been reported in mice. McKhann et al (2003) gave subcutaneous injections of 6 – 12mg/kg KA every 30 – 90 minutes until Class II seizures were observed. In all these studies, an increase in severity and inter-individual uniformity was reported along with a decrease in mortality.

We also provide evidence that the effect of prolonging the period of severe SE extends to an effect during the 'latent period'. Following an incremental dosing regimen approximately doubles the frequency of IEDs between 3 and 7 days post-SE. The frequency of IEDs is a strong predictor of chronic epilepsy (Staley

et al, 2011). Longitudinal studies investigating neuronal loss, mossy fibre sprouting and spontaneous seizures would offer confirmation of whether this method has the potential to offer a useful model of TLE in the C57BL/6J strain, in which current methods induce only mild epileptogenic indicators. Because this strain is the most popular background for genetic manipulations, the development of a more useful model of chronic epilepsy would be a major step forward.

6.7 Epileptogenesis – Pharmacological interventions

In the early epileptogenic period, L-NPA treatment reduced the frequency of IEDs (figure 4.7), suppressed reactive gliosis in the CA3 region (figure 4.8) and reactive synaptogenesis in the OML and MML of the dentate gyrus (figure 4.9) These observations might suggest a potential disease-modifying action of L-NPA on the epileptogenic process by modulation of the initiating event. Recently, an increase in nNOS expression following early-life seizures has been reported (Kim, 2010), which increased susceptibility to spontaneous seizures later in life in an nNOS-dependent manner, giving further evidence for how nNOS may play a role in the development of chronic epilepsy from a precipitating event.

The administration of Tat-NR2B9c post-SE reduces the frequency of IEDs during the ‘latent period’ in comparison with placebo treated controls and slightly reduces reactive gliosis, involving both astrocytes and microglia, in the CA3 region of the hippocampus associated with epileptogenesis three days after the

induction of SE with an incremental dosing regimen of KA. This adds to the work of Dykstra et al (2009) who reported that Tat-NR2B9c administration could reduce neuronal loss in the rat hippocampus following a period of pilocarpine-induced SE and suggests that perturbing NMDA receptor-PSD-95 protein interactions can retard disease progression in animal models of TLE.

High levels of glutamate signalling associated with seizures, and particularly, the excessive stimulation of NMDA receptors, can lead to a series of potentially neurotoxic events (Hellier et al, 2009). The Ca^{2+} influx, vital to normal signalling, when in excessive quantities, can lead to neurodegeneration and the perturbation of neural networks, leading to a chronic state of seizure susceptibility (Mody & Macdonald, 1995). By dissociating PSD-95 from the NR2B subunit of the NMDA receptor, the neurotoxic effects of Ca^{2+} influx can be reduced whilst largely retaining the normal functioning of the synapse. PSD-95 is linked to the C-terminal PDZ ligand of NR2B, and also binds to nNOS. When the interaction of NR2B and PSD-95 is disrupted, the NMDAR becomes uncoupled from nNOS activation. As reported in chapter 4, nNOS signalling is involved in modulating the severity of seizures. By uncoupling NMDAR signalling from nNOS, NMDAR-dependent excitotoxicity can be reduced (Doucet et al, 2012).

We found that systemic administration with 1400W decreased the frequency of IEDs between three and seven days post-SE, suggesting that the drug has some ability to modulate disease progression. However, no effect was found on

neuronal cell loss at either 7 or 14 days post SE, nor did 1400W administration have any effect on the epileptogenic proliferation in nNOS expression.

References

Aarts, M., Liu, Y., Liu, L., Besshoh, S., Arundine, M., Gurd, J.W., Wang, Y-T., Salter, M.W & Tymianski, M (2002) Treatment of Ischemic Brain Damage by perturbing NMDA Receptor-PSD-95 Protein Interactions. *Science, **298**, 846 – 850.*

Abercrombie, M & Johnson, M.L (1946) Quantitative histology of Wallerian degeneration I. Nuclear population in rabbit sciatic nerve. J. Anat. Rec. 80, 191 – 202.

Acharya, M.M., Hattiangady, B & Shetty, A.K (2008) Progress in neuroprotective strategies for preventing epilepsy. Prog. Neurobiol **870**, 1 – 42

Adrian, E.D (1936) The spread of activity in the cerebral cortex. *J. Physiol. **88**, 127 – 161.*

Al-Ghoul, W.M., Meeker, R.B & Greenwood R.S (1995) Kindling induces a long-lasting increase in brain nitric oxide synthase activity. NeuroReport **6(3)**, 457 - 460.

Alici, K., Gloveli, T., Weber-Luxenburger, G., Motine, V & Heinemann, U (1996) Comparison of effects induced by toxic applications of kainate and glutamate and

by glucose deprivation on area CA1 of rat hippocampal slices. *Brain Res.* ***738(1)****, 109 – 120.*

Amara, S.G & Kuhar, M.J (1993) Neurotransmitter transporters: Recent progress. *Ann. Rev. Neurosci.* ***16****, 73 – 93.*

Anderson, P., Morris, R., Amaral, D., Bliss, T & O'Keefe, J (2006) The Hippocampus Book. *Oxford University Press.*

Antunes, F., Boveris, A & Cadenas, E (2007) On the biological role of the reaction of NO with oxydized cytochrome C oxidase. *Antioxidants and Redox signalling* ***9(10)****, 1569 – 1579*.

Arhan, E., Serdaroglu, A., Ozturk, B., Ozturk, H.S., Ozcelik, A., Kurt, N., Kutsal, E & Sevinc, N. (2011) Effects of epilepsy and antiepileptic drugs on nitric oxide, lipid peroxidation and xanthine oxidase system in children with idiopathic epilepsy. Seizure **20(2),**138-42.

Aronica, E & Gorter, JA (2007) Gene expression profile in temporal lobe epilepsy. The Neuroscientist **13(2)**, 100 - 108.

Ayala, G.F., Dichter, M & Gumnit, R.J. (1973) Genesis of epileptic interictal spikes. New knowledge of cortical feedback systems suggests a neurophysiological explanation of brief paroxysms. *Brain Res.* ***52****, 15 – 21.*

Ayala, G.F. (1983) The paroxysmal depolarisation shift. *Prog. Clin. & Biolog. Res.* ***124****, 15 – 21.*

Bak, P. and Tang, C. and Wiesenfeld, K. (1987). "Self-Organized Criticality: An Explanation of 1/*ƒ* Noise". *Phys. Rev. Lett.* ***59*** *(4): 381–384*

Bal-Price, A & Brown, G.C (2001) Inflammatory neurodegeneration mediated by nitric oxide from activated glia-inhibiting neuronal respiration, causing glutamate release and excitotoxicity. *J. Neurosci.* ***21(17)****, 6480 – 6491.*

Bannerjee, S & Bhat, M.A (2007) Neuron-Glia interactions in blood-brain barrier formation. *Annu. Rev. Neurosci.* ***30****, 235 – 258*

Bansalam, M.K & Fakhoury, T.A (2003) Toparimate and status epilepticus: report of three cases. *Epilepsy & Behav. 4, 757 – 760.*

Baram, T.Z., Gerth, A & Shultz, L (1997) Febrile seizures: an age appropriate model. *Brain Res. Dev. Brain. Res.* ***246****, 134 – 143.*

Barbarosie, M & Avolie, M (1997) CA3-driven hippocampla-entorhinal loop controls rather than sustains in vitro limbic seizures. *J. Neurosci.* ***17****, 9308 – 9314.*

Bates, T.E., Loesch, A., Burnstock, G & Clark, J.B (1995) Immunocytochemical evidence for a mitochondrially located nitric oxide synthase in brain and liver. *Biochem. & Biophys. Res. Comm.* ***213(3)****, 896 – 900.*

Bauer, J & Bien, C.G (2009) Encephalitis and epilepsy. *Semin. Immunopathol.* ***31****, 537 – 544.*

Baulac, S. (2010) Channelopathies in human epilepsies. *Epilepsies* ***22(3)****, 226 – 229.*

Beamer, E.H., Otahal, J., Sills, G.J & Thippeswamy, T (2012) N^{W}-Propyl-L-arginine (L-NPA) reduces status epilepticus and early epileptogenic events in a mouse model of epilepsy: behavioural, EEG and immunohistochemical analyses. *Eur. J. Neurosci.* ***36****, 3194 – 3203*

Beer, J., Mielke, K., Zipp, M., Zimmermann, M & Herdegen, T (1998) Expression of c-jun, junB, c-Fos, fra-1 and fra-2 mRNA in the rat brain following seizure activity and axotomy. *Brain Res.* ***794(2)****, 255 – 266*.

Ben-Ari, Y & Logowska, J (1978) Epileptogenic action of intra-amygdaloid injection of kainic acid. *C R Acad. Sci. Hebd. Seances Aca. Sci. D.* ***287(8)****, 813 – 816*.

Ben-Ari, Y & Cossart, R (2000) Kainate, a double agent that generates seizures: two decades of progress. Trends Neurosci. **23**, 580 - 587.

Benkovic, S.A., O'Callaghan, J.P & Miller, D.B (2004) Sensitive indicators of injury reveal hippocampal damage in C57BL/6J mice treated with kainic acid in the absence of tonic-clonic seizures. *Brain res.* ***1024(1-2)****, 59 – 76*.

Bensalem, M.K & Fakhoury, T.A (2003) Topiramate and status epilepticus: report of three cases. *Epilepsy Behav.* ***4(6)****, 757 – 760*.

Berg, A. T (2008) The natural history of mesial temporal lobe epilepsy. Current opinion in neurology **21**, 173 – 178

Betts, T., Waegemans, T & Crawford, P (2000) A multicentre, double-blind, randomized, parallel group study to evaluate the tolerability and efficacy of two oral doses of levetiracetam, 2000 mg daily and 4000 mg daily, without titration in patients with refractory epilepsy. *Seizure* ***9****, 80 - 87.*

Bialer, M & White, S.H (2010) Key factors in the discovery and development of new antiepileptic drugs. *Nat. Rev. Drug Discov.* ***9****, 68 – 82*.

Biton, V., Mirza, W & Montouris, G (2001) Weight change associated with valproate and lamotrigine monotherapy in patients with epilepsy. *Neurology* ***56****, 172 – 7.*

Bleakman, D & Collingridge, G.L (1999) Kainate receptors are involved in synaptic plasticity. Nature 402(6759), 297 – 301.

Block, M.L., Zecca, L & Hong, J.S (2007) Microglia-mediated neurotoxicity: uncovering the molecular mechanisms. *Nat. Rev. Neurosci.* ***8(1)****, 57 – 69.*

Boer, R., Ulrich, W-R., Klein, T., Mirau, B., Haas, S & Baur, I (2000) The inhibitory potency and selectivity of Arginine Substrate Site Nitric-Oxide Synthase Inhibitors is Solely Determined by Their Affinity toward the Different Isoenzymes. *Mol. Pharmacol.* ***58(5)****, 1026 – 1034*.

Bolkvadze, T & Pitkanen, A (2012) Development of post-traumatic epilepsy after controlled cortical impact and lateral fluid percussion-induced brain injury in the mouse. J. Neurotrauma 29(5), 789 – 812.

Bonfoco, E., Krainc, D., Ankarcrona, M., Nicotera, P & Lipton, S.A (1995) Apoptosis and necrosis: Two distinct events induced, respectively, by mild and intense insults with N-methyl-D-aspartate or nitric oxide/superoxide in cortical cell cultures. *PNAS, **92**, 7162 – 7166*

Bonneto, J., Iliadis, A., Genton, P., Dravet, C., Viallet, D & Mesdjian, E (1993) Steady state pharmacokinetics of conventional versus controlled release Carbamazapine in patients with epilepsy. *Epilepsy Res. **14**, 257 – 263.*

Bootsma, H.P.R., Ricker, L., Diepman, L., Gehring, J., Hulsman, J., Lambrechts, D., Leenen, L., Majoie, M., Schellekens, A., de Krom, M & Aldenkamp, A.P (2008) Long-term effects of Levetiracetam and topiramate in clinical practice: a head-to-head comparison. *Seizure **17(1)**, 19 – 26.*

Borges, K., McDermott, D., Irier, H., Smith, Y & Dingledine, R (2006) Degeneration and proliferation of astrocytes in the mouse dentate gyrus after pilocarpine-induced status epilepticus. *Exp. Neurol. **201**, 416 – 417.*

Bortolotto, Z.A., Lauri, S., Isaac, J.T.R & Collingridge, G (2003) Kainate receptors and the induction of mossy fibre long-term potentiation. *Philos. Trans. R. Soc. Lond. B. Biol. Sci. **358(1432)**, 657 – 666*

Bourgeois, B (2000) Pharmacokinetics and Pharmacodynamics of Topiramate. *J. Child Neurol.* ***15****, S27 – 30.*

Bradford, H.F (1995) Glutamate, GABA and epilepsy. *Prog. Neurobiol.* ***47(6)****, 477 – 511.*

Brailowsky, S., Menini, C., Silva-Barrat, C & Naquet, R (1987) Epileptogenic gamma-aminobutyric acid-withdrawal syndrome after chronic, intracortical infusion in baboons. *Neurosci. Lett.* ***74****, 75 – 80*.

Bredt, D.S & Snyder, S.H. (1992) Nitric oxide, a novel neuronal messenger. *Neuron* ***8(1)****, 3 – 11.*

Bredt, D.S & Nicoll, R.A (2003) AMPA receptor trafficking at excitatory synapses. *Neuron* ***40(2)****, 361 – 379*.

Brock, L.G & Coombs, J.S & Eccles, J.C (1951) Action potentials of motor neurons to stimulation by internal microelectrodes. *Proc. Univ. Otago Med. Sch.* ***31****, 19 – 20.*

Brown, G.C & Bal-Price, A (2003) Inflammatory Neurodegeneration Mediated by Nitric Oxide, Glutamate, and Mitochondria. *Mol. Neurobiol.* ***27(3)****, 325 – 355.*

Bruce, A.J., Sakhi, S., Schreiber, S.S & Baudry, M (1995) Development of Kainic Acid and N-Methyl-D-Aspartic Acid Toxicity in Organotypic Hippocampal Cultures. *Exp. Neurol.* ***132****, 209 – 219*

Buckmaster, P.S & Dudek, F.E (1997) Neuron loss, granule cell axon reorganisation, and functional changes in the dentate gyrus of epileptic kainate-treated rats. *J. Comp. Neurol.* ***385(3)****, 385 – 404.*

Burette, A., Zabel, U., Weinburg, R.J., Schmitt, H.H.H.W & Valtschanoff, J.G (2002) Synaptic localization of nitric oxide synthase and soluble guanylyl cyclase in the hippocampus. J. Neurosci. **22(20)**, 8961 - 8970.

Buskila, Y., Farkash, S., Hershfinkel, M & Amitai, Y (2005) Rapid and reactive nitric oxide production by astrocytes in mouse neocortical slices. *Glia* ***52****: 169–176.*

Buzsaki, G. (1997) Functions for interneuronal nets in the hippocampus. *Can. J. Physiol. & Pharmacol.* ***75(5)****, 598 – 515.*

Cantallops, I & Routtenberg, A (2000) Kainic acid Induction of Mossy Fiber sprouting: Dependence on Mouse Strain. *Hippocampus* ***10****, 269 – 273*.

Cavalheiro, E.A., Riche, D.A & LaSalle, G.L.G (1982) Long-term effects of intrahippocampal kainic acid injection in Rats: a method for inducing spontaneous recurrent seizures. *Electroencephalogr. Clin. Neurophysiol.* ***53****, 581 – 589*

Cavazos, J.E & Sutula, T.P (1990) Progressive neuronal loss induced by kindling: a possible mechanism for mossy fibre synaptic reorganisation and hippocampal sclerosis. *Brain Res.* ***527****, 1 – 6*

Cavazos, J.E., Das, I & Sutula, T.P (1994) Neuronal loss induced in limbic pathways by kindling: evidence for induction of hippocampal sclerosis by repeated brief seizures. *J. Neurosci.* ***14****, 3106 – 3121*

Cazauvieilh, B.C (1825) De l'epilepsie consideree dans ses rapports avec la l'alienation mentale. *Arch. Gen. Med.* ***9****, 510 – 542*

Chan, S.H., Wang, L.L., Wang, S.H & Chan, J.Y (2001) Differential cardiovascular responses to blockade of nNOS or iNOS in rostral ventrolateral medulla of the rat. *Br. J. Pharmacol.* ***133****, 606 – 614*

Chatterton, J.E., Awobuluyi, M., Premkumar, L.S., Takahashi, H., Talantova, M., Shin, Y., Cui, J., Tu, S., Sevarino, K.A., Nakanishi, N., Tong, G., Lipton, S.A &

Chauviere, L., Doublet, T., Ghestem, A., Siyoucef, S.S., Wendling, F., Huys, R., Jirsa, V., Bartolomei, F., Bernard, C (2012) Changes in Interictal Spike Features Precede the Onset of Temporal Lobe Epilepsy*. Ann. Neurol. **71**, 805 – 814*

Chavko, M., Xing, G & Keyser, D.O (2001) Increased sensitivity to seizures in repeated exposures to hyperbaric oxygen: role of NOS activation. Brain Res. **900(2),** 227-33

Chen, X., Nelson, C.D., Li, X., Winters, C.A., Azzam, R., Sousa, A.A., Leapman, R.D., Gainer, H., Sheng, M & Reese, T.S (2011) PSD-95 is required to sustain the Molecular Organization of the Postsynaptic Density. *J. Neurosci.* ***31(17)**, 6329 – 6338*

Chen X, Vinade L, Leapman RD, Petersen JD, Nakagawa T, Phillips TM, Sheng M, Reese TS *(*2005*)* Mass of the postsynaptic density and enumeration of three key molecules*. Proc Natl Acad Sci USA **102**,11551 – 11556*

Cho, K.O., Hunt, C.A & Kennedy, M.B (1992) The rat brain postsynaptic density fraction contains a homolog of the Drosophila discs-large tumour suppressor protein. *Neuron, **9**(5), 929 – 942*

Choi, D.W (1992) Excitotoxic cell death. *J. Neurobiol.* ***23(9)****, 1261 – 1276.*

Chung, Y.H., Kim, Y.S & Lee, W.B (2004) Distribution of neuronal nitric oxide synthase-immunoreactive neurons in the cerebral cortex and hippocampus during post-natal development. *J. Mol. Histol.* ***35(8 – 9)****, 765 – 770*.

Cohen-Gadol, A.A., Wilhelmi, B.G., Collingnon, F., White, J.B., Britton, J.W., Cambier, D.M., Christianson, T.J.H & Cascino, G.D (2006) Long-term outcome of epilepsy surgery among 399 patients with nonlesional seizure foci including mesial temporal lobe sclerosis. *J. Neurosurgery.* ***104(4)****, 513 – 524*.

Collins, R.C., McLean, M & Olney, J.W (1980) Cerebral metabolic response to systemic kainic acid: 14-C-deoxyglucose studies. *Life Sci.* ***27****, 855 – 862.*

Colom, L.V & Saggau, P (1994) Spontaneous interictal-like activity originates in multiple areas of the CA2-CA3 region of hippocampal slices. *J. Neurophysiol.* ***71(4)****, 1574 – 1585.*

Conn, P.J & Pinn, J-P (1997) Pharmacology and functions of metabotropic glutamate receptors. *Ann. Rev. Pharmacol. And Toxicity* ***37****, 205 – 237*

Cook, D.J., Teves, L & Tymianski, M (2012) Treatment of stroke with a PSD-95 inhibitor in the gyrencephalic primate brain. *Nature* ***483****, 213 – 217*.

Coons, A.H & Kaplan, M.H (1950) Localization of antigen in tissue cells; improvements in a method for the detection of antigen by means of fluorescent antibody. *J. Exp. Med.* ***91****, 1 – 13.*

Cork, R.J., Perrone, M.L., Bridges, D., Wandell, J., Scheiner, C.A & Mize, R.R (1998) A web-accessible digital atlas of the distribution of nitric oxide synthase in the mouse brain. *Prog. Brain Res.* ***118****, 37 – 50.*

Cosgrave, A.S., McKay, J.S., Bubb, V., Morris, R., Quinn, J.P & T. Thippeswamy (2008) Regulation of activity-dependent neuroprotective protein (ADNP) by the NO-cGMP pathway in the hippocampus during kainic acid-induced seizure. Neurobiol. Dis. **30(3)**, 281 - 292.

Cosgrave, A.S., McKay, J.S., Morris, R., Quinn, J.P & Thippeswamy, T (2010) The effects of nitric oxide inhibition prior to kainic acid treatment on neuro- and gliogenesis in the rat dentate gyrus in vivo and in vitro. Histol. & Histopathol. **25(7)**, 841 - 856

Coulter, D.A & Eid, T (2012) Astrocytic Regulation of Glutamate Homeostasis in Epilepsy. *Glia* ***60****, 1215 – 1226*.

Crawley, J.N (2008) Behavioural Phenotyping Strategies for Mutant Mice. *Neuron* ***57(6)****, 809 – 818.*

Crespel, A., Coubes, P., Rousset, M-C., Brana, C., Rougier, A., Rondouin, G., Bockaert, J & Lerner-Natoli, M (2002) Inflammatory reactions in human medial temporal lobe epilepsy with hippocampal sclerosis. *Brain Res.* ***952(2)****, 159 – 169*.

Cui, H., Hayashi, A., Sun, H-S., Belmares, M.P., Cobey, C., Phan, T., Schweizer, J & Tymianski, M (2007) PDZ protein interactions underlying NMDA receptor-mediated excitotoxicity and neuroprotection by PSD-95 inhibitors. *J. Neurosci.* ***27(37)****, 9901 – 9915.*

Danysz, W & Parsons, C.G (1998) Glycine and N-Methyl-D-Aspartate Receptors: Physiological significance and possible Therapeutic Applications. *Pharmacol. Rev.* ***50(4)****, 597 – 664*

Davalos, D., Grutzendler, J., Yang, G., Kim, J.V., Zuo, Y., Jung, S., Littman, D.R., Dustin, M.L & Gan, W-B (2005) ATP mediates rapid microglial response to local brain injury *in vivo. Nat. Neurosci.* ***8(6)****, 752 – 758.*

De Lanerolle, N.C., Kim, J.H., Robbins, R.J & Spencer, D.D (1989) Hippocampal interneuron loss and plasticity in human temporal lobe epilepsy. Brain Res. 495(2), 387 – 395.

Del-Rio Hortega, P (1932) *in Cytology and Cellular Pathology of the Nervous System (Penfield, W., ed.), 481 – 534, Hoeber.*

Denninger, J.W & Marletta, M.A (1999) Guanylate cyclase and the NO/cGMP signalling pathway. *Biochim. Biophys. Acta.* ***1411****, 334 – 350*.

Desthexe, A & Sejnowski, T.J (2003) Interactions between membrane conductances underlying thalamocortical slow-wave oscillations. *Physiol. Rev.* ***83(4)****, 1401 – 1453*.

Derkach, V., Barria, A & Soderling, T.R (1999) CA2+/calmodulin-kinase II enhances channel conductance of α-amino-3-hydroxy-5-methyl-4-isoxazolepropionate type glutamate receptors. *Proc. Natl. Acad. Sci.* ***96(6)****, 3269 – 3274*.

De Vries, H.E., Kuiper, J., De Boer, A.G., Van Berkel, T.J & Breimer, D.D (1997) The Blood-Brain Barrier in Neuroinflammatory Diseases. *Pharmacol. Revs.* ***49(2)****, 143 - 156*

Dichter, M.A & Ayala, G.F (1987) Cellular mechanisms of epilepsy: a status report. *Science* ***237****, 157 – 164.*

Do Nascimento, A.L., Dos Santos, N.F., Campos Pelagio, F., Aparecida Teixeira, S., De Moraes Ferrari, E.A & Langone, F (2012) Neuronal degeneration and gliosis time-course in the mouse hippocampal formation after pilocarpine-induced status epilepticus. *Brain Res.* ***1470****, 98 – 110*.

Doucet, M.V., Harkin, A & Dev, K.K (2012) The PSD-95/nNOS complex: new drugs for depression? *Pharmacol. and Therapeutics* ***133(2)****, 218 – 229*.

Dudek, F.E (2003) High-frequency Oscillations and Neocortical Seizures: Do they have a role in seizure onset, and which mechanisms generate them? *Epilepsy Curr.* ***3(3)****, 80 – 81.*

Dragoi, G & Buszaki, G (2006) Temporal Encoding of Place Sequences by Hippocampal Cell Assemblies. *Neuron* ***50(1)****, 145 – 157.*

Dragunow, M & Faull, R (1989) The use of c-Fos as a metabolic marker in neuronal pathway tracing. *J. Neurosci. Methods* ***29(3)****, 261 – 265*.

Duchen, M.R (2000) Mitochondria and calcium: From cell signalling to cell death. *J. Physiol.* ***529(1)****, 57 – 68.*

Dumas, T.C (2005) Developmental regulation of cognitive abilities: Modified composition of a molecular switch turns on associative learning. *Prog. Neurobiol.* ***76(3)****, 189 – 211.*

Duncan, J.S., Sander, J.W., Sisodiya, S.M & Walker, M.C. (2006) Adult Epilepsy. *Lancet* ***367(9516)****, 1087 – 1100.*

Dykstra, C.M., Ratnam, M & Gurd, J.W (2009) Neuroprotection after status epilepticus by targetting protein interations with postsynaptic density protein 95. *J. Neuropathol. Exp. Neurol.* ***68****, 823 – 831*.

Eid, T., Thomas, M.J., Spencer, D.D., Runden-Pran, E., Lai, J.C., Malthankar, G.V., Kim, J.H., Danbolt, N.C., Ottersen, O.P & de Lanerolle NC (2004) Loss of glutamine synthetase in the human epileptogenic hippocampus: Possible mechanism for raised extracellular glutamate in mesial temporal lobe epilepsy. *Lancet* ***363****, 28 – 37*.

Ellman, G.L., Courtney, K.D., Andres Jr, V & Featherstone, R.M. (1961) A new and rapid colorimetric determination of acetylcholinesterase activity. *Biochem. Pharmacol.* ***7(2)****, 88 – 90.*

Engel Jr, J. (2008) Progress in epilepsy: Reducing the treatment gap and the promise of biomarkers. *Curr. Opinions in Neurol.* ***21(2)****, 150 – 154.*

Engel, J & Ackermann, R.F (1980) Interictal spikes correlate with decreased, rather than increased epileptogenicity in amygdaloid kindled rats. *Brain. Res.* ***190****, 543 – 548.*

Engstrom, F.L & Woodbury, D.M (1988) Seizure Susceptabiilty in DBA and C57 Mice: The Effects of Various Convulsants. *Epilepsia,* ***29(4)****, 389 – 395*

Engstrom, F.L & Woodbury, D.M (1986) The effects of various convulsants on seizure activity in DBA/2 and C57/6 mice. *Proc. West. Pharmacol. Soc.* ***29****, 219 - 222*

Erdemli, G & Krnjevic, K (1995) Nitric oxide tonically depresses a voltage- and Ca-dependent outward current in hippocampal slices. Neurosci. Let. **201(1)**, 57 – 60.

Errante, L.D & Petroff, O.A.C (2003) Acute effects of gabapentin and pregabalin on rat forebrain cellular GABA, glutamate, and glutamine concentrations. *Seizure* ***12(5)****, 300 – 306.*

Faught, E., Sachdeo, R.C. Remler, M.R. Chayasirisobhon, S. Ramsay, F. Iragui, V. Kanner, A. Kramer L.D. & Rosenberg, A (1992) Felbamate double-blind monotherapy trial, *Neurology* ***42(suppl. 3)****, 311 – 315.*

Fellin, T & Haydon, P.G (2005) Do astrocytes contribute to excitation underlying seizures? *Trends Mol. Med.* ***11(12)****, 530 – 533.*

Fellin, T., Pascual, O., Gobbo, S., Pozzan, T., Haydon, P.G & Carmignoto, G. (2004) Neuronal synchrony mediated by astrocytic glutamate through extrasynaptic NMDA receptors. *Neuron* ***43(5)****, 729 – 743.*

Ferraro, T.N., Golden, G.T., Smith, G.G & Berrettini, W.H (1995) Differential susceptability to seizures induced by systemic kainic acid treatment in mature DBA/2J and C57BL/6J mice. *Epilepsia* ***36(3)****, 301 – 307*.

Fink-Jensen, A., Suzdak, P.D., Swedberg, M.D.B., Judge, M.E., Hansen, J.L & Nielsen, P.G (1992) The γ-aminobutyric acid (GABA) uptake inhibitor, tiagabine, increases extracellular brain levels of GABA in awake rats. *Eur. J. Pharmacol.* ***220(2-3)****, 197 – 201.*

Finnocchietto, P.V., Franco, M.C., Holod, S., Gonzalez, A.S., Converso, D.P., Antico Arciuch, V.G., Serra, M.P., Poderoso, J.J & Carreras, M.S (2009) Mitochondrial nitric oxide synthase: a masterpiece of metabolic adaption, cell growth, transformation and death. *Exp. Biol. Med.* ***234(9)****, 1020 – 1028.*

Fisher, R.S (1989) Animal models of the epilepsies. *Brain Res. Revs.* ***14****, 245 – 278.*

Fisher, R.S., van Emde Boas, W., Blume, W., Elger, C., Genton, P., Lee, P & Engel, Jr, J (2005) Epileptic seizures and Epilepsy: Definitions Proposed by the International League against Epilepsy (ILAE) and the International Bureau for Epilepsy (IBE). Epilepsia 46(4), 470 – 472.

Foresti, M.L., Arisi, G.M & Shapiro, L.A (2011) Role of glia in epilepsy-associated neuropathology, neuroinflammation and neurogenesis. *Brain res. Rev.* ***66(1)****, 115 – 122*.

Freund, T.F & Buzsaki, G (1996) Interneurons of the hippocampus. *Hippocampus* ***6(4)****, 347 – 470*.

Furchgott, R.F & Zawadzki, J.V (1980) The obligatory role of endothelial cells in the relaxation of arterial smooth muscle by ACh. *Nature* ***288****, 373 – 376*.

Gahwiler, B.H (1981) Organotypic monolayer cultures of nervous tissue. *J. Neurosci. Methods* ***4****, 329 – 342*

Gaitanis, J.N & Drislane, F.W (2003) Status epilepticus: A review of different syndromes, their current evaluation, and treatment. *Neurologist* ***9(2)****, 61 – 72.*

Gall, C.M., Hess, U.S & Lynch, G (1998) Mapping brain networks engaged by, and changed by, learning. *Neurbiol. Learn Memory* ***70****, 14 – 36*.

Gallassi, R., Morreale, A., Lorusso, S., Procaccianti, G., Lugaresi, E & Baruzzi, A (1990) Cognitive effects of valproate. *Epilepsy Res.* ***5(2)****, 160 – 164*.

Garthwaite, J., Garthwaite, G., Palmer, R. M., & Moncada, S (1989) NMDA receptor activation induces nitric oxide synthesis from arginine in rat brain slices. Eur. J. Pharmac. **172**, 413 - 416.

Garthwaite, J (2008) Concepts of neural nitric oxide-mediated transmission. Eur. J. Neurosci. **27**, 2783 – 2802.

Garvey, E.P., Oplinger, J.A., Furfine, E.S., Kiff, R.J., Laszlo. F., Whittle, B.J & Knowles, R.G (1997) 1400W is a slow, tight binding, and highly selective inhibitor of inducible nitric-oxide synthase in vitro and in vivo, *J. Biol. Chem.* ***272****, 4959–4963.*

Gass, P., Herdegen, T., Bravo, R & Kiessling, M (1992) Induction of immediate early gene encoded proteins in the rat hippocampus after biccuculine-induced seizures: Differential expression of KROX-24, FOS and JUN proteins. *Neurosci.* ***48(2)****, 315 – 324*.

Giardina, W.J (1994) Anticonvulsant action of tiagabine, a new GABA-uptake inhibitor. *J. Epilepsy* ***7****, 161 – 166.*

Gibbs, F.A., Lennox, W.G & Gibbs, E.L. (1936) The electro-encephalogram in diagnosis and in localization of epileptic seizures. *Arch Neurol Psychiatry* ***36****, 1225 -35.*

Gidal, B.E., Anderson, G.D., Spencer, N.W., Maly, M.M., Murty, J., Pitterie, M.E., Collins, D.M & Davis, L.A (1996) Valproate-associate weight gain: Potential relation to energy expenditure and metabolism in patients with epilepsy. *J. Epilepsy* ***9(4)****, 234 – 241*.

Gilliam, F.G., Mendiratta, A., Pack, A.M & Bazil, C.W (2008) Epilepsy and common comorbidities: improving the outpatient epilepsy encounter. *Epileptic Disord.* ***7(SUPPL. 1)****, S27 – S33.*

Glass, C.K., Saijo, K., Winner, B., Marchetto, M.C & Gage, F.H (2010) Mechanisms underlying Inflammation in Neurodegeneration. *Cell 140, 918 – 934.*

Glien, M., Brandt, C., Potschka, H., Voigt, H., Ebert, U., Loscher, W (2001) Repeated low-dose treatment of rats with pilocarpine: low mortality but high proportion of rats developing epilepsy. *Epilepsy Res.* ***46****, 111 – 119*.

Goddard, G.V (1967) Development of epileptic seizures through brain stimulation at low intensity. *Nature* ***214****, 1020 – 1023.*

Golgi, C (1873) Sulla struttura della sostanza grigia del cervello. *Gazzetta Medica Italiana (Lombardia)* ***33****, 244 – 246.*

Gotman, J (1991) Relationship between interictal spiking and seizures: human and experimental evidence*. Can. J. Neurol. Sci.* ***18****, 573 – 576.*

Gotman, J & Koffler, D.J (1990) Interictal spiking increasing after seizures but does not after decrease in medicine. *Electroencephalogr. Clin. Neurophysiol.* ***75****, 358 – 360.*

Gowers, W.R (1881) Epilepsy and other chronic convulsive disorders: their causes, symptoms and treatment. *London: J & A Churchill.*

Grabenstatter, H.L., Ferraro, D.J., Williams, P.A., Chapman, P.L & Dudek, F.E (2005) Use of chronic epilepsy models in antiepileptic drug discovery: the effect of topiramate on spontaneous motor seizures in rats with kainate-induced epilepsy. *Epilepsia* ***46****, 8 – 14*.

Gray EG. (1959) Axo-somatic and axo-dendritic synapses of the cerebral cortex: An electron microscope study. *J. Anat.* ***93****, 420 – 433.*

Greenwood, R.S., Godar, S.E & Winstead, K.K (1983) Focal penicillin seizures – motor activity and cellular physiology and morphology. *Brain res. Bull.* ***11(1)****, 91 - 101*

Griffith, W.H & Taylor, L (1988) Sodium valproate decreases synaptic potentiation and epileptiform activity in hippocampus. *Brain Res.* ***474****, 155 - 164*

Griffiths, M.J., Messent, M., MacAllister, R.J & Evans, T.W (1993) Aminoguanidine selectively inhibits inducible nitric oxide synthase. *Br. J. Pharmacol.* ***110(3)****, 963 – 968*

Hagioka, S., Takeda, Y., Zhang, S., Sato, T & Morita, K (2005) Effects of 7-nitroindazole and N-nitro-L-arginine methyl ester on changes in cerebral blood flow and nitric oxide production preceding development of hyperbaric oxygen-induced seizures in rats. Neurosci. Let. **382(3)**, 206 – 210

Haneka, M.T., Rodriquez, J.J & Verkhradsky, A (2010) Neuroglia in neurodegeneration. *Brain Res. Revs.* ***63(1 – 2)****, 189 – 211.*

Hawkins, R.D., Son, H & Arancio, O. (1998) Nitric oxide as a retrograde messenger during long-term potentiation in the hippocampus. *Prog. Brain Res.* ***118****, 155 – 172.*

Hayashi, M.K., Tang, C., Verpelli, C., Narayanan, R., Stearns, M.H., Xu, R-M., Li, H., Sala, C & Hayashi, Y (2009) The Postsynaptic Density Proteins Homer and Shank Form a Polymeric Network Structure. *Cell* ***137(1)****, 159 – 171*.

Heales, S.J.R., Bolanos, J.P., Stewart, V.C., Brookes, P.S., Land, J.M & Clark, J.B (1999) Nitric oxide, mitochondria and neurological disease. *Biochimica et Biophysica Acta- Bioenergetics* ***1410(2)****, 215 – 228*.

Hebb, D (1949) The Organisation of Behaviour. *John Wiley & Sons.*

Heilbroner, P.L & Devinsky, O (1997) Monotherapy with Gabapentin for partial epilepsy: A review of 30 cases. *J. Epilepsy* ***10****, 220 – 224.*

Heinemann, U., Gabriel, S., Schuchmann, S. & Eder, C. (1999).Contribution of astrocytes to seizure activity. *Adv. Neurol.* ***79****, 583–590.*

Hellier, J.L., Patrylo, P.R., Buckmaster, P.S & Dudek, F.E (1998) Recurrent spontaneous motor seizures after repeated low-dose systemic treatment with

kainate: assessment of a rat model of temporal lobe epilepsy. *Epilepsy Res.* ***31****, 73 – 84*.

Hellier, J.L., White, A., Williams, P.A., Dudek, F.E & Staley, K.J (2009) NMDA receptor-mediated long-term alterations in epileptiform activity in chronic epilepsy. *Neuropharmacol.* ***56****, 414 – 421*.

Hendrikson, H., Datson, N.A., Ghijsen, W.E.J.M., van Vliet, E.A., Lopes de Silva, F.H., Gorter, J.A & Vreugdenhil (2001) Altered hippocampal gene expression prior to the onset of spontaneous seizures in the rat post-status epilepticus model. *Eur. J. Neurosci.* ***14****, 1475 – 1484*.

Hess, J., Angel, P & Schorpp-Klstner (2004) AP-1 subunits: quarrel and harmony among siblings. *J. Cell. Sci.* ***117****, 5965 – 5973.*

Hodgkin, A.L. & Huxley, A.F (1952) A quantitative description of membrane current and its application to conduction and excitation in nerve. *J. Physiol.* ***117****, 500 – 544.*

Hopfield, J.J & Tank, D.W. (1986) Computing with neural circuits: A model. *Science* ***233****, 625 – 633.*

Hopper, R.A & Garthwaite, J (2006) Tonic and phasic nitric oxide signals in hippocampal long-term potentiation. J. Neurosci. **26(45)**, 11513 - 11521.

Hororbin, R & Kiernan, J (2002) Conn's Biological stains: A Handbook of dyes, stains and fluorochromes for use in Biology and Medicine. *Taylor & Francis.*

Houser, C.R (1990) Granule cell dispersion in the dentate gyrus of humans with temporal lobe epilepsy. *Brain Res. **535**, 195 - 204.*

Hsueh, Y.P & Sheung, M (1999) Requirement of N-terminal cysteines of PSD-95 for PSD-95 multimerization and ternary complex formation but not for binding to potassium channel Kv1.4. *J. Biol. Chem. **274(1)**, 532 – 536*

Hu, R.Q., Koh, S., Torgerson, T & Cole, A.J (1998) Neuronal stress and injury in C57/BL mice after systemic kainic acid administration. *Brain Res. **810**, 229 – 240*

Huttenlocher, P.R. (1976) Ketonemia and seizures: metabolic and anticonvulsant effects of two ketogenic diets in childhood epilepsy. *Pediatric Res. **10(5)**, 536 – 540.*

Ignarro, L.J., Buga, G.M., Wood, K.S., Byrns, R.E & Chaudhuri, G (1987) Endothelium-derived relaxing factor produced and released from artery and vein is nitric oxide. *Proc. Natl. Acad. Sci. U.S.A **84(24)**, 9265 – 9269.*

Ikeda, H & Murase, K (2004) Glial nitric oxide-mediated long-term presynaptic facilitation revealed by optical imaging in rat spinal dorsal horn. *J. Neurosci.* ***24****, 9888 – 9896.*

Jackson, J.H (1890) On convulsive seizures. *Lancet* ***1****, 685 – 688, 735 – 738, 785 – 788.*

Jafarian-Tehrani, M., Louin, G., Royo, N.C., Besson, V.C., Bohme, G.A., Plotkine, M & Marchand-Verrecchia, C (2005) 1400W, a potent, selective inducible NOS inhibitor, improves histopathological outcome following traumatic brain injury in rats. *Nitric Oxide* ***12****, 61 – 69*.

Janszky, J., Fogarasi, A., Jokeit, H., Schulz, R., Hoppe, M & Ebner, A (2001) Spatiotemporal relationship between seizure activity and interictal spikes in temporal lobe epilepsy. *Epilepsy Res.* ***47(3)****, 179 – 188.*

Jeffreys, J.G.R (1995) Nonsynaptic modulation of neuronal activity in the brain: Electric currents and extracellular ions. *Physiol. Rev.* ***75(4)****, 689 – 723.*

Jian, K., Chen, K., Cao, X., Zhu, X.-H., Fung, M.-L & Gao, T.-M (2007) Nitric oxide modulation of voltage-gated calcium current by S-nitrosylation and cGMP

pathway in cultured rat hippocampal neurons. Biochem. and Biophys. Res. Comms. **359(3)**, 481 - 485.

Jiminez-Mateos, E.M & Henshall, D.C (2009) Seizure preconditioning and epileptic tolerance: models and mechanisms. *Int. J. Physiol. Pathophysiol. Pharmacol. **1**, 180 – 191*.

Jinno, S., Aika, Y., Fukada, T & Kosaka, T (1998) Quantitative analysis of GABAergic neurons in the mouse hippocampus, with optical dissector using confocal laser scanning microscope. *Brain Res. **814(1 – 2)**, 55 – 70.*

Jiruska, P., Powell, A.D., Chang, W.C & Jeffreys, J.G.R (2010) Electrographic high-frequency activity and epilepsy. Epilepsy Res. **89(1)**, 60 - 65

Joels, M (2009) Stress, the hippocampus, and epilepsy. Epilepsia **50(4)**, 586 - 597.

Johannessen, C.U (2000) Mechanisms of action of valproate: a commentary. *Neurochem. Intl. **37**, 103 – 110.*

Johnstone, D & Brown, T.H (1981) Giant synaptic potential hypothesis for epileptiform activity. *Science **211**, 294 – 297.*

Jones, E.G (1999) Golgi, Cajal and the Neuron Doctrine. *J. Hist. Neurosci.* ***8(2)****, 170 – 178.*

Kaila, K (1994) Ionic basis of GABA(A) receptor channel function in the brain. *Prog. Neurobiol.* ***42(4)****, 489 – 537.*

Kalinchuk, A.V., Stenberg, D., Rosenberg, P.A & Porkka-Heiskanen, T (2006) Inducible and neuronal nitric oxide synthases (NOS) have complementary roles in recovery sleep induction. *Eur. J. Neurosci.* ***24(5)****, 1443 – 1456.*

Kalis, M.M & Huff, N.A (2001) Oxcarbazepine, An Antiepileptic agent. *Clin. Therapeutics* ***23(5)****, 680 – 700*.

Kaminow, L., Schimschock, J.R., Hammer, A.E & Vuong, A (2003) Lamotrigine monotherapy compared with Carbamazapine, phenytoin, or valproate monotherapy in patients with epilepsy. *Epilepsy & Behav.* ***4****, 659 – 666.*

Kandel, E.R. (2001) The Molecular Biology of Memory Storage: A Dialogue Between Genes and Synapses. *Science* ***294****, 1030 1038.*

Kaneko, K., Itoh, K., Berliner, L.J., Miyasaka, K & Fujii, H (2002) Consequences of nitric oxide generation in epileptic-seizure rodent models as studied by in vivo EPR. *Magnetic Resonance in Med.* ***48(6)****, 1051 – 1056*.

Kaibara, M & Blume, W.T (1988) The post-ictal electroencephalogram. *Electroencephalogr. Clin. Neurophysiol.* ***70****, 99 – 104.*

Karin, M., Liu, Z-G & Zandi, E (1995) AP-1 function and regulation. *Curr. Op. Cell Biol.* ***9(2)****, 240 – 246*.

Katz, A., Marks, D.A., McCarthy, G., Spencer, S.S (1991) Does interictal spiking change prior to seizures? *Electroencephalogr. Clin. Neurophysiol.* ***79****, 153 – 156.*

Kelly, M.E & McIntyre, D.C (1994) Hippocampal kindling protects several structures from the neuronal damage resulting from kainic acid-induced status epilepticus. *Brain Res.* ***634(2)****, 245 – 256.*

Kennedy, M (1997) The postsynaptic density at glutamatergic synapses. *Trends. Neurosci.* ***20****, 264 – 268*

Khartatishvili, I., Nissinen, J.P., McKintosh, T.K & Pitkanen (2006) A model of posttraumatic epilepsy induced by lateral fluid-percussion brain injury in rats. *Neurosci.* ***140(2)****, 685 – 697.*

Kiemann, C.J.H.M., Roubos, E.W (2011) The gray area between synapse structure and function- Gray's synapse types I and II revisited. *Synapse, **65**(11), 1222 – 1230*

Kim, H.P., Ryter, S.W & Choi, A.M (2006) CO as a cellular signalling molecule. *Annu. Rev. Pharmacol. Toxicol. **46**, 411 - 449*.

Kim, D-K (2010) Increased seizure susceptibility and upregulation of nNOS expression in hippocampus following recurrent early-life seizures in rats. *J. Korean Med. Sci. **25**, 905 - 911*

Kim, Y & Rho, J.M (2008) The ketogenic diet and epilepsy. *Curr. Op. Clin. Nutr. Metab. Care **11(2)**, 113 – 120*

Klemann, C.J.H.M & Roubos, E.W. (2011) The Gray Area Between Synapse Structure and Function – Gray's Synapse Types I and II revisited. *Synapse **65**, 1222 – 1230.*

Knowles, R.G & Moncada, S (1994) Nitric oxide synthases in mammals. *Biochem. Journal **298(2)**, 249 – 258*.

Koponen, S., Kurkinen, K., Akerman, K.E.O., Mochly-Rosen, D., Chan, P.H & Koistinaho, J (2003) Prevention of NMDA-induced death of cortical neurons by

inhibition of protein kinase Cz: Inhibition of PKCz blocks NMDA neurotoxicity. *J. Neurochem.* ***86(2)****, 442 – 450*.

Kornyei, Z., Czirok, A., Vicsek, T & Madarasz, E (2000) Proliferative and Migratory responses of Astrocytes to in vitro Injury. *J. Neuosci. Res.* ***61****, 421 - 429*

Kovacs, R., Rabanus, A., Otahal, J., Patzak, A., Kardos, J., Albus, K., Heinemann, U & Kann, O (2009) Endogenous Nitric Oxide Is a Key Promoting Factor for Initiation of Seizure-Like Events in Hippocampal and Entorhinal Cortex Slices. *J. Neurosci.* ***29(26)****, 8565 - 8577.*

Koyama, R & Ikegaya, Y (2005) To BDNF or not to BDNF: that is the epileptic hippocampus. *Neuroscientist* ***11****, 282 – 287*.

Krall, R.L., Penry, J.K., White, B.G., Kupferberg, H.J & Swinyard, E.A (1978) Antiepileptic drug development: II. Anticonvulsant drug screening. *Epilepsia* ***19****, 409 – 428.*

Kreutzberg, G.W (1996) Microglia: a sensor for pathological events in the CNS. *Glia* ***19(8)****, 312 – 318.*

Kudryashova, I.V (2007) Synaptic and Extrasynaptic NMDA receptors: Problems and prospects. *Neurochem. Journal* ***1(4)****, 275 – 280.*

Kurschner, V.C., Petruzzi, R.L., Golden, G.T., Berrettini, W.H & Ferraro, T.N (1998) Kainate and AMPA receptor binding in seizure-prone and seizure-resistant inbred mouse strains. *Brain Res.* ***780(1)****, 1 – 8*

Kwan, P & Brodie, M.J (2000) Early identification of refractory epilepsy. *N. Eng. J. Med.* ***342(5)****, 314 – 319.*

Kream, R.M & Stefano, G.B (2009) Endogenous morphine and nitric oxide coupled regulation of mitochondrial processes. *Med. Sci. Monit.* ***15****, RA263 - 268.*

Lamas, S., Lowenstein, C.J & Michael, T (2007) Nitric oxide signalling comes of age: 20 years and thriving. *Cardiovasc. Res.* ***75****, 207 – 209.*

Landau, W.M & Kleffner, F.R (1957) Syndrome of aquired aphasia with convulsive disorder in children. *Neurol.* ***7(8)****, 523 – 530.*

Laursen, M.A (1984) The Contribution of in vitro studies to the understanding of Epilepsy. *Acta Neurol. Scandinavia* ***69****, 367 – 375*

Leach, M.J., Baxter, M.G & Critchley, M.A.E (1991) Neurochemical and behavioural aspects of Lamotrigine. *Epilepsia* ***32(SUPPL 2)****, S4 – S8*.

Lee ,C-H., Lee, C-Y., Tsai, T-S & Liou, H-H (2008) PKA-mediated phosphorylation is a novel mechanism of Levetiracetam, an antiepileptic drug, activating ROMK1 channels. *Biochem. Pharmacol.* ***76(2)****, 225 – 235*.

Lees, G & Leach, M.J (1993) Studies of the mechanism of action of the novel anticonvulsant Lamotrigine (Lamictal) using primary neuroglial cultures from rat cortex. *Brain Res.* ***612****, 190 – 199*.

Lefer, D.J (2007) A new gaseous signalling molecule emerges: Cardioprotective role of hydrogen sulphide. *Proc. Natl. Acad. Sci.* ***104(46)****, 17907 – 17908*.

Lehmuke, M.J., Thomson, K.E., Scheerlinck, P., Pouliot, B., Greger, B & Dudek, F.E (2009) A simple quantitative method for analyzing electrographic status epilepticus in rats. *J. Neurophysiol.* ***101****, 1660 – 1670*.

Leppik, I.E., Dreifuss, F.E, Pledger, G.W (1991) Felbamate for partial seizures: results of a controlled clinical trial. *Neurology* ***41****, 1785–1789*.

Li, Q., Guo, M., Xu, X., Xiao, X., Xu, W., Sun, X., Tao, H & Li, R (2008) Rapid decrease of GAD-67 content before the convulsion induced by hyperbaric oxygen exposure. *Neurochem. Res.* ***33(1)****, 185 – 193.*

Li, G., Bauer, S., Nowak, M., Norwood, B., Tackenberg, B., Rosenow, F., Knake, S., Oertel, W.H & Hamer, H.M (2011) Cytokines and Epilepsy. *Seizure 20, 249 – 256.*

Lim, I.A., Merrill, M.A., Chen, Y & Hell, J.W (2003) Disruption of the NMDA receptor-PSD-95 interaction in hippocampal neurons with no obvious short-term effect. *Neuropharmacol.* ***45(6)****, 738 – 754*.

Liotta, A., Caliskan, G., Ul Haq, R., Hollnagel, J.O., Rosler, A., Heinemann, U & Behrens, C.J (2011) Partial disinhibition is required for transition of stimulus-induced sharp wave-ripple complexes into recurrent epileptiform discharges in rat hippocampal slices. *J. Neurophysiol.* ***105(1)****, 172 - 187*

Llinas, R., Sugimori, M., and Silver, R.B. (1992). Microdomains of high calcium concentration in a presynaptic terminal. *Science* ***256****, 677–679.*

Loewi, O. (1921) Über humorale Übertragbarkeit der Herznervenwirkung. I. *Pflügers Archiv*, ***189****, 239–242.*

Loescher, W (2011) Critical review of current animal models of seizures and epilepsy used in the discovery and development of new antiepileptic drugs. *Seizure* ***20****, 359 – 368.*

Lothman, E.W., Hatlelid, J.M., Zorumski, C.F., Conry, J.A., Moon, P.F & Perlin, J.B (1985) Kindling with rapidly recurring hippocampal seizures. *Brain Res.* ***360(1-2)****, 83 – 91.*

Lothman, E.W., Collins, R.C & Ferrendelli, J.A (1981) Kainic acid-induced limbic seizures: electrophysiologic studies. *Neurology* ***31****, 806 – 812*

Lu, Y.-F., Kandel, E.R & Hawkins, R.D (1999) Nitric Oxide Signaling Contributes to Late-Phase LTP and CREB Phosphorylation in the Hippocampus. *J. Neurosci.* ***19(23)****, 10250 - 10261.*

Lucas, S-M., Rothwell, N., Gibson, R.M (2006) The role of cytokines in CNS injury and disease. *Br. J. Pharmacol. 147(S1), S232 – 240*.

Lynch, D.R., Shim, S.S., Seifert, K.M., Karupathi, S., Mutel, V., Gallagher, M.J & Guttmann, R.P (2001) Pharmacological characterization of interactions of RO 25-6981 with the NR2B (ξ2) subunit. *Eur. J. Pharmacol.* ***416****, 185 – 195.*

Magloszczky, Zs., Halasz, P., Vajda, J., Czirjak, S & Freund, T.F (1997) Loss of calbindin-D(28K) immunoreactivity from dentate granule cells in human temporal lobe epilepsy. *Neurosci.* ***76(2)****, 377 – 385*.

Mahanty, N.K & Sah, P (1998) Calcium-permeable AMPA receptors mediate long-term potentiation in interneurons in the amygdala. *Nature* ***394(6694)****, 683 – 687*.

Malenka, R.C & Bear, M.F (2004) LTP and LTD: an embarrassment of riches. *Neuron* ***44(1)****, 5 – 21.*

Malherbe, P., Mutel, V., Broger, C., Perin-Dureau, F., Kemp, J.A., Neyton, J., Pauletti, P & Kew, J.N (2003) Identification of critical residues in the amino terminal domain of the human NR2B subunit involved in the RO 25-6981 binding pocket. *J. Pharmacol. Exp. Ther.* ***307****, 897 – 905*.

Malick, J.B & Bell, R.M.S. (1976) Enkephalins and endorphins: a major discovery. *JAMA* ***236****, 2887 – 2888*.

Manilow, R & Malenka, R.C (2002) AMPA receptor trafficking and synaptic plasticity. *Annu. Rev. Neurosci.* ***25****, 103 – 126*

Marangos, P.J., Post, R.M., Patel, J., Zander, K., Parma, A & Weiss, S (1983) Specific and potent interactions of Carbamazapine with brain adenosine receptors. *Eur. J. Pharmacol.* ***93****, 175 – 182.*

Martin, R.C., Kuzniecky, R., Ho, S., Hetherington, H., Pan, J., Sinclair, K., Gilliam, F & Faught, E (1999) Cognitive effects of topiramate, gabapentin, and lamotrigine in healthy young adults. *Neurol.* ***52(2)****, 321 – 327.*

Maskey, D., Pradhan, J., Oh, C.K & Kim, M.J (2012) Changes in the distribution of calbindin D28K, parvalbumin, and calretinin in the hippocampus of the circling mouse. *Brain Res.* ***1437****, 58 – 68*.

Matsomoso, H & Marsan, C.A (1964) Cortical cellular phenomena in experiment epilepsy: interictal manifestations. *Exp. Neurol.* ***9(4)****, 286 - 304*

McBain, C.J & Fisahn, A (2001) Interneurons unbound. Nat. rev. Neurosci. **2**, 11 - 23.

McCormick, D.A & Contreras, D (2001) On the cellular and network bases of epileptic seizures. *Ann. Rev. Physiol.* ***63****, 815 – 846.*

McGeer, E.G., Olney, J.W & McGeer, P.L (1978) Kainic acid as a tool in neurobiology. Raven, New York.

McGeer, P.L & McGeer, E.G (1995) The inflammatory response system of brain: implications for therapy of Alzheimer and other neurodegenerative diseases. *Brain Res. Rev.* ***21(2)****, 195 – 218.*

McKee, P (2004) Treating refractory epilepsy with tiagabine: clinical experience. *Seizure* ***13(7)****, 478 – 480.*

McKhann, G.M., Wenzel, H.J., Robbins, C.A., Susunov, A.A & Schwartzkroin (2003) Mouse strain differences in kainic acid sensitivity, seizure behaviour, mortality, and hippocampal pathology. *Neurosci.* ***122****, 551 – 561.*

McLean, M.J (1986) Sodium Valproate, but not Ethosuximide, produces use- and voltage-dependent limitation of high frequency repetitive firing of action potentials of mouse central neurons in cell culture. *J. Pharmacol. And Exp. Therapeutics* ***237****, 1001 – 1011*.

McLean, M.J (2002) Oxcarbazepine: mechanism of action. In: Levy RH, Mattson RH, Meldrum BS, Perucca E, editors. *Antiepileptic drugs. 5th ed. Philadelphia: Lippincott Williams & Wilkins; pp. 451–8*.

Medvedev, A., MacKenzie, L., Hiscock, J.J & Willoughby, J.O (2000) Kainic acid induces distinct types of epileptiform discharge with differential involvement of hippocampus and neocortex. *Brain Res. Bull.* ***52(2)****, 89 – 98*.

Meldrum, B (1984) GABAergic agents as anticonvulsants in baboons with photosensitive epilepsy. *Neurosci. Letts.* ***47(3)****, 345 – 349.*

Meldrum, B.S (2000) Glutamate as a neurotransmitter in the brain: Review of physiology and pathology. *J. Nutrition* ***130(SUPPL. 4)****, S1007 – S1015*

Meyer, B & Andrew, P (1998) Nitric oxide synthases: catalytic function and progress towards selective inhibition. *Naunyn Schmiedebergs Arch. Pharmacol.* ***358(1)****, 127 – 133*.

Miles, R. & Wong, R.K (1983) Single neurones can initiate synchronized population discharge in the hippocampus. *Nature* ***306****, 371–373*

Mita, T., Kawazu, I., Hirano, H., Ohmori, O., Janjua, N & Shibata, K (2001) E1 mice epilepsy shows genetic polymorphism for s-Adenosyl-L-homocysteine hydrolase. *Neurochem. Intl.* ***38(4)****, 349 – 357.*

Moddel, G., Jacobson, B., Ying, Z., Janigro, D., Bingaman, W., Gonzalez-Martinez, J., Kellinghaus, C & Najm, I.M (2005) The NMDA receptor NR2B

subunit contributes to epileptogenesis on human cortical dysplasia. *Brain Res.* ***1046(1 – 2)****, 10 – 23*.

Mody, I & Macdonald, J.F (1995) NMDA receptor-dependent neurotoxicity: The role of intracellular CA2+ release. *Trends. Pharmacol. Sci.* ***16(10)****, 527 – 532*.

Montpied, P., Winsky, L., Dailey, J.W., Jobe, P.C., Jacobowitz, D.M (1995) Alteration in levels of expression of brain Calbindin D-28K and calretinin mRNA in genetically epilepsy-prone rats. *Epilepsia* ***36(9)****, 911 – 921*.

Montezuma, K., Biojone, K., Lisboa, C., Cunha, F.Q., Guimaraes, F.S & Joca, S.R.L (2012) Inhibition of iNOS induces antidepressant-like effects in mice: Pharmacological and genetic evidence. *Neuropharmacol.* ***62(1)****, 485 - 491*

Moore, P.K., Al-Swayeh, O.A., Chong, N.W.S., Evans, R.A., Gibson, A (1990) L-N(G)-nitro-arginine (L-NOARG), a novel L-arginine-reversible inhibitor of endothelium-dependent vasodilation in vitro. *Br. J. Pharmacol.* ***99(2)****, 408 – 412*.

Moore, W.M., Webber, RK., Jerome, G.M., Tioeng, F.S., Misko, T.P & Currie, M.G (1994) L-N6-(1-iminoethyl)lysine: a selective inhibitor of inducible nitric oxide synthase. *J. Med. Chem.* ***37(23)****, 3886 - 3888*

Mori, M., de Cassia Ribiero de Silva Lapa, R., Scerni, D.A., Funke, M.G., Cavalheiro, E.A & da Graca Naffah-Mazzacoratti, M (1998) Study of hippocampal synaptogenesis and epilepsy: Experimental model. *Brazilian J. Epilepsy and Clin. Neurophysiol.* ***4(3)****, 125 – 135.*

Morimoto, K., Fahnestock, M & Racine, R.J (2004) Kindling and status epilepticus models of epilepsy: Rewiring the brain. *Prog. Neurobiol. 73(1), 1 – 60*.

Moser, E.I (2011) The multi-laned hippocampus. *Nat. Neurosci.* ***14****, 407 – 408*.

Moyner, H., Sprengel, R., Schoepfer, R., Herb, A., Higuchi, M., Lomeli, H., Burnashev, N & Seeburg, P.H (1992) Heteromeric NMDA receptors: Molecular and functional distinction of subtype. *Science* ***256(5060)****, 1217 – 1221*.

Mrak, R.E & Griffin, S.T (2005) Glia and their cytokines in progression of neurodegeneration. *Neurobiol. Ageing* ***26(3)****, 349 – 354.*

Mullen, R.J Buck, C.R. & Smith A.M. (1992) NeuN, a neuronal specific nuclear protein in vertebrates, *Development* ***116****, 201 – 211.*

Mumford, J.P & Dam, M (1989) Meta-analysis of European placebo controlled studies of Vigabatrin in drug resistant epilepsy. *Br. J. Clin. Pharmacol.* ***27(S1)****, 101 – 107*.

Murakami, S., Takemoto, T & Shimizu, Z (1953) The effective principle of Digenea simplex Aq. I. separation of the effective fraction by liquid chromatography. *J. Pharm. Soc. Japan* ***73****, 1026 – 1028*.

Nadler, J.V. Perry, B.W & Cotman, C.W (1978) Intraventricular kainic acid preferentially destroys hippocampal pyramidal cells. *Nature* ***271(5646)****, 676 – 677*.

Nadler, J.V (1981) Minireview: KA as a tool for the study of temporal lobe epilepsy. *Life Sciences* ***29(20)****, 2031 – 2048*.

Nadler, J.V (2003) The Recurrent Mossy Fiber Pathway of the Epileptic Brain. Neurochem. Res. **28(11)**, 1649 - 1658.

Nagarkatti, N., Deshpande, L.S & DeLorenzo, R.J (2008) Levetiracetam inhibits both ryanadine and IP3 receptor activated calcium induced calcium release in hippocampal neurons in culture. *Neurosci. Lett.* ***436(3)****, 289 – 293*.

Namiki, S., Kakizawa, S., Hirose, K & Iiono, M (2005) NO signaling decodes frequency of neuronal activity and generates synapse-specific plasticity in mouse cerebellum. J. Physiol. 566(3), 849 - 863.

Naka, M., Nanbu, T., Kobayashi, K., Kamanaka, Y., Komeno, M., Yanase, R., Fukotomi, T., Seo, H.G., Fujiwara, N., Ohuchida, S., Suzuki, K., Kondo, K & Taniquchi, N (2000) A potent inhibitor of inducible nitric oxide synthase, ONO-1714, a cyclic amidine derivative. *Biochem. Biophys. Res. Commun.* ***270(2)****, 663 – 667.*

Nakane, M., Klinghofer, V., Kuk, J.E., Donnelly, J.L., Budzik, G.P., Pollock, J.S., Basha, F & Carter, GW (1995) Novel potent and selective inhibitors of inducible nitric oxide synthase. *Mol. Pharmacol.* ***47(4)****, 831 – 834.*

Neher, E & Sakaba, T (2008) Multiple roles of Calcium Ions in the Regulation of Neurotransmitter Release. *Neuron* ***59****, 861 – 872.*

Newcomer, J.W., Farber, N.B., Jevtovic-Todorovic, C., Selke, G., Melson, A.K., Hershey, T., Craft, S & Olney, J.W (1999) Ketamine-induced NMDA receptor hypofunction as a model of memory impairment and psychosis. *Neuropyschopharmacol.* ***20(2)****, 106 – 118*.

Nimmerjahn, A., Kirchoff, F., Helmchen, F (2005) Resting microglial cells are highly dynamic surveillants of brain paranchyma in vivo. *Science* ***308(5726)****, 1314 – 1318*.

Nishi, M., Hinds, H., Lu, H.P., Kawata, M & Hayashi, Y (2001) Motoneuron-specific expression of NR3B, a novel NMDA-type glutamate receptor subunit that works in a dominant-negative manner. *J. Neurosci.* ***21(23)****, RC185*

Nitecka, L., Tremblay, E & Charton, G (1984) Maturation of kainic acid seizure-brain damage syndrome in the rat. II. Histopathological sequalae. *Neurosci.* ***13(4)****, 1073 – 1094*.

Nitta, I., Watase, H & Tomiie, Y (1958) Structure of kainic acid and its isomer, allokainic acid. *Nature* ***181****, 761 – 762*.

Nowak, L., Bregestovski, P & Ascher, P. (1984) Magnesium gates glutamate-activated channels in mouse central neurones. *Nature* ***307(5950)****, 462 – 465.*

Ohshima, M., Tsuji, M., Taguchi, A., Kasahara, Y., Ikeda, T (2012) Cerebral blood flow during reperfusion predicts later brain damage in a mouse and a rat model of neonatal hypoxic-ischemic encephalopathy. *Exp. Neurol.* ***233(1)****, 481 – 489*.

Ojemann, L.M., Friel, P.N., Tempkin, N.R., Chemlin, T., Ricker, B.A & Wallace, J (1992) Long-term treatment with Gabapentin for partial epilepsy. *Epilepsy Res.* ***13****, 159 – 165.*

Oliva, C., Escobedo, P., Astorga, C., Molina, C & Sierralta, J (2012) Role of the maguk protein family in synapse formation and function. *Dev. Neurobiolog.* ***72(1)****, 57 – 72.*

Ortinski, PI., Dong, J., Mungenast, A., Yue, C., Takano, H., Watson, D.J., Haydon, P.G & Coulter, D.A (2010) Selective induction of astrocytic gliosis generates deficits in neuronal inhibition. *Nat. Neurosci.* ***13(5)****, 584 – 591.*

Ohshima, M., Tsuji, M., Taguchi, A., Kasahara, Y., Ikeda, T (2012) Cerebral blood flow during reperfusion predicts later brain damage in a mouse and a rat model of neonatal hypoxic-ischemic encephalopathy. *Exp. Neurol.* ***233(1)****, 481 – 489*.

Ozawa, S., Kamiya, H & Tsuzuki, K. (1998) Glutamate receptors in the mammalian central nervous system. *Prog. Neurobiol.* ***54(5)****, 581 – 618.*

Palva, J.M., Palva, S & Kaila, K. (2005) Phase synchrony among neuronal oscillations in the human cortex. *J. Neurosci.* ***25(15)****, 3962 – 3972.*

Parmentier, S., Bohme, G.A., Lerouet, D., Damour, D., Stutzmann, J.M., Margaill, I &

Paoletti, P & Neyton, J (2007) NMDA receptor subunits: function and pharmacology. *Curr. Opinion in pharmacol.* ***7****, 39 – 47*

Pasti, L., Zonta, M., Pozzan, T., Vicini, S & Carmignoto, G (2001) Cytosolic calcium oscillations in astrocytes may regulate exocytotic release of glutamate. *J. Neurosci.* ***21(2)****, 477 – 484*.

Peeters, M., Gunthorpe, M.J., Strijbos, P.J.L.M., Goldsmith, P., Upton, N & James, M.F (2007) Effects of pan- and subtype-selective N-methyl-D-aspartate receptor antagonists on cortical spreading depression in the rat: Therapeutic potential for migraine. *J. Pharmacol. And Exp. Therapeutics* ***321(2)****, 564 – 572*.

Penfield, W & Jasper, H. Epilepsy and the Functional anatomy of the Human Brain *(Little Brown, Boston. 1954).*

Periera de Vasconcelos, A., Bouilleret, V., Riban, V., Wasterlain, C & Nehlig, A (2005) Role of nitric oxide in cerebral blood flow changes during kainate seizures in mice: genetic and pharmacological approaches. Neurobiol. of Disease **18**, 270 - 281.

Perry, V.H., Andersson, P-B & Gordon, S (1993) Macrophages and inflammation in the central nervous system. *Trends Neurosci.* ***16****, 268 – 273*

Pinault, D., Uresche, N., Charpier, S., Deniau, J-M., Marescaux, C., Vergnes, M., Crunelli, V (1998) Intracellular recordings in thalamic neurons during spontaneous spike and wave discharges in rats with absence epilepsy. *J. Physiol.* ***509****, 449 – 456.*

Pitkanen, A & Lukasiuk (2011) Mechanisms of epileptogenesis and potential treatment targets. *Lancet Neurol.* ***10****, 173 – 186.*

Pitkanen, A & Sutula, T.P (2002) Is epilepsy a progressive disorder? Prospects for new therapeutic approaches in temporal-lobe epilepsy. *Lancet Neurol.* ***1****, 173 – 181.*

Plotkine, M (1999) Selective inhibition of inducible nitric oxide synthase prevents ischaemic brain injury. *Br. J. Pharmacol.* ***127****, 546 - 552*

Poddar, R., Deb, I., Mukherjee, S & Paul, S (2010) NR2B-NMDA receptor mediated modulation of the tyrosine phosphatase STEP regulates glutamate induced neuronal death. *J. Neurochem.* ***115(6)****, 1350 – 1360*.

Price, D.J (1989) Intravenous valproate: experience in neurosurgery. In: Chadwick, D (Ed.), *Fourth International Symposium of Sodium Valproate and Epilepsy, Royal Society of Medicine Services, London, pp 197 – 203.*

Priestly, J.B (1775) Elements and Atoms

Puranam, R.S & McNamara, J.O (1999) Seizure disorders in mutant mice: relevance to human epilepsies. *Curr. Opin. Neurobiol.* ***9****, 281 – 287.*

Racine, R.J (1972) Modification of seizure activity by electrical stimulation. II. Motor seizure. Electroencephalography and Clin. Neurophysiol. **32**, 281 - 294.

Rajesekaran (2005) Seizure-induced oxidative stress in rat brain regions: Blockade by nNOS inhibition. Pharmacol. Biochem. & Behaviour **80(2)**, 263 - 272

Ralay Ranaivo, H & Wainwright, M.S (2010) Albumin activates astrocytes and microglia through mitogen-activated protein kinase pathways. *Brain Res.* ***1313****, 222 – 231*.

Ralston, B.L (1958) The mechanism of transition of interictal spiking into ictal seizure discharges. *Electroencephalogr. Clin. Neurophysiol.* ***10****, 217 – 232.*

Rasband, W.S (1997 – 2011) ImageJ, U. S. National Institutes of Health, Bethesda, Maryland, USA, http://imagej.nih.gov/ij/

Rasmussen, T., Olszewski, J., Lloyd-Smith, D (1958) Focal seizures due to chronic localized encephalitis. *Neurology* ***8(6)****, 435 – 445*.

Ratovitski, E. A., Alam, M. R., Quick, R. A., McMillan, A., Bao, C., Kozlovsky, C., Hand, T. A., Johnson, R. C., Mains, R. E., Eipper, B. A. and Lowenstein, C. J. (1999) Kalirin inhibition of inducible nitric-oxide synthase. J. Biol. Chem. ***274***, 993 – 999

Ravizza, T., Gagliardi, B., Noe, F., Boer, K., Aronica, E & Vezzani, A (2008) Innate and adaptive immunity during epileptogenesis and spontaneous seizures: evidence from experimental models and human temporal lobe epilepsy. *Neurobiol. Disease* ***29(1)****, 142 – 160*.

Relo. A & Feldon, J (2002) Specific neuronal protein: a new tool for histological evaluation of excitotoxic lesions, Physiol. Behav. **76** *449– 456*.

Rho, J.M., Donevain, S.D & Rogawski, M.A (1994) Mechanism of action of the anti-convulsant Felbamate: opposing effects on N-Methyl-d-Aspartate and GABA A receptors. *Ann. Neurol.* ***35****, 224 – 234.*

Riban, V., Bouilleret, V., Pham-Le, B.T., Fritschy, J-M., Marescaux, C., Depaulis, A (2002) Evolution of hippocampal epileptic activity during the development of

hippocampal sclerosis in a mouse model of temporal lobe epilepsy. *Neurosci.* ***112(1)****, 101 – 111*.

Ricker, J.H (ed) (2003) Differential Diagnosis in Adult Neuropsychological Assesment. *Springer Publishing Company. pp 109*

Rigo, J.M., Hans, G., Nguyen, L., Rocher, V., Belachew, S & Malgrange, B (2002) The anti-epileptic drug Levetiracetam reverses the inhibition by negative allosteric modulators of neuronal GABA- and glycine- gated currents. *Br. J. Pharmacol.* ***136****, 5 – 8.*

Robinson, J.H & Deadwyler, S.A (1981) Kainic acid produces depolarization of CA3 pyramidal cells in the in vitro hippocampal slice. *Brain Res.* ***221****, 117 – 127.*

Rogawski, M.A. & Loscher, W. (2004).The neurobiology of antiepileptic drugs. *Nat. Rev. Neurosci.* ***5****, 553–564*

Romero, T.R., Galdino, G.S., Silva, G.C., Resende, L.C., Perez, A.C., Cortez, S.F & Duarte, I.D (2012) Involvement of the L-arginine/nitric oxide/cyclic guanosine monophosphate pathway in peripheral antinociception induced N-palmitoyl-ethanolamine in rats. *J. Neurosci. Res.* ***90(7)****, 1474 – 1479.*

Rothman, S.M (1985) The Neurotoxicity of Excitatory Amino Acids is Produced by Passive Chloride Influx. *J. Neurosci.* ***5(6)****, 1483 – 1489*

Sah, P & Louise-Faber, E.S (2002) Channels underlying neuronal calcium-activated potassium currents. *Prog. Neurobiol.* ***66(5)****, 345 – 353.*

Samoriski, G.M., Piekut, D.T & Applegate, C.D (1997) Differential spatial patterns of *Fos* induction following generalized clonic and generalized tonic seizures. Exp. Neurol. **143(2)**, 255 - 268.

Sanes, J.R & Lichtman, J.W (2001) Induction, assembly, maturation and maintenance of a postsynaptic apparatus. *Nat. Rev. Neurosci.* ***27(7)****, 370 – 377.*

Santizo, R., Baughman, V.L & Pelligrino (2000) Relative contributions from neuronal and endothelial nitric oxide synthases to regional cerebral blood flow changes during forebrain ischemia in rats. NeuroReport **11(7)**, 1549 – 1553.

Sarkisian, M.R (2001) Overview of the current animal models for human seizure and epileptic disorders. *Epilepsy Behav.* ***2(3)****, 201 – 216*.

Sarkisova, K & van Luijtelaar, G (2011) The WAG/Rij strain: A genetic animal model of absence epilepsy with comorbidity of depression. *Prog. In Neuro-Psychopharmacol. and Biol. Psychia.* ***35(4)****, 854 – 876.*

Scharfman, H.E (2007) The CA3 “backprojection”. *Prog. Brain res.* ***163****, 627 – 637*

Schauwecker, P.E & Steward, O (1997) Genetic determinants of susceptibility to excitotoxic cell death: implications for gene targetting approaches. *Proc. Natl. Acad. Sci.* ***94(8)****, 4103 – 4108*.

Schmidt, D., Gram, L., Brodie, M., Kraemer, G., Perucca, E., Kaelviaeinen, R & Elger, C.E (2000) Tiagabine in the treatment of epilepsy – a clinical review with a guide for the prescribing physician. *Epilepsy Res.* ***41****, 245 – 251*.

Schmidt, D & Elger, C.E (2004) What ist he evidence that Oxcarbazepine and carbazepine are distinctly different antiepileptic drugs? *Epilepsy & Behav. 5, 627 – 635*.

Schmidt, H. H. H. W., Hofmann, H., Schindler, U., Shutenko, Z.S., Cunningham, D. D & Feelisch, M (1996) No NO from NO synthase. PNAS **93(25)**, 14492 - 14497

Schwob, J.E., Fuller, T., Price, J.L & Olney, J.W (1980) Widespread patterns of neuronal damage following systemic or intracerebral injections of kainic acid: A histological study. *Neurosci.* ***5(6)****, 991 – 1014*.

Sennlaub, F., Cortois, Y., Goureau, O (2002) Inducible Nitric Oxide Synthase Mediates Retinal Apoptosis in Ischemic Proliferative Retinopathy. *J. Neurosci.* ***22(10)****, 3987 – 3993.*

Sergott, R.C., Bittman, R.M., Christen, E.M & Sagar, S.M (2010) Vigabentin-induced peripheral visual field defects in patients with refractory partial epilepsy. *Epilepsy Res.* ***92(2-3)****, 170 – 176*.

Shapiro, L.A., Wang, L & Ribak, C.E (2008) Rapid astrocyte and microglial activation following pilocarpine-induced seizures in rats. *Epilepsia* ***49(2)****, 33 – 41*.

Shibley, H & Smith, B.N (2002) Pilocarpine-induced status epilepticus results in mossy fibre sprouting and spontaneous seizures in C57BL/6J and CD-1 mice. *Epilepsy Res.* ***49****, 109 – 120.*

Shikhanov, N.P., Ivanov, N.M., Khovryakov, A.V., Kasperson, K., McCann, G.M., Kruglyakov, P.P & Susonov, A.A (2005) Studies of damage to hippocampal neurons in inbred mouse lines in models of epilepsy using kainic acid and pilocarpine. *Neurosci and Behav.* ***35(6)****, 623 – 628.*

Shimizu, T., Hayashi, Y., Yamasaki, R., Yamada, J., Zhang, J., Ukai, K., Koike, M & Nakanishi, H (2005) Proteolytic degradation of glutamate decarboxylase

mediates Disinhibition of hippocampal CA3 pyramidal cells in cathepsin-D difficient mice. *J. Neurochem.* ***94(3)****, 680 – 690.*

Sik, A., Penttonen, M & Buzsak, G (1997) Interneurons on the Hippocampal Dentate Gyrus: an in vivo Intracellular Study. Eur. J. Neurosci **9**, 573 - 588.

Sills, G.J (2007) Seizures beget seizures: A lack of Experimental Evidence and Clinical Relevance Fails to dampen enthusiasm. Epilepsy Curr. 7(4), 103 – 104.

Siviotti, L & Nistri, A. (1991) GABA receptor mechanisms in the central nervous system. *Prog. Neurobiol.* ***36(1)****, 35 – 92*

Sloviter, R.S. (1996) Hippocampal pathology and pathophysiology in temporal lobe epilepsy. *Neurologia* ***11****, 29–32*

Sloviter, R.S (1999) Status epilepticus-induced neuronal injury and network reorganisation. *Epilepsia* ***40(SUPPL. 1)****, S34 – S39.*

Snead III, O.C. (1995) Basic mechanisms of generalized absence seizures. *Annals of Neurol.* ***37(2)****, 146 – 157.*

Song, H., Stevens, C.F & Gage, F.H. (2002) Astroglia induce neurogenesis from adult neural stem cells. *Nature* ***417(6884)****, 39 – 44.*

Soriano, F.X., Martel, M-A., Papadia, S., Vaslin, A., Baxter, P., Rickman, C., Forder, J., Tymianski, M., Duncan, R., Aarts, M., Clarke, P.G.H., Wyllie, D.J.A & Hardingham, G.E (2008) Specific Targetting of pro-death NMDA Receptor signals with Differing Reliance on the NR2B PDZ ligand. J. Neuroscience **28(42)**, 10696 – 10710

Southan, G.J., Szabo, C & Thiemermann (1995) Isothioureas: potent inhibitors of nitric oxide synthases with variable isoform selectivity. *Br. J. Pharmacol.* ***114(2)****, 510 - 516*

Sperk, G., Lassmann, H & Baran, H (1983) Kainic acid induced seizures: Neurochemical and histopathological changes. *Neurosci.* ***10(4)****, 1301 – 1315*.

Sperk, G (1994) Kainic acid seizures in the Rat. *Prog. Neurobiol.* ***42(1)****, 1 – 32.*

Staley, K.J., Bains, J.S., Yee, A., Hellier, J & Longacher, J.M (2001) Statistical model relating CA3 burst probability to recovery from burst-induced depression at recurrent collateral synapses. *Nat. Neurosci., 201 – 209*.

Stamler, J.S.. Singel, D.J & Loscalzo, J (1992) Biochemistry of nitric oxide and its redox-activated forms. *Science* ***258(5090)****, 1898 – 1902*.

Starkey, S.J., Grant, A.L & Hagan, R.M (2001) A rapid and transient synthesis of nitroc oxide (NO) by a constitutively expressed type II NO synthase in the guinea-pig suprachiasmatic nucleus. *Br J Pharmacol* ***134****: 1084–1092.*

Steele, M.L & Robinson, S.R (2012) Reactive astrocytes give neurons less support: implications for Alzheimer's disease. *Neurobiol. Aging* ***33(2)****, e1 – 13*.

Steinert, J.R., Chernova, T & Forsythe, I.D (2010) Nitric Oxide signalling in Brain Function, Dysfunction and Dementia. *Neuroscientist* ***16****, 435 – 452*

Stolp, H.B (2012) Neuropoietic cytokines in normal brain development and neurodevelopmental disorders. Mol. & Clin. Neurosci. IN PRESS

Sudhof, T.C (1995) The synaptic vesicle cycle: a cascade of protein-protein interactions. *Nature* ***375****, 645 – 653*

Sudhof, T.C (2004) The synaptic vesicle cycle. *Ann. Rev. Neurosci.* ***27****, 509 – 547*

Sutula, T., Cascino, G., Cavazos, J., Parada & I., Ramirez, L (1989) Mossy fiber synaptic reorganization in the epileptic human temporal lobe. *Ann. Neurol.* ***26****, 321 - 330.*

Sykova, E & Chvatal, A. (2000) Glial cells and volume transmission in the CNS. *Neurochem. Int.* ***36(4-5)****, 397 – 409.*

Szabadits, E., Cserep, C., Ludanyi, A., Katona, I., Gracia-Llanes, J., Freund, T.F & Nyiri, G (2007) Hippocampal GABAergic Synapses Possess the Molecular Machinery for Retrograde Nitric Oxide Signaling. J. Neurosci. **27(30)**, 8101 - 8111.

Takei, Y., Takashima, S., Ohyu, J., Matsuura, K., Katoh, N., Takami, T., Miyajima, T & Hoshika, A (2001) Different effects between 7-nitroindazole and L-NAME on cerebral hemodynamics and hippocampal lesions during kainic acid-induced seizures in newborn rabbits. *Brain and dev.* ***23(6)****, 406 - 413.*

Tallent, M.K & Siggins, G. R (1999) Somatostatin Acts in CA1 and CA3 to reduce Hippocampal Epileptiform Activity. *J. Neurophysiol.* ***81****, 1626 – 1635.*

Tanaka, K., Watase, K., Manabe, T., Yamada, K., Watanabe, M., Takahashi, K., Iwama, H., Nishikawa, T., Ichihara, N., Kikuchi, T., Okuyama, S., Kawashima, N., Hori, S., Takimoto, M & Wada, K (1997) Epilepsy and exacerbation of brain injury in mice lacking the glutamate transporter GLT-1. *Science* ***276****, 1699 – 1702.*

Taylor B. S. and Geller D. A. (2000) Molecular regulation of the human inducible nitric oxide synthase (iNOS) gene. *Shock* **13,** 413–424.

Tauck, D.L & Nadler, J.V (1985) Evidence of functional mossy fibre sprouting in hippocampal formation of kainic acid-treated rats. *J. Neurosci.* ***5(4)****, 1016 – 1022.*

Timofeev, I., Grenier, F & Steriade, M (2004) Contribution of intrinsic cellular factors in the generation of cortically generated electrographic seizures. *J. Neurophysiol.* ***92****, 1133–1143.*

Tomita, S., Adesnik, H., Sekiguchi, M., Zhang, W., Wada, K., Howe, J.R., Nicoll, R.A & Bredt, D.S (2005) Stargazin modulates AMPA receptor gating and trafficking by distinct domains. *Nature* ***435(7045)****, 1052 – 1058*

Treiman, D.M., Walton, N.Y., Kendrick, C (1990) A progressive sequence of electroencephalographic changes during generalized convulsive status epilepticus. *Epilepsy Res.* ***5****, 49 – 60.*

Treiman, D.M (1993) Generalized convulsive status epilepticus in the adult. *Epilepsia* ***34(SUPPL. 1)****, S2 – S11.*

Tsacopoulos, M & Magistretti, P.J. (1996) Metabolic coupling between glia and neurons. J. Neurosci. 16(3), 877 – 885.

Tsien, J.Z. (2000) Linking Hebb's coincidence detection to memory formation. *Curr. Op. Neurobiol.* ***10(2)****, 266 – 273.*

Tunnicliff, G (1996) Basis of the antiseizure action of phenytoin. *Gen. Pharmacol.* ***27(7)****, 1091 – 1097*.

Twarog BM (1954): Responses of a molluscan smooth muscle to acetylcholine and 5-hydroxytryptamine. *J. Cell. Comp. Physiol.* ***44****, 141 – 163.*

Uhlhaas, P.J & Singer, W. (2006) Neural Synchrony in Brain Disorders: Relevance for Cognitive Dysfunctions and Pathophysiology. *Neuron* ***52(1)****, 155 – 168*.

Ullian, E.M., Christopherson, K.S & Barres, B.A (2004) Role for glia in synaptogenesis. *Glia* ***47(3)****, 209 – 216.*

Verkhratsky, A & Butt, A. (2007) Glial neurobiology: A textbook. Wiley

Verkhratsky, A & Kettenmann, H. (1996) Calcium signalling in glial cells. *Trends Neurosci.* ***19(8)****, 346 – 352.*

Vernadakis, A (1996) Glia-neuron intercommunications and synaptic plasticity. *Prog. Neurobiol.* ***49(3)****, 185 – 214.*

Vezzani, A & Granata, T (2005) Brain inflammation and epilepsy: Experimental and Clinical evidence. *Epilepsia* ***46(11)****, 1724 – 1743.*

Vezzani, A., Ravizza, T., Balosso, S & Aronica, E (2008) Glia as a source of cytokines: implications for neuronal excitability and survival. *Epilepsia* ***49 (SUPPL. 2)****, 24 – 32.*

Vezzani, A., Bartfai, T., Bianchi, M., Rossetti, C & French, J (2011) Therapeutic potential of new anti-epileptic drugs. *Epilepsia* ***52****, 67 – 69*.

Vezzani, A., Friedman, Dingledine, R.J (2012) The role of inflammation in epileptogenesis. *Neuropharmacol.* ***69****, 16 – 24*.

Vitkovic, L., Bockaert, J & Jacque, C (2000) “Inflammatory” cytokines: Neuromodulators in the normal brain? *J. Neurochem.* ***74(2)****, 457 – 471.*

Volterra, A & Meldolesi, J (2005) Astrocytes, from brain glue to communication elements: The revolution continues. *Nat. Rev. Neurosci.* ***6****, 626 – 640.*

Von Krosigk, M., Bal, T., McCormick, D.A (1993) Cellular mechanism of a synchronised oscillation in the thalamus. *Science* ***261****, 361 – 364.*

von Zahn, J., Moller, T., Kettenmann, H & Notte, C (1997) Microglial phagocytosis is modulated by pro- and anti- inflammatory cytokines. *Neuroreport **8**, 3851 – 3856.*

Walker, M.C & Sander, J.W.A.S (1996) Topiramate: a new antiepileptic drug for refractory epilepsy. *Seizure **5**, 199 – 203.*

Wang, C.X., Schuaib, A (2005) NMDA/NR2B selective antagonists in the treatment of ischemic brain injury. *Curr. Drug Targets CNS Neurol. Disord. **4**, 143 – 151*.

Wang, W., Sun, Y-J., Xi, T & Zhu, D-Y (2004) Effect of 1400W on neurogenesis after transient focal cerebral ischemia in the adult rat hippocampus*. Chinese Pharmacol. Bull. **20(1)**, 33 – 37*.

Wang, J., Wang Q & Ye, F (2002) Effects of antisense glutamic acid decarboxylase oligodeoxynucleotide on epileptic rats induced by pentylenetrazol. *Chinese Med. Journal **115(3)**, 425 – 429.*

Wang, Z & Chow, S-Y (1994) Effect of kainic acid on unit discharge in CA1 area of hippocampal slice of DBA and C57 mice. *Epilepsia, **35(5)**, 915 – 921*

Watanabe, T., Morimoto, K., Hirao, T., Suwaki, H., Watase, K & Tanaka, K (1999) Amygdala-kindled and pentylenetetrazole-induced seizures in glutamate transporter GLAST-deficient mice. *Brain Res.* ***845****, 92 – 96*.

Waurin, J-P & Dudek, F.E (2001) Excitatory Synaptic input to granule cells Increases with time after kainate treatment. *J. Neurophysiol.* ***85****, 1067 – 1077*.

Wenzel, H.J., Woolley, C.S., Robbins, C.A & Schwartzkroin, P.A (2000) Kainic acid-induced mossy fibre sprouting and synapse formation in the dentate gyrus of rats. *Hippocampus* ***10(3)****, 244 – 260.*

Whittington, M.A., Traub, R.D., Kopell, N., Ermentrout, B & Buhl, E.H (2000) Inhibition-based rhythms: Experimental and mathematical observations in network dynamics. *Int. J. Psychophysiol.* ***38(3)****, 315 – 336.*

Wiebe, S., Blume, W.T., Girvin, J.P & Eliasziw, M. (2001) A randomized, controlled trial of surgery for temporal-lobe epilepsy. *N. Eng. J. Med.* ***345(5)****, 311 – 318.*

Wieser, H-G (2004) Mesial temporal lobe epilepsy with hippocampal sclerosis. *Epilepsia* ***45(6)****, 695 – 714*.

Williams, P., White, A., Ferraro, D., Clark, S., Staley, K & Dudek, F.E (2006) The use of radiotelemetry to evaluate electrographic seizures in rats with kainite-induced epilepsy. *J. Neurosci. Methods* ***155(1)****, 39 – 48.*

Wink, D.A & Mitchell, J.B (1998) Chemical biology of nitric oxide: insights into regulatory, cytotoxic, and cytoprotective mechanism of nitric oxide. *Free radical Biol. Med.* ***25****, 434 – 456.*

Wolf, H.K., Buslei, R., Schmidt-Kastner, R., Schmidt-Kastner, P.K., Pietsch, T., Wiestler, O.D & Blumke, I (1996) NeuN: A Useful Neuronal Marker for Diagnostic Histopathology. *J. Histochem. & Cytochem.* ***44(10)****, 1167 – 1171.*

Willoughby, J.O., Mackenzie, L., Medvedev, A & Hiscock, J.J (1997) Fos induction following systemic kainic acid: early expression in hippocampus and later widespread expression correlated with seizure. Neurosci. **77(2)**, 379 - 392

Willow, M., Gonoi, T & Catterall, W.A (1985) Voltage clamp analysis of the inhibitory actions of diphenylhydantoin and carbamazepine on the voltage-sensitive sodium channels in neuroblastoma cells. *Mol. Pharmacol.* ***27****, 549 - 558*

Yang, S & Cox, C.L (2007) Modulation if inhibitory activity by nitric oxide in the thalamus. J Neurophysiol **97(5)**, 3386 – 3395.

Zarri, I., Bucossi, G., Cupello, A., Rapallino, M.V & Robello, M (1994) Modulation by nitric oxide of rat brain GABA(A) receptors. Neurosci. Let. **180(2)**, 239 - 242.

Zhang, H.Q., Fast, W., Marletta, M.A., Martasek, P & Silverman, R.B (1997) Potent and selective inhibition of neuronal nitric oxide synthase by Nw-propyl-L-arginine. J. Med. Chem. **40(24)**, 3869 – 3870.

Zheng, H., Zhu, Wei., Zhao, H., Wang, X., Wang, W & Li, Z (2010) Kainic Acid-Activated Microglia Mediate Increased Excitability of Rat Hippocampal Neurons in vitro and in vivo: Crucial Role of Interleukin-1beta. *Neuroimmunomodulation **17**, 31-38.*

Zucker, R.S (1996) Exocytosis: A molecular and Physiological perspective. *Neuron **17**, 1049 – 1055*

Appendix: Beamer, E.H., Otahal, J., Sills, G.J & Thippeswamy, T (2012) N^{W}-Propyl-L-arginine (L-NPA) reduces status epilepticus and early epileptogenic events in a mouse model of epilepsy: behavioural, EEG and immunohistochemical analyses. *Eur. J. Neurosci.* ***36****, 3194 – 3203*

This text box is where the unabridged thesis included the following third party copyrighted material:

Beamer, E.H., Otahal, J., Sills, G.J & Thippeswamy, T (2012) *N*W-Propyl-L-arginine (L-NPA) reduces status epilepticus and early epileptogenic events in a mouse model of epilepsy: behavioural, EEG and immunohistochemical analyses. *Eur. J. Neurosci.* ***36****, 3194 – 3203*